Theoretical Concepts of Photocatalysis

Mohammad Mansoob Khan

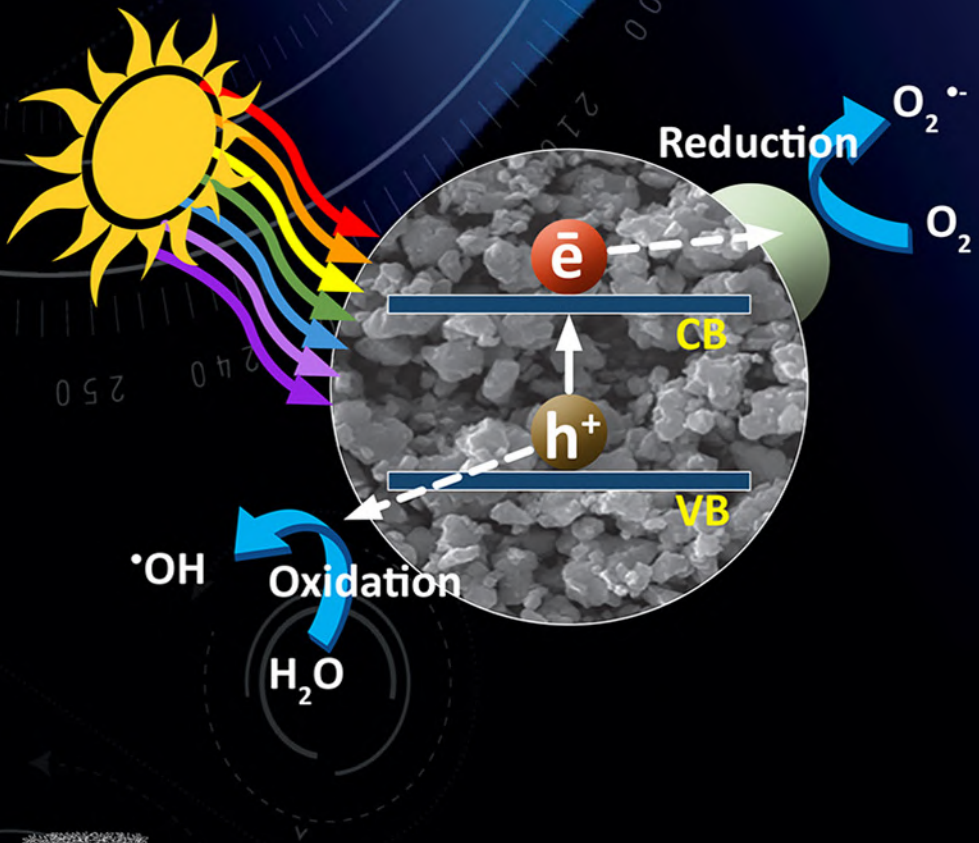

ELSEVIER

Theoretical Concepts of Photocatalysis

Theoretical Concepts of Photocatalysis

Mohammad Mansoob Khan
Chemical Sciences, Faculty of Science,
Universiti Brunei Darussalam,
Gadong, Brunei Darussalam

ELSEVIER

Elsevier
Radarweg 29, PO Box 211, 1000 AE Amsterdam, Netherlands
The Boulevard, Langford Lane, Kidlington, Oxford OX5 1GB, United Kingdom
50 Hampshire Street, 5th Floor, Cambridge, MA 02139, United States

Notices

Knowledge and best practice in this field are constantly changing. As new research and experience broaden our understanding, changes in research methods, professional practices, or medical treatment may become necessary.

Practitioners and researchers must always rely on their own experience and knowledge in evaluating and using any information, methods, compounds, or experiments described herein. In using such information or methods they should be mindful of their own safety and the safety of others, including parties for whom they have a professional responsibility.

To the fullest extent of the law, neither the Publisher nor the authors, contributors, or editors, assume any liability for any injury and/or damage to persons or property as a matter of products liability, negligence or otherwise, or from any use or operation of any methods, products, instructions, or ideas contained in the material herein.

ISBN: 978-0-323-95191-3

Publisher: Joseph P. Hayton
Editorial Project Manager: Catherine Costello
Production Project Manager: Bharatwaj Varatharajan
Cover Designer: Christian J. Bilbow

Typeset by MPS Limited, Chennai, India

Dedication

I would like to dedicate this book to my lovely family members—wife, Arshia Tauseef; son, Mohammad Muaz Khan; and daughters, Asma Khan and Madihah Khan.

Along with the above, I would also like to dedicate this book to the Universiti Brunei Darussalam, Brunei Darussalam.

—***Mohammad Mansoob Khan***

Contents

About the author

Mohammad Mansoob Khan is a professor of inorganic chemistry at Chemical Sciences, Faculty of Science, Universiti Brunei Darussalam, Brunei Darussalam. He earned his PhD degree from the Aligarh Muslim University, Aligarh, India, in 2002. He has worked in India, Ethiopia, Oman, and South Korea and has established excellence in teaching and novel research. He used to teach various courses at the undergraduate and post-graduate levels. He has edited three books and authored two books. He has published about 160 research and review articles.

His expertise is in the cutting-edge area of nanochemistry, nanosciences, nanotechnology, materials sciences, and materials chemistry, especially in the field of inorganic and nanohybrid materials such as synthesis of noble metal nanoparticles, their nanocomposites, metal oxides (such as TiO_2, ZnO, SnO_2, and CeO_2), and chalcogenides (such as CdS, ZnS, and MoS_2). He is also extensively working on the bandgap engineering of semiconductors (such as metal oxides and chalcogenides). The synthesized nanostructured materials are used for heterogeneous photocatalysis, hydrogen production, photoelectrodes, solar cells, sensors, and biological applications such as anti-bacterial, antifungal, and antibiofilm activities.

Preface

This book *Theoretical Concepts of Photocatalysis* provides the fundamentals and theoretical concepts of photocatalysis and related applications. This book includes synthesis, properties, and applications of photocatalysts and strategies on the usefulness and major challenges associated with successful scale-up of the photocatalysts. This book offers a concisely structured and systematic overview of photocatalysis, exploring the theoretical studies of charge carrier dynamics and introducing the fundamental concepts of photocatalytic reactions which involves different types of photocatalysts for various applications. Photocatalysis using different types of photocatalysts (metal oxides, chalcogenides, etc.) is a green technology that has been widely applied for environmental remediation and energy production. Its significant advantages, such as low cost, high efficiency, harmlessness, and stability, are discussed alongside future perspectives and challenges of photocatalysis. Focusing on nanostructure synthesis methods, control, activity enhancement strategies, environmental applications, and perspectives of semiconductor-based nanostructures, this book offers guidelines for designing new semiconductor-based photocatalysts to meet the demands of the efficient utilization of solar energy in the area of energy production and environmental remediation.

This book is an essential textbook for the present and future research in photocatalysis for recyclable, sustainable, and eco-friendly methods for highly innovative and applied nanomaterials. The chapters provide the latest and cutting-edge findings on the use of photocatalysts for energy and environmental applications. This book also describes materials characteristics and significant enhancements in physical, chemical, catalytic, and photocatalytic properties.

This book contains the following nine chapters that deal with several types of photocatalysts and their applications as photocatalysts in various photocatalytic reactions and applications:

Chapter 1 covers the fundamentals of photocatalysis and photocatalysts. This chapter in brief discusses the introduction and fundamental principles of photocatalytic processes and photocatalysts.

Chapter 2 focuses on the fundamentals and principles of photocatalysis and photocatalysts. This chapter also discusses the background necessary to

understand the heterogeneous photocatalysis shown by metal oxides, chalcogenides, etc.

Chapter 3 provides details of photocatalysts that are active under UV light irradiation. This chapter also discusses the background necessary to understand the heterogeneous photocatalysis shown by semiconducting photocatalytic materials under UV light irradiation.

Chapter 4 discusses the photocatalysts that are active under visible light irradiation. This chapter also covers the principles and fundamentals of photocatalysis that takes place under visible light irradiation. This chapter also discusses the fundamentals and principles of heterogeneous photocatalysis shown by semiconducting photocatalytic materials under visible light irradiation.

Chapter 5 covers the synthetic strategies of various types of photocatalysts in order to obtain desired properties for novel photocatalytic applications. In this chapter, various synthesis methods of photocatalysts such as sol−gel method, hydrothermal method, solvothermal method, microwave method, and sonochemical method have been discussed.

Chapter 6 discusses various characterizations of photocatalytic materials in detail and deals with various characterization methods such as spectroscopic, physicochemical, and electrochemical characterization techniques.

Chapter 7 discusses various photocatalytic applications that involve semiconductor-based photocatalysts. This chapter deals with the photocatalytic applications of selected semiconductors such as metal oxides, chalcogenides, and their composites.

Chapter 8 presents selected applications, techniques, and materials that are well studied and tested. Techniques that have been launched in the markets are discussed.

Chapter 9 discusses various future challenges for photocatalysts. The future of semiconductors as photocatalysts in real-life applications such as water purification, air purification, energy, environment, and food packaging has been proposed and discussed.

Mohammad Mansoob Khan

Acknowledgments

First, I would like to thank God for giving me the idea, strength, and opportunity to propose, write, and successfully complete this book, that is, *Theoretical Concepts of Photocatalysis*.

Second, I would like to thank and acknowledge the Universiti Brunei Darussalam, Brunei Darussalam, for continuous encouragement and all types of support.

Third, I would like to thank all the Elsevier team members, Susan Dennis, Catherine Costello, etc. for their assistance, valuable time, and dedicated involvement throughout the process.

I would like to sincerely thank my mother for her unconditional support and prayers. Also, I would like to acknowledge my wife (Arshia) and children (Muaz, Asma, and Madihah) for their full support throughout the writing of this book.

Last, but not least, I would like to acknowledge my PhD students, Shaidatul and Ashmalina, for their help and support.

Mohammad Mansoob Khan
Chemical Sciences, Faculty of Science,
Universiti Brunei Darussalam,
Gadong, Brunei Darussalam

Chapter 1

Introduction of photocatalysis and photocatalysts

Mohammad Mansoob Khan

1.1 Introduction

Various environmental pollutions and lack of sufficient clean and natural energy resources are some of the most serious problems that are presently faced by human beings at the international level. The increase in world population and the widespread unregulated industrial growth have also led to faster energy consumption and source of pollution. However, the persistent release of industrial waste and toxic chemicals into the air and watercourses has resulted in pollution-related diseases, global warming, and abnormal climatic changes. Hence, there is a need to contribute to the growth of environmentally pleasant, ecologically clean and safe, sustainable, and energy-efficient chemical technologies. These are the most urgent challenges to which scientists need to pay attention [1].

Photocatalysis is a process in which the inexhaustibly abundant, clean, and safe energy of the sun can be harvested for sustainable, harmless, and economically feasible technologies and is a major development in this direction. Studies of well-defined photocatalytic reaction systems, detailed reaction mechanisms, and kinetics using several molecular spectroscopies have led to the development of various novel photocatalytic materials [1,2]. Photocatalysis has been attracting extra attention as it finds applications in a variety of products across a broad range of research areas, mainly environmental and energy-related fields. Recently, metal oxides, such as TiO_2, ZnO, SnO_2, and CeO_2, have been the main choice for most studies in basic research and practical applications because of their high activity, low cost, high stability, nontoxicity, and chemical inertness, which makes them suitable for applications in water and air purification, sterilization, hydrogen evolution, etc. [2,3].

In general, photocatalysts have been used for important applications, such as cleansing polluted water and polluted air, self-cleaning glasses, tiles, and tents coated with materials with unique photoinduced super-hydrophilicity. Studies have also been carried out for the advancement of visible light-responsive photocatalysts by incorporating small amounts of dopants (impurities) such as

Theoretical Concepts of Photocatalysis. DOI: https://doi.org/10.1016/B978-0-323-95191-3.00005-5

metals and non-metals by chemical doping and physical ion-implantation methods. Moreover, it has also been possible to prepare photocatalysts, enabling the absorption of light not only in the ultraviolet region but also in the visible light region to function effectively under natural sunlight irradiation [1−3].

1.1.1 Historical developments of photocatalysis

In early 1911, the term photocatalysis appeared in many scientific publications. In Germany, Eibner started this concept in his studies on the effect of ZnO on the bleaching of Prussian blue. The relevance of the term "photocatalysis" was achieved more when the term was used in the title of a few articles reporting the degradation of oxalic acid under light irradiation [4]. A few years later, Baly et al. studied the production of formaldehyde. This was done under visible light illumination using uranium salts and ferric hydroxides as catalysts [5]. In the late 1930s, Doodeve and Kitchener for the first time investigated the ability of TiO_2 to act as a photosensitizer for bleaching dyes in the presence of oxygen species [2,3].

In the 1960s, a Russian group headed by Filimoov began to explore the odds of using materials, for example, TiO_2 and ZnO, for isopropanol photooxidation. At the same time, different Japanese groups studied the heterogenous photooxidation of organic solvents in the presence of ZnO. In parallel, in Germany, Doerffler and collaborators observed the promotion of CO oxidation over irradiated ZnO [1−3,6].

In the early 1970s, Teichner's group showed interest in the photocatalytic oxidation processes in which the partial oxidation of paraffin and olefins over TiO_2 was performed. At the same time, Tanaka and Blyholde studied the photocatalytic decomposition of nitrous oxide. In 1972, two Japanese researchers (Fujishima and Honda) reported electrochemical photolysis of water using a rutile TiO_2 electrode exposed to near UV light and connected to a platinum counter electrode through an electrical load [1−3,6]. This novel idea was created following the oil crisis in the 1970s which led to an unprecedented impulse of research into alternative energy sources.

This led to the potential of hydrogen (H_2) production using abundant and inexpensive water and sunlight. In 1977, Nozik et al. reported that the splitting of water molecules did not require external potential and the photoactivity could be boosted if a noble metal (e.g., Pt) was incorporated. During the same time, Frank and Bard first reported the decomposition of CN^- and SO_3^{2-} by TiO_2, ZnO, and CdS under light [1−3].

The influence of Fujishima's work on the relevance of TiO_2 among photoactive materials was established and progressively increased with works in which in 1973, Bickley et al. reported the photooxidation of isopropanol on rutile TiO_2 [7]. Later, Fujishima et al. reported photocatalytic CO_2 reduction using various inorganic semiconductor materials as photocatalysts. These early efforts extended the applications of photocatalysis, drawing significant research attention in the 1980s to similar reactions using TiO_2 nanoparticles as photocatalysts [3,6,8].

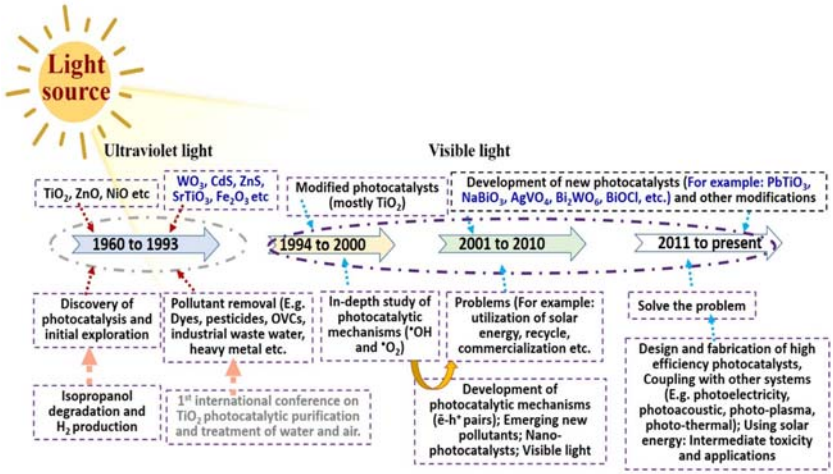

FIGURE 1.1 Historical development of photocatalysis and search for novel photocatalysts intended for energy and environmental remediation.

For instance, subsequent investigations were carried out in 1980 by Wagner and Somorjai on the photogeneration of H_2 over platinized $SrTiO_3$ single crystals with and without potential. In 1981, Sakata and Kawai reported the production of H_2 and CH_4 upon irradiation of Pt/TiO_2 suspension in aqueous ethanol with high quantum efficiency. Since then, investigations have been focused on understanding the fundamental principles, enhancing the photocatalytic efficiencies, searching for new photocatalysts and visible light-active photocatalysts as well as expanding the scope of photocatalysis [1−3,8−11]. These developments have been summarized and shown in Fig. 1.1.

1.2 Photocatalysis

From history, we have learned that the human race has been motivated by nature to discover intelligent answers to complicated problems in their everyday life. Similarly, natural photosynthesis drives chemical pathways using solar radiation. Hence, photocatalysis has arisen as a nature-inspired method for harvesting and converting sun energy to facilitate challenging synthetic conversions for various applications. In 1972, Fujishima and Honda first reported "photocatalysis" by water splitting under UV irradiation. Since then, research in this field has increased many folds [1,2]. The term photocatalysis is composed of two words: photo and catalysis. Photo means "light" whereas catalysis is the process where a substance participates in modifying the rate of a chemical reaction by the transformation of the reactants without

being changed in the end. The substance is known as a catalyst which increases the rate of a reaction by minimizing the activation energy [9,11].

Generally speaking, photocatalysis is a reaction that uses light to activate a substance which modifies the rate of a chemical reaction without being used up. Chlorophyll found in plants is a typical natural photocatalyst. The difference between chlorophyll as a photocatalyst to human-made nano TiO_2 photocatalyst is that usually chlorophyll captures sunlight to convert water and carbon dioxide into oxygen and glucose. However, on the contrary, a photocatalyst forms or generates electrons and hole pairs ($\bar{e}-h^+$ pairs) which helps in the formation of free radicals ($^{\bullet}OH$, $O_2^{\bullet}$, etc.) which are strong oxidizing and reducing agents and are used to decompose the organic pollutants to carbon dioxide and water in the presence of the photocatalyst, light, and water (Fig. 1.2) [6,8,9,11,12].

In other words, photocatalysis is a chemical reaction that takes place in the presence of a photocatalyst and suitable light. A photocatalyst accelerates the rate of a reaction under light which acts either directly or by exciting that in turn catalyzes the reaction. Photocatalysis could be used for the removal of organic or inorganic pollutants from the environment by the photooxidation and photoreduction process driven by light, which takes place at ambient temperature and pressure without requiring any other energy inputs [9,12].

Photocatalysis, which induces efficient and effective reactions at room temperature under sunlight irradiation, has been the focus of much attention for its potential to establish ideal and green technologies which can convert clean, safe, and abundant solar energy into electrical and/or chemical energy [12]. Photocatalysis can be used for the removal of organic or inorganic pollutants and degradation of organic pollutants from the environment by a photocatalytic reaction in the presence of suitable light at ambient temperature without external inputs [9].

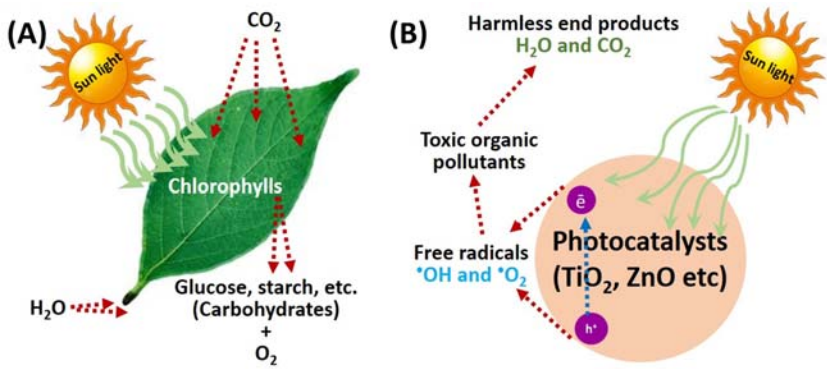

FIGURE 1.2 Fundamentals of photocatalysis (A) natural photosynthesis in leaf and (B) using TiO_2.

A few examples of photocatalytic reactions are stated below and shown in Fig. 1.3:

- Photocatalytic water purification: Photocatalysts in the presence of suitable light can oxidize organic pollutants into nontoxic by-products such as CO_2 and H_2O. They can also disinfect several bacteria and viruses.
- Photocatalytic dye degradation is a process in which large dye molecules can be decomposed (oxidized and/or reduced) chemically into smaller molecules. The resulting products can be water, carbon dioxide, and/or mineralized by-products. Examples of photocatalysts: TiO_2, ZnO, and CdS.
- Inorganic antimicrobial materials have gained significant attention due to their ability to withstand adverse processing conditions and improved mechanical and chemical stability at high temperatures and pressures. Examples of inorganic antimicrobial photocatalysts are ZnO, MgO, CuO, and Fe_2O_3.
- Self-cleaning glass is a specific type of glass with a surface that keeps itself free of dust and grime. Broadly, self-cleaning coatings are of two types: (1) hydrophobic self-cleaning coatings and (2) hydrophilic self-cleaning coatings. These types of coatings can clean themselves through the action of water. The former by rolling down the water droplets and the latter by sheeting water that carries away dust, etc. Hydrophilic coatings based on TiO_2, however, have an additional property. They can chemically break down the adsorbed dust in the presence of sunlight.

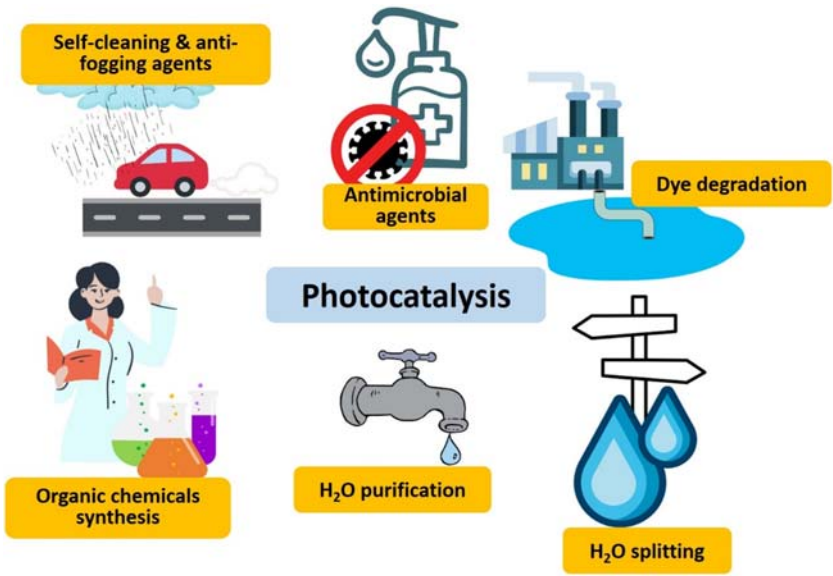

FIGURE 1.3 A few examples of photocatalysis.

- Photocatalytic water splitting is an artificial photosynthesis process with photocatalysis that takes place in a photoelectrochemical cell and is used for the dissociation of water into hydrogen (H_2) and oxygen (O_2), using either artificial or natural light. Theoretically, only light energy (photons), water, and a suitable photocatalyst are needed. This topic is the focus of much interest and research. So far, no technology has been commercialized. Hydrogen fuel production has gained much attention as public understanding of global warming has grown. Methods such as photocatalytic water splitting are being investigated to produce H_2 gas, which is a clean-burning fuel. Water splitting holds particular promise since it utilizes water, an inexpensive renewable resource. Photocatalytic water splitting has the simplicity of using a photocatalyst and sunlight to produce H_2 gas from water. Examples of photocatalysts: CdS, $Cd_{1-x}Zn_xS$. [8,9,12].
- Antifogging: Mostly applied on windshields to keep visibility high and improve driving safety. Antifogging coatings have been proposed which involve the enhancement of attractive forces between water and surface to overcome surface tension as well as disperse the water droplets to form an invisible water layer [13]. Examples of photocatalysts include TiO_2, SiO_2, and CeO_2 [14–16].
- Photocatalytic organic synthesis: Organic chemicals are essential for the manufacture of a vast number of products. Conventional industrial routes to produce organic chemicals typically require harsh operating conditions. Therefore, the photocatalytic organic synthesis route is developed as it only requires light as an energy source and milder reaction conditions [17–19].
- Photocatalytic removal of agricultural pollutants: To improve the production of crops, agricultural chemicals including fertilizers, additives for soil remediation, growth regulators, pesticides, and herbicides are widely used. Very few of these agricultural chemicals are completely mineralized after biotic or abiotic degradation. Some of their degradation intermediates, which possess even higher toxicity, have been detected at higher concentrations in drinking water and surface water compared to their parent forms. Therefore, heterogeneous photocatalysis can be used as an effective process for removing agricultural pollutants from water bodies. Dispersed powder of TiO_2 and ZnO has been widely used to degrade agricultural pollutants under irradiation of light [20,21].
- Photocatalytic removal of pharmaceutical pollutants: Pharmaceutically active compounds are widely emerging as contaminants in water environments, and they possess high potential risks to aquatic life and human health. Generally, conventional wastewater and biological treatments have failed to separate drugs from a waste watercourse. A heterogeneous photocatalysis process becomes a productive approach for reducing the harmful effects of pharmaceutical wastes, their by-products, and unreacted reactants in the environment [22,23].

- Photocatalytic reduction of CO_2 is similar to natural photosynthesis. It is a process in which plants convert CO_2 and H_2O to oxygen and carbohydrates in the presence of sunlight. As a result of photocatalysis, CO_2 can be reduced to various chemicals, such as CH_4, CH_3OH, HCOOH, and CO. Among them, methanol is of prime interest due to its vast industrial use and applicability in the energy-related sector [24].
- Air purification: Photocatalytic air purification is a promising technology that mimics nature's photochemical process. The main advantages of photocatalytic air purification are that no chemicals or external energy input are required except light, which is not costly when utilizing ambient light or sunlight. It is a safe operation under ambient conditions and is a relatively humidity-insensitive activity, and it possesses the ability to fully mineralize volatile organic compounds to CO_2 and H_2O [25].
- Photoantioxidant: Antioxidants neutralize free radicals either by providing the extra electron needed to make the pair or by breaking down the free radical molecule to render it harmless under the irradiation of light [26]. Under the influence of visible light irradiation, $\bar{e}$ in the metal oxide gets photoexcited after the absorption of photons from valence band to conduction band generating $\bar{e}-h^+$ pairs. The generated electrons from the absorption act as reducing agents. The h^+ on the surface of the metal oxide has a considerable oxidizing capacity, as a result, hydroxyl radicals that have a high oxidizing potential formed could interact with free radicals.
- Photocatalytic removal of heavy metals: Heavy metals are a group of metals and metalloids that have a relatively high density and are toxic even at low concentrations. Conventional methods have several drawbacks including low efficiency, high cost, and by-products. Photocatalysis is an emerging advanced catalytic oxidation technology that uses light energy as the only source of energy. It is a clean new technology that can be widely used in the treatment of organic pollutants in water [27,28].

1.2.1 Photocatalysts

A photocatalyst is a substance that participates in a chemical reaction without being consumed which results in a change in the rate of a photoreaction. A photoreaction is a chemical reaction that involves the absorption of light by one or more reacting species [12].

In other words, a photocatalyst is a substance that can absorb suitable light (photons, quanta, etc.) which helps in chemical transformations of the reactants by lowering the activation energy and repeatedly coming in contact with intermediate chemical species which helps to convert the reactants to final harmless end products. In short, a photocatalyst is a material which absorbs light to bring it to a higher energy level and provides such

energy to the reactants to make a chemical reaction take place [11]. The physicochemical properties of the photocatalysts are crucial for their good performance. These properties and characteristics are usually established according to the nature of the photocatalyst (composition, size, shape, morphology, purity, defects, etc.) and the source of the material, i.e., how it was fabricated [29,30].

Usually, an ideal photocatalyst should have some basic properties. They must be active either under UV light, visible light, or solar light. They should have the property of chemical and biological robustness as well as be stable toward photocorrosion. The other most important characteristic that they must have is that they should be nontoxic and must have a low cost and easy availability [12]. The most typical photocatalysts are solid semiconductors, such as metal oxides, chalcogenides, and carbonaceous materials [30–32]. A few examples of photocatalysts are listed below [26,33–44]:

- Metal oxides: TiO_2, ZnO, CeO_2, and SnO_2.
- Chalcogenides: CdS, ZnS, MoS, Sb_2S_3, CdSe, and CdTe.
- Ternary compounds: $ZnAl_2O_4$, $AgAlO_2$, and $ZnFe_2O_4$.
- Quaternary compounds: $Sm_2Ti_2S_2O_5$, $AgInZn_7S_9$, and $ZnIn_2S_4$.
- Nanocomposites materials: TiO_2/CNT and graphitic carbon nitride (g-C_3N_4).
- Metals: Au, Pt, Ag, Ti, Zn, Ce, and Fe.

1.3 Importance of photocatalysis and photocatalysts

1.3.1 Photocatalysis

It is generally described as a process in which light is used to activate a substance, a photocatalyst that modifies the rate of a chemical reaction without being used up in the chemical reaction. Photocatalysis is a favorable, green, and environmentally friendly method for the conversion of solar energy to chemical energy or chemical conversion over a suitable semiconductor such as metal oxide and chalcogenide nanostructures. The best example is photocatalytic degradation of pollutants and hydrogen production. Photocatalysis is a rapidly emerging area with a high possibility of an extensive range of industrial applications, such as disinfection of water and air, mineralization of toxic organic pollutants, production of renewable fuels, and organic syntheses [30,31,45].

1.3.2 Photocatalysts

Generally, photocatalysts are semiconducting materials that are of great technological importance in the electronics industry and environmental remediation. This is because of their ability to generate charge carriers ($\bar{e}-h^+$ pairs) when activated with a certain amount of threshold energy. The favorable

combination of electronic band structure, light absorption properties, charge transport characteristics, and excited lifetimes of some semiconductors have made possible their application as photocatalysts [30,31,45]. Therefore, metal oxides, such as TiO_2, ZnO, SnO_2, and CeO_2, and chalcogenides, such as CdS, MoS_2, and ZnS have been the prime choice for basic research and practical applications owing to their light-harvesting properties, electronic band structures, excited-state lifetimes, charge transport characteristics, charge carrier mobility, high activity, good stability, easy availability, low-cost, nontoxicity, and chemical inertness.

Hence, the chemistry that takes place at the surface of semiconductors such as metal oxides and chalcogenides has attracted considerable attention for a range of industrial applications, including catalysis, photocatalysis, water purification, deodorization, air purification, self-cleaning, self-sterilizing, antifogging surfaces in optical display technology, chemical synthesis, solar energy devices, antibacterial activities, batteries, and energy production and storage [11,29–32].

1.4 Future perspective

The key to the outstanding performance of nanomaterials is based on their composition, size, shape, morphology, purity, defects, etc. A metal oxide semiconductor shows unique properties which are capable of absorbing UV light because their band gap energy corresponds to the energy of the UV light. Their properties can be used to create a UV-induced system. However, since UV light is only a small proportion of solar energy ($\sim$3%–4%), numerous efforts have been made to develop new photocatalytic systems that are capable of effectively utilizing the visible light which constitutes the main part of the solar spectrum. Various methods which include metal and non-metal doping as well as surface decorations have been applied to produce visible light-active materials. In general, chalcogenides, ternary compounds, quaternary compounds as well as nanocomposites have been reported to excellently improve the photocatalytic degradation efficiency of pollutants under visible light irradiation. This will make the photocatalyst nanomaterials to be more widely applied for many chemical reactions in several fields, such as environment, energy, and medical sciences.

1.5 Summary

Photocatalysis is an astonishing development that can be used for numerous applications such as hydrogen production, photocatalytic degradation of various organic pollutants in wastewater, air purification, and antibacterial activity. When compared with other methods, photocatalysis is fast developing and gaining much attention because of its several benefits, such as nontoxicity, low cost, high stability, and high efficiency. Photocatalysis is an

exclusive development for solving energy and environmental issues. Different types of available photocatalysts have been presented along with issues related to physicochemical characteristics, response to light, and photochemical stability.

References

[1] J.M. Coronado, F. Fresno, M.D. Hernández-Alonso, R. Portela, Design of advanced photocatalytic materials for energy and environmental applications, Green Energy and Technology 71 (2013) 1–4. Available from: https://doi.org/10.1007/978-1-4471-5061-9.

[2] S. Zhu, D. Wang, Photocatalysis: basic principles, diverse forms of implementations and emerging scientific opportunities, Advanced Energy Materials 7 (2017) 1–24. Available from: https://doi.org/10.1002/aenm.201700841.

[3] A. Hernández-Ramírez, I. Medina-Ramírez, Photocatalytic Semiconductors: Synthesis, Characterization, and Environmental Applications, Springer, Cham, 2015. Available from: https://doi.org/10.1007/978-3-319-10999-2.

[4] J.M. Coronado, F. Fresno, M.D. Hernández-Alonso, R. Portela, Design of Advanced Photocatalytic Materials for Energy and Environmental Applications, Springer, London, 2013. Available from: https://doi.org/10.1007/978-1-4471-5061-9.

[5] E.C.C. Baly, I.M. Heilbron, W.F. Barker, CX.—Photocatalysis. Part I. The synthesis of formaldehyde and carbohydrates from carbon dioxide and water, Journal of the Chemical Society, Transactions 119 (1921) 1025–1035. Available from: https://doi.org/10.1039/CT9211901025.

[6] M.M. Khan, Principles and mechanisms of photocatalysis, Photocatalytic Systems by Design, Elsevier, 2021, pp. 1–22. Available from: https://doi.org/10.1016/B978-0-12-820532-7.00008-4.

[7] R. Bickley, Photoadsorption and photocatalysis at rutile surfaces II. Photocatalytic oxidation of isopropanol, Journal of Catalysis 31 (1973) 398–407. Available from: https://doi.org/10.1016/0021-9517(73)90311-4.

[8] M.M. Khan (Ed.), Chalcogenide-Based Nanomaterials as Photocatalysts, first ed., Elsevier, 2021. Available from: https://doi.org/10.1016/C2019-0-01819-5.

[9] X. Chen, Y. Hu, Z. Xie, H. Wang, Materials and Design of Photocatalytic Membranes, Elsevier Inc., 2018. Available from: https://doi.org/10.1016/B978-0-12-813549-5.00003-7.

[10] J. Zhang, B. Tian, L. Wang, M. Xing, J. Lei, Photocatalysis: Fundamentals, Materials and Applications, 1st, Springer, 2018. Available from: https://doi.org/10.1007/978-981-13-2113-9.

[11] Y. Oshida, Oxidation and oxides, Bioscience and Bioengineering of Titanium Materials, Elsevier, 2013, pp. 87–115. Available from: https://doi.org/10.1016/b978-0-444-62625-7.00004-2.

[12] J. Zhang, B. Tian, L. Wang, M. Xing, J. Lei, Photocatalysis, Springer Singapore, Singapore, 2018. Available from: https://doi.org/10.1007/978-981-13-2113-9.

[13] J.-B. Chemin, S. Bulou, K. Baba, C. Fontaine, T. Sindzingre, N.D. Boscher, et al., Transparent anti-fogging and self-cleaning TiO2/SiO2 thin films on polymer substrates using atmospheric plasma, Scientific Reports 8 (2018) 9603. Available from: https://doi.org/10.1038/s41598-018-27526-7.

[14] F.M. Fardo, R.S. Ribeiro, J.A. Strauss, J. Nardi, L.C. Ferreira, G. Schmökel, et al., Double layer SiO_2 –TiO_2 sol–gel thin films on glass for antireflection, antifogging, and UV recoverable self-cleaning, Applied Optics 59 (2020) 7720. Available from: https://doi.org/10.1364/AO.397484.

[15] A. Tricoli, M. Righettoni, S.E. Pratsinis, Anti-fogging nanofibrous SiO_2 and nanostructured SiO_2-TiO_2 films made by rapid flame deposition and in situ annealing, Langmuir 25 (2009) 12578−12584. Available from: https://doi.org/10.1021/la901759p.

[16] F.L. Heale, I.P. Parkin, C.J. Carmalt, Slippery liquid infused porous TiO_2/SnO_2 nanocomposite thin films via aerosol assisted chemical vapor deposition with anti-icing and fog retardant properties, ACS Applied Materials & Interfaces 11 (2019) 41804−41812. Available from: https://doi.org/10.1021/acsami.9b14160.

[17] D. Friedmann, A. Hakki, H. Kim, W. Choi, D. Bahnemann, Heterogeneous photocatalytic organic synthesis: state-of-the-art and future perspectives, Green Chemistry 18 (2016) 5391−5411. Available from: https://doi.org/10.1039/C6GC01582D.

[18] X. Zhu, Y. Lin, J. San Martin, Y. Sun, D. Zhu, Y. Yan, Lead halide perovskites for photocatalytic organic synthesis, Nature Communications 10 (2019) 2843. Available from: https://doi.org/10.1038/s41467-019-10634-x.

[19] B. König, Photocatalysis in organic synthesis − past, present, and future, European Journal of Organic Chemistry 2017 (2017) 1979−1981. Available from: https://doi.org/10.1002/ejoc.201700420.

[20] N. Vela, M. Calín, M.J. Yáñez-Gascón, A. el Aatik, I. Garrido, G. Pérez-Lucas, et al., Removal of pesticides with endocrine disruptor activity in wastewater effluent by solar heterogeneous photocatalysis using ZnO/Na2S2O8, Water, Air, and Soil Pollution 230 (2019). Available from: https://doi.org/10.1007/s11270-019-4185-y.

[21] N.T. Hanh, N. le Minh Tri, D. van Thuan, M.H. Thanh Tung, T.D. Pham, T.D. Minh, et al., Monocrotophos pesticide effectively removed by novel visible light driven Cu doped ZnO photocatalyst, Journal of Photochemistry and Photobiology A: Chemistry 382 (2019). Available from: https://doi.org/10.1016/j.jphotochem.2019.111923.

[22] D. Ranjith Kumar, K.S. Ranjith, Y. Haldorai, A. Kandasami, R.T.R. Kumar, Nitrogen-implanted ZnO nanorod arrays for visible light photocatalytic degradation of a pharmaceutical drug acetaminophen, ACS Omega 4 (2019) 11973−11979. Available from: https://doi.org/10.1021/acsomega.9b00557.

[23] C.P. Sajan, A. Naik, H.N. Girish, H.R. Ravi, R. Singh, Template-free processing of Ag-anchored ZnO polyscale sheets and their application in the photocatalytic degradation of organics present in pharmaceutical waste, Water Conservation Science and Engineering 2 (2017) 31−41. Available from: https://doi.org/10.1007/s41101-017-0022-6.

[24] O. Shtyka, R. Ciesielski, A. Kedziora, W. Maniukiewicz, S. Dubkov, D. Gromov, et al., Photocatalytic reduction of CO_2 over Me (Pt, Pd, Ni, Cu)/TiO_2 catalysts, Topics in Catalysis 63 (2020) 113−120. Available from: https://doi.org/10.1007/s11244-020-01241-y.

[25] F. He, W. Jeon, W. Choi, Photocatalytic air purification mimicking the self-cleaning process of the atmosphere, Nature Communications 12 (2021). Available from: https://doi.org/10.1038/s41467-021-22839-0.

[26] S.N. Matussin, M.H. Harunsani, A.L. Tan, A. Mohammad, M.H. Cho, M.M. Khan, Photoantioxidant studies of SnO_2 nanoparticles fabricated using aqueous leaf extract of Tradescantia spathacea, Solid State Sciences 105 (2020) 106279. Available from: https://doi.org/10.1016/j.solidstatesciences.2020.106279.

[27] P. Somu, S. Paul, Casein based biogenic-synthesized zinc oxide nanoparticles simultaneously decontaminate heavy metals, dyes, and pathogenic microbes: a rational strategy for wastewater treatment, Journal of Chemical Technology and Biotechnology 93 (2018) 2962−2976. Available from: https://doi.org/10.1002/jctb.5655.

[28] Y. Zhang, T. Bian, J. Gu, X. Zheng, Z. Li, Controllable ZnO architectures with the assistance of ethanolamine and their application for removing divalent heavy metals (Cu, Pb, Ni) from water, New Journal of Chemistry 42 (2018) 3356−3362. Available from: https://doi.org/10.1039/c7nj04669c.

[29] J.C. Colmenares, Y.J. Xu, Heterogeneous Photocatalysis, Springer, 2006. Available from: https://doi.org/10.1201/9781420015751.

[30] M.M. Khan, S.F. Adil, A. Al-Mayouf, Metal oxides as photocatalysts, Journal of Saudi Chemical Society 19 (2015) 462−464. Available from: https://doi.org/10.1016/j.jscs.2015.04.003.

[31] M.M. Khan, Metal Oxide Powder Photocatalysts, Elsevier Ltd., 2018. Available from: https://doi.org/10.1016/B978-0-08-101977-1.00002-8.

[32] M.M. Khan, D. Pradhan, Y. Sohn, Nanocomposites for Visible Light-Induced Photocatalysis, Springer International Publishing, Cham, 2017. Available from: https://doi.org/10.1007/978-3-319-62446-4.

[33] S.N. Matussin, A.L. Tan, M.H. Harunsani, M.H. Cho, M.M. Khan, Green and phytogenic fabrication of Co-doped SnO_2 using aqueous leaf extract of Tradescantia spathacea for photoantioxidant and photocatalytic studies, Bionanoscience 11 (2021) 120−135. Available from: https://doi.org/10.1007/s12668-020-00820-3.

[34] S.N. Matussin, M.H. Harunsani, A.L. Tan, M.H. Cho, M.M. Khan, Effect of Co^{2+} and Ni^{2+} co-doping on SnO_2 synthesized via phytogenic method for photoantioxidant studies and photoconversion of 4-nitrophenol, Materials Today Communications 25 (2020) 101677. Available from: https://doi.org/10.1016/j.mtcomm.2020.101677.

[35] S.N. Matussin, A.L. Tan, M.H. Harunsani, A. Mohammad, M.H. Cho, M.M. Khan, Effect of Ni-doping on the properties of the SnO_2 synthesized using Tradescantia spathacea for photoantioxidant studies, Materials Chemistry and Physics (2020) 123293. Available from: https://doi.org/10.1016/j.matchemphys.2020.123293.

[36] A. Rahman, M.M. Khan, Chalcogenides as photocatalysts, New Journal of Chemistry 45 (2021) 19622−19635. Available from: https://doi.org/10.1039/D1NJ04346C.

[37] A. Rahman, M.H. Harunsani, A.L. Tan, N. Ahmad, M.M. Khan, Antioxidant and antibacterial studies of phytogenic fabricated ZnO using aqueous leaf extract of Ziziphus mauritiana Lam, Chemical Papers 75 (2021) 3295−3308. Available from: https://doi.org/10.1007/s11696-021-01553-7.

[38] A. Rahman, A.L. Tan, M.H. Harunsani, N. Ahmad, M. Hojamberdiev, M.M. Khan, Visible light induced antibacterial and antioxidant studies of ZnO and Cu-doped ZnO fabricated using aqueous leaf extract of Ziziphus mauritiana Lam, Journal of Environmental Chemical Engineering (2021) 105481. Available from: https://doi.org/10.1016/j.jece.2021.105481.

[39] A. Rahman, M.H. Harunsani, A.L. Tan, N. Ahmad, M. Hojamberdiev, M.M. Khan, Effect of Mg doping on ZnO fabricated using aqueous leaf extract of Ziziphus mauritiana Lam. for antioxidant and antibacterial studies, Bioprocess and Biosystems Engineering 44 (2021) 875−889. Available from: https://doi.org/10.1007/s00449-020-02496-1.

[40] A. Rahman, M.H. Harunsani, A.L. Tan, N. Ahmad, B.K. Min, M.M. Khan, Influence of Mg and Cu dual-doping on phytogenic synthesized ZnO for light induced antibacterial and radical scavenging activities, Materials Science in Semiconductor Processing 128 (2021) 105761. Available from: https://doi.org/10.1016/j.mssp.2021.105761.

[41] S.N. Naidi, M.H. Harunsani, A.L. Tan, M.M. Khan, Structural, morphological and optical studies of CeO_2 nanoparticles synthesized using aqueous leaf extract of Pometia pinnata, BioNanoScience 12 (2022) 393−404. Available from: https://doi.org/10.1007/s12668-022-00956-4.

[42] S.N. Naidi, M.H. Harunsani, A.L. Tan, M.M. Khan, Green-synthesized CeO_2 nanoparticles for photocatalytic, antimicrobial, antioxidant and cytotoxicity activities, Journal of Materials Chemistry B 9 (2021) 5599−5620. Available from: https://doi.org/10.1039/D1TB00248A.

[43] S.N. Naidi, F. Khan, A.L. Tan, M.H. Harunsani, Y.-M. Kim, M.M. Khan, Photoantioxidant and antibiofilm studies of green synthesized Sn-doped CeO_2 nanoparticles using aqueous leaf extracts of Pometia pinnata, New Journal of Chemistry 45 (2021) 7816−7829. Available from: https://doi.org/10.1039/D1NJ00416F.

[44] S.N. Naidi, F. Khan, A.L. Tan, M.H. Harunsani, Y.-M. Kim, M.M. Khan, Green synthesis of CeO_2 and Zr/Sn-dual doped CeO_2 nanoparticles with photoantioxidant and antibiofilm activities, Biomaterials Science 9 (2021) 4854−4869. Available from: https://doi.org/10.1039/D1BM00298H.

[45] J.C. Colmenares, Y.-J. Xu, Heterogeneous Photocatalysis, first ed., Springer Berlin Heidelberg, Berlin, Heidelberg, 2016. Available from: https://doi.org/10.1007/978-3-662-48719-8.

Chapter 2

Fundamentals and principles of photocatalysis

Mohammad Mansoob Khan

2.1 Introduction

Photocatalysis is a term that dates back nearly 100 years. It could simply be defined as the change in the rate of a chemical transformation under the action of light and in the presence of a photocatalyst that absorbs suitable light and is involved in a chemical reaction without being changed at the end of a reaction. While one can find examples of heterogeneous photocatalysis that span this period, a significant growth period for the field of photocatalysis took place in the 1970s. A notable discovery during this time was the observation of Fujishima and Honda that water could be photoelectrochemically split into H_2 and O_2 gases using a semiconductor TiO_2 as a photocatalyst [1,2].

Consequently, there was a tremendous increase in activities in the field of photocatalysis fueled by the energy crisis of the late 1970s. The promise of a future H_2 gas-based economy coupled with the discovery of dye-sensitized solar cells by Grätzel and coworkers continued to increase interest in photocatalysis. In addition, the exponential growth of heterogeneous photocatalysis studied was observed in the 1980s particularly on the TiO_2 [3]. Later, in 1996, the Nobel Prize in chemistry was awarded to Smalley, Kroto, and Curl for the discovery of fullerenes. Owing to this, there was an understanding that nanotechnology and nanoscience could have a significant impact on photoconversion processes [1,2,4,5].

2.2 Fundamentals of photocatalysis

Photocatalysis is a type of catalytic reaction that is influenced by light and a photocatalyst. It is a reaction that uses a suitable light to activate a photocatalyst which modifies the rate of a chemical reaction without being used up. Precisely, photocatalysis is a chemical reaction that takes place in the presence of a photocatalyst and suitable light. In other words, it is a reaction that uses light to generate

Theoretical Concepts of Photocatalysis. DOI: https://doi.org/10.1016/B978-0-323-95191-3.00008-0

a pair of excited electrons and positive holes to induce redox reactions, as the first step, with both positive and negative Gibbs-energy change.

An efficient photocatalyst is a conductive nanomaterial that absorbs incident light to bring itself up to higher energy states, which provides such energy to a reacting substance to make a chemical reaction happen. When used for thermodynamically uphill reactions such as photosynthesis, photocatalysis promises a sustainable solution to large-scale solar energy production, conversion, and storage [2,4,5]. Photocatalysis also promises a huge contribution to environmental remediation.

Photocatalysis is motivated by natural photosynthesis (please refer to Chapter 1). The fundamental processes driven by light are frequently mentioned as the "Z-scheme" as shown in Fig. 2.1.

The most important components are the two photosystems, i.e., photosynthesis I and photosynthesis II (PSI and PSII). Upon light irradiation, the chlorophyll in PSII absorbs photons with a maximum wavelength of 680 nm (P680) and transfers energy to PSI. The energy is then used to extract electrons from H_2O, producing O_2 through water oxidation catalysis (WOCs). The electrons are separated and transferred to PSI, where the chlorophyll absorbs photons with a maximum wavelength of 700 nm (P700). The energy of the newly absorbed photons further excites the electrons transferred from PSII, making them energetic enough to reduce nicotinamide adenine dinucleotide phosphate ($NADP^* \rightarrow NADPH$). Together with the proton gradient built during the process, NADPH drives the downstream transformations such as CO_2 to hydrocarbons by the Calvin cycle.

The most important principle of natural photosynthesis is the ability to drive chemical reactions using light energy. The concept of photocatalysis was traced back to Edmond Becquerel as early as 1839. Determined research on this topic did not gain mainstream attention until the late 1960s. Most recently, the research interest in photocatalysis benefited from the rising

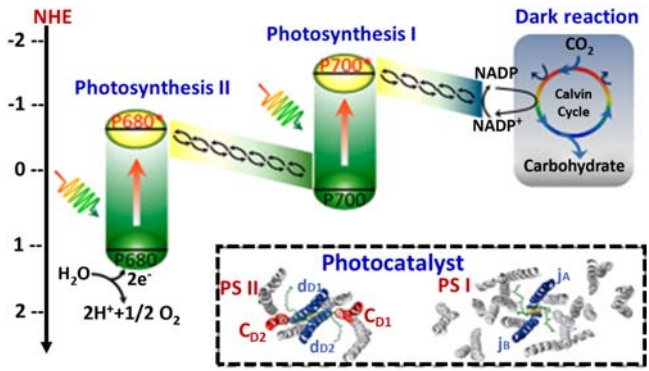

FIGURE 2.1 Z-scheme charge separation process of nature photosynthesis I and photosynthesis II (PS I and PS II) with protein photocatalysts. P680* and P700* stand for the excited states of chlorophyll P680 and P700, respectively; NADP is nicotinamide adenine dinucleotide phosphate reductase.

awareness of sustainability. One promising application of photocatalysis is to store solar energy directly in chemicals. Hence, the names solar fuels and artificial photosynthesis developed [1,2,4]. A few important examples of photocatalysis are listed below:

1. Bacteria and fungi are the main source for the decomposition of different types of building materials (such as wood, paints, curtains, and pipes) and also for many health-related artifacts. Photocatalysis using semiconductor nanomaterials can be effective in handling these problems, especially indoor environments and building applications. Both zinc oxide (ZnO) and titanium dioxide (TiO_2) can be used for antibacterial coatings, photocatalytic paints, photocatalytic tiles, etc. The antibacterial activity of ZnO nanoparticles (NPs) has received significant interest worldwide. ZnO is a metal oxide widely used in different types of nanomaterial applications. It is a promising direct wide band gap semiconductor with low cost and simple production through a variety of fabrication methods. As TiO_2 is a concern, adding it with a particle size of $\sim$21 nm to a bacterial colony is enough to destroy all bacteria within 2 h. The free radicals formed, i.e., hydroxyl radicals ($^{\bullet}OH$) and superoxide radicals ($O_2^{\bullet -}$) are the main factors responsible for the bactericidal capacity of photocatalysis that possesses a decomposition capacity of 1000−10,000 times which is more effective than the chemical disinfection of microorganisms such as bacteria.
2. Au−Cu_9S_5 NPs were also tested for contrast enhancement in computed tomography (CT) imaging, which is a widely used medical imaging technique for diagnosis due to its deep tissue penetration and high-resolution characteristics. High atomic number elements such as gold (Au) have shown excellent X-ray attenuation ability, which triggered research on using biocompatible Au NPs as contrast-enhancing agents for CT imaging.
3. Super-hydrophilic coatings are made of metal oxides, polymers, or mixtures. Metal oxide coatings are thermally stable over long term and are used in harsh environments. Super-hydrophilicity is created either by micro-nano-scale texture (nano wicking) or by functional (e.g., hydroxyl, OH^-) groups on the material surface. For example, the super-hydrophilicity of TiO_2 is attributed to its photochemical activity and amphiphilic surface. In fact, without ultraviolet (UV) radiation, TiO_2 surfaces lose their super-hydrophilicity quite rapidly. Similarly, silica is also super-hydrophilic at a high surface concentration of OH^- groups, especially for flame-made SiO_2.

2.2.1 Types of catalysis

2.2.1.1 Homogeneous catalysis

Homogenous catalysis is a type of catalysis in which the catalyst operates in the same phase as the reactants, usually dissolved in a suitable solvent.

Simply defined, it is when both the semiconductor (photocatalyst) and reactant are in the same phase (i.e., gas, solid, or liquid). Fig. 2.2 shows the schematic diagram of homogeneous catalysis. Mechanistic studies of homogenous catalysts are generally easier than those of heterogeneous catalysts, which help in optimization. Homogenous catalysts can be difficult to separate from the products, and thus, their recycling.

Homogenous catalysts based on complexes of low-valence transition metals favor the reactions of carbon monoxide and formate with molecular hydrogen, alkenes, alkynes, alcohol, amines, and organometallic compounds and the addition of hydrogen halides to unsaturated bonds. Examples of homogenous catalysis are listed below:

Example 1: Acid catalysis

The proton is a pervasive homogeneous catalyst because water is the most common solvent. Water forms protons through the process of self-ionization of water. In an illustrative case, acids accelerate (catalyze) the hydrolysis of esters:

$$CH_3CO_2CH_3 + H_2O \rightleftharpoons CH_3CO_2H + CH_3OH$$

Example 2: Lead chamber process

Oxides of nitrogen can also serve as catalysts for the oxidation of sulfur dioxide in the lead chamber process for producing sulfuric acid, an instance of homogeneous catalysis in which the catalyst and reactants are gases.

$$2SO_2(g) + O_2(g) \overset{NO}{\longleftrightarrow} 2SO_3$$

2.2.1.2 Heterogeneous catalysis

Heterogeneous catalysis is a type of catalysis in which the catalyst has a different phase than the reaction mixture. In other words, when both the semiconductor (photocatalyst) and reactant are in different phases. In general, heterogeneous catalysts are solids that are nanostructured materials because they have a high number of active sites (high surface area) to get a high catalytic activity. In heterogeneous catalysis, the reactants adsorb onto binding

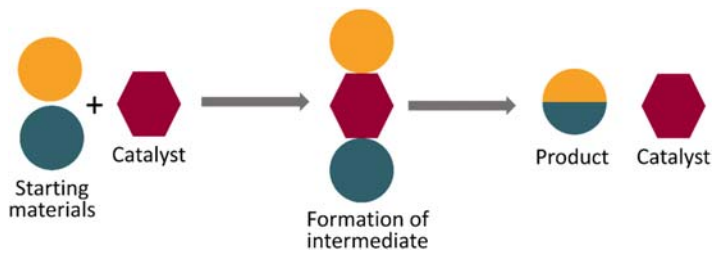

FIGURE 2.2 Schematic diagram of homogeneous catalysis.

sites on the surface of the catalyst as illustrated in Fig. 2.3, and the availability of these reaction sites can limit the rate of heterogeneous reactions.

Examples of heterogeneous catalysis are listed below:

Example 1: Oxidation of SO_2 to SO_3 in the presence of Pt metal as a catalyst in the contact process for the manufacture of sulfuric acid.

$$2SO_2(g) + O_2(g) \xrightarrow{Pt} 2SO_3$$

Example 2: Catalytic oxidation of ammonia.

$$NH_3 + O_2(g) \xrightarrow{Pt} NO + H_2O$$

In general, photocatalysis is a type of heterogeneous catalytic reaction that takes place in the presence of suitable light and photocatalysts [4–6].

2.2.2 Principles of photocatalysis

The term photocatalysis derives from two words: photo comes from the term photon and catalyst comes from a substance altering the reaction rate in its presence. By definition, photocatalysis is a process that takes place when a light source interacts with the surface of semiconductor materials, i.e., photocatalysts. During this process, there must be at least two simultaneous reactions that take place, i.e., oxidation from photogenerated holes and reduction from photogenerated electrons. The photocatalyst itself should not undergo any change and remain unused at the end of a reaction. Therefore, precise synchronization of the two processes needs to take place. Fig. 2.4 shows the different principles that govern light absorption and charge separation processes [1].

Where molecular photocatalysts (A) are concerned, the molecular orbital theory will be most suitable to describe the system, where the alignment of the highest occupied molecular orbital (HOMO) or the lowest unoccupied molecular orbital (LUMO) of the photocatalyst with the reactant molecular orbitals is most relevant. For semiconducting photocatalysts (B), the band theory is most suitable. When the size of the photocatalysts is minimized to

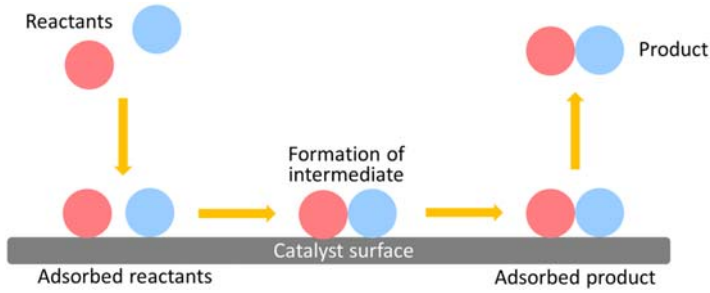

FIGURE 2.3 Schematic diagram of heterogeneous catalysis.

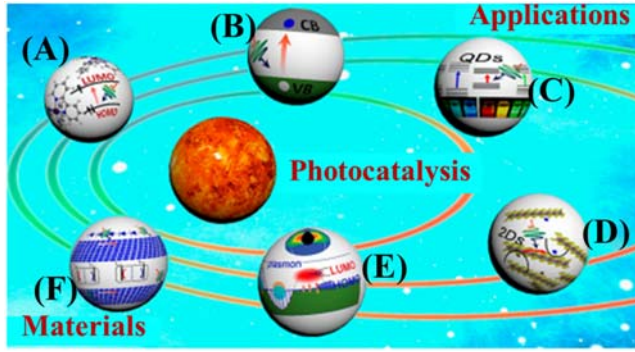

FIGURE 2.4 Schematic showing the classification of artificial photosynthesis: (A) molecular dye as a photocatalyst, (B) traditional semiconductor-based photocatalyst, (C) quantum-dots-based photocatalyst, (D) two-dimensional material-based photocatalyst, (E) plasmonic metal-based photocatalyst, (C−E) new emerging materials, and (F) traditional semiconductor-based photovoltaic power-driven electrocatalysis as "photocatalysts."

be comparable to the Bohr radii of excitons, the quantum effect becomes significant, where the optical and electrical behaviors are highly sensitive to the sizes. This is the situation where quantum dots (QDs) photocatalysts attract significant attention (C). When the size is small enough, even conductive materials (e.g., carbon dots <10 nm) could become semiconducting, opening up novel possibilities for using them as photocatalysts.

The use of conductive materials for photocatalysis, such as metals, has been applied as photocatalysts due to their plasmonic effects. Two-dimensional (2D) materials (e.g., ultrathin films, monolayers of black phosphorus, transition metal oxides, and dichalcogenides) are also explored as photocatalysts (D). The interest in this class of materials originates from their unique structures, which gives rise to the anisotropy required for charge separation for photocatalytic applications. Finally, the presence of photovoltaic in conjunction with catalysts, (E), is mainly meant to be inclusive, as this class of applications signifies efforts for the same purpose of using light-catalyzed chemical reactions that are difficult (e.g., pollutant degradation) or thermodynamically unfavored (e.g., photosynthesis). The advantage is clear—light absorption as well as charge separation. Hence, photocatalysis can be optimized alone on conventional semiconductor photovoltaic devices [1,2,4−7].

2.2.3 Mechanisms of the photocatalytic process

It has been well proven that the photocatalytic process initiates when photons of energy higher or equal to the band gap energy (E_g) are absorbed by a semiconductor particle. An electron ($\bar{e}$) from the valence band (VB) is transferred to the conduction band (CB) creating a hole (h^+) in the VB. Therefore, the hole acts as a charge carrier with a $+$ve charge. The number of holes in the

VB per unit volume is called "hole concentration." Similarly, the number of electrons in the CB per unit volume is called "electron concentration." The absorption of these photons creates within the bulk electron-hole pairs, which dissociate into free photoelectrons in the CB and holes in the VB.

Several fundamental mechanistic processes have been described in the photocatalytic degradation of organic pollutants over TiO_2 surfaces. For example, TiO_2 absorbs a photon of energy equal to or greater than its band gap energy (E_g), an electron ($\bar{e}$) will be promoted from the VB to the CB leaving behind an electron vacancy or "hole" (h^+) in the VB as shown in Fig. 2.5. The $\bar{e}$ and h^+ can recombine on the surface or in the bulk of the particle releasing the energy as heat or migrating to the surface where they can react with adsorbed molecules (mainly H_2O or reactants) on the surface of the particle as illustrated in Fig. 2.5.

These oxidative reactions would result in the direct absorption of light by the dye (organic pollutants), which can further lead to charge injection from the excited state of the dye to the CB of the semiconductor as summarized by the following equations:

$$\mathrm{Dye_{ads} + h^+ \rightarrow Dye_{ads}},$$

$$\mathrm{Dye_{ads} + TiO_2 \rightarrow Dye_{ads}^+ + TiO_2^{\bullet}(\bar{e})},$$

$$\mathrm{Dye + {}^{\bullet}OH \rightarrow degraded\ products},$$

$$\mathrm{Dye + h_{VB}^+ \rightarrow oxidized\ products},$$

$$\mathrm{Dye + \bar{e}_{CB} \rightarrow reduced\ products}.$$

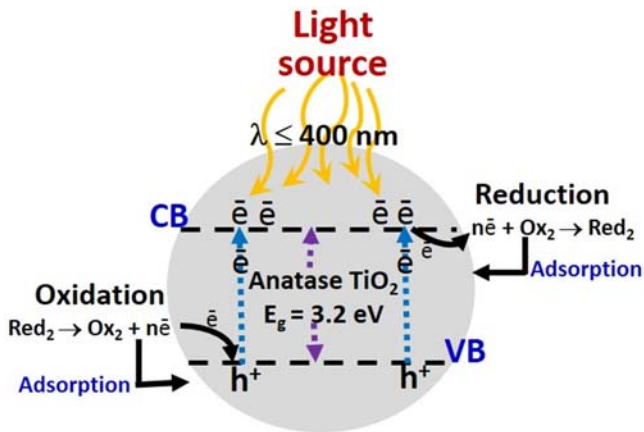

FIGURE 2.5 Schematic representation of the electron transfer reactions on anatase TiO_2 nanoparticles.

In summary, the efficiency of a photocatalyst depends on its light-harvesting ability, competition of different interface charge transfer processes involving electrons and holes, and decrease in $\bar{e}-h^+$ recombination [6].

2.3 Effect of photocatalyst type, size, surface area, morphology, dose, light intensity, time, temperature, etc. on photocatalysis

Photocatalysts are of different types and photocatalytic reactions depend on several parameters. The parameters such as catalyst type, size, morphology, dose, light intensity, time, and temperature play an important role in photocatalysis in deciding the fate of the reaction. The extent of photocatalysis is influenced by several factors (Fig. 2.6), be it related to the semiconductor itself or the surrounding environment of the photocatalyst. For example, photocatalytic degradation of the pollutants depends on the size and surface of the photocatalysts. Any change in the characteristics of the parameter can alter the photocatalytic activities of the photocatalyst which are discussed below [5–14].

2.3.1 Effect of the type of photocatalysts on photocatalysis

There are different types of photocatalysts such as metal oxides (TiO_2, ZnO, SnO_2, CeO_2, etc.) and chalcogenides (CdS, ZnS, CdSe, MoS_2, etc.) [6]. Both semiconductor photocatalysts possess different properties and one of them is their band gap energy and band edge position. TiO_2 has a band gap energy of $\sim$3.2 eV whereas CdS has a band gap energy of $\sim$2.4 eV. Both respond differently if applied under UV and visible light irradiation in which TiO_2 is active under UV light whereas CdS is active under visible light.

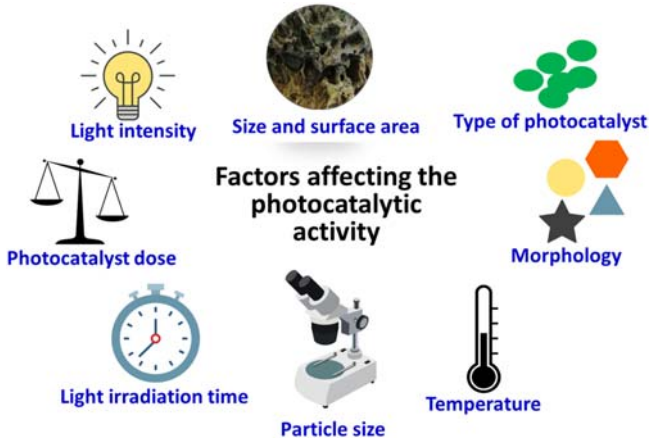

FIGURE 2.6 Factors affecting photocatalytic activities of nanomaterials.

In detail, heterogeneous photocatalysts (e.g., TiO_2 and ZnO) appear to be the most promising materials for organic dye degradation. However, one of the major drawbacks of using TiO_2 as a catalyst is the low photo-quantum efficiency which arises from the fast recombination of the photogenerated electrons and holes. Moreover, TiO_2 is inactive under visible light due to its wide band gap energy. This inherently causes the inability to make use of the vast potential of solar photocatalysis. Various techniques have been used to make TiO_2 absorb photons of lower energy as well. These techniques include surface modification via organic materials, semiconductor coupling, creating defects, band gap modification by creating oxygen vacancies, and oxygen sub-stoichiometry, by metal doping, non-metals doping, co-doping with non-metals, and metals. Dopants, such as transition metals, have been added to the TiO_2 catalyst to improve its response and also reduce the recombination of photogenerated electrons and photogenerated holes. The main aim of doping is to reduce the band gap and introduction of intra-band gap states which results in more visible light harvesting [7].

2.3.2 Effect of size and surface area of the photocatalyst on photocatalysis

Generally, in catalysis, the size and surface area of the catalysts play a crucial role in determining the rate of a reaction. Similarly, in photocatalytic reactions, the small size and high surface area of NPs are important characteristic properties of photocatalysts to achieve high performance. By increasing the surface area of the photocatalyst, there will be more active sites for photocatalytic reactions. It is because of its high surface area to volume ratio. In this way, photocatalysts with a small size and high surface area show more photocatalytic reactivity compared to bulk materials.

In heterogeneous catalysis, crystal size is of primary importance because it is directly related to its specific surface area which improves the efficiency of a catalyst. A study done by Li et al. proved that the enhancement of photocatalytic activity was due to the high surface area, special twist-like helix morphology, large pore size, and better crystallinity of the anatase TiO_2 [8]. In another study, copper sulfide (CuS) was used for methylene blue (MB) degradation because it is nontoxic, inexpensive, and stable under ambient conditions. It has an efficient catalytic ability because of its high surface area to volume ratio allowing for better contact between the reactants and CuS [4].

Furthermore, Adhikari et al. reported similar behavior. A smaller particle size exhibits higher 4-nitroaniline reduction which may be due to the high density of active sites as the surface area increases. The photogenerated carriers in smaller particles are also likely to transfer more quickly to the sample surface without recombination [15].

2.3.3 Effect of the morphology of the photocatalyst on photocatalysis

The photocatalytic activity of the samples tested with methyl orange (MO) was strongly influenced by its corresponding morphology. It was found that the efficiency of the spherical ZnO morphology is much better than the flower-like ZnO, due to its higher specific surface area and pore volume rather than the flower-like nanostructure. Therefore, adsorption of pollutants is likely to occur faster on ZnO with spherical morphology and in this case, the rate of oxidation and reduction is greater than the ZnO with flower-like morphology. It was found that the performance of the spherical ZnO nanostructure was better than that of the flower-like nanostructure.

Zu et al. prepared prism-shaped active faceted rutile Ti(III)-doped TiO_2 with the control of the morphology under acidic conditions and hydrothermal treatment at 200°C for 12 h [9]. They proved that the facet effect is an important factor for heterogeneous photocatalysts due to the surface atom arrangement and coordination which intrinsically determine the reactant adsorption on the surface of photocatalyst, surface distribution between photoexcited electrons and reactant molecules, as well as the desorption of product molecules.

Moreover, SnO_2 NPs also performed better than SnO_2 nanowedges and nanospheres due to the number of surface defects available to the high surface area material as reported by Kar et al. [16].

2.3.4 Effect of the photocatalyst dose on photocatalysis

The photocatalyst dose or loading for photoactivity in the reaction is one of the important parameters that control the rate of reaction. It has been generally found that photoactivity increases with an increase in the dose of the catalyst.

The increased dose or loading contributes to the high activity because of the presence of more active catalyst sites at higher concentrations, which help in the formation of more free radicals such as hydroxyl radicals ($^{\bullet}OH$) and superoxide radicals ($O_2^{\bullet -}$). Furthermore, when the catalytic dose is increased above the optimum value, no substantial increase in the photoactivity is observed. This is due to the reason that the increased amounts of catalyst particles in the solution make it turbid, and thus, block and scatter the light for the reaction to proceed. Therefore, the percentage degradation of the pollutant starts decreasing. At high concentrations of photocatalysts, the chances for particle agglomeration increase, which results in a decrease in the available surface area for light absorption. Hence, this reduces the generation of photoexcited electrons and holes which affects the photocatalytic activity, and the rate of reaction drops significantly [10].

Elaziouti et al. reported the effect of the amount of catalyst (m/v) on photocatalytic degradation of dyes over a range of catalyst amounts from 0.25 to 3 g/L. The degradation rate of Congo red (CR) increased from

68.73% to 95.02% in the case of CR and from 46.29% to 97.24% in the case of benzopurpurine (BP4B) when the ZnO amount was increased from 0.25 to 0.5 g/L for CR and from 0.25 to 1 g/L for BP4B, respectively. This increase in the photocatalytic degradation rate with the photocatalyst amount can be explained in terms of the availability of active sites on the catalyst surface and the penetration of UV light into the suspension as a result of the increased screening effect and scattering of light [11].

On the other hand, the opposite observation was reported by Alkaykh et al. [17]. The percentage of MB degradation was decreased when the amount of $MnTiO_3/TiO_2$ (photocatalyst) was increased (0.005−0.04 g). This can be explained in terms of active site availability (as mentioned above) and the light penetration of photo-activating light into the system. Moreover, at a higher catalyst dosage, the rate of reaction may be reduced due to the deactivation of activated molecules by collision with ground state catalysts.

2.3.5 Effect of light intensity on photocatalysis

Generally, light intensity too affects photocatalytic reactions. It has been shown that at low light intensities (0−20 mW/cm^2), the rate would decrease linearly with the increasing light intensity (first-order), whereas at intermediate light intensities ($\sim$25 mW/cm^2), the rate would depend on the square root of the light intensity. At high light intensities, the rate is independent of light intensity, because at a low light intensity, reactions involving electron-hole formation are predominant and electron-hole ($\bar{e}-h^+$) recombination is negligible. On the other hand, when light intensity is increased, the electron-hole pair separation competes with recombination, thereby, causing a lower effect on the reaction rate [7].

Elaziouti et al. reported that the intensity of the light irradiated is an important parameter influencing the degradation of organic pollutants by photocatalytic activity. The effect of light intensity on the rate of photocatalytic degradation of dyes was investigated by varying the light intensity of UV-A between 50 and 90 J/cm^2. The degradation efficiency of benzopurpurine (BP4B) increased linearly with the light intensity, whereas that of CR increased up to 70 J/cm^2 and after that no changes were observed. The linear increase of the degradation efficiency for CR and BP4B at a light intensity, ranging from 50 to 70 J/cm^2 and 50 to 90 J/cm^2 for CR and BP4B, respectively, was assigned to more photons that would be available for excitation at the semiconductor surface, and in turn, more electron-hole pairs had generated. Thus, this resulted in an enhanced rate of photocatalytic degradation of CR and BP4B [11]. Moreover, Sujatha et al. have studied the effect of varying the output of UV lamp power from 16 to 64 W on the degradation of coffee using TiO_2 as a photocatalyst [18]. It was observed that the photocatalytic degradation performance of TiO_2 increases with an increase in the light irradiation due to the generation of more electrons and holes.

In other words, low light intensity produces low energy to excite electron-hole pairs. Consequently, the production of radicals ($^{\bullet}OH$, $O_2^{\bullet-}$, etc.) is also limited leading to low efficiency of photocatalytic degradation. On the contrary, when the light intensity is high, more electron-hole pairs are generated by a photocatalyst. Following that, free radicals production are more which results in high efficiency of photocatalytic degradation [19].

2.3.6 Effect of light irradiation time on photocatalysis

Usually, light irradiation time also influences photocatalytic reactions. In general, in the case of photocatalytic organic pollutant degradation, the duration of irradiation time is directly proportional to the percentage of organic pollutant degradation. As the time increases, the degradation percentage also increases until it reaches an optimum value.

This can be explained by the formation of more free radicals such as hydroxyl radicals ($^{\bullet}OH$) and superoxide radicals ($O_2^{\bullet-}$). By definition, the irradiation time of the photocatalytic degradation process is the duration of interaction between the photocatalyst and the absorbed or harvested rays to produce free radicals, and the interaction between the free radicals and the substrate of organic compounds. Free radicals are strong oxidizing agents that are used in degrading organic pollutants. The more free radicals are formed, the greater the percentage of photocatalytic degradation of organic pollutants [20].

For example, Shaban et al. reported the evaluation of photocatalytic properties of TiO_2 nanoribbons (NRs) and TiO_2 NRs/CNTs nanocomposite through their efficiency in the degradation of MB dye under sunlight. The photocatalytic degradation tests were performed at different dye concentrations within a time ranging from 30 to 300 min. The degradation of dye using only 0.02 g TiO_2 NRs shows an increase in the degradation efficiency from about 51% to about 97.5% with increasing the irradiation time from 30 to 300 min at an initial dye concentration of 5 mg/L [12]. In another study, Zhou et al. varied the irradiation time of visible light from 0 to 8 min and WO_3/Ag_2CO_3 exhibited the highest degradation of rhodamine B about 99.7% within 8 min [21].

2.3.7 Effect of temperature on photocatalysis

The temperature effect is not substantial if the reaction under observation has a small temperature variation. However, if the temperature will be excessively higher or lower, it might change the course of the photocatalytic degradation reaction rate. Dissolved oxygen is one of the key elements that drive photocatalysis, as it helps in scavenging CB electrons that leads to the formation of hydroxyl radicals. The higher or lower temperature causes the change in the percentage of the dissolved oxygen in the samples, and hence, changes the

rate of the photocatalytic reaction. Furthermore, higher temperatures cause the desorption of organic compounds from the photocatalyst surface. This also affects the overall photocatalytic efficiency of the reaction [10].

The effect of temperature is related to the interactions between the photocatalysts and the pollutants in terms of kinetic and thermodynamic studies. Decreasing or increasing the temperature to extremes would reduce the photocatalytic activity of the photocatalytic materials.

For example, Hu et al. proposed that the rate constant increases greatly over a temperature range of 38°C−100°C. The photocatalytic reactions at the temperature of 38°C−100°C all followed the pseudo-first-order rate law, and the temperature has a great effect on the reaction rate [22]. In addition, another study by Chen et al. reported that the temperature range between 50°C and 80°C is regarded as the ideal temperature for effective photocatalytic degradation of organic matter. It was found that the recombination of charge carriers will increase if the temperature is beyond 70°C, and thus, the photocatalysis activity will decrease [23]. Moreover, Azad et al. reported that the photocatalytic degradation performance of Ca/La@TiO_2 increased about two to three times if the temperature increased from 30°C to 40°C. At 40°C, about 88% photocatalytic degradation of MO was observed, while at 30°C, only 76% was observed [24].

2.3.8 Effect of pollutant's concentration and type on photocatalysis

Generally, pollutants type and concentration also affect photocatalytic reactions. This could be another main factor to determine the photocatalytic degradation rate of the pollutants. Table 2.1 shows the different types of pollutants used in photocatalysis. Many researchers have reported photocatalytic activity under similar operating conditions and using similar catalysts, but the variation in the initial concentration of pollutants results in different irradiation times necessary to achieve complete mineralization [7]. This shows that the irradiation time and pollutant's concentration and type play important roles in photocatalysis

For example, Alkaykh et al. reported on the effect of the MB concentration which varied from 2×10^{-6} M to 1.5×10^{-5} M in the presence of 0.005 g of the photocatalyst. It was found that at a lower concentration of the MB dye, the removal efficiency of the dye increases. This is because the adsorption capacity is higher at lower concentrations because of the higher availability of more active sites for MB molecules to be adsorbed on the surface of the photocatalyst [17].

Similarly, pollutant types also play a very important role in photocatalysis. For example, all the dyes (organic pollutants) are not the same. Some of the dyes are cationic dyes and some are anionic dyes. At the same time, these dyes have different functional groups and molecular masses. That

TABLE 2.1 Different photocatalysts used to remove various types of pollutants using photocatalysis.

Photocatalyst	Model pollutant	Type of pollutant	Performance	References
Ag@graphene	Congo red dye	Anionic diazo dye	90% of Congo red was degraded after 5 h under visible light irradiation	[25]
ZnO	Rose Bengal dye	Anionic dye	ZnO exhibited an excellent photocatalytic degradation efficiency >80% within 1 h	[26]
MoS_2	Crystal violet	Cationic dye	Degraded about 92% crystal violet within 50 min	[27]
Chitosan/Ce doped ZnO composites	Malachite green	Cationic dye	About 87% degradation of malachite green	[28]
MoS_2	Rhodamine B	Cationic dye	Rhodamine B dye is degraded by 39.9% and 67.4% respectively for ordinary and concentrated sunlight irradiation within 120 min	[29]
Co/Ni-doped Cu_2MoS_4	Rhodamine B	Cationic dye	93.5% degraded within 1 h	[30]
MoS_2	Methylene blue	Cationic dye	Complete degradation of methylene blue is achieved in 20 under sunlight	[31]
Ag@TiO_2	Methyl orange	Anionic dye	Degraded 98.9% within 60 min under UV, and 99.3% within 80 min under solar irradiation	[32]
Cu-doped ZnO	Methyl orange	Anionic dye	99% of methyl orange degradation was obtained after 120 min of solar exposure	[33]

makes them interact with the photocatalyst differently. Hence, these dyes show different photocatalytic degradation rates even with the same photocatalyst. For instance, eosin yellow (anionic dye) was easily decolorized and mineralized using TiO_2 under UV light irradiation than malachite green oxalate (cationic dye). This indicates that the type of dye, its ionic character, and its molecular formula may be determining factors influencing the degradation [34].

2.4 Characteristics of good photocatalysts

The efficiency of a photocatalytic reaction depends on several parameters, characteristics, conditions, etc. of a photocatalyst. Based on the above discussion, a good photocatalyst should have the following characteristics [2,4,13,14]:

1. Appropriate electronic band structure and band gap energy: The range of energy levels that contain electrons within as well as the ranges of energy that they may not have (band gap).
2. Precise band edge positions that overlap with the water redox potentials.
3. Efficient light absorption or light-harvesting ability: To be able to excite electrons to the VB.
4. Capable of generating charge carriers when stimulated with the required amount of light energy. In other words, smaller band gap materials are more appropriate.
5. Favorable charge transport characteristics and high charge carrier mobility.
6. Promising excited lifetimes of the photocatalyst.
7. Should not be susceptible to photo corrosion: This will cause the deactivation of a photocatalyst over time.
8. Chemically stable in a variety of conditions: Highly stable without changing the properties of a photocatalyst when various conditions are applied.
9. Commercially available.
10. Reusable: Easily recover and reuse with no considerable decrease in photocatalytic activity.
11. Nontoxic: Environmentally safe to use and nontoxic to humans.

2.5 Summary

This chapter mainly discusses the fundamentals of semiconductor-based heterogeneous photocatalysis. It also focuses on the basic concepts involved, such as the theory and background necessary to understand the heterogeneous photocatalysis of metal oxides and chalcogenides. This chapter also

includes a discussion on the principles of semiconductor-based photocatalysis, thermodynamics, and kinetic aspects, which regulate photocatalytic performance. The efficiency of photocatalysis is affected by various parameters. Therefore, a good photocatalyst must possess certain characteristics such as appropriate size, morphology, high surface area, excellent light-harvesting properties, dose, light intensity, time, and temperature. Finally, the characteristics of good photocatalysts have been discussed.

References

[1] X. Yang, D. Wang, Photocatalysis: from fundamental principles to materials and applications, ACS Applied Energy Materials 1 (2018) 6657−6693. Available from: https://doi.org/10.1021/acsaem.8b01345.

[2] M.M. Khan, Principles and mechanisms of photocatalysis, Photocatalytic Systems by Design, Elsevier, 2021, pp. 1−22. Available from: https://doi.org/10.1016/B978-0-12-820532-7.00008-4.

[3] N. Serpone, A.v Emeline, Semiconductor photocatalysis − past, present, and future outlook, Journal of Physical Chemistry Letters 3 (2012) 673−677. Available from: https://doi.org/10.1021/jz300071j.

[4] M.M. Khan, Chalcogenide-Based Nanomaterials as Photocatalysts, first ed., Elsevier, 2021. Available from: https://doi.org/10.1016/C2019-0-01819-5.

[5] A. Hernández-Ramírez, I. Medina-Ramírez, Photocatalytic Semiconductors: Synthesis, Characterization, and Environmental Applications, Springer International Publishing, Cham, 2015. Available from: https://doi.org/10.1007/978-3-319-10999-2.

[6] M.M. Khan, D. Pradhan, Y. Sohn, Nanocomposites for Visible Light-Induced Photocatalysis, Springer International Publishing, Cham, 2017. Available from: https://doi.org/10.1007/978-3-319-62446-4.

[7] A. Kumar, A review on the factors affecting the photocatalytic degradation of hazardous materials, Material Science & Engineering International Journal 1 (2017) 106−114. Available from: https://doi.org/10.15406/mseij.2017.01.00018.

[8] J. Li, J. Xu, W.L. Dai, H. Li, K. Fan, One-pot synthesis of twist-like helix tungsten-nitrogen-codoped titania photocatalysts with highly improved visible light activity in the abatement of phenol, Applied Catalysis B: Environmental 82 (2008) 233−243. Available from: https://doi.org/10.1016/j.apcatb.2008.01.022.

[9] F. Zuo, K. Bozhilov, R.J. Dillon, L. Wang, P. Smith, X. Zhao, et al., Active facets on titanium(III)-doped TiO_2: an effective strategy to improve the visible-light photocatalytic activity, Angewandte Chemie − International Edition 51 (2012) 6223−6226. Available from: https://doi.org/10.1002/anie.201202191.

[10] J. Zhang, B. Tian, L. Wang, M. Xing, J. Lei, Photocatalysis: Fundamentals, Materials and Applications, 1st ed., Springer, 2018. Available from: https://doi.org/10.1007/978-981-13-2113-9.

[11] Elaziouti, N. Laouedj, B. Ahmed, ZnO-assisted photocatalytic degradation of congo red and benzopurpurine 4B in aqueous solution, Journal of Chemical Engineering & Process Technology 02 (2011). Available from: https://doi.org/10.4172/2157-7048.1000106.

[12] M. Shaban, A.M. Ashraf, M.R. Abukhadra, TiO_2 nanoribbons/carbon nanotubes composite with enhanced photocatalytic activity; fabrication, characterization, and application, Scientific Reports 8 (2018) 781. Available from: https://doi.org/10.1038/s41598-018-19172-w.

[13] M.M. Khan, S.F. Adil, A. Al-Mayouf, Metal oxides as photocatalysts, Journal of Saudi Chemical Society 19 (2015) 462–464. Available from: https://doi.org/10.1016/j.jscs.2015.04.003.

[14] M.M. Khan, Metal Oxide Powder Photocatalysts, Elsevier Ltd., 2018, pp. 5–18. Available from: https://doi.org/10.1016/B978-0-08-101977-1.00002-8.

[15] S.P. Adhikari, A. Lachgar, Effect of particle size on the photocatalytic activity of $BiNbO_4$ under visible light irradiation, Journal of Physics: Conference Series, Institute of Physics Publishing (2016). Available from: https://doi.org/10.1088/1742-6596/758/1/012017.

[16] A. Kar, J. Olszówka, S. Sain, S.R.I. Sloman, O. Montes, A. Fernández, et al., Morphological effects on the photocatalytic properties of SnO_2 nanostructures, Journal of Alloys and Compounds 810 (2019) 151718. Available from: https://doi.org/10.1016/j.jallcom.2019.151718.

[17] S. Alkaykh, A. Mbarek, E.E. Ali-Shattle, Photocatalytic degradation of methylene blue dye in aqueous solution by $MnTiO_3$ nanoparticles under sunlight irradiation, Heliyon 6 (2020) e03663. Available from: https://doi.org/10.1016/j.heliyon.2020.e03663.

[18] G. Sujatha, S. Shanthakumar, F. Chiampo, UV light-irradiated photocatalytic degradation of coffee processing wastewater using TiO_2 as a catalyst, Environments 7 (2020) 47. Available from: https://doi.org/10.3390/environments7060047.

[19] G. Jia, G. Wang, Y. Zhang, L. Zhang, Effects of light intensity and H_2O_2 on photocatalytic degradation of phenol in wastewater using TiO_2/ACF, in: Proceedings – 2010 International Conference on Digital Manufacturing and Automation, ICDMA 2010, 2010, pp. 623–626. https://doi.org/10.1109/ICDMA.2010.431.

[20] S. Wardhani, D. Purwonugroho, C.W. Fitri, Y.P. Prananto, Effect of pH and irradiation time on TiO_2-chitosan activity for phenol photo-degradation, in: AIP Conference Proceedings, American Institute of Physics Inc., 2018. https://doi.org/10.1063/1.5062759.

[21] M. Zhou, X. Tian, H. Yu, Z. Wang, C. Ren, L. Zhou, et al., WO_3/Ag_2CO_3 mixed photocatalyst with enhanced photocatalytic activity for organic dye degradation, ACS Omega 6 (2021) 26439–26453. Available from: https://doi.org/10.1021/acsomega.1c03694.

[22] Q. Hu, B. Liu, Z. Zhang, M. Song, X. Zhao, Temperature effect on the photocatalytic degradation of methyl orange under UV-vis light irradiation, Journal Wuhan University of Technology, Materials Science Edition 25 (2010) 210–213. Available from: https://doi.org/10.1007/s11595-010-2210-5.

[23] Y.W. Chen, Y.H. Hsu, Effects of reaction temperature on the photocatalytic activity of TiO_2 with Pd and Cu cocatalysts, Catalysts 11 (2021). Available from: https://doi.org/10.3390/catal11080966.

[24] K. Azad, P. Gajanan, Photodegradation of methyl orange in aqueous solution by the visible light active Co:La:TiO_2 nanocomposite, Chemical Sciences Journal 08 (2017). Available from: https://doi.org/10.4172/2150-3494.1000164.

[25] M.E. Khan, M.M. Khan, M.H. Cho, Biogenic synthesis of a Ag–graphene nanocomposite with efficient photocatalytic degradation, electrical conductivity and photoelectrochemical performance, New Journal of Chemistry 39 (2015) 8121–8129. Available from: https://doi.org/10.1039/C5NJ01320H.

[26] C. Vidya, M.N.C. Prabha, M.A.L.A. Raj, Green mediated synthesis of zinc oxide nanoparticles for the photocatalytic degradation of Rose Bengal dye, Environmental Nanotechnology, Monitoring and Management 6 (2016) 134–138. Available from: https://doi.org/10.1016/j.enmm.2016.09.004.

[27] P. Sharma, M.K. Singh, M.S. Mehata, Sunlight-driven MoS_2 nanosheets mediated degradation of dye (crystal violet) for wastewater treatment, Journal of Molecular Structure 1249 (2022) 131651. Available from: https://doi.org/10.1016/j.molstruc.2021.131651.

[28] A.M. Saad, M.R. Abukhadra, S. Abdel-Kader Ahmed, A.M. Elzanaty, A.H. Mady, M.A. Betiha, et al., Photocatalytic degradation of malachite green dye using chitosan supported ZnO and Ce−ZnO nano-flowers under visible light, Journal of Environmental Management 258 (2020) 110043. Available from: https://doi.org/10.1016/j.jenvman.2019.110043.

[29] J.S. Roy, G. Dugas, S. Morency, Y. Messaddeq, Rapid degradation of Rhodamine B using enhanced photocatalytic activity of MoS_2 nanoflowers under concentrated sunlight irradiation, Physica E: Low-Dimensional Systems and Nanostructures 120 (2020) 114114. Available from: https://doi.org/10.1016/j.physe.2020.114114.

[30] J. Ma, F. Zhu, P. Ji, Q. Zou, H. Wang, G. Xu, Enhanced visible-light photocatalytic performance of Co/Ni doped Cu_2MoS_4 nanosheets for Rhodamine B and erythromycin degradation, Journal of Alloys and Compounds 863 (2021) 158612. Available from: https://doi.org/10.1016/j.jallcom.2021.158612.

[31] H.K. Sadhanala, S. Senapati, K.V. Harika, K.K. Nanda, A. Gedanken, Green synthesis of MoS_2 nanoflowers for efficient degradation of methylene blue and crystal violet dyes under natural sun light conditions, New Journal of Chemistry 42 (2018) 14318−14324. Available from: https://doi.org/10.1039/C8NJ01731J.

[32] R. Saravanan, D. Manoj, J. Qin, Mu Naushad, F. Gracia, A.F. Lee, et al., Mechanothermal synthesis of Ag/TiO_2 for photocatalytic methyl orange degradation and hydrogen production, Process Safety and Environmental Protection 120 (2018) 339−347. Available from: https://doi.org/10.1016/j.psep.2018.09.015.

[33] P.M. Perillo, M.N. Atia, Solar-assisted photodegradation of methyl orange using Cu-doped ZnO nanorods, Materials Today Communications 17 (2018) 252−258. Available from: https://doi.org/10.1016/j.mtcomm.2018.09.010.

[34] N. Laid, N. Bouanimba, R. Zouaghi, T. Sehili, Comparative study on photocatalytic decolorization of an anionic and a cationic dye using different TiO_2 photocatalysts, Desalination and Water Treatment 57 (2016) 19357−19373. Available from: https://doi.org/10.1080/19443994.2015.1099470.

Chapter 3

Semiconductors as photocatalysts: UV light active materials

Mohammad Mansoob Khan

3.1 Introduction

A semiconductor is defined as a material with electrical resistivity lying in the range of $10^{-2}-10^{9}$ Ω/cm. It can also be defined as a material whose energy gap is between 0 and about 4 eV for electronic excitations [1]. It has been considered that wide band gap metal oxides such as titanium oxide (TiO_2), zinc oxide (ZnO), cerium oxide (CeO_2), and tin oxide (SnO_2) can photocatalytically degrade a variety of organic pollutants under ultraviolet (UV) light irradiation [2–17]. Nano and/or mesoporous materials such as metal oxides, chalcogenides, and nanocomposites have been synthesized by several methods and their applications have been thoroughly investigated [18–20]. The absorption of UV light by wide band gap semiconductors results in the formation of electrons ($\bar{e}$) and holes (h^+) during a process of electronic excitation from the valence band (VB) to the conduction band (CB). These photogenerated charge carriers ($\bar{e}$ and h^+) can migrate to the surface of the semiconductors and participating in redox reactions with adsorbed molecules. For practical applications, it is necessary to develop novel catalysts that can function effectively under UV light. ZnO is one of the promising functional materials, being appropriate for many superior applications such as field-effect transistors, lasers, photodiodes, chemical and biological sensors, and solar cells [18,19,21]. ZnO was found to be more efficient than TiO_2 for the treatment of effluents from the paper industry as well as for photocatalytic dye degradation [4,18].

Additionally, zinc sulfide (ZnS) is one of the main II − VI semiconductor materials, also known as chalcogenides, which has two phases, (1) a cubic form (c-ZnS) with a sphalerite structure and (2) a hexagonal form (h-ZnS) equivalent to wurtzite [20]. These two forms have wide band gaps of 3.7 and 3.8 eV, respectively. ZnS has also been a focus of interest for several applications, such as photocatalysis, photoconductors, optical sensors, and electroluminescent materials.

Theoretical Concepts of Photocatalysis. DOI: https://doi.org/10.1016/B978-0-323-95191-3.00004-3

The band gap energy of ZnS is larger than the ZnO (3.2 eV). Theoretical calculations confirmed that the mixture of these two semiconductors could yield a novel composite with a photoexcitation threshold energy less than those of the individual components [22,23]. Therefore, this chapter will mainly cover the fundamentals of UV light active semiconductor photocatalysts and related recent developments.

3.2 Fundamentals of semiconductors

A semiconductor is a material that is an insulator at a very low temperature (absolute zero, i.e., 0K or −273.15°C) but has a substantial electrical conductivity at room temperature. It is a substance, usually a solid chemical in element or compound form, which can conduct electricity under some conditions, making it a good medium for the control of electrical current. The distinction between a semiconductor and an insulator is not very well-defined. However, a semiconductor is a material with a band gap small enough that its CB is appreciably thermally populated at room temperature [24,25].

In other words, semiconductors are solid materials whose conductivity lies between the conductivity of conductors and insulators. Unlike metals, the conductivity of semiconductors increases with increasing temperature which leads to bond breaking and the formation of free electrons. At the location at which the electron was displaced, a so-called defect electron, i.e., "hole" is formed. For example, silicon (Si) as a semiconductor in which:

1. An electron breaks free from a Si atom (e.g., due to an energy supply such as heat) and acts as a free negative charge carrier.
2. After the electron has moved, a positively charged hole forms and remains in the atom.
3. Another nearby electron can recombine with this hole. Thus, a new hole is generated.
4. In addition to free electrons, which are negative charge carriers, these holes can move in the lattice and act as positive charge carriers.

3.3 Semiconductors as photocatalysts

As mentioned earlier in this chapter, a semiconductor is a solid substance that has a conductivity between insulators and conductors such as glass and metals, respectively. Si and germanium (Ge) are examples of elemental semiconductors. They are considered the best-known semiconductors. There are many semiconductors besides Si and Ge which include minerals such as zinc-blende (ZnS), cuprite (Cu_2O), and galena (PbS). Materials with zero band gap energy are considered metals (conductors). A metal has a partially filled CB and there is no energy gap between filled and unfilled regions. Semiconductors have a considerable band gap energy (E_g) between the VB and the CB. In semiconductors, a

significant number of electrons can be excited by heat into empty energy levels (CB) and move easily throughout the material, allowing the material to conduct electricity. On the other hand, insulators are materials with large E_g. An insulator possesses a considerable wide energy gap between the VB and the CB. It is difficult to excite electrons from the VB to the CB in insulators. As a result, an insulator does not conduct electricity (Fig. 3.1).

Electrical properties can be indicated by resistivity. Conductors such as gold (Au), silver (Ag), and copper (Cu) have low resistance, thus, conducting electricity easily. Insulators such as rubber, glass, and ceramics have high resistance and are difficult to conduct electricity. Semiconductors have properties somewhere between conductors and insulators. Their resistivity might change according to the temperature. For example, at a low temperature, almost no electricity passes through these materials. However, when the temperature increases, electricity passes through these materials easily. Semiconductors containing almost no impurities conduct almost no electricity. But when some elements such as impurities and/or dopants are incorporated into the semiconductors, electricity starts passing through these modified semiconductors easily.

Some examples of semiconductors are Si, Ge, gallium arsenide (GaAs), and elements near the so-called "metalloid staircase" in the periodic table. After Si, GaAs is the second most common semiconductor that is used in laser diodes, solar cells, microwave frequency integrated circuits, etc. Si is a critical element that is used for fabricating most electronic circuits. Semiconductors are broadly divided into two types:

1. Intrinsic semiconductor
2. Extrinsic semiconductor

3.3.1 Intrinsic and extrinsic semiconductors

Semiconductors can be categorized into two types. Based on its purity and impurity, it can be intrinsic semiconductors or extrinsic semiconductors (Table 3.1). Briefly, intrinsic semiconductors are composed of only one kind

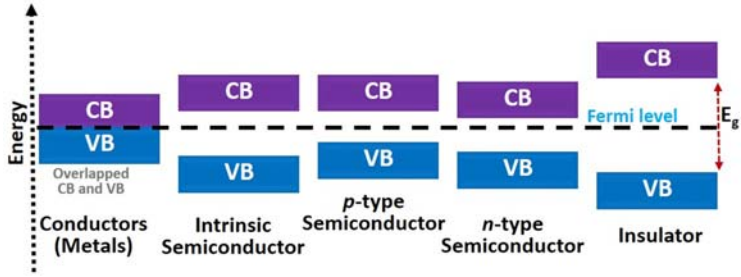

FIGURE 3.1 Electronic band structures of conductors, semiconductors, and insulators indicate Fermi level and band gap energy (E_g).

TABLE 3.1 Difference between intrinsic and extrinsic semiconductors.

Intrinsic semiconductor	Extrinsic semiconductor
1. Pure semiconductor	1. Impure semiconductor
2. Electrons density is equal to holes density	2. Electrons density is not equal to holes density
3. Low electrical conductivity	3. High electrical conductivity
4. Temperature-dependent	4. Temperature and amount of impurity dependent
5. No impurities	5. Trivalent and pentavalent impurity

of material and are considered pure materials. However, extrinsic semiconductors are composed of more than one type of material and are considered impure materials. For example, Si and Ge are intrinsic semiconductors. These semiconductors are also called "undoped semiconductors." Extrinsic semiconductors, on the other hand, are intrinsic semiconductors with other substances (impurities) added to alter their properties. In short, they have been doped with another element and are also called "doped semiconductors."

In other words, semiconductors that are chemically pure and free from impurities (dopants) are termed intrinsic semiconductors. The number of holes (h^+) and electrons ($\bar{e}$) is determined by the properties of the material itself instead of the impurities. In intrinsic semiconductors, the number of excited electrons ($\bar{e}s$) is equal to the number of holes, i.e., $n\bar{e}s = nh^+$. These semiconductors are also termed undoped semiconductors or i-type semiconductors. Si (Fig. 3.2) and Ge are examples of i-type semiconductors. These elements belong to group IV of the periodic table and their atomic numbers are 14 and 32, respectively. Therefore, intrinsic semiconductors are also known as pure semiconductors or i-type semiconductors.

The electronic configuration of Si and Ge is $1s^2$, $2s^2$, $2p^6$, $3s^2$, $3p^2$ and $1s^2$, $2s^2$, $2p^6$, $3s^2$, $3p^6$, $4s^2$, $3d^{10}$, $4p^2$, respectively. The electronic configurations show that both elements have four electrons in their outermost shell or valence shell. As the temperature of the semiconductor is increased, the electrons gain more thermal energy, and thus, break free from their valence shell. The process of ionization of the atoms in the crystal lattice creates a vacancy in the bond between the atoms. The position from which the electron gets dislodged forms a hole (h^+) which is equivalent to an effective positive charge. The h^+ is then occupied by an adjacent free $\bar{e}$ because of which the latter vacant position becomes an h^+ and the former becomes a neutral position. This way, the hole or the effective positive charge is transferred from one position to another (Fig. 3.2). In an intrinsic semiconductor, the number of free electrons is equal to the number of holes. Mathematically,

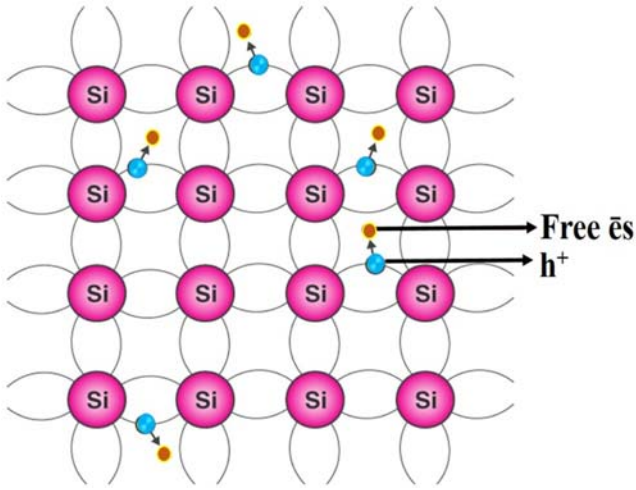

FIGURE 3.2 Free electrons and holes in silicon.

$n\bar{e} = nh^+ = ni$. Here, ni is the number of total intrinsic carrier concentrations which is equal to the total number of h^+s or the total number of ēs.

When the temperature of an intrinsic semiconductor is T = 0K, it behaves like an insulator. When the temperature is increased further (T > 0), the electrons get excited and move from the VB to the CB of the semiconductor. These electrons occupy the CB partially, leaving a correspondingly equal number of holes in the VB.

An extrinsic semiconductor or a doped semiconductor is a semiconductor that has been intentionally doped to modulate its electrical, optical, and structural properties. In the case of semiconductor detectors of ionizing radiation, doping is the intentional incorporation of impurities into an intrinsic semiconductor to improve their electrical properties.

The addition of a small percentage of impurity atoms in the regular crystal lattice of Si or Ge produces dramatic changes in their electrical properties. These impurity atoms incorporated into the crystal structure of the semiconductor provide free charge carriers (ēs or h^+) in the semiconductor. In an extrinsic semiconductor, impurity dopant atoms in the crystal lattice mainly provide the charge carriers which carry electric current through the crystal. In general, there are two types of dopant atoms resulting in two types of extrinsic semiconductors. These dopants that produce the desired controlled changes are classified as either electron acceptors or electron donors. The corresponding doped semiconductors based on charge carriers are of two types and are known as:

1. n-type semiconductors
2. p-type semiconductors

3.3.1.1 n-Type semiconductors

An extrinsic semiconductor that has been doped with electron donor atoms is called an n-type semiconductor because the majority of charge carriers in the crystal are negative electrons (Fig. 3.3). Since Si is a tetravalent element, the normal crystal structure contains four covalent bonds from four valence electrons. In silicon, the most common dopants are group III and group V elements. However, group V elements (pentavalent) have five valence electrons, which allows them to act as a donor. It means that the addition of these pentavalent impurities such as arsenic, antimony, or phosphorus contributes to free electrons, which greatly increases the conductivity of the intrinsic semiconductor.

At room temperature, these loosely attached fifth valence electrons of impurity atoms can come out from their position due to thermal excitation. The free electrons in addition to the free electrons created due to the breakdown of a semiconductor causes the total free electrons in the crystal. Furthermore, as a free electron is created, a hole is also created. In the n-type, electrons are the main mobile charge carriers. For example, a crystal doped with phosphorus (group V) results in an n-type semiconductor.

The conduction electrons are completely dominated by the number of donor electrons. Therefore, the total number of conduction electrons is approximately equal to the number of donor sites, i.e., $n \approx ND$. The charge neutrality of the semiconductor material is maintained because excited donor sites balance the conduction electrons. The net result is that the number of conduction ēs has increased, while the number of h^+ has reduced. The imbalance of the carrier concentration in the respective bands is expressed by the different absolute numbers of electrons and holes. Electrons are the majority carriers, while holes are minority carriers in the n-type of semiconductors.

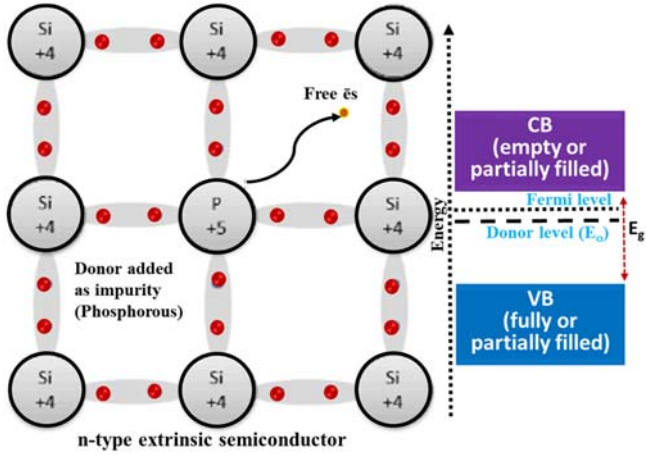

FIGURE 3.3 The n-type extrinsic semiconductor.

3.3.1.2 p-Type semiconductors

An extrinsic semiconductor that has been doped with electron acceptor atoms is called a p-type semiconductor because the majority of charge carriers in the crystal are holes (h^+, positive charge carriers) (Fig. 3.4). The pure semiconductor, such as silicon, is a tetravalent element. Its normal crystal structure contains four covalent bonds from four valence electrons. However, as opposed to the n-type semiconductors, the group III elements (trivalent) which contain three valence electrons make them function as acceptors when used to dope silicon. When an acceptor atom replaces a tetravalent Si atom in the crystal, a vacant state (an electron-hole) is formed. It is one of the two types of charge carriers that are responsible for creating an electric current in semiconducting materials. These positively charged holes can move from atom to atom in semiconducting materials as electrons leave their positions. The addition of trivalent impurities such as boron (B), aluminum (Al), or gallium (Ga) to an intrinsic semiconductor creates these positive electron holes in the structure. For example, a Si crystal doped with boron (group III) creates a p-type semiconductor.

The number of electron holes is completely dominated by the number of acceptor sites. Therefore, the total number of holes is approximately equal to the number of donor sites, i.e., $p \approx N_A$. The charge neutrality of this semiconductor material is also maintained. The net result is that the number of electron holes is increased, while the number of conduction electrons is reduced. The imbalance of the carrier concentration in the respective bands is expressed by the different absolute numbers of ēs and h^+. Electron holes are the majority carriers, while electrons are the minority carriers in p-type semiconductors. Table 3.2 shows some of the differences between the p-type and n-type semiconductors.

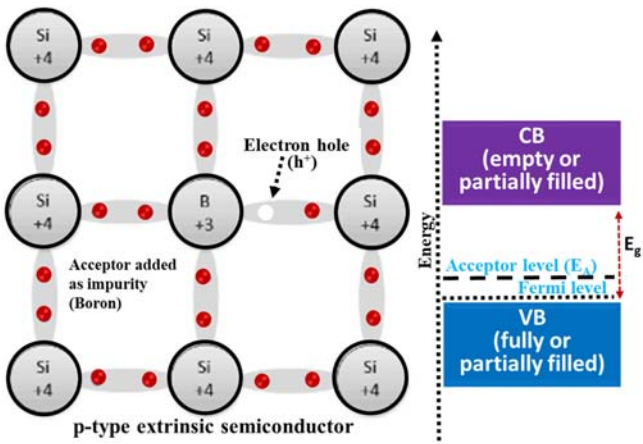

FIGURE 3.4 The p-type extrinsic semiconductor.

TABLE 3.2 The differences between p-type and n-type semiconductors.

p-Type semiconductor	n-Type semiconductor
1. Formed by adding trivalent impurities	1. Formed by adding pentavalent impurities
2. Charge carriers are holes	2. Charge carriers are electrons
3. Addition of impurities creates holes or vacancies of electrons. This is called an acceptor atom.	3. Addition of impurities creates extra electrons and this is called a donor atom.
4. Fermi level lies among the energy level of acceptor and the valence band	4. Fermi level lies among the energy level of the donor and the conduction band
5. Energy level of the acceptor is near to the valence band and absent from the conduction band	5. Energy level of the donor is near to the conduction band and absent from the valence band

3.3.1.3 Donor level

From the energy gap perspective, some impurities "create" energy levels in the band gap close to CB so that electrons can be easily excited from these levels into the CB. The electrons are said to be the "majority carriers" for current flow in an n-type semiconductor. This shifts the effective Fermi level to a point about halfway between the donor levels (E_o) and the CB (Fig. 3.3).

3.3.1.4 Fermi level

The highest occupied energy level in a solid at absolute zero temperature is known as the Fermi level.

It is the term used to describe the top of the collection of electron energy levels at absolute zero temperature. The Fermi level is the surface of the Fermi sea at absolute zero temperature where no electrons will have enough energy to rise above the surface. In pure semiconductors, the position of the Fermi level is within the band gap, approximately in the middle of the band gap.

3.3.1.5 Acceptor level

As of the energy gap view, a few impurities "create" energy levels within the band gap close to the VB so that electrons can be easily excited from the VB into these levels, leaving mobile holes in the VB. They create "shallow" levels, i.e., levels that are very close to the VB, so the energy required to ionize the atom (accept the electron that fills the hole and creates another hole further from the substituted atom) is small. This shifts the effective Fermi level to a point about halfway between the acceptor levels (E_A) and the VB (Fig. 3.4).

3.3.2 Band gap energy

The main difference between conductors, semiconductors, and insulators is the extent of the band gap energy (E_g). The energy difference between the CB and VB of a semiconductor is called the band gap energy (E_g). Thus, the band gap of semiconductors (1−4 eV) lies in the appropriate range for a semiconductor photocatalyst as shown in Fig. 3.1. Besides band gap energy and charge carrier mobility, band edge position is important for the photocatalytic activity of semiconductors because this is a crucial and important parameter for catalytic reactions that take place at the surface of the photocatalyst [24−26]. Following are a few selected examples of semiconductors showing their respective band gap energies:

1. Titanium dioxide (TiO_2), $E_g = 3.20$ eV
2. Zinc oxide (ZnO), $E_g = 3.3$ eV
3. Gallium nitride (GaN), $E_g = 3.4$ eV
4. Cubic zinc sulfide (ZnS), $E_g = 3.54$ eV
5. Hexagonal zinc sulfide (ZnS), $E_g = 3.91$ eV
6. Aluminum nitride (AlN), $E_g = 6.02$ eV

3.3.3 Band edge positions

In an electronic energy level diagram of a semiconductor (Fig. 3.5), the upper edge of the VB (E_{VB}) corresponds to the energy that determines the *oxidizing ability* of the holes, and the energy level at the bottom of the CB (E_{CB}) is the energy that determines the *reduction ability* of the ēs. The energies of electrons in a solid are referred to as the vacuum level, which is taken as the reference of zero energy value.

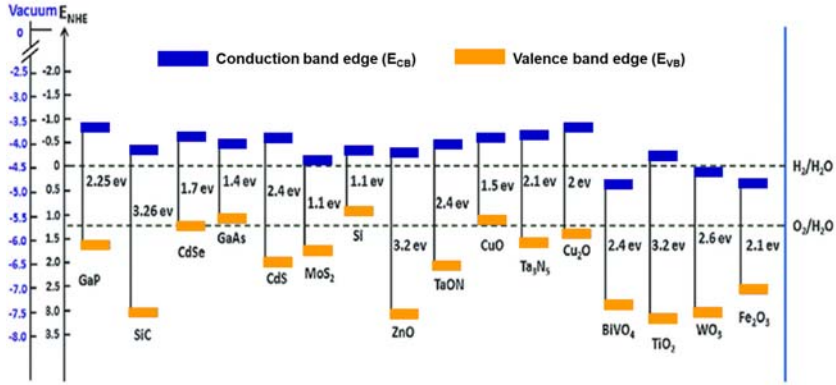

FIGURE 3.5 Band edge positions of semiconductors at pH = 0 relative to NHE and the vacuum level.

The bands in the semiconductors relate to the VB and CB. The VB is the range of energies at which an electron can exist in its normal or unexcited state. The CB is the range of energies at which an electron can exist in its excited state. The edges of the bands refer to the highest energy state that an electron can exist in the VB, and the lowest energy an electron can have in the CB. The band edge positions are important for photocatalytic activities of semiconductors because these are critical for catalytic reactions which take place at the surface of semiconductors [24–26]. The band edge positions of semiconductors regulate their functionality in various optoelectronic applications such as photoelectrochemical cells, photovoltaics, and light-emitting diodes. Following are some examples of semiconductors showing band edge positions:

1. TiO_2 with a band gap energy of 3.2 eV has a CB edge position of −0.51 V at pH 5–7 versus normal hydrogen electrode (NHE).
2. Cadmium sulfide (CdS) with a band gap energy of 2.4 eV has a CB edge position of −0.91 V at pH 5–7 versus NHE.
3. $SrTiO_3$ and $KTaO_3$ have high negative CB levels around −0.3 to 0.4 V versus NHE.

3.3.4 Ultraviolet light active semiconductors

Semiconductors such as metal oxides and some of the selected chalcogenides as semiconductors are considered ultraviolet light active semiconducting materials because of their wide band gap energy ($E_g > 3.0$ eV). Hence, these semiconducting materials can easily absorb UV light and show photocatalytic activities under UV light irradiation.

3.3.4.1 Metal oxides

Metal oxides, generally binary semiconducting compounds, are one of the most important and widely characterized solids which are considered heterogeneous catalysts. Binary oxides, for example, TiO_2, ZnO, CeO_2, SnO_2, WO_3, and Fe_2O_3, have been the most studied metal oxides for photocatalytic activities. Among them, TiO_2 is the photocatalyst mainly used owing to its nontoxicity, water insolubility, hydrophilicity, low cost, stability, and resistance to photocorrosion. TiO_2 is an odorless white powder. It is found in three crystalline forms such as anatase, rutile, and brookite as shown in Fig. 3.6.

Crystalline TiO_2 is found naturally in three polymorphs or phases such as anatase, rutile, and brookite (Fig. 3.6). Among these, anatase is considered the most stable polymorph. In the presence of light with energy equal to or higher than the band gap energy of TiO_2, an electron is promoted from the VB to the CB, leaving behind a positive hole (h^+). These characteristics of TiO_2 offer it a wide range of applications, such as air purification, water

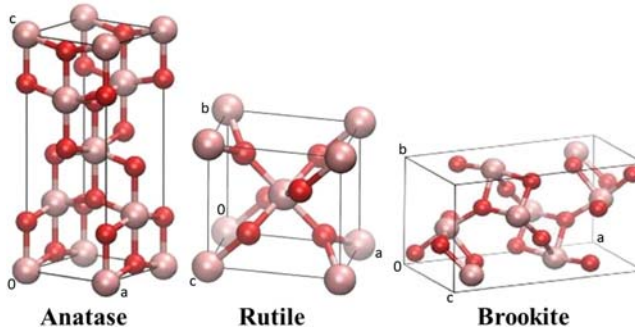

FIGURE 3.6 Three phases of TiO_2.

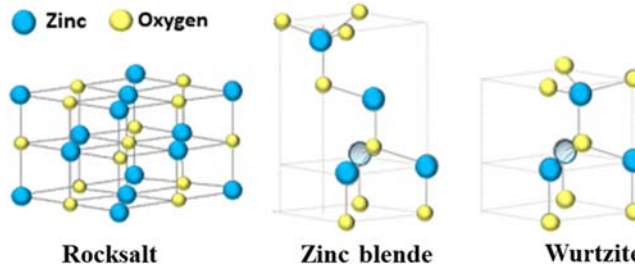

FIGURE 3.7 Three different phases and crystal structures of ZnO.

purification, and self-cleaning glasses. Consequently, the photoactivation of nano-TiO_2 can be achieved by irradiation with UV-A, UV-B, and UV-C lights, visible light, fluorescent light, and X-ray radiation. The photocatalytic activity results in the formation of highly reactive free radicals ($O_2^{\bullet -}$ and $^{\bullet}OH$) that are capable of reacting with most of the adjacent organic substances or pollutants and oxidizing them to harmless end byproducts [24–26].

Another example of metal oxide is ZnO. It is an n-type semiconductor whose thermodynamically stable phase is a hexagonal wurtzite structure where each anion is surrounded by four cations at the corners of a tetrahedron and vice versa (Fig. 3.7). This tetrahedral coordination is typical of sp^3 covalent bonding in nature. However, this material also has a substantial ionic character that tends to increase the band gap beyond the one expected from the covalent bonding. Despite this fact, ZnO is the second most used semiconductor after TiO_2 because of its good optoelectronic, catalytic, and photochemical properties along with its low cost and nontoxic nature [4,27].

ZnO is a white powder that is insoluble in water. Owing to its broad-spectrum UV light absorption and anti-bacterial and anti-viral properties, it is used as an additive in several materials and products including sunscreens,

oral care products, vitamins, rubbers, plastics, ceramics, glass, cement, lubricants, paints, ointments, adhesives, sealants, pigments, foods, batteries, ferrites, fire retardants, and first-aid tapes. Though it is found naturally as the mineral zincite, most of the ZnO is produced synthetically. ZnO has a relatively large direct band gap of ~3.3 eV at room temperature. The advantages associated with a large band gap of ZnO include higher breakdown voltages, the ability to sustain large electric fields, lower electronic noise, and high-temperature and high-power operation.

SnO_2 is an n-type metal oxide semiconductor reported with a band gap energy of ~3.6 eV at 300K. The two common oxidation states of Sn cations are +2 and +4, which are known to be stannous ion (Sn^{2+}) and stannic ion (Sn^{4+}). SnO_2 is known as a good photocatalyst because of its high chemical stability, low cost, and good photoactivity. SnO_2 has been synthesized with different methods, for instance, hydrothermal, sol-gel, co-precipitation, solvothermal, gel-combustion, and microwave methods. It has a rutile-type ($P4_2/mnm$) tetragonal shape with lattice parameters of a = 4.738 Å and c = 3.187 Å (JCPDS no. 00-041-1445). However, similar to silica, SnO_2 has various polymorphs (Fig. 3.8), such as (A) $CaCl_2$-type (*Pnnm*), (B) α-PbO_2-type (*Pbcn*), (C) pyrite-type (*Pb3*), (D) ZrO_2-type orthorhombic phase I (*Pbca*), and (E) fluorite-type (*Fm3m*). For instance, Bhosale et al. have synthesized a UV-active SnO_2 with a tetragonal crystal structure using aqueous leaf extract of *Calotropis gigantea* for photocatalytic degradation of methyl orange (MO) dye [28].

Cerium belongs to the lanthanide series and is a rare earth metal, possessing two common oxidation states, Ce^{3+} and Ce^{4+}. CeO_2 has outstanding electronic, magnetic, and luminescence properties due to the unfilled 4f electronic structure of cerium. They show good photocatalytic and radical

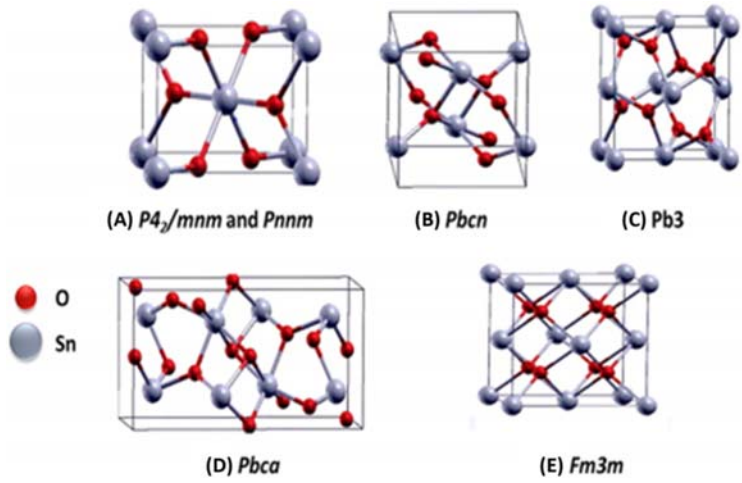

FIGURE 3.8 Different crystal structures of SnO_2.

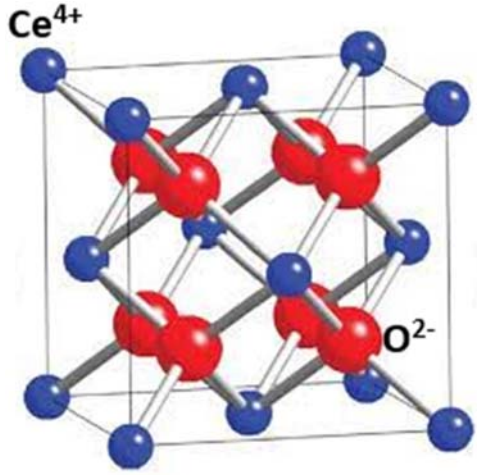

FIGURE 3.9 Fluorite structure of CeO_2.

scavenging activity due to the reversible transition between Ce^{3+} and Ce^{4+} oxidation states in CeO_2 crystals and the high mobility of oxygen species. However, with a wide band gap ($\sim$3.19 eV) and fast recombination of electrons and holes, CeO_2 is more active under UV light as compared to visible light irradiation. CeO_2 can be synthesized using various physical and chemical methods. Physical methods such as ball milling, spray pyrolysis, thermal decomposition, and laser irradiation are used. While, the chemical approach includes hydrothermal, spray hydrolysis, sol-gel, and sonochemical methods. CeO_2 has a fluorite structure with space group Fm3m and it consists of a simple cubic oxygen sub-lattice with the cerium ions occupying alternate cube centers as shown in Fig. 3.9. Venkataswamy et al. have studied the effect of metal doping on the photocatalytic performance of CeO_2 under UV light [29]. They found out that Mn-doped CeO_2 exhibited the highest photocatalytic degradation of rhodamine B (RhB) rate constant of 6.64×10^{-3} min^{-1}.

3.3.5 Chalcogenides

In addition to metal oxides, several chalcogenides have been investigated regarding their photocatalytic activities. Among them, metal sulfides are the most common semiconducting materials studied because of their low band gap energy (1.3−2.40 eV) which has the advantage of solar energy utilization. There are various sulfide semiconductor materials possessing narrow band gaps (i.e., CdS, Sb_2S_3, Bi_2S_3, MoS_2, etc.) with appropriate characteristics to be used in the photocatalytic process. The representative chalcogenide photocatalyst is CdS which is active for H_2 evolution under visible light irradiation.

Among other metal sulfides such as ZnS, Sb_2S_3, Bi_2S_3, and MoS_2, only ZnS possesses a wide band gap of ~3.5 eV. However, ZnS has the advantage to be nontoxic, exhibiting good photocatalytic activity for photocatalytic removal of hazardous compounds. Juine et al. have successfully synthesized ZnS using zinc acetate dehydrates and thiourea via microwave-assisted method [30]. The authors reported about 95% photocatalytic degradation of methylene blue (MB) and MO dyes was achieved by ZnS under different UV light sources namely UV-C, UV-B, and UV-A as well as visible light. Moreover, MO dye degraded completely within 20 min with a rate constant of 0.015 min^{-1} under the UV-C light source and by 190 min under visible light.

Cadmium selenide (CdSe) and cadmium telluride (CdTe) can reduce water for hydrogen production because of the negative CB position versus NHE. However, these chalcogenides are unable to oxidize water because the VB redox potential is lower than 1.23 V; thereby, CdSe and CdTe exhibit poor photocatalytic activity for oxidation of organic pollutants [26]. MgS is a wide band gap direct semiconductor of interest as a blue-green emitter. The wide band gap property allows the use of MgS as a photodetector for short wavelength ultraviolet light. A study by Kokilavani et al. showed that the photocatalytic performance of MgS could be improved when coupled with Ag_2MoO_4 [31]. The degradation efficiency of MgS/Ag_2MoO_4 (90%) was about 1.5 and 2.2 times greater than bare Ag_2MoO_4 (62%) and MgS (41%). The strong interactions between the MgS and Ag_2MoO_4 interfacial surfaces are responsible for the increase in charge separation owing to the superior activity of MgS/Ag_2MoO_4.

3.3.6 Ternary semiconductors

Most photocatalytic ternary semiconductors such as metalates, oxysulfides, oxyhalides, and oxynitrides can be activated with light irradiation. Metalates such as aluminates, ferrites, niobates, tantalates, titanates, tungstates, and vanadates have been tested as photocatalytic semiconductors for the photocatalytic degradation of different organic dyes, mainly MB, RhB, and MO.

Aluminates such as $ZnAl_2O_4$ and $AgAlO_2$ have band gap energies of 4.11 and 3.2 eV, respectively. These aluminates presented lower activity in the visible region due to their wide band gap. However, $ZnAl_2O_4$ and $AgAlO_2$ were found responsive to UV light. These ternary semiconductors have been tested for photocatalytic degradation of organic pollutants under UV light irradiation [27,32].

3.4 Photocatalysis under ultraviolet light irradiation

Photocatalysis is a chemical reaction that takes place in the presence of a photocatalyst and suitable light. In other words, it is a reaction that uses light to generate a pair of excited electrons and a positive hole to induce redox reactions, as the first step, with both positive and negative Gibbs-energy

change. Photocatalysis depends on the ability of the photocatalyst to harvest the light (UV or visible light). In photocatalysis, the photocatalytic activity depends on the ability of the catalyst to create electron-hole pairs, which helps in generating free radicals [e.g., hydroxyl radicals ($^{\bullet}OH$) or superoxide radicals ($O_2^{\bullet -}$)]. These free radicals help to undergo secondary reactions and facilitate the degradation of the organic pollutants. Moreover, the excited electrons ($\bar{e}$) in CB can be used for the removal of toxic and heavy metals and other inorganic pollutants [2,24,25].

The photoactivation of semiconductors is based on its electronic excitation by photons (light) with energy greater than the band gap energy (E_g). The electrons migrate after the excitation generating vacancies in the VB, i.e., the formation of holes (h^+) and forming regions with high electron density ($\bar{e}$) in the CB. These holes are pH dependent and have high positive electrochemical potentials in the range of +2.0 to +3.5 V measured against a saturated calomel electrode. This potential is sufficiently positive to form hydroxyl radicals ($^{\bullet}OH$) from water molecules adsorbed on the surface of the semiconductor (Eq. 3.1−3.3). The photocatalytic efficiency of the semiconductors depends on the competition between the formation of the $\bar{e}/h^+$ pairs and the recombination of these pairs (Eq. 3.4) on the surfaces of the semiconductor photocatalysts.

$$\text{Photocatalysts} + h\nu \rightarrow \text{Photocatalysts}\left(\bar{e}_{CB} + h^+_{VB}\right) \tag{3.1}$$

$$h^+ + H_2O_{ads.} \rightarrow {}^{\bullet}OH + H^+ \tag{3.2}$$

$$h^+ + OH^-_{ads.} \rightarrow {}^{\bullet}OH \tag{3.3}$$

$$\text{Photocatalysts}\left(\bar{e}_{CB} + h^+_{VB}\right) \rightarrow \text{Photocatalysts} + \Delta \tag{3.4}$$

The oxidation reactions caused by the formed holes (h^+) take place at the VB. The electrons transferred to the CB are responsible for the reduction reactions, such as the formation of gaseous hydrogen and the formation of other important oxidizing species such as superoxide anion ($O_2^{\bullet -}$), which is a free radical. In the case of semiconductors such as metal oxides and chalcogenides, the E_g is between 2.80−3.40 eV and 1.8−2.7 eV, respectively. The overall procedure is shown schematically in Fig. 3.10.

In the electronic energy level diagram, the upper edge of the E_{VB} corresponds to the energy that determines the *oxidizing ability* of the holes, and the energy level at the bottom of the E_{CB} is the energy of the electrons that determines the *reduction ability* of the excited $\bar{e}$s. The positive hole formed in the semiconductor photocatalysts dissociates the H_2O molecules to form H_2 gas and hydroxyl radicals ($^{\bullet}OH$). The negative electron reacts with the adsorbed oxygen molecules to form superoxide anions ($O_2^{\bullet -}$). This cycle continues till suitable light of appropriate intensity and wavelength is available. The complete mechanism of photocatalytic reaction that happens at the

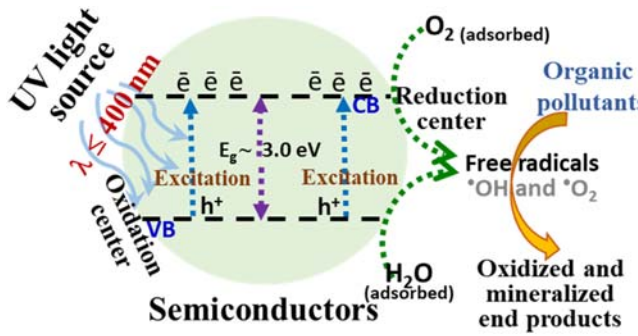

FIGURE 3.10 Photocatalytic reactions at the surface of the semiconductors under UV light irradiation.

surface of the semiconductors, in presence of a suitable light, is shown in Fig. 3.10.

The ultimate leading and advanced oxidation reactions are based on the formation of $^{\bullet}OH$ and $O_2^{\bullet-}$ which are extremely powerful oxidizing agents, second only to fluorine in power. Through the use of the strong oxidation strength of $^{\bullet}OH$ and $O_2^{\bullet-}$ radicals, photocatalytic oxidation can efficiently decompose, degrade, disinfect, deodorize, and purify air, water, and different types of surfaces [2,33–35].

3.5 Summary

Light absorption efficiencies of semiconductors are important in photocatalytic applications. Semiconductors such as metal oxides have wide band gap energy. Therefore, these materials are active under UV light irradiation. This chapter has discussed the fundamentals of semiconductor-based heterogeneous photocatalysis. It also focuses on the basic concepts involved, such as the theory and background necessary to understand the heterogeneous photocatalysis of metal oxides and some selected chalcogenides which are UV light-responsive materials. This chapter also includes a discussion on the principles of semiconductor-based photocatalysis, which regulate photocatalytic performance. Hence, a good photocatalyst must possess certain desirable characteristics for efficient and applied photocatalytic applications.

References

[1] P.Y. Yu, M. Cardona, Introduction, Fundamentals of Semiconductors, Springer, Berlin, Heidelberg, 2010, pp. 1–15. Available from: https://doi.org/10.1007/978-3-642-00710-1_1.

[2] M.M. Khan, Principles and mechanisms of photocatalysis, Photocatalytic Systems by Design, Elsevier, 2021, pp. 1–22. Available from: https://doi.org/10.1016/B978-0-12-820532-7.00008-4.

[3] M.M. Khan, S.A. Ansari, D. Pradhan, M.O. Ansari, D.H. Han, J. Lee, et al., Band gap engineered TiO_2 nanoparticles for visible light induced photoelectrochemical and photocatalytic studies, Journal of Materials Chemistry 2 (2014) 637–644. Available from: https://doi.org/10.1039/c3ta14052k.

[4] A. Rahman, M.H. Harunsani, A.L. Tan, M.M. Khan, Zinc oxide and zinc oxide-based nanostructures: biogenic and phytogenic synthesis, properties and applications, Springer Berlin, Heidelberg (2021). Available from: https://doi.org/10.1007/s00449-021-02530-w.

[5] A. Rahman, M.H. Harunsani, A.L. Tan, N. Ahmad, M.M. Khan, Antioxidant and antibacterial studies of phytogenic fabricated ZnO using aqueous leaf extract of Ziziphus mauritiana Lam, Chemical Papers 75 (2021) 3295–3308. Available from: https://doi.org/10.1007/s11696-021-01553-7.

[6] A. Rahman, A.L. Tan, M.H. Harunsani, N. Ahmad, M. Hojamberdiev, M.M. Khan, Visible light induced antibacterial and antioxidant studies of ZnO and Cu-doped ZnO fabricated using aqueous leaf extract of Ziziphus mauritiana Lam, Journal of Environmental Chemical Engineering (2021) 105481. Available from: https://doi.org/10.1016/j.jece.2021.105481.

[7] A. Rahman, M.H. Harunsani, A.L. Tan, N. Ahmad, M. Hojamberdiev, M.M. Khan, Effect of Mg doping on ZnO fabricated using aqueous leaf extract of Ziziphus mauritiana Lam. for antioxidant and antibacterial studies, Bioprocess and Biosystems Engineering 44 (2021) 875–889. Available from: https://doi.org/10.1007/s00449-020-02496-1.

[8] A. Rahman, M.H. Harunsani, A.L. Tan, N. Ahmad, B.K. Min, M.M. Khan, Influence of Mg and Cu dual-doping on phytogenic synthesized ZnO for light induced antibacterial and radical scavenging activities, Materials Science in Semiconductor Processing 128 (2021) 105761. Available from: https://doi.org/10.1016/j.mssp.2021.105761.

[9] S. Matussin, M.H. Harunsani, A.L. Tan, M.M. Khan, Plant-extract-mediated SnO_2 nanoparticles: synthesis and applications, ACS Sustainable Chemistry & Engineering 8 (2020) 3040–3054. Available from: https://doi.org/10.1021/acssuschemeng.9b06398.

[10] S.N. Matussin, A.L. Tan, M.H. Harunsani, M.H. Cho, M.M. Khan, Green and phytogenic fabrication of Co-doped SnO_2 using aqueous leaf extract of Tradescantia spathacea for photoantioxidant and photocatalytic studies, Bionanoscience 11 (2021) 120–135. Available from: https://doi.org/10.1007/s12668-020-00820-3.

[11] S.N. Matussin, M.H. Harunsani, A.L. Tan, M.H. Cho, M.M. Khan, Effect of Co^{2+} and Ni^{2+} co-doping on SnO_2 synthesized via phytogenic method for photoantioxidant studies and photoconversion of 4-nitrophenol, Materials Today Communications 25 (2020) 101677. Available from: https://doi.org/10.1016/j.mtcomm.2020.101677.

[12] S.N. Matussin, M.H. Harunsani, A.L. Tan, A. Mohammad, M.H. Cho, M.M. Khan, Photoantioxidant studies of the SnO_2 nanoparticles fabricated using aqueous leaf extract of Tradescantia spathacea, Solid State Sciences (2020) 106279. Available from: https://doi.org/10.1016/j.solidstatesciences.2020.106279.

[13] S.N. Matussin, A.L. Tan, M.H. Harunsani, A. Mohammad, M.H. Cho, M.M. Khan, Effect of Ni-doping on the properties of the SnO_2 synthesized using Tradescantia spathacea for photoantioxidant studies, Materials Chemistry and Physics (2020) 123293. Available from: https://doi.org/10.1016/j.matchemphys.2020.123293.

[14] S.N. Naidi, M.H. Harunsani, A.L. Tan, M.M. Khan, Structural, morphological and optical studies of CeO_2 nanoparticles synthesized using aqueous leaf extract of Pometia pinnata, Bionanoscience (2022). Available from: https://doi.org/10.1007/s12668-022-00956-4.

[15] S.N. Naidi, M.H. Harunsani, A.L. Tan, M.M. Khan, Green-synthesized CeO_2 nanoparticles for photocatalytic, antimicrobial, antioxidant and cytotoxicity activities, Journal of

Materials Chemistry B 9 (2021) 5599–5620. Available from: https://doi.org/10.1039/D1TB00248A.

[16] S.N. Naidi, F. Khan, A.L. Tan, M.H. Harunsani, Y.-M. Kim, M.M. Khan, Photoantioxidant and antibiofilm studies of green synthesized Sn-doped CeO_2 nanoparticles using aqueous leaf extracts of Pometia pinnata, New Journal of Chemistry 45 (2021) 7816–7829. Available from: https://doi.org/10.1039/D1NJ00416F.

[17] S.N. Naidi, F. Khan, A.L. Tan, M.H. Harunsani, Y.-M. Kim, M.M. Khan, Green synthesis of CeO_2 and Zr/Sn-dual doped CeO_2 nanoparticles with photoantioxidant and antibiofilm activities, Biomaterials Science 9 (2021) 4854–4869. Available from: https://doi.org/10.1039/D1BM00298H.

[18] S. Chakrabarti, B.K. Dutta, Photocatalytic degradation of model textile dyes in wastewater using ZnO as semiconductor catalyst, Journal of Hazardous Materials 112 (2004) 269–278. Available from: https://doi.org/10.1016/j.jhazmat.2004.05.013.

[19] A. di Paola, E. García-López, G. Marcì, L. Palmisano, A survey of photocatalytic materials for environmental remediation, Journal of Hazardous Materials 211–212 (2012) 3–29. Available from: https://doi.org/10.1016/j.jhazmat.2011.11.050.

[20] A. Rahman, M.M. Khan, Chalcogenides as photocatalysts, New Journal of Chemistry 45 (2021) 19622–19635. Available from: https://doi.org/10.1039/D1NJ04346C.

[21] R. Delgado-Balderas, L. Hinojosa-Reyes, J.L. Guzmán-Mar, M.T. Garza-González, U.J. López-Chuken, A. Hernández-Ramírez, Photocatalytic reduction of Cr(VI) from agricultural soil column leachates using zinc oxide under UV light irradiation, Environmental Technology (United Kingdom) 33 (2012) 2673–2680. Available from: https://doi.org/10.1080/09593330.2012.676070.

[22] A. Kudo, Y. Miseki, Heterogeneous photocatalyst materials for water splitting, Chemical Society Reviews 38 (2009) 253–278. Available from: https://doi.org/10.1039/b800489g.

[23] W. Bai, L. Cai, C. Wu, X. Xiao, X. Fan, K. Chen, et al., Alcohothermal synthesis of flower-like ZnS nano-microstructures with high visible light photocatalytic activity, Materials Letters 124 (2014) 177–180. Available from: https://doi.org/10.1016/j.matlet.2014.03.073.

[24] M.M. Khan, Metal Oxide Powder Photocatalysts, Elsevier Ltd., 2018. Available from: https://doi.org/10.1016/B978-0-08-101977-1.00002-8.

[25] M.M. Khan, S.F. Adil, A. Al-Mayouf, Metal oxides as photocatalysts, Journal of Saudi Chemical Society 19 (2015) 462–464. Available from: https://doi.org/10.1016/j.jscs.2015.04.003.

[26] M.M. Khan, Chalcogenide-Based Nanomaterials as Photocatalysts, first ed., Elsevier, 2021. Available from: https://doi.org/10.1016/C2019-0-01819-5.

[27] S.K. Sampath, D.G. Kanhere, R. Pandey, Electronic structure of spinel oxides: Zinc aluminate and zinc gallate, Journal of Physics: Condensed Matter 11 (1999) 3635–3644. Available from: https://doi.org/10.1088/0953-8984/11/18/301.

[28] T.T. Bhosale, H.M. Shinde, N.L. Gavade, S.B. Babar, V.v Gawade, S.R. Sabale, et al., Biosynthesis of SnO_2 nanoparticles by aqueous leaf extract of Calotropis gigantea for photocatalytic applications, Journal of Materials Science: Materials in Electronics 29 (2018) 6826–6834. Available from: https://doi.org/10.1007/s10854-018-8669-0.

[29] P. Venkataswamy, D. Jampaiah, A.E. Kandjani, Y.M. Sabri, B.M. Reddy, M. Vithal, Transition (Mn, Fe) and rare earth (La, Pr) metal doped ceria solid solutions for high performance photocatalysis: effect of metal doping on catalytic activity, Research on Chemical Intermediates 44 (2018) 2523–2543. Available from: https://doi.org/10.1007/s11164-017-3244-5.

[30] R.N. Juine, B.K. Sahu, A. Das, Recyclable ZnS QDs as an efficient photocatalyst for dye degradation under the UV and visible light, New Journal of Chemistry 45 (2021) 5845−5854. Available from: https://doi.org/10.1039/D1NJ00588J.

[31] S. Kokilavani, A. Syed, B.H. Kumar, A.M. Elgorban, A.H. Bahkali, B. Ahmed, et al., Facile synthesis of MgS/Ag_2MoOV_4 nanohybrid heterojunction: outstanding visible light harvesting for boosted photocatalytic degradation of MB and its anti-microbial applications, Colloids and Surfaces A: Physicochemical and Engineering Aspects 627 (2021) 127097. Available from: https://doi.org/10.1016/j.colsurfa.2021.127097.

[32] X. Li, Z. Zhu, Q. Zhao, L. Wang, Photocatalytic degradation of gaseous toluene over ZnAl2O4 prepared by different methods: a comparative study, Journal of Hazardous Materials 186 (2011) 2089−2096. Available from: https://doi.org/10.1016/j.jhazmat.2010.12.111.

[33] H. Tong, S. Ouyang, Y. Bi, N. Umezawa, M. Oshikiri, J. Ye, Nano-photocatalytic materials: possibilities and challenges, Advanced Materials 24 (2012) 229−251. Available from: https://doi.org/10.1002/adma.201102752.

[34] A.A. Ismail, D.W. Bahnemann, Photochemical splitting of water for hydrogen production by photocatalysis: a review, Solar Energy Materials and Solar Cells 128 (2014) 85−101. Available from: https://doi.org/10.1016/j.solmat.2014.04.037.

[35] M.M. Khan, D. Pradhan, Y. Sohn, Nanocomposites for Visible Light-induced Photocatalysis, Springer International Publishing, Cham, 2017. Available from: https://doi.org/10.1007/978-3-319-62446-4.

Chapter 4

Semiconductors as photocatalysts: visible-light active materials

Mohammad Mansoob Khan

4.1 Introduction

In a continuously developing technology-driven society, an urgent need for efficient solar light harvesting to achieve sustainable solutions in science, engineering, and industry is needed. The rapid growth of industries and some unavoidable human activities cause environmental pollution to be a threat to society. Over the last few decades, a significant effort has been made to develop visible-light active and efficient materials including inorganic, organic, ceramic, polymeric, carbonaceous, and their composites with tunable size, morphology, and structures. These characteristics provide materials with unique properties, such as narrow band-gap energy, efficient light-harvesting, charge carriers' separation, minimum or no recombination, which can assist in efficient visible-light-induced photocatalysis. Solar light consists of $\sim$5% ultraviolet (UV) light ($\sim$200−400 nm), $\sim$43% visible light ($\sim$400−700 nm), and $\sim$52% infrared light ($\sim$700−2500 nm). This shows that UV light only contributes a small portion of the sunlight and a large part of solar energy cannot be utilized [1−3].

In the renewable energy resources industry, sunlight is used as a source of energy. However, considering the cycle between day and night and dependence on seasons and weather conditions as well as low sunlight power, relying on sunlight as an energy source might create some problems. Thus, it is necessary to design materials that can be used efficiently during the day and can accumulate energy for long periods. Some studies reported the synthesis of semiconductors which showed efficient photocatalytic systems [4]. For instance, one study showed high activity for the photoreduction of CO_2 to methanol using TiO_2 nanoparticles (NPs) incorporated inside the mesoporous of SBA-15 silica [5]. SBA-15 is among the mesoporous silica that has the highest porosity and largest surface area. Moreover, its large pore volume, surface area, and adsorption capacity characteristics make it suitable for composite material preparation.

Theoretical Concepts of Photocatalysis. DOI: https://doi.org/10.1016/B978-0-323-95191-3.00007-9

Moreover, technically, there are a lot of issues in using UV-light active photocatalysts for applications such as artificial photosynthesis and water treatment [6]. Therefore, designing new semiconducting materials that are active under visible light has attracted a lot of attention since it can maximally utilize the clean, safe, and abundant solar energy treatment [6]. Moreover, it has become a major challenge to design a photocatalyst with a wide-ranging absorption range of solar irradiation, high mobility, and prolonged lifetime for charge carriers as well as a small number of recombination centers for redox catalytic activity enhancement. Therefore, this chapter discusses the design of visible-light-active materials.

4.2 Visible-light active semiconductors

As the best-known photocatalyst, TiO_2 has attracted much attention and interest from many researchers due to its exceptional properties, such as high refractive index and UV absorption, excellent incident photoelectric conversion efficiency and dielectric constant, good photocatalytic activity, photostability, chemical stability, and long-time corrosion resistance as well as nontoxicity. To recap, a good photocatalyst must show desirable properties which are listed in Table 4.1.

However, there are three main drawbacks of TiO_2 which limit its practical applications. These drawbacks are as follows:

First, its large band-gap energy ($\sim$3.2 eV for the anatase phase and $\sim$3.0 eV for the rutile phase of TiO_2). It is well-known that photon absorption of semiconductors depends greatly on their band-gap energy. The photons can only be absorbed by the photocatalyst if the photon energies are higher than the semiconductor's band-gap energy. Consequently, its surface photoactivation can be exclusively achieved under UV radiation ($\lambda \leq 390$ nm) or it can only respond and generate electron-hole ($\bar{e}-h^+$) pairs under UV light irradiation.

Second, a high recombination rate of $\bar{e}-h^+$ pairs is another disadvantage of TiO_2 which affects the photocatalytic efficiency of TiO_2. This results in a low quantum yield rate and a limited photooxidation rate.

TABLE 4.1 Desirable properties of photocatalysts.

Property	Effect of the property
High surface area	High adsorption
Efficient light absorption	Higher efficiency
Efficient charge separation	Low recombination
Long lifetime of charge separation	Possibility of chemical reactions
High mobility of charge carriers	More efficient charge separation

Third, the weak separation efficiency of the charge results in low photocatalytic activity. These three limitations greatly influence the wide practical applications of TiO_2.

To overcome the above-mentioned shortcomings, several studies have been conducted in the past decades based on the idea of extending the absorption wavelength range of the photoactivation of semiconductors toward the visible-light region and enhancing the utilization efficiency of solar energy. In this way, an increased amount of energy from the solar light spectrum can be harvested and very well utilized. Selected semiconductors such as some metal oxides and chalcogenides are considered visible-light active semiconducting materials owing to their narrow band-gap energy ($E_g < 3.0$ eV) and appropriate band edge positions. These semiconducting materials can easily absorb visible light and respond to photocatalytic activities under visible-light irradiation. To achieve the above-mentioned characteristics of the semiconducting photocatalytic materials, several strategies have been adopted and some of them are discussed under the following headings [2,3,7].

4.3 Metal-loaded or decorated semiconductors

Metal-loaded or decorated semiconductors can be obtained through surface modification. In this process, modification of the surface of the main photocatalyst material is achieved by bringing physical, chemical, and/or biological characteristics different from the one originally found on the surface of a photocatalytic semiconducting material. Various materials can be used as surface modifiers which include metal ions, metallic NPs (zero-valent), and their compounds. One of the first studies showing the visible-light activity of TiO_2 modified with metal compounds was presented by Macyk and Kisch for platinum(IV) chloride as a surface modifier. The proposed mechanism is shown in Fig. 4.1A (similar to the sensitization of TiO_2 by dyes). The excited platinum complex by visible light undergoes homolytic cleavage of the platinum−chloride bond giving the Pt(III) intermediate and a surface-bound chlorine atom. Then, electron transfer from the former to the conduction band (CB) of TiO_2 and from the electron donor (4-chlorophenol, ArOH) to the chlorine atom regenerates the sensitizer. The reduction of adsorbed oxygen through several steps leads to the formation of hydroxyl free radicals ($^{\bullet}OH$) [8−10].

Noble metals (NMs) (Au, Ag, Pt, Pd, and Ir) in the form of either adsorbed complexes or metal NPs deposits have been used for the improvement of photocatalytic activities of semiconductors for several years. The enhancement of the photoactivity (under UV light irradiation) originates from extending the lifetime of the charge carriers (photogenerated electrons and holes) since the NM serves as an electron sink (Fig. 4.1B), thus, accelerating the transfer of electrons from semiconductors to metal NPs.

In general, the Fermi levels of these NMs are lower than that of the catalysts in which the photoexcited electrons can be transferred from the CB of

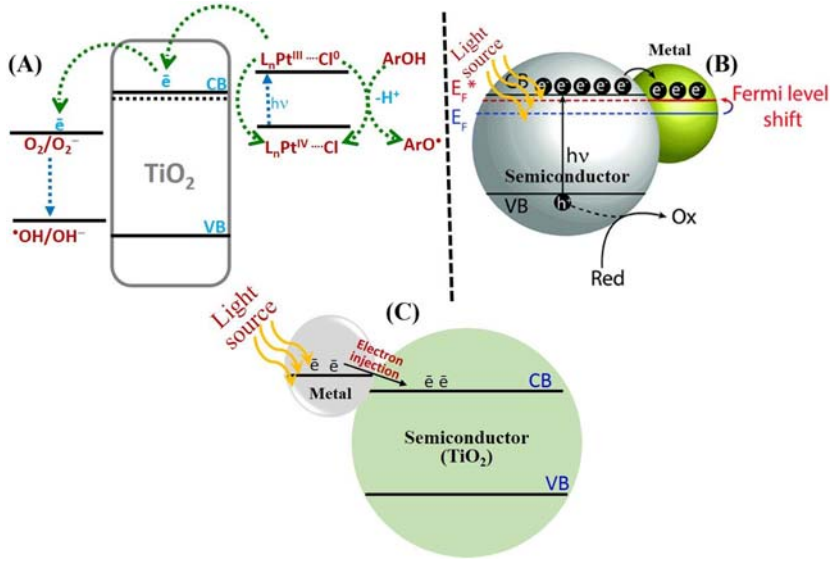

FIGURE 4.1 (A) Sensitization of TiO_2 by platinum(IV) chloride complexes, (B) electron transfer from semiconductor to metal, and (C) semiconductor by metal using LSPR.

semiconductors to metal particles deposited on the surface of the semiconductors. Meanwhile, the photogenerated valence band (VB) holes remain on the semiconductors. These activities greatly reduce the possibility of the electron-hole recombination, resulting in efficient separation of charge carriers and stronger photocatalytic reactions. The metal NPs deposited on the surface of the semiconductors act as an electron sink which promotes interfacial charge transfer and reduces charge recombination. Other semiconducting materials such as CeO_2, SnO_2, Fe_2O_3, ZnO, and $KNbO_3$ have also been reported for surface modification or decoration.

Another strategy to improve the performance of the semiconductors is the use of localized-surface plasmon resonance (LSPR) energy of irradiated NMs loaded, decorated, or deposited on the surface of the semiconductors. This approach is adopted purposely to selectively activate various electron states localized at the surface and subsurface of the photoactive semiconductors. This results in the adjustment of reaction pathways and gives the effect of spectral selectivity.

Recently, an alternative property of NMs, that is, visible-light absorption due to plasmon resonance has been used for activation of wide band-gap semiconductors toward visible light (Fig. 4.1C). Gold-modified TiO_2 (Au/TiO_2) was used as visible-light-responsive photocatalytic material for the decomposition of methyltert-butyl ether (MTBE). The first report directly showed that plasmon resonance was responsible for the visible-light activity which was

confirmed by action spectrum (AS) analyses for photocurrent generation and photooxidation of 2-propanol. With these studies, AS resembled respective absorption spectra confirming that plasmonic resonance of gold is responsible for the activity of Au/TiO_2 under visible-light irradiation. Three main mechanisms have been proposed for plasmonic photocatalysis under visible-light irradiation:

1. Charge transfer (mainly electron transfer)
2. Energy transfer
3. Plasmonic heating.

In general, the mechanism of photocatalytic decomposition of organic compounds (OCs) by Au/TiO_2 under visible-light irradiation is similar to that of activation using sensitizers, such as metal complexes or dyes. Thus, NMs are also called "plasmonic photosensitizers." At first, incident photons are absorbed by NM NPs through the LSPR excitation (Fig. 4.1C), and then, electrons "hot electrons" are transferred from NM NPs into the CB of TiO_2. Then, these hot electrons reduce the molecular oxygen adsorbed on the surface of TiO_2 to superoxide radicals ($O_2^{\bullet -}$) and the resultant electron-deficient NM NPs can oxidize OCs to recover their original metallic state.

Ag, Au, and Cu NPs exhibit plasmon resonance in the visible spectral region. Hence, Au and Ag NMs are mainly used for plasmonic photocatalysis. However, other NMs have also been used such as Pd, Pt, and Cu. It is also possible that the mechanism of action of TiO_2 modified with other metals (non-NMs) could be similar to plasmonic photocatalysis. For example, electron transfer confirmed by the time-resolved microwave conductivity (TRMC) method has been proposed for fine bismuth nanoclusters deposited on TiO_2 [7–10].

It is also noted that light harvesting also depends on the loading of NMs. An appropriate amount of NMs loading on the surface of the semiconductor facilitates plasmonic photocatalysis. However, loading too many NMs NPs on the surface of semiconductors reduces photon absorption and becomes electron-hole recombination centers which, therefore, results in lower efficiency. Metal NPs decorated/ loaded metal oxides such as $Ag@TiO_2$, $Au@TiO_2$, Ag@ZnO, $Au@SnO_2$, $Ag@SnO_2$, $Ag@CeO_2$, and, $Au@CeO_2$ have been extensively studied and used for photocatalytic degradation of different types of colored organic dyes and non-colored organic pollutants under visible-light irradiation.

4.4 Metal-doped semiconductors

Doping means the incorporation of impurities (metals or non-metals) into a lattice of a semiconductor crystal structure for the modification or alteration of its electrical, optical, and structural properties. In other words, doping is the deliberate introduction of impurities into an intrinsic semiconductor to modulate its electrical, optical, and structural properties. The doped material

is referred to as an extrinsic semiconductor. Dopants can be metals, non-metals, or both [7,8].

Properties of metals such as transition metals with 3d or 4d electrons are influenced by many factors, such as the number of d-electrons in transition metal ions, crystalline structures, defects, and preparation methods. Therefore, in such a case, the band-gap energy, band edge positions, Fermi level, and d-electron configuration of the electronic structure of TiO_2 can be effectively modulated when transition metal ions are incorporated into the TiO_2 lattice. Subsequently, it forms a wide range of new energy levels below CB arising from their partially filled d-orbitals, which result in an obvious red shift in the band-gap energy. This increases the visible-light-harvesting ability of the metal-doped semiconductors. In addition, transition metal ions alter the carrier equilibrium concentration by serving as electron-hole trapping, suppressing the recombination rate of electron-hole pairs, and enhancing the photocatalytic activity rates. In this way, the photocatalytic performance of TiO_2 can be effectively improved through transition metal doping.

Furthermore, semiconductors doped with a transition metal as photocatalysts have been extended to achieve improved properties, in particular, to induce a narrow band-gap energy in their electronic structure. Thus, the doped metal oxides with a variety of transition metal ions represent interesting properties such as low recombination of charge carriers and enhanced photocatalytic activities. This might be due to the incorporation of dopants (impurities) in a semiconductor crystal lattice contributing extra electrons or extra holes which inhibit or delay the recombination. This improves the semiconductor efficiency in becoming an ideal photocatalyst.

In short, the doping of semiconductors such as metal oxides (substitutional or interstitial) with metal is responsible for a change in the chemical nature of solid materials. This influences the improvement in electronic properties described as band-gap engineering. Recently, many theoretical and experimental studies have been developed to investigate metal (Fe, Cr, V, Mo, Re, Ru, Mn, Co, Rh, Bi, etc.) (Fig. 4.2A) and non-metal (N, S, B, C, and F) (Fig. 4.2B) doping which affects the electronic band structure of the TiO_2 photocatalyst. To make semiconductors better photocatalysts, incorporate impurities (dopants) to contribute extra electrons or extra holes which can inhibit or delay recombination, such as

- elements with five outer electrons contributing an extra electron to the lattice (donor dopant).
- elements with three outer electrons accepting an electron (acceptor dopant).

The efficiency of photocatalysts depends on various charge transfer events and the migration of charges to the surface. Hence, dopants influence the intrinsic properties of semiconductors resulting in lowering the band-gap

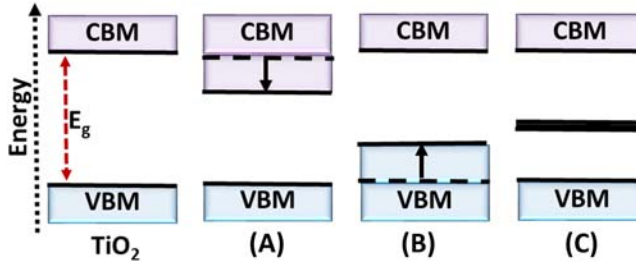

FIGURE 4.2 Three schemes of the band-gap modifications of semiconductors for visible-light sensitization with (A) lower shift of CBM, (B) higher shift of VBM, and (C) formation of impurity states.

energy and shifting light absorption into the visible spectral region. Dopants should be both good electrons and hole traps. For example, TiO_2's visible-light response activity incorporated by doping can result from (1) a lower shift of the conduction band minimum (CBM) (which is generally affected by metal ion dopants), (2) a higher shift of valence band maximum (VBM) (which is generally affected by non-metal ion dopants), and (3) formation of impurity states in the band gap, as shown in Fig. 4.2C. Hence, the following requirements are identified for the doped photocatalysts:

1. The CBM should be higher than the redox potential of the H_2/H_2O level, while the VBM should be lower than the O_2/H_2O level to ensure photoreduction and photooxidation activities for water splitting, respectively.
2. The states in the gap should be shallow or mixed with the band states of TiO_2 which should be enough to transfer photoexcited or thermally excited charge carriers to reactive sites at the photocatalyst surface within their lifetime.

Metal ion incorporation was successfully used for the modification of the properties of TiO_2 with metal doping. Metal ion incorporation into TiO_2 revealed that various ions occupy substitutional sites by replacing Ti atoms. The replacement of Ti atoms depends on the size mismatch energy of the implanted ions. It was proposed that for the metal ion-implanted TiO_2, the overlap of the CB due to Ti(d) orbital of TiO_2 and the metal(d) orbitals of the implanted metal ions can decrease the band-gap energy of TiO_2 to enable visible-light absorption. The substitution of Ti ions with the isolated metal ions implanted into the lattice position of the bulk TiO_2 is the determining factor for the utilization of visible light. Fig. 4.3 shows the narrowing of the bandgap when TiO_2 was doped with Ag [7].

It is known that doping of metal ions could expand the photoresponse of semiconductors into the visible-light spectrum. As metal ions are incorporated into the lattice, impurity energy levels in the band gap are formed. Metal ions should be doped near the surface of the semiconductor for a

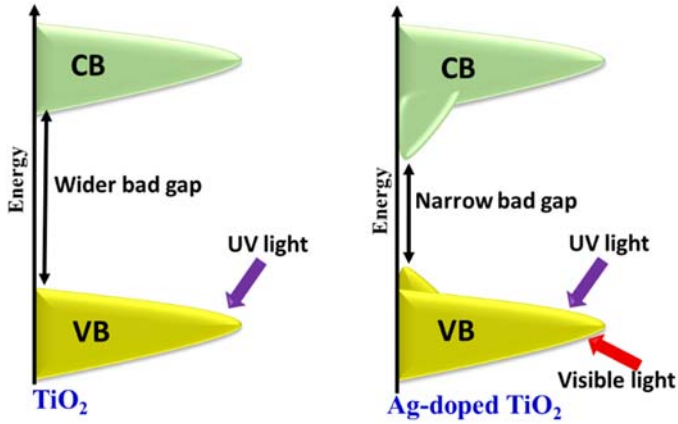

FIGURE 4.3 Band-gap narrowing of the TiO_2 when doped with Ag.

better charge transfer. In the case of deep doping, metal ions likely behave as recombination centers, since electron/hole transfer to the interface is quite difficult. Generally, doping near the surface of the semiconductors is beneficial whereas deep doping leads to poor performance. Also, doping of $\sim 1\%-5\%$ metal ions is optimal. However, a higher percentage of doping might show the opposite response. The overall effect of incorporating dopants includes band-gap lowering, no or minimum recombination, and light absorption shifts into the visible spectral range. Therefore, the photocatalytic response of doped semiconductors is very sensitive to the metal ion doping methods, doping content, and doping depth.

4.5 Non-metal-doped semiconductors

Doping of semiconductors by non-metal elements with high ionization energies and high electronegativities, such as nitrogen (N), carbon (C), boron (B), sulfur (S), fluorine (F), and chlorine (Cl) is another efficient strategy to enhance the visible-light photocatalytic activity. For instance, a high performance for photocatalytic water oxidation under visible light using N-doped ZnO has been reported by Zong et al. and they found that the amount of O_2 evolved on N-doped ZnO samples prepared at 873K, 973K, and 1073K was about 2.4, 5.7, and 1.1 μmol/h, respectively [11]. In another study, cabbage-like N-doped ZnO showed an improved photocatalytic degradation efficiency (98.6% and 96.2%) and kinetic degradation rates of methylene blue (MB) ($k = -0.0579\ min^{-1}$ and $k = -0.0585\ min^{-1}$) under UV light and visible-light irradiation [12]. The basic phenomenon is that the non-metal dopants influence the VB through interaction with the O 2p orbitals. The localized states or p states of non-metal dopants generally form the impurity levels just above the VB, which extends the optical absorption edge of

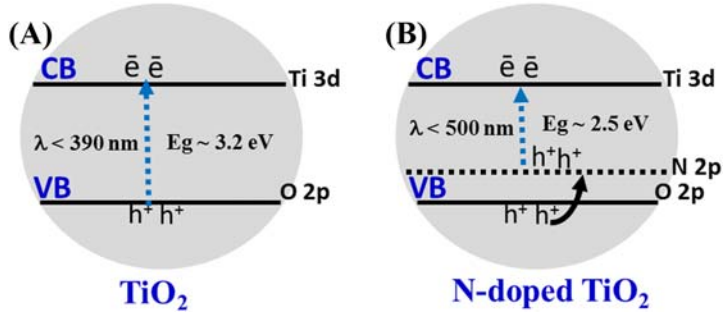

FIGURE 4.4 Schematic showing (A) TiO_2 under UV light ($\lambda < 390$ nm) illumination and (B) band-gap narrowed N-doped TiO_2 under visible-light ($\lambda < 500$ nm) irradiation.

semiconductors toward the visible-light region (Fig. 4.4). Therefore, the distribution of the dopant impurity states is above the VB maximum, which has a greater potential for realizing visible-light photoactivity [3,7,13]. This results in higher photocatalytic activity of non-metal-doped semiconductors in the visible-light region owing to the band-gap narrowing and the shift of the absorption edge in the higher wavelength region.

Among non-metal elements, N has been established to be one of the most efficient dopants for visible-light-responsive TiO_2 photocatalyst (Fig. 4.4). Since Asahi et al. made a breakthrough work in 2001 and found that N-doped TiO_2 could enhance its photocatalytic activity for the photocatalytic degradation of MB under visible-light irradiation, many theoretical calculations and experiments have shown and confirmed that N is one of the most promising dopants for the redshift of the absorption edge so far. Some researchers suggested a model in which the incorporation of N via O substitution results in band-gap narrowing due to the mixing of the N 2p and O 2p states, which shows a remarkable redshift of the spectrum onset. In other words, N-doped TiO_2 is a promising photocatalyst for enhanced light harvest in the visible region because it has strongly localized N 2p states (0.3−0.5 eV) at the VB maximum.

4.6 Dye-sensitized semiconductors

Photosensitization has been extensively used to extend the photoresponse of semiconductor photocatalytic materials into the visible-light region of the electromagnetic spectrum. Dye sensitization is widely used to utilize visible light for energy conversion. Some dyes having redox properties and visible-light sensitivity can be used in solar cells as well as photocatalytic systems. Under visible-light irradiation, dyes (S) can easily absorb the energy, and the excited dyes (S^*) can inject electrons into the CB of semiconductors to initiate the catalytic reactions as illustrated in Fig. 4.5. The mechanism of

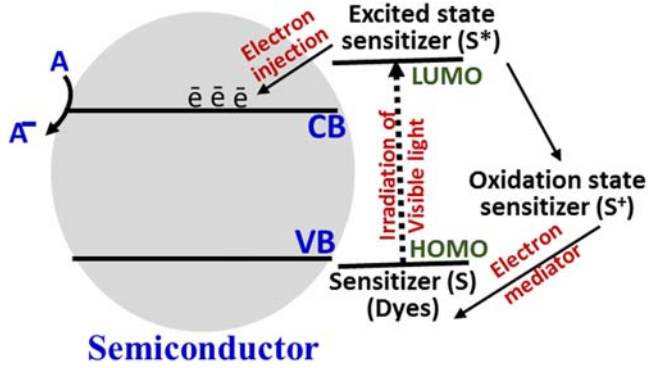

FIGURE 4.5 Primary electron transfer pathway in a dye-sensitized semiconductor photocatalyst.

dye-sensitized photocatalysis is highly dependent on the transfer (or injection) of ēs from the excited state of the dye molecule (S^*) to the semiconductor surface (Fig. 4.5) [7,14,15].

For example, visible light excites the sensitizer molecules, i.e., dyes, adsorbed on the semiconductor and subsequently inject ēs to the CB of the semiconductor. The VB remains unaffected in a typical photosensitization, while the CB acts as a mediator for transferring electrons from the sensitizer to the substrate (electron acceptors) on the surface of the semiconductor. In other words, as the dye molecule absorbs visible light, excitation of electrons proceeds from the highest occupied molecular orbital (HOMO) to the lowest unoccupied molecular orbital (LUMO) of the dye. Consequently, the excited dye molecule transfers the LUMO electrons into the CB of the semiconductor photocatalyst, while the dye itself gets changed into its cationic radicals (S^+) and later can be regenerated and reused.

The sensitization of a semiconductor has been used for different technological purposes which include the development of new solar cells, H_2 production by H_2O splitting, and for the photocatalytic degradation of organic dyes from industrial effluents. In this area, the activity of the photocatalyst has been considerably improved by its sensitization to extend the range in the solar spectrum. Hence, the use of organic dyes/semiconductor material systems in the process of wastewater treatment via a photosensitization mechanism is a promising field to solve environmental problems. A great variety of chemical substances has been proposed as effective photosensitizers of a semiconductor. For example, Nimpoeno et al. have utilized methyl red dye as a photosensitizer on ZnO for phenol degradation under visible-light irradiation [16]. They reported that the photocatalytic activity of ZnO increased from 0.1% phenol degradation to 4.1%, 6.8%, and 6.4% phenol degradation with the addition of 1%, 2%, and 3% methyl red, respectively. In another study, Kim et al. reported that they loaded dye-sensitized TiO_2

simultaneously with Pt and Al_2O_3 overlayer ($Al_2O_3/TiO_2/Pt$) for photocatalytic activity under visible-light irradiation [17]. These materials have significantly enhanced the visible-light activities for the production of H_2 (in the presence of ethylenediaminetetraacetic acid (EDTA) as an electron donor) and the dechlorination of CCl_4.

Among these, the most relevant photosensitizers belong to the families of inorganic sensitizers, coordination metal complexes, organic dyes, and organic dyes with molecular complex structures.

For the first type, the use of inorganic sensitizers involves semiconductors with narrow band gaps suitable for the absorption of visible light. Among the main physical properties of these compounds are their high stability toward the photocorrosion process and their absorption in a wide wavelength region. Inorganic sensitizers with substantial performance include metal ions of transition series such as V, Cr, Mn, Fe, and Ni as well as metallic alloys of the type Pt-Au and Au-Ag. The second type, such as coordination metal complexes, is a type of sensitizer widely used owing to its high efficiency to extend the absorption region of TiO_2. Mostly, ruthenium and osmium complexes have been intensely used for this purpose.

A dye-sensitized solar cell (DSSC) is a semiconductor-based photovoltaic device that directly converts both artificial and natural (solar) radiation into electric current. The sensitization of a semiconductor has been used for different technological purposes such as the development of solar cells, H_2 production by H_2O splitting, and degradation of organic dyes coming from industrial effluents [14,15]. DSSC has three main components:

1. The dye which absorbs solar energy to generate excitons.
2. Nanostructured metal oxide (photoanode) which captures electrons from the dye.
3. Redox electrolyte which transports ēs and holes from the metal oxide and oxidized dyes to electrodes. Thus, the conversion efficiency of DSSC is mainly influenced by transparent conductive oxide (TCO) (photoanode), sensitizer (dye), electrolyte, electrodes, etc.

4.6.1 Disadvantage of dye-sensitized semiconductors and dye-sensitized solar cell

Noble metal-based sensitizers including ruthenium, osmium, and rhenium exhibit high efficiency, but their high cost and difficult synthesis limit their wide applications. Furthermore, to reduce the cost of fabrication of DSSCs, researchers are concentrating their interest on organic sensitizers. Organic dyes have provided numerous options in this respect as improving their molecular structure brings about improvement in the light-harvesting ability of the dyes, and with the help of such dyes, optimal DSSCs have been fabricated [18]. An important disadvantage of the sensitization of semiconductors

with an organic dye is its instability that causes the gradual decomposition of organic dye molecules by photocatalytic degradation due to the natural tendency of the organic dyes to undergo redox reactions. To solve this problem, the incorporation of electron donors into the reaction medium can be an effective solution. For example, EDTA is used as an effective electron donor. Moreover, to reduce the cost of DSSCs, researchers are also focusing on natural sensitizers, such as betacyanin and anthocyanin or chlorophyll, as they are easy to prepare, cost-effective, and environmentally friendly. However, these natural sensitizers are less efficient.

DSSCs are not yet considered an option for large-scale deployments where higher-cost higher-efficiency cells are more viable. DSSCs are not yet manufactured at a commercial scale. Another major drawback is the electrolyte solution, which sometimes contains volatile organic solvents. To avoid evaporation, the container must be carefully sealed.

4.7 Coupled semiconductors

The coupling (Fig. 4.6) of two or more nanocrystalline semiconductors allows the design of semiconductors heterostructures that are potentially useful in photocatalytic reactions, such as water splitting, microelectronics, and electrode materials [8,9,19]. Coupled semiconductors are also called composite semiconductors. The advantage of using coupled semiconductors is twofold:

1. To extend the photoresponse by coupling a large band-gap semiconductor with a narrow band-gap semiconductor.
2. To retard the recombination of photogenerated charge carriers by injecting electrons into the lower-lying CB of the large band-gap energy semiconductor.

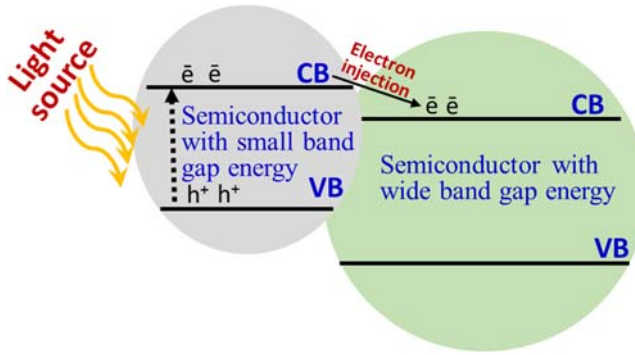

FIGURE 4.6 Electron transfer mechanism and $\bar{e}-h^{+}$ separation in the coupled semiconductors.

A successful coupling of the two semiconductors should meet the following conditions:

1. The semiconductors should be photocorrosion-free.
2. The small band-gap semiconductor should be excited by visible-light.
3. The CB of the small band-gap semiconductor should be more negative than that of the large band-gap semiconductor.
4. The CB of the large band-gap semiconductor should be more negative than the CO_2 redox potential.
5. The electron injection should be fast as well as efficient.

To improve the photocatalytic capacity of the semiconductors, it is important to develop visible-light-active photocatalysts that can harvest a wide range of photons in the solar spectrum. In general, a decrease in the band-gap energy of the photocatalyst increases the absorption of visible-light photons. Then, the redox potentials of CB and VB are compromised in the process to delay the recombination of electrons and holes. This feature affects the yield of photocatalytic reactions including the degradation of organic pollutant contaminants. Hence, it is desirable to develop photocatalytic systems which are capable of absorbing visible-light without compromising the redox potentials of CB and VB of the semiconductors. Recently, considerably enhanced activities of diode structures made of n- and p-type semiconductors were successfully established compared to individual semiconductors. The improved performance of such coupled systems (Fig. 4.6) was attributed to

1. The coupling of semiconductors with distinctive band-gap energies (low and high) for the extension of the spectral range of light absorption,
2. formation of p−n junction between the coupled photocatalysts to facilitate the separation of electron-hole pairs (for the least recombination of photoexcited electron-hole pairs), and
3. retaining the high redox potentials of the individual semiconductors in the coupled semiconductor system so that reactions can take place simultaneously at different semiconductor surfaces to activate redox reactions.

The applicability of the coupled semiconductors with various combinations has been explored to facilitate visible-light absorption and efficient charge carrier separation. A small band-gap energy semiconductor ($CaFe_2O_4$) can be coupled with a large band-gap energy semiconductor (such as TaON, ZnO, TiO_2, and Ag_3VO_4) to assist in light absorption and the separation of charge carriers. Other examples of coupled semiconductors are $CoFe_2O_4/TiO_2$, $BiOI/TiO_2$, WO_3/TiO_2, $ZnFe_2O_4/TiO_2$, ZnO/CuO, $Sm_2Ti_2O_7/SmCrO_3$, $BiOI/BiPO_4$, ZnO/SnO_2, and $CaBi_6O_{10}/Bi_2O_3$. Thin film of SnO_2/TiO_2 coupled semiconductors was also effectively employed for the photocatalytic degradation of azo dyes [8,9,19].

In addition to binary coupled semiconductors, ternary coupled heterostructured composite photocatalysts, such as $AgIO_3/AgI/TiO_2$, $AgBr-Ag-Bi_2WO_6$,

$MgO/ZnO/In_2O_3$, $Pt/TiO_2 - {}_xN_x/SrTiO_3$, and $BiVO_4{-}Cu_2O{-}TiO_2$, have also been explored to attain the improvement of photocatalytic degradation activity or synergic effects, such as enhanced light absorption and charge transfer along with the least $\bar{e}{-}h^+$ recombination.

4.8 Defective semiconductors

Defects can be a bonus as well as a curse for semiconductors. They depend on the origin, synthesis method, usage, and applications. Defects can be divided into different classes according to their dimensionality. Thus, zero (point defect), one- (line defect), two- (plane defect), and three- (volume defect) dimensional defects may be found in semiconductors. Each defect has its own significance and is considered accordingly although two- and three-dimensional defects have been taken together as these two types of defects show similar behavior. Moreover, the performance of two- and three-dimensional defects can be considered to be extensions of zero- and one-dimensional behaviors [9,20,21].

Therefore, defective semiconductors such as defective TiO_2 (Fig. 4.7) can be made visible-light-active either by introducing structural defects such as Ti^{3+} formation (low-valent ion formation) and oxygen vacancies or by incorporation of non-metals such as N, C, and S, and transition as well as rare-earth ions. These defects and dopants create sub-band states (defect states) in the band gap of TiO_2 and shift the absorption edge of TiO_2 toward the visible-light region of the electromagnetic spectrum, thereby, enhancing the visible-light photocatalytic activity of the semiconductors. Structural defects, formed by doping, can effectively tune the band structure and control the photocatalytic activity. For example, Fe, Ce-codoped TiO_2, doping of these

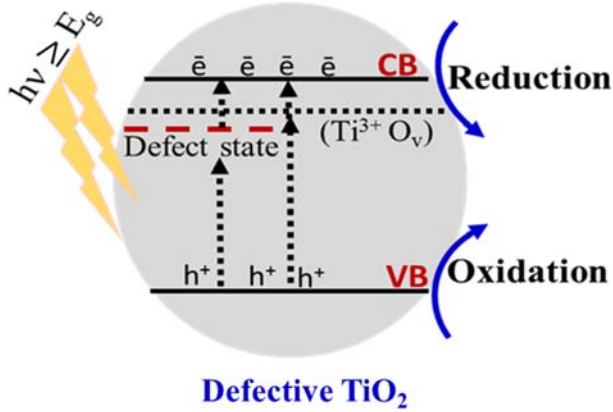

FIGURE 4.7 Defective TiO_2 showing the formation of $\bar{e}{-}h^+$ pairs, Ti^{3+} formation, and oxygen vacancy.

ions leads to the formation of grain boundary defects which result in the bending of the VB and CB. These defects limit electron mobility to the interface and prevent charge carrier recombination.

The introduction of defects into metal oxides appears to be a promising approach for shifting the optical absorption edge to lower energies, thereby, increasing the absorption in the visible-light region of the electromagnetic region. In conclusion, defects in the metal oxide nanostructures are caused mainly by the formation of low-valent cations as well as oxygen vacancies, which affect the band-gap narrowing significantly [7,20,21].

4.9 Chalcogenides

Chalcogenides have emerged as promising materials for visible-light-induced photocatalysis as they are well-known for their narrow band-gap energy. Chalcogenides are compounds consisting of at least one chalcogen anion (S^{2-}, Se^{2-}, or Te^{2-}) and at least one electropositive element [22,23]. Furthermore, they have drawn significant attention due to their great and highly demanded properties including narrow band-gap energy, non-toxic, bio-compatibility, low cost, and facile synthesis. In short, chalcogenides are narrow band-gap semiconductors that have been widely used as photocatalysts. These narrow band-gap materials allow more efficient absorption of over 40% of solar energy in the visible-light range which will eventually improve its photocatalytic properties. Upon visible-light irradiation, these materials generate electron and hole ($\bar{e}-h^+$) pairs. The photogenerated $\bar{e}-h^+$ pairs have been utilized to split water into H_2 and O_2 gas to remove and degrade industrial, pharmaceutical, and agricultural organic/inorganic/biological pollutants that have been accumulated in the environment [22–25].

Metal cations of the metal sulfide semiconductor catalysts mostly have d^0, d^5, and d^{10} electron configurations in which *d* and *sp* orbitals together form the CB, while the VB is composed of S 3p orbitals. As the 3p orbital of S is more negative than the 2p orbital of O, the VB position of the metal sulfide is higher than that of the metal oxide with a narrower band-gap structure.

For example, cadmium sulfide (CdS) and cadmium selenide (CdSe) are typical chalcogenides quantum dot materials. Their quantum size effect can lead to more separation of CB and VB energy levels which reduce the recombination rate of photogenerated carriers to a great extent, thus, improving the photocatalytic activity. CdS NPs show strong absorption in the visible-light spectrum because of the ideal band-gap energy of $\sim$2.4 eV. The band-gap width of CdSe is $\sim$1.7 eV, which is smaller than that of CdS and can utilize more sunlight. Under the influence of the quantum limiting effect, the CB potential of CdSe becomes more negative with the decrease of particle size, so it has a greater driving force for photocatalytic hydrogen reduction. Table 4.2 shows the band-gap energies of the chalcogenides which make them responsive to visible-light irradiation [22–25].

TABLE 4.2 Chalcogenides and their corresponding band-gap energies.

S. No.	Transition metal chalcogenides	E_g (eV)tc[a]
1	MoS_2	1.8
2	$MoSe_2$	2.0
3	WS_2	2.4
4	WSe_2	2.3
5	ZnSe	2.0
6	CdS	2.3
7	CdSe	1.2
8	CuS	2.1
9	Ba_2ZnSe_3	2.75
10	Cu_2WS_4	2.15
11	$Cu_2ZnSnSe_4$	1.4
12	Cu_2FeSnS_4	1.4

[a]*Approximate band-gap energy.*

4.10 Ternary compounds

In recent years, novel ternary metal chalcogenides have raised extensive attention of researchers. Various metalates, oxysulfides, oxyhalides, and oxynitrides can be classified as photocatalytic ternary semiconductors which can be activated with visible-light irradiation. Many of these compounds have been mainly investigated for O_2 and H_2 evolution from H_2O splitting. Other than that photocatalytic degradation of organic pollutants has also been carried out under visible or solar light irradiation. Aluminates, ferrites, niobates, tantalates, titanates, tungstates, and vanadates are some examples of metalates that have been tested as photocatalytic semiconductors for the degradation of different organic dyes, mainly MB, rhodamine B (RhB), and methyl orange (MO), among others [8,9].

Aluminates, such as $ZnAl_2O_4$ and $AgAlO_2$, have a band-gap energy of 4.11 and 3.2 eV, respectively. These aluminates presented lower activity in the visible region due to their wide band gap. However, ferrites, such as $ZnFe_2O_4$ and $BiFeO_3$, have been investigated for the photocatalytic degradation of organic pollutants. The photocatalytic activity of $ZnFe_2O_4$ ($E_g = \sim 1.9$ eV) was tested for the degradation of phenol under solar light and artificial UV light irradiation, while the activity of $BiFeO_3$ was investigated for the decomposition of MO under UV and visible-light irradiation. However, this catalyst showed efficient photocatalytic activity only under UV light irradiation.

On the other hand, several niobates, tantalates, and titanates possess layered perovskite structures in which they can also be activated with visible light, especially for H_2O splitting. A few selected examples are $Ca_2Nb_2O_7$, $Ba_5Nb_4O_{15}$, $NaTaO_3$, $KTaO_3$, $AgTaO_3$, $KTaO_3$, $Ca_2Ta_2O_7$, $Sr_2Ta_2O_7$, $CaTiO_3$, and $SrTiO_3$. Out of these examples, $KTaO_3$ and $SrTiO_3$ have high negative CB levels (-0.3 to 0.4 V versus Normal Hydrogen Electrode (NHE)) which can split H_2O into H_2 and O_2. Moreover, $SrTiO_3$ is also active in the reduction of NO_3^- using water as an electron donor.

Furthermore, oxysulfides, oxyhalides, and oxynitrides can also induce a significant increase in visible-light absorption. For example, tantalum oxynitride (TaON) exhibits a narrow band gap of ~ 2.5 eV. Under visible-light irradiation, TaON enabled the effective evolution of H_2 and O_2 from the methanol and $AgNO_3$ solution [8,9,26,27].

The AB_mC_n-type metal chalcogenides, such as cubic spinel structure (AB_2X_4) and chalcopyrite structure (ABX_2), have good stability and high catalytic activity under visible-light irradiation. For example, the ternary sulfur compound, $ZnIn_2S_4$, is a novel photocatalytic material with three common crystal structures: cubic phase, hexagonal phase, and rhombohedral phase. The band-gap energy of $ZnIn_2S_4$ is relatively narrow ($2.06-2.85$ eV) with a good visible-light response, appropriate band structure, and lower environmental toxicity.

$CuInS_2$ is an I-III-VI-type direct band-gap semiconductor with a band-gap width of about 1.45 eV. It has a high light absorption coefficient (10^{-5} cm^{-1}) in the visible-light region, does not contain toxic elements, and has special radiation intensity absorption and superior defect tolerance. $CuInS_2$ is usually composed of the chalcopyrite sphalerite and wurtzite phase, which corresponds to different optical properties.

4.11 Quaternary compounds

Various metalates, oxysulfides, oxyhalides, and oxynitrides can be classified as photocatalytic quaternary semiconductors in which they can be activated by visible-light irradiation. Many of these compounds have been mainly investigated for O_2 and H_2 evolution from H_2O splitting. Oxides, oxynitrides, oxysulfides, and oxyhalides as quaternary compounds have also been investigated for the evaluation of their photocatalytic activity for photocatalytic degradation of organic pollutants and H_2O splitting. Photocatalytic materials applied for environmental remediation or H_2O splitting include a wide range of semiconductor materials such as binary, ternary, and quaternary semiconductors. Additionally, many sulfides, nitrides, and oxynitrides (CdS, Ta_3N_5, and LaTiON) have also been investigated as alternative materials to TiO_2 for visible-light or solar photocatalysis. Oxynitrides such as LaTiON and oxysulfides such as $Sm_2Ti_2S_2O_5$ can also effectively harvest visible light and exhibit higher photocatalytic activity for H_2O splitting and organic contaminant degradation than their oxide counterparts.

Among the non-metal elements, S can often completely replace O to convert an oxide into a sulfide, because both O and S belong to group 16. A series of sulfides has been reported, for example, $AgInZn_7S_9$ and $ZnIn_2S_4$, in which the visible-light absorption is better than their oxide analogs. These sulfides, thus, exhibit high photocatalytic activity for the evolution of H_2 under visible-light irradiation [8,9,23,26,27].

Bi-based layered oxyhalides were also tested for the photocatalytic degradation of MO under UV and visible-light illumination. Bi_4NbO_8Cl (E_g = 2.38 eV) showed an excellent visible-light efficiency and was more active than the ternary oxychloride Bi_3O_4Cl (E_g = 2.80 eV). Meanwhile, $Na_{0.5}Bi_{1.5}O_2Cl$ with a band-gap energy of 3.04 eV was more efficient than BiOCl (E_g = 3.44 eV) under visible-light illumination but less active under UV light. Table 4.3 summarizes some of the quaternary semiconductors with their respective band-gap energy which is active under visible-light irradiation.

Zhang et al. have reported $K_2FeCu_3Q_4$ (where Q = S and Se) as a new photocatalyst for the counter electrodes in the DSSCs system. The as-prepared $K_2FeCu_3Q_4$ possessed suitable energy band alignments and showed a robust electrocatalytic activity for triiodide reduction [15].

4.12 Characteristics of visible-light active photocatalysts

Solar energy is the richest energy source on earth, which has enormous potential for the fulfillment of total energy requirements. Since the UV light

TABLE 4.3 Quaternary semiconductors with their respective band-gap energy.

Semiconductor	Band-gap energy (eV)[a]
Bi_4NbO_8Cl	2.38
$PbBi_2Nb_2O_9$	2.88
$LaTaO_2N$	2.00
$LaTiO_2N$	2.10
$Y_2Ta_2O_5N_2$	2.20
Cu_2ZnSnS_4	1.40–1.60
$AgInZn_7S_9$	2.30
Ag_2SrSiS_4	2.08
Ag_2SrGeS_4	1.73

[a]*Approximate band-gap energy.*

only occupies a small portion of the sunlight and a large part of solar energy cannot be utilized using UV-light active materials, producing visible-light-active materials is preferred. Hence, there is a growing interest in designing semiconductor photocatalysts that can utilize visible light [3,4,7–9,27–29]. Following are a few characteristics of a visible-light active photocatalyst:

1. Large surface area to volume ratio
2. Superior light absorption or harvesting
3. Efficient charge separation
4. Narrow band-gap energy
5. Long lifetime of charge separation
6. Higher photostability
7. Economical.

4.13 Photocatalysis under visible-light irradiation

By taking into consideration that visible light makes up to 44% of the entire solar spectrum, the development of visible-light-active photocatalysts is a crucial necessity by combining with optimized structural modification to achieve long-lived charge carriers for various applications. Most of the widely used photocatalytic materials including ZnO and TiO_2 are wide-band-gap semiconductors and cannot directly absorb visible light. To shift the band gap to the visible-light region, there are numerous methods utilized, including doping, metal decoration, dye sensitizing, fabrication of defective, ternary, and quaternary compounds as well as the formation of heterojunctions as mentioned above.

In the semiconductors, the absorption of light photons generates electron-hole ($\bar{e}$–h^+) pairs within the bulk which dissociate into free photoelectrons ($\bar{e}$) in the CB and photo holes (h^+) in the VB. These $\bar{e}$s and h^+s can recombine on the surface or in the bulk of the particle releasing the energy as heat. Also, these $\bar{e}$s and h^+s can migrate to the surface where they can react with the adsorbed molecules (H_2O and O_2) on the surface of the particle. In the presence of adsorbed H_2O, electrons transfer from the H_2O molecule to the positive holes produces $^{\bullet}OH$ free radicals. This step is the direct oxidation by the holes or primary reaction. These powerful oxidants ($^{\bullet}OH$) react with the organic and toxic compounds and oxidize them. Similarly, the adsorbed O_2 reacts with the excited $\bar{e}$s in the CB and produces $O_2^{\bullet-}$ free radicals. This is the direct reduction by $\bar{e}$s or primary reaction. These $O_2^{\bullet-}$ free radicals are powerful oxidants and react with the organic pollutants and oxidize them into harmless end products such as H_2O and CO_2 (Fig. 4.8) [3,7–9].

These $^{\bullet}OH$ and $O_2^{\bullet-}$ free radicals play an important role in initiating oxidation reactions, especially for substances that weakly adsorb on the surface of the semiconductors. The adsorbed pollutants get completely oxidized

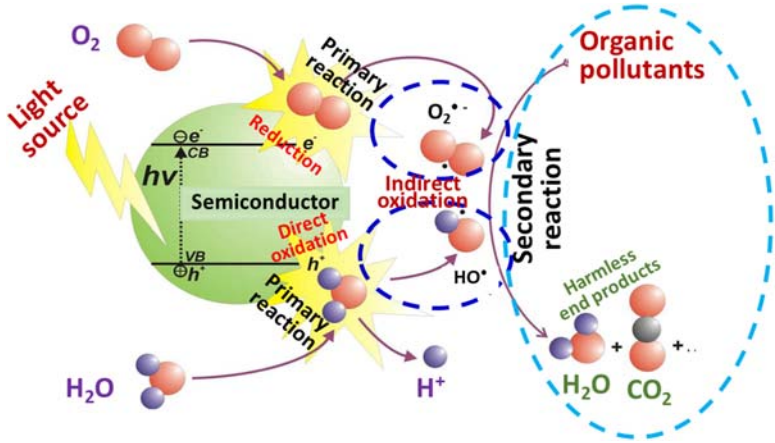

FIGURE 4.8 Photocatalytic reactions at the surface of semiconductors are induced by visible-light irradiation.

using $^{\bullet}OH$ and $O_2^{\bullet-}$ free radicals into harmless end products, i.e., H_2O and CO_2. This oxidation pathway is known as indirect oxidation or secondary reaction. The efficiency of a photocatalyst depends on the competition of different interface charge carriers' transfer processes involving electrons and holes and their deactivation by recombination. The efficiency of photocatalysis also depends on how well one can prevent the charge recombination, i.e., electrons and holes from recombining.

4.14 Parameters affecting the photocatalytic process

The photocatalytic activity of a semiconductor photocatalyst depends on several parameters. These are intrinsic and extrinsic parameters of the photocatalytic semiconductors [3,7–9,27–29]. These parameters affect the kinetics and mechanisms of photocatalytic reactions in aqueous media.

Following are the intrinsic parameters that affect the photocatalytic reactions:

- Crystallographic phase,
- crystallite size and particle size,
- surface area
- nature of the photocatalyst (the ability of the material to absorb and utilize the light)
- presence of dopants,
- impurities (type and amount),
- vacancies, and
- different surface states.

Following are the extrinsic parameters that affect the photocatalytic reactions:

1. Surrounding environment
2. Photocatalytic reaction conditions:
   a. pH of the solution,
   b. type of pollutants,
   c. the initial concentration of pollutants
   d. light intensity,
   e. catalyst dosage,
   f. flow rate,
   g. support, and
   h. utilization of sacrificial reagents.

4.15 Summary

This chapter includes different types of visible-light active photocatalytic semiconducting materials with an emphasis on the photocatalytic mechanism. Moreover, the possible reaction pathways occurring during the visible or solar photocatalytic processes are highlighted. The optical response of the photocatalysts into the visible-light region through surface modification/decoration, doping with non-metals or metals, coupling, sensitization, defect formation, etc. has been discussed. The characteristics of visible-light active semiconducting materials have also been discussed. This chapter also discusses the principles of photocatalysis that take place using narrow band-gap energy photocatalytic materials. In conclusion, a visible-light active photocatalyst must possess certain desirable characteristics, which regulate the photocatalytic performance for efficient photocatalytic applications.

References

[1] N. Serpone, A.V. Emeline, Semiconductor photocatalysis – past, present, and future outlook, Journal of Physical Chemistry Letters 3 (2012) 673–677. Available from: https://doi.org/10.1021/jz300071j.

[2] M.M. Khan, S.F. Adil, A. Al-Mayouf, Metal oxides as photocatalysts, Journal of Saudi Chemical Society 19 (2015) 462–464. Available from: https://doi.org/10.1016/j.jscs.2015.04.003.

[3] M.M. Khan, Metal Oxide Powder Photocatalysts, Elsevier Ltd., 2018. Available from: https://doi.org/10.1016/B978-0-08-101977-1.00002-8.

[4] Ş. Neaţu, J.A. Maciá-Agulló, H. Garcia, Solar light photocatalytic CO_2 reduction: general considerations and selected bench-mark photocatalysts, International Journal of Molecular Sciences 15 (2014) 5246–5262. Available from: https://doi.org/10.3390/ijms15045246.

[5] H.-C. Yang, H.-Y. Lin, Y.-S. Chien, J.C.-S. Wu, H.-H. Wu, Mesoporous TiO_2/SBA-15, and Cu/TiO_2/SBA-15 composite photocatalysts for photoreduction of CO_2 to methanol, Catalysis Letters 131 (2009) 381–387. Available from: https://doi.org/10.1007/s10562-009-0076-y.

[6] L. Mohapatra, K. Parida, A review of solar and visible light active oxo-bridged materials for energy and environment, Catalysis Science and Technology 7 (2017) 2153−2164. Available from: https://doi.org/10.1039/c7cy00116a.

[7] M.M. Khan, Principles and mechanisms of photocatalysis, Photocatalytic Systems by Design, Elsevier, 2021, pp. 1−22. Available from: https://doi.org/10.1016/B978-0-12-820532-7.00008-4.

[8] M.M. Khan, D. Pradhan, Y. Sohn, Nanocomposites for Visible Light-Induced Photocatalysis, Springer International Publishing, Cham, 2017. Available from: https://doi.org/10.1007/978-3-319-62446-4.

[9] A. Hernández-Ramírez, I. Medina-Ramírez, Photocatalytic Semiconductors: Synthesis, Characterization, and Environmental Applications, 2015. https://doi.org/10.1007/978-3-319-10999-2.

[10] G.H. Waly, Effect of incorporating undoped or silver-doped photocatalytic titanium dioxide on the antifungal effect and dynamic viscoelastic properties of long-term acrylic denture liners, Future Dental Journal 4 (2018) 8−15. Available from: https://doi.org/10.1016/j.fdj.2018.03.002.

[11] X. Zong, C. Sun, H. Yu, Z.G. Chen, Z. Xing, D. Ye, et al., Activation of photocatalytic water oxidation on N-doped ZnO bundle-like nanoparticles under visible light, Journal of Physical Chemistry C 117 (2013) 4937−4942. Available from: https://doi.org/10.1021/jp311729b.

[12] E. Prabakaran, K. Pillay, Synthesis of N-doped ZnO nanoparticles with cabbage morphology as a catalyst for the efficient photocatalytic degradation of methylene blue under UV and visible light, RSC Advances 9 (2019) 7509−7535. Available from: https://doi.org/10.1039/C8RA09962F.

[13] S.A. Ansari, M.M. Khan, M.O. Ansari, M.H. Cho, Nitrogen-doped titanium dioxide (N-doped TiO_2) for visible light photocatalysis, New Journal of Chemistry 40 (2016) 3000−3009. Available from: https://doi.org/10.1039/C5NJ03478G.

[14] T.H. Meen, J.K. Tsai, Y.S. Tu, T.C. Wu, W.D. Hsu, S.J. Chang, Optimization of the dye-sensitized solar cell performance by mechanical compression, Nanoscale Research Letters 9 (2014) 1−8. Available from: https://doi.org/10.1186/1556-276X-9-523.

[15] G. Zhang, M. Zhu, L. Zhai, J. Cao, Z. Gao, T. Zeng, $ThCr_2Si_2$-type quaternary chalcogenides as efficient Pt-free counter electrodes for dye-sensitized solar cells, Journal of Alloys and Compounds 817 (2020) 152797. Available from: https://doi.org/10.1016/j.jallcom.2019.152797.

[16] W.A. Nimpoeno, H.O. Lintang, L. Yuliati, Methyl red dye-sensitized zinc oxide as photocatalyst for phenol degradation under visible light, in: AIP Conference Proceedings, American Institute of Physics Inc., 2020, p. 020048. https://doi.org/10.1063/5.0005797.

[17] W. Kim, T. Tachikawa, T. Majima, W. Choi, Photocatalysis of dye-sensitized TiO_2 nanoparticles with thin overcoat of Al_2O_3: enhanced activity for H_2 production and dechlorination of CCl_4, The Journal of Physical Chemistry C 113 (2009) 10603−10609. Available from: https://doi.org/10.1021/jp9008114.

[18] P. Chawla, M. Tripathi, Novel improvements in the sensitizers of dye-sensitized solar cells for enhancement in efficiency—a review, International Journal of Energy Research 39 (2015). Available from: https://doi.org/10.1002/er.3366. n/a-n/a.

[19] A. di Paola, L. Palmisano, A.M. Venezia, V. Augugliaro, Coupled semiconductor systems for photocatalysis. preparation and characterization of polycrystalline mixed WO_3/WS_2 powders, The Journal of Physical Chemistry B 103 (1999) 8236−8244. Available from: https://doi.org/10.1021/jp9911797.

[20] S. Boston, Defects in semiconductors, in: The Materials Science of Semiconductors, 2008. https://doi.org/10.1515/9783110289039.734.

[21] R. Schmitt, A. Nenning, O. Kraynis, R. Korobko, A.I. Frenkel, I. Lubomirsky, et al., A review of defect structure and chemistry in ceria and its solid solutions, Chemical Society Reviews 49 (2020) 554–592. Available from: https://doi.org/10.1039/c9cs00588a.

[22] A. Rahman, M.M. Khan, Chalcogenides as photocatalysts, New Journal of Chemistry 45 (2021) 19622–19635. Available from: https://doi.org/10.1039/D1NJ04346C.

[23] M.M. Khan (Ed.), Chalcogenide-Based Nanomaterials as Photocatalysts, first ed., Elsevier, 2021. Available from: https://doi.org/10.1016/C2019-0-01819-5.

[24] Y.I. Choi, S. Lee, S.K. Kim, Y. Kim, D.W. Cho, M.M. Khan, et al., Fabrication of ZnO, ZnS, Ag-ZnS, and Au-ZnS microspheres for photocatalytic activities, CO oxidation and 2-hydroxyterephthalic acid synthesis, Journal of Alloys and Compounds 675 (2016) 46–56. Available from: https://doi.org/10.1016/j.jallcom.2016.03.070.

[25] M.E. Khan, M.M. Khan, M.H. Cho, CdS-graphene nanocomposite for efficient visible-light-driven photocatalytic and photoelectrochemical applications, Journal of Colloid and Interface Science 482 (2016) 221–232. Available from: https://doi.org/10.1016/j.jcis.2016.07.070.

[26] M. Hojamberdiev, Y. Cai, J.J.M. Vequizo, M.M. Khan, R. Vargas, K. Yubuta, et al., Binary flux-promoted formation of trigonal $ZnIn_2S_4$ layered crystals using ZnS-containing industrial waste and their photocatalytic performance for H_2 production, Green Chemistry 20 (2018) 3845–3856. Available from: https://doi.org/10.1039/C8GC01746H.

[27] S. Ghosh, Visible-Light Active Photocatalysis – Research and Technological Research Frontiers in Solar Light Harvesting, (n.d.).

[28] J. You, Y. Guo, R. Guo, X. Liu, A review of visible light-active photocatalysts for water disinfection: features and prospects, Chemical Engineering Journal 373 (2019) 624–641. Available from: https://doi.org/10.1016/j.cej.2019.05.071.

[29] K.R. Tolod, S. Hernández, E.A. Quadrelli, N. Russo, Visible light-driven catalysts for water oxidation: toward solar fuel biorefineries, Studies in Surface Science and Catalysis 178 (2019) 65–84. Available from: https://doi.org/10.1016/B978-0-444-64127-4.00004-5.

Chapter 5

Synthesis methods for photocatalytic materials

Mohammad Mansoob Khan

5.1 Introduction

The characteristics of materials are very crucial for deciding the fate of photocatalytic semiconductor materials in terms of use and applications. Therefore, the synthesis methods used are crucial to developing semiconductor photocatalysts with desirable characteristics. Several methods have been developed to produce photocatalytic semiconductor materials. In general, two synthesis approaches have been identified which are known as top-down and bottom-up approaches as illustrated in Fig. 5.1. The top-down comprises milling, lithography, repeated quenching, etc. This approach does not have good control of the particle size and structure; hence, the characteristics of the materials are quite difficult to control. A bottom-up method is an approach that is mostly used by researchers for the synthesis of photocatalytic semiconductor materials as this approach involves building up material from the bottom, that is, atom-by-atom, molecule-by-molecule, and cluster-by-cluster. Several chemical routes have been identified to synthesize the colloidal metal nanoparticles (NPs) from different precursors using chemical reductants in different solvents such as aqueous solvents and nonaqueous solvents. The chemical and biological routes that have been studied for various applications include precipitation, sol−gel, hydrothermal, sonochemical, and green synthesis method.

In the synthesis of NPs, control of the size and morphology of nanomaterials are very important. The size, shape, and morphology-controlled synthesis of NPs is crucial and has emerged as an efficient strategy not only for the optimization of desired properties but also to investigate and solve structure-performance relationships. Solution-phase synthesis methods based on the reduction or decomposition of precursors to generate the desired growth species have been successful in the synthesis of NPs with controlled physical and chemical features. However, the synthesis of

Theoretical Concepts of Photocatalysis. DOI: https://doi.org/10.1016/B978-0-323-95191-3.00006-7

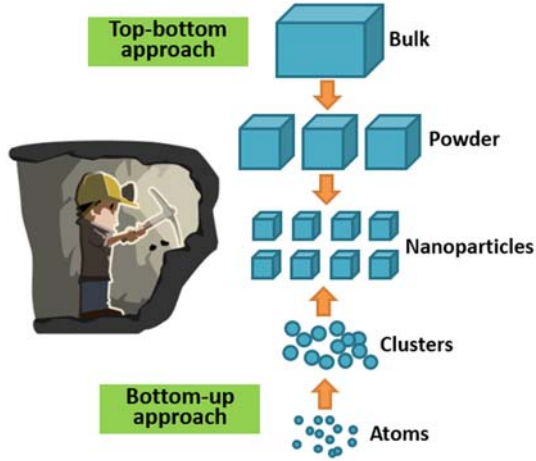

FIGURE 5.1 Top-bottom and bottom-up approaches for fabrication of photocatalyst.

really controlled NPs can require relatively high temperature and it is limited in terms of versatility.

Moreover, there is still a need for synthetic approaches that are relatively simple, robust, and scalable for fabricating-controlled NPs. Although controlled NPs could be obtained in some cases, however, control of size and shape can be very challenging owing to the slow molecular and ion diffusion as well as different reactivities of precursors in the relative solid to liquid phases. Therefore, Oliveira et al. have proposed a mechano-colloidal approach to generate the target NPs morphology [1].

The following headings discuss some of the selected synthesis methods such as the sol−gel method, hydrothermal method, microwave method, sonochemical method, chemical vapor deposition (CVD), physical vapor deposition (PVD), and green synthesis method for photocatalytic semiconductor materials.

5.2 Sol−gel method

The term sol-gel refers to a process in which solid NPs are dispersed in a liquid (a sol) which agglomerate together to form a continuous three-dimensional network extending throughout the liquid (a gel). It is a wet-chemical method that uses either a chemical solution (sol short for solution) or colloidal particles (sol for nanoscale particle) to produce an integrated network (gel). The process involves the conversion of monomers into a colloidal solution (sol) that acts as the precursor for an integrated network (or gel) of either discrete particles or network polymers. It is a method for producing solid materials from small molecules. It is used for the fabrication of metal

NPs, and semiconductors such as metal oxides, especially the oxides of titanium and silicon.

In materials science, the sol-gel process is a method for producing solid materials from small atoms or molecules, that is, a bottom-up approach. Typical precursors in the sol-gel method are metal alkoxides. The precursor sol can either be deposited on a substrate to form a film (e.g., by dip-coating or spin coating), cast into a suitable container with the desired shape (e.g., to obtain monolithic ceramics, glasses, fibers, membranes, aerogels), or used to synthesize powders (e.g., microspheres, nanospheres). The process is summarized in Fig. 5.2.

The sol−gel method involves two main reactions: hydrolysis of the precursor in the acidic or basic mediums and polycondensation of the hydrolyzed products. In general, the sol−gel method can be defined as the conversion of a precursor solution into an inorganic solid via inorganic polymerization reactions induced by water. It uses a precursor and aqueous or alcoholic mixture of metalorganic (alkoxides) or inorganic salts (chloride, nitrate, sulfate, acetate, etc.). The sol−gel method consists of the following steps:

1. preparation of a homogeneous solution of precursors,
2. conversion of the homogeneous solution into a sol by treatment with a suitable reagent (generally water with or without any acid/base),
3. gelation via a polycondensation or polyesterification
4. gel aging, which causes the gel network to contract, as well as phase transformations and Ostwald ripening,
5. shaping and drying of the gel which removes liquid phases which may lead to fundamental changes in the structure of the gel, and
6. thermal treatment $\sim 500^{\circ}C$ (sintering) which leads to the desired ceramic material.

The precursors are hydrolyzed and condensed to form inorganic polymers composed of metal-oxygen-metal (M-O-M) bonds (Fig. 5.2). Further condensation results in a gel. The gel can be dried under hypercritical conditions and aerogels are produced. When the gel is dried under ambient conditions, a xerogel is obtained. The gel is then thermally treated to yield the desired material and several forms such as monoliths, films, fibers, and monosized powders can be shaped [2,3].

For example, the synthesis of TiO_2 NPs using the sol−gel method at low temperatures and the ability to prepare TiO_2 of various morphologies. Titanium alkoxides or titanium halides are usually used as the titanium precursor in this method. First, the hydrolysis of titanium precursor forms a sol. After aging the sol for a certain time, a three-dimensional cross-linked gel is obtained, and amorphous white powder is obtained by grinding the gel. Finally, crystalline TiO_2 is obtained after calcination at a certain high temperature. Similarly, Shivaraju et al. synthesized N-doped TiO_2 via the

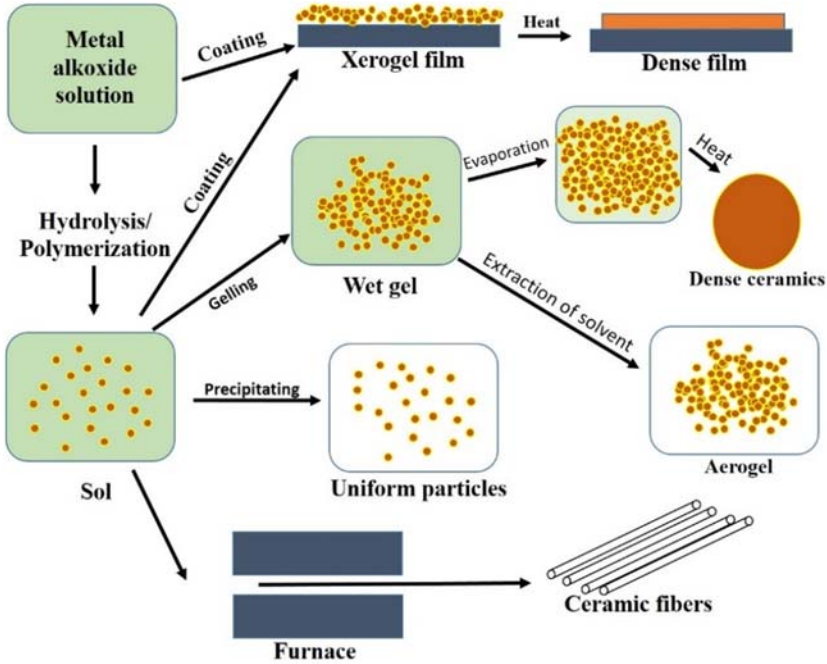

FIGURE 5.2 Schematic representation of the different stages of the sol−gel method to obtain different types of materials.

sol−gel technique using titanium tetra isopropoxide (TTIP) as the precursor and ammonia as the nitrogen source [4]. Arham et al. also reported the synthesis of Ni-doped SnO_2 via the same technique in which $SnCl_4$ and $NiCl_2$ were used as the starting materials [5]. Another example is the synthesis of visible light active material $BiVO_4$, using the same synthesis method. Two solutions were prepared: $Bi(NO_3)_3$ in HNO_3 mixed with citric acid (labeled as solution A) and NH_4VO_3 in distilled water mixed with citric acid (labeled as solution B). Both solutions were mixed and the pH was adjusted to 6.5 using ammonia solution. After stirring at moderate temperature (80°C), dark blue sol−gel was obtained [6].

Several approaches have been described to improve the control of the size and shape of sol−gel-prepared particles, including the addition of acid or base catalysts which can also permit the separation of hydrolysis and condensation processes. For instance, highly crystalline anatase TiO_2 with different triangular prismatic shapes, rectangular and rod-like elongated shapes, exposing different crystal surfaces, have been prepared by polycondensation of titanium alkoxides in the presence of tetramethylammonium hydroxide [7].

In this chemical procedure, a "sol" (a colloidal solution) is formed that then gradually changes to the formation of a gel-like diphasic system

containing both a liquid phase and solid phase whose morphologies range from discrete particles to continuous polymer networks. In the case of colloids, the volume fraction of particles (or particle density) may be so low that a significant amount of fluid may need to be removed initially for the gel-like properties to be recognized. This can be accomplished in several ways. The simplest method is to allow some time for sedimentation to take place, then pour off the residual liquid. Centrifugation can also be used to speed up the process of phase separation. The removal of the remaining liquid (solvent) phase requires a drying process, which is typically accompanied by a significant amount of shrinkage and densification. The rate at which the solvent can be removed is ultimately determined by the distribution of porosity in the gel. The ultimate microstructure of the final product strongly influences the changes imposed upon the structural template during this phase of processing. Subsequently, a thermal treatment is often required to accelerate further polycondensation and enhance mechanical properties and structural stability through final sintering, densification, and grain growth.

5.2.1 Advantages of the sol–gel method

1. It does not require complicated instruments and provides simple and easy means for preparing undoped, doped, and coupled nanomaterials.
2. One of the distinct advantages of using this methodology as compared to the traditional methods is that densification is often achieved at a much lower temperature.
3. Another great advantage of the sol–gel method is that during any stage of the process, it is possible to incorporate different types of dopants. The incorporation of an active dopant in the sol during the gelation stage allows doping elements to have direct interaction with the main material in such a way that the photocatalytic properties of the materials can be improved.
4. It can produce thin bond-coating to provide excellent adhesion between the metallic substrate and the top coat.
5. It can produce a thick coating to provide corrosion protection performance.
6. It can produce high-purity products because the precursor of the desired ceramic oxides can be mixed, dissolved in a specified solvent, and hydrolyzed into a sol, and subsequently to a gel.
7. It can easily shape materials into complex geometries in a gel state.
8. The composition can be highly controllable.
9. It can have low-temperature sintering capability, usually 200°C–600°C.
10. It can provide a simple, economic, and effective method to produce high-quality coatings.
11. It can provide high chemical homogeneity, particularly for the multicomponent system.

Depending on the specific application, the different stages in the sol−gel method can be extended, altered, or manipulated to respond to different needs. The concentration and type of precursor, the nature of the solvent, the pH of the solution, the type and concentration of additives (catalysts, surfactants, structure directing agents), the pre- and postheat treatment of the materials, and the aging time are all variables that can be controlled using the sol−gel method.

5.3 Hydrothermal method

The term hydrothermal usually refers to any heterogeneous reaction in the presence of aqueous solvents and/or mineralizers under high temperature and pressure or a process in water at high temperature and pressure. In short, the hydrothermal synthesis method can be defined as a method of synthesis of single crystals that depends on the solubility of the precursors in hot water under high pressure. The hydrothermal method is one of the liquid-phase chemical synthesis methods in which the main factors influencing the properties of the product are vessel volume, reaction temperature, heating rate, and reaction time.

This method is mostly used in the laboratory for the fabrication of nanomaterials. The crystal growth is performed in an apparatus consisting of a steel pressure vessel called an autoclave (Fig. 5.3) in which a nutrient is supplied along with water. A temperature gradient is maintained at the opposite ends of the growth chamber. At the hotter end, the nutrient and solute dissolve, while at the cooler end, products are deposited on a seed crystal which grows to the desired crystals. Using aqueous solution as the reaction system, through heating or other means, the target products can be synthesized in a sealed reaction vessel (autoclave) which creates an environment of high temperature and high pressure

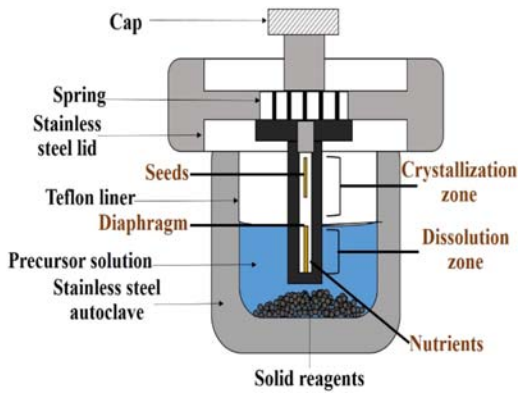

FIGURE 5.3 Schematic of the stainless steel autoclave with Teflon liner.

during the hydrothermal process. In this condition, with an increase in the water vapor pressure, the density and surface tension of materials decrease, and the ion products increase, leading to the fast dissolution and the recrystallization of the substances which can be dissolved in water at room temperature. The synthesis under hydrothermal conditions is usually performed below the supercritical temperature of water (374°C). In general, hydrothermal synthesis involves:

- An aqueous chemical process
- Starting precursors can be inexpensive oxides, hydroxides, chlorides, and nitrates
- Typical reaction temperature 100°C−374°C
- Pressure range 0−15 MPa
- The product is crystalline anhydrous powders with controlled particle size, particle shape, and stoichiometry. Calcination is not necessary

When selecting a suitable autoclave, the most important parameters are the experimental temperature, pressure, and corrosion resistance in that temperature-pressure range in a given solvent or hydrothermal fluid. If the reaction is taking place directly in the vessel, the corrosion resistance is a prime factor in the choice of the autoclave material. The most successful materials which are corrosion resistant are high-strength alloys, such as 300 series (austenitic) stainless steel, iron, nickel, cobalt-based superalloys as well as titanium and its alloys. An autoclave should be of good materials having the following characteristics:

- can bear high temperature
- can bear high pressure
- inert to acids, bases, and oxidizing agents.
- corrosion resistant
- should be of high-strength alloys, such as 300 series (austenitic) stainless steel, iron, nickel, cobalt-based superalloys, and titanium and its alloys
- it should be easily assembled and dissembled
- it should have sufficient length to obtain the desired temperature gradient
- it should be leak-proof at desired temperature and pressure.

Based on the above discussion and points, there are several types of autoclaves.

Types of autoclaves:

1. Gravity displacement type autoclave: It is the most commonly used type of autoclave in laboratories. It is available in various sizes and dimensions.
   a. Vertical type (small volume capacity)
   b. Horizontal autoclave (large volume capacity)
2. Positive pressure displacement type autoclave
3. Negative pressure (vacuum) displacement type.

Several researchers have been using the hydrothermal method to obtain NPs with desirable photocatalytic properties. For example:

1. TiO_2 NPs can be obtained by the hydrothermal method of peptized precipitates of a titanium precursor with water. The precipitates are prepared using titanium butoxide as a precursor in the presence of tetraalkylammonium hydroxide (peptizer). Under the same concentration of the peptizer, the particle size decreased with increasing alkyl chain length. The peptizers and their concentrations influenced the morphology of the particles. Furthermore, TiO_2 nanotubes have received increasing attention, and an extensive review on TiO_2-based nanotubes synthesized via hydrothermal technique has been recently published by Liu et al. In this article, the formation mechanism, structure modification, and photocatalytic applications of TiO_2 nanotubes have been discussed. The factors during the hydrothermal reaction that influence the formation of nanotubes (TiO_2 precursor, hydrothermal temperature, and duration), auxiliary methods (ultrasonication and microwave assistance), and posttreatment (acid washing and calcination) on the formation of TiO_2 nanotubes have been reviewed [2,3,8].
2. Hu et al. prepared Ag@SnO_2 using the hydrothermal method. Sodium stannate rehydrates and urea were dissolved in ultra-pure water, while silver nitrate and ammonium hydroxide were mixed. Two prepared solutions were mixed and transferred into a Teflon-lined autoclave and heated at 150°C [9].
3. Bi_2WO_6 nanoplates were obtained via the same synthesis method. The aqueous solution of sodium tungstate was normally stirred at room temperature. Bismuth nitrate was added followed by the addition of NaOH until the pH was 10. It was subsequently heated hydrothermally at 100°C−200°C and the obtained product was used for characterization and applications [10].
4. Chen et al. reported the synthesis of Se-doped MoS_2 using sodium molybdenum oxide dehydrates, L-cysteine, and Se powder via the hydrothermal method [11]. The hydrothermal process was performed at 200°C for 18 h. They reported that Se-doped MoS_2 exhibited enhanced photocatalytic degradation of Congo red with 95.4% degradation which is approximately 5.26−6.25 times higher compared to bulk MoS_2 (62.4%) and MoSe (58.3%) after 60 min under visible light.

5.3.1 Advantages of the hydrothermal synthesis method

1. Ability to synthesize crystals of substances which are unstable near the melting point
2. Ability to synthesize crystals of high quality
3. Can hybridize with other methods

4. New materials can be synthesized
5. Easy and relatively cheap method
6. One synthetic procedure
7. Produce desired materials with minimal loss of products, that is, produce a high yield of products

5.3.2 Disadvantages of the hydrothermal synthesis method

1. High cost of equipment, that is, autoclave.
2. Unable to monitor crystals during the process of their growth.
3. It can affect both under temperatures and pressures below the critical point for a specific solvent above which differences between liquid and vapor disappear and under supercritical conditions.
4. Difficult to control morphology and size.
5. Cannot be used for all materials.
6. May obtain variation in the size of particles.
7. The hydrothermal synthesis has to be carried out within pressurized vessels which hinders its large-scale production.
8. Even though the method is relatively simple, it needs a longer reaction duration.

5.4 Solvothermal method

The solvothermal synthesis method is the wet-chemical synthesis method for producing nanomaterials. It is very similar to the hydrothermal method (where the synthesis is conducted in a stainless steel autoclave). The only difference is that the solvent used is usually nonaqueous solvents. Using the solvothermal method one can get the benefits of both the sol−gel method and hydrothermal method. Thus, the solvothermal synthesis method allows for precise control over the size, shape and size distribution, and crystallinity of metal oxide NPs or nanostructure products. These characteristics can be altered by changing certain experimental parameters, including reaction temperature, reaction time, solvent type, surfactant type, and precursor type. The system can be:

- in subcritical or in supercritical conditions of the solvent used,
- homogeneous or heterogeneous.

Generally, particle size, shape, size distribution, and crystallinity of the semiconductor can be better controlled using the solvothermal method than the hydrothermal method. The solvothermal method is a useful method for the synthesis of a variety of NPs with narrow size distribution and dispersity and has been employed to synthesize metal oxide NPs and nanorods with or without the aid of surfactants. In the solvothermal synthesis method, the solvent plays a very important role in determining the size and morphology of

crystals. Solvents with different physical and chemical properties can influence the solubility, reactivity, and diffusion behavior of the reactants; in particular, the polarity and coordinating ability of the solvent can influence the morphology and the crystallization behavior of the final products. Following are the main factors which affect the crystal growth in the solvothermal process:

1. Chemical factors
   a. nature of the solvent,
   b. nature of the nutrient,
   c. nature of the seeds,
   d. the interactions of solvent/ wall of the autoclave/vessel.
2. Physical factors
   a. the crystal-growth temperature (T_{growth}),
   b. the ΔT value,
   c. the pressure value,
   d. the hydrodynamics in the crystal-growth system.
3. Kinetic factors
   a. the crystal-growth temperature (T_{growth}),
   b. the ΔT value,
   c. the pressure value,
   d. the hydrodynamics in the crystal-growth system.

Following are some of the examples that show the role of the solvents, temperature, etc. during the solvothermal synthesis:

1. The presence of ethanol at a high concentration not only can cause the polarity of the solvent to change but also strongly affects the ζ potential values of the reactant particles and increases solution viscosity.
2. In the absence of ethanol, short and wide flake-like structures of TiO_2 are obtained instead of nanowires. When chloroform is used, TiO_2 nanorods are obtained. The nonaqueous solvothermal method usually provides better control over the size, crystallinity, and agglomeration behavior of the NPs. For instance, mesoporous TiO_2 microspheres with rough surfaces generally have a high specific surface area, which is an important feature for semiconductor activity because more active sites are available for photocatalytic reactions. Several forms of mesoporous TiO_2 NPs of different sizes have been prepared via solvothermal methods.
3. Synthesis of hierarchical mesoporous TiO_2 microspheres with high crystallinity and high Brunauer–Emmett–Teller (BET)-specific surface area was carried out using tetrabutyl titanate as a precursor into the polyethylenimine solution mixed with absolute ethanol. The activity of the obtained TiO_2 microspheres was evaluated for the degradation of methyl orange (MO) and phenol aqueous solutions under simulated solar light irradiation. The results showed that the specific surface area was high

($118.3\ m^2/g$) and the pore-size distribution revealed a narrow distribution centered at 2.4 and 10.1 nm, respectively. The TiO_2 microspheres exhibited excellent photodegradation activities on both MO and phenol, compared to P25 [2,3].

4. Jeevitha et al. synthesized WO_3 through a solvothermal method using WCl_6 as the precursor and urea and ethanol as the solvents [12]. The mixture was stirred at room temperature before it was heated at 180°C for 12 h. The precipitates were centrifuged, dried at 60°C, and calcined at 450°C.
5. Qian et al. synthesized $Gd_2O_3:Eu^{3+}$ using the same procedure. The authors used $Gd(NO_3)_3$ and $Eu(NO_3)_3$ as the precursors and polyvinylpyrrolidone (PVP) and ethanol as the solvents [13]. Thiourea was added to the solution and dissolved using ultrasound. After the solution was evenly stirred, sodium hydroxide was added before the mixed solution was transferred to Teflon. It was heated for 24 h at 200°C.

5.4.1 Advantages of the solvothermal synthesis method

- solvents other than water can be used
- work at a higher temperature
- solvents with different characteristics provide unique properties to synthesized materials
- almost any material can be dissolved in the solvent by increasing the temperature and pressure to its critical point.

5.4.2 Disadvantages of the solvothermal synthesis method

- high cost of autoclave and muffle furnace
- It is very often that the solvothermal technique requires the use of solvents that are unfriendly to the environment
- Long reaction times
- The cooling process is very slow

5.5 Sonochemical method

Sonochemistry involves ultrasounds which are sound waves with frequencies higher than the upper audible limit of human hearing (20 kHz). Ultrasound devices operate with frequencies from 20 kHz up to several gigahertz. Ultrasound is very useful in the synthesis of a wide range of nanostructured materials, including high-surface-area transition metals, alloys, carbides, oxides, and colloids. Sonochemistry is concerned with understanding the effect of ultrasound in forming acoustic cavitation in liquids, resulting in the initiation of the chemical activity in the solution. The application of ultrasound

under specific conditions allows the possibility of synthesizing nanomaterials in a short time, under mild conditions, in air, and without calcination.

The effect of ultrasound on chemicals (atoms/molecules) does not come from a direct interaction of the ultrasonic sound waves with the molecules in the solution. The simplest explanation for this is that sound waves propagate through a liquid at ultrasonic frequencies (or λ) which are significantly longer than that of the bond length between the atoms in a molecule. The sound wave cannot affect the vibrational energy of the bond. Therefore, ultrasonic sound waves cannot directly increase the internal energy of a molecule. Instead, sonochemistry arises from acoustic cavitation, that is, the cavity formation, cavity growth, and implosive collapse of bubbles in a liquid. The collapse of these bubbles is an almost adiabatic process, resulting in the massive build-up of energy inside the bubble, resulting in extremely high temperature and pressure in a microscopic region of the sonicated liquid. The high temperature and pressure result in the chemical excitation of any matter that was inside or in the immediate surroundings of the bubble as it rapidly imploded or collapsed.

High-intensity ultrasound can be used for the production of novel materials and provides an unusual route to known materials without high temperatures, high pressures, or long reaction times. Ultrasound irradiation causes acoustic cavitation, that is, formation, growth, and implosive collapse of the bubbles in a liquid. Several phenomena are responsible for sonochemistry and specifically the production or modification of nanomaterials during ultrasonic irradiation. When ultrasound waves are passed through a liquid medium, it causes mechanical vibration of the liquid and acoustic streaming within it. If the liquid medium contains dissolved gas nuclei, they can be grown and collapsed by the action of ultrasound. When cavitation bubbles oscillate and collapse, physical effects are generated. The phenomenon of growth and collapse of microbubbles under an ultrasonic field is known as *acoustic cavitation*. The collapse of acoustic cavitation bubbles is near adiabatic condition and generates high temperature within the bubbles for a short time. Under this extremely high temperature, highly reactive radicals are generated. Hence, these radicals are used to achieve chemical reactions, that is, synthesis of nanomaterials. The implosive collapse of the microbubbles generates a localized hot spot of extremely high temperature ($\sim$5000K) and pressure ($\sim$20 MPa).

The sonochemical method is advantageous as it is nonhazardous, rapid in reaction rate, and produces very small nanoparticles. The most notable effects are the formation of *acoustic cavitation* (formation, growth, and implosive collapse of the microbubbles), and can be categorized as follows:

1. *primary sonochemistry* (gas-phase chemistry occurring inside collapsing bubbles),

2. *secondary sonochemistry* (solution-phase chemistry occurring outside the bubbles), and
3. *physical modifications* (caused by high-speed jets or shock waves derived from bubble collapse).

In other words, sonochemistry is the application of ultrasound to chemical reactions and processes. The mechanism causing sonochemical effects in liquids is the phenomenon of acoustic cavitation. Ultrasonic cavitation intensifies and speeds up chemical reactions such as synthesis and catalysis.

High-intensity ultrasound has found many important applications in organic synthesis, materials and organometallic synthesis, and industrial manufacturing processes. Sonochemistry originates from the extreme transient conditions induced by ultrasound, which produces unique hot spots that can achieve temperatures above 5000K, pressures exceeding 1000 atmospheres, and heating and cooling rates over 10^{10} K/s. These conditions are distinct from other conventional synthetic techniques such as photochemistry, wet chemistry, hydrothermal synthesis, or flame pyrolysis [2,3]. Fig. 5.4 shows the schematic diagram of the experimental setup of the sonicator for the sonochemical synthesis of nanomaterials.

The speed of sound in a typical liquid is 1000 to 1500 ms^{-1}, and the ultrasonic frequency range of 20 kHz to 15 MHz is much larger than the molecular size scale. The chemical and physical effects of ultrasound do not arise from a direct interaction between chemical species and sound waves but from the physical phenomenon of acoustic cavitation, that is, formation of cavities (micro- or nanocavities), growth, and implosive collapse of bubbles. When sound waves with sufficient amplitude propagate through a liquid, the liquid is under dynamic tensile stress and the density changes with

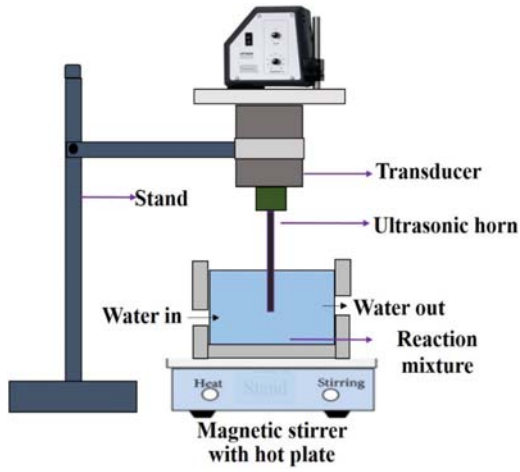

FIGURE 5.4 Sonochemical synthesis using a sonicator.

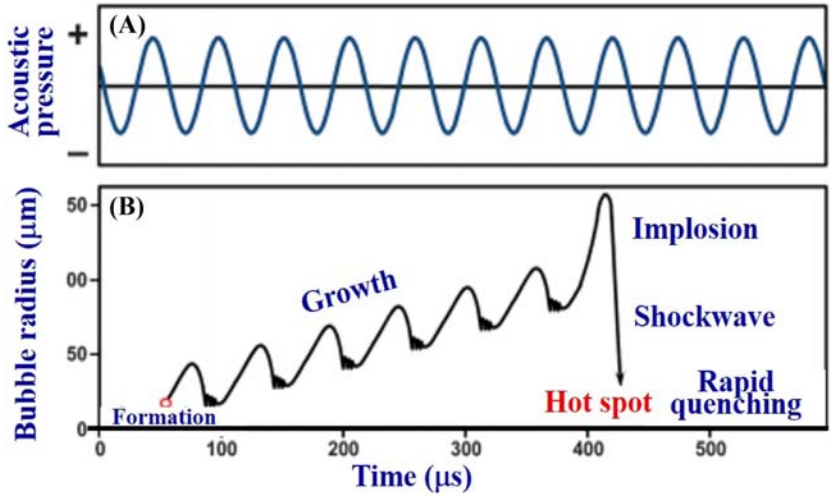

FIGURE 5.5 Schematic shows the process of acoustic cavitation: (A) the formation, and (B) growth and implosive collapse of bubbles in a liquid irradiated with high-intensity ultrasound.

alternating expansive and compressive waves. Bubbles are generated from preexisting impurities (e.g., gas-filled crevices in dust motes) and oscillate with the applied sound field. Fig. 5.5 shows that bubbles can grow through a slow pumping of gas from the bulk liquid into the oscillating bubble (rectified diffusion). Bubbles at a critical size (usually tens of micrometers) can couple strongly to the acoustic field and undergo a rapid inertial overgrowth during expansion, followed by a catastrophic collapse. The implosive collapse process is nearly adiabatic in its final stage and is responsible for the extreme condition which is the characteristic of sonochemistry [14,15].

Sonochemical synthesis of nanomaterials depends on several parameters and factors. Following are some factors which affect the sonochemical synthesis:

1. *Frequency*: As the frequency is increased, pressure changes abruptly causing high turbulence inside the liquid known as acoustic streaming and it dominates acoustic cavitation.
2. *Power input*: Applied power reflects on the pressure amplitude increasing power drastically, disrupting bubble dynamics, thus, resulting in poor cavitation. Therefore, the applied power and frequency should always correlate in balancing the bubble growth.
3. *Solution*: The solution as a whole incorporates various sonochemical ingredients such as precursor/solvent/additives/chemical agents and dissolved gas. Changing one of them can bring remarkable changes in the process.
4. *Sonication time*: Effect of time of experiment and number of cycles induced morphological variation in nanomaterials formation. When the sonication time increases, the formation of a new structure will take place.

The sonochemical synthesis method has several advantages over other conventional and wet-chemical synthesis methods. Following are the advantages of using the sonochemical synthesis method:

1. High reaction rate which saves time.
2. Controllable reaction conditions, capacity to form uniform shapes, narrow distributions of particle size, and high purity.
3. The energy efficient method saves $\sim 80\%$ of energy as compared to that utilized by the conventional synthesis method.
4. Generally, no need for heating, calcination, or sintering.
5. Sonochemistry is a very important tool for intensifying various physical and chemical processes to render economy, reduce time, and increase product quality.
6. Sonochemistry has facilitated numerous advancements and new applications in sciences and engineering.

Disadvantages of the sonochemical synthesis method:

1. Noise hazard
2. It is difficult to control the temperature of a certain reaction. This is because the solutions tend to warm up when they are exposed to high ultrasonication, resulting in an inconsistent temperature. Many sonochemical reactions need to be at a certain temperature, so this serves as a major disadvantage.

Various reports exist in the literature regarding the synthesis of metal- and nonmetal-doped TiO_2 by sonochemical methods. For example:

1. Wang et al. prepared N-doped TiO_2 nanocrystalline by the sonication of the solution of tetraisopropyl titanium and urea in water and isopropyl alcohol at 80°C for 150 min. The effect of the sonication time on the formation of N-doped TiO_2 NPs was investigated. The crystallinity of the sample increased at a higher sonication time (60, 120, 150, and 180 min). However, 150 min was the optimal sonication time where the crystallization of TiO_2 was completed.
2. Kumar et al. reported the synthesis of Ag NPs through the sonochemical synthesis method using starch and $AgNO_3$ as the precursor. Ultrasound was carried out with an ultrasonic processor immersed directly into the solution [16].
3. Another study using the same synthesis method was conducted by Goswami et al. in which cobalt acetate and iron (II) acetate were subjected to sonication for 30 min in a pulse mode [14].

5.6 Microwave method

Microwave (MW) heating in the laboratory started to gain extensive attention in 1986 although the use of microwave heating in chemical modification

can be traced back to the 1950s. Microwave synthesis is also known by acronyms as Microwave-Assisted Organic Synthesis (MAOS), Microwave-Enhanced Chemistry (MEC), and Microwave-organic Reaction Enhancement (MORE) synthesis. These acronyms have quite a low acceptance among researchers. Microwaves (MW) are a form of electromagnetic energy radiations with frequencies in the range of 300 MHz to 300 GHz. The commonly used frequency is 2.45 GHz. The vessel wall is transparent to MW. It involves direct in-core heating (Fig. 5.6). It is known that MW irradiation is not sufficiently energetic to break the hydrogen or covalent bonds. Thus, it cannot induce chemical reactions since no bond breaking can take place by direct absorption of microwave energy. Heat is generated by molecular collision and friction. It is a clean, fast, cost-effective, and convenient pathway for the synthesis of photocatalytic materials [2,3].

The differences between conventional heating by conduction versus heating by microwave irradiation can be found in Fig. 5.6 and Table 5.1.

"Microwave chemistry" is the science of applying microwave irradiation to chemical reactions which is based on the efficient heating of matter by microwave dielectric heating. Microwave dielectric heating depends on the ability of a specific material (e.g., solvent and/or reagents) to absorb microwave energy and convert it into heat. MW acts as high-frequency electric fields that generally heat any material containing mobile electric charges, such as polar molecules in a solvent or conducting ions in a solid. Polar solvents are heated as their component molecules are forced to rotate with the field and lose energy during collisions. Semiconducting and conducting samples get heated when ions or electrons within these materials form an electric current and energy is lost due to the electrical resistance of the material.

In the liquid-phase synthesis of nanomaterials, microwave irradiation activates heating by two main mechanisms, namely (1) dipolar polarization (Fig. 5.7A) and (2) ionic conduction (Fig. 5.7B). In the dipolar mechanism of polarization (or rotation), the dipoles in the reaction mixture (e.g., polar

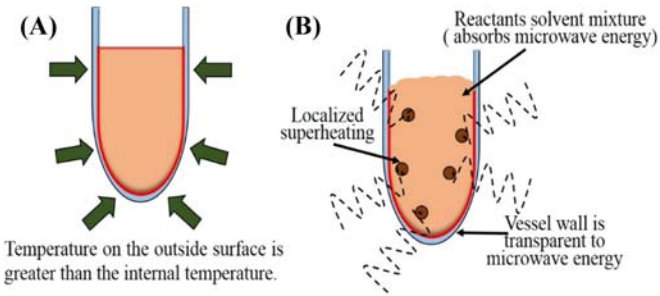

FIGURE 5.6 (A) Conventional heating by conduction and (B) heating by microwave irradiation.

TABLE 5.1 Differences between conventional heating and microwave heating.

Conventional heating by conduction	Heating by microwave
• Conductive heat. • Heating by convection currents. • Slow and energy inefficient process. • The heat gradient is from the heating device to the medium. • The temperature on the outside surface is more than the boiling point of a liquid. • Heat transfer depends on thermal conductivity, the temperature difference across the material, and convection currents. • Hence, the temperature increase is rather slow and so this method is inefficient.	• Solvent/reagent absorbs MW energy. • Vessel wall transparent to MW. • Direct in-core heating. • Instant on-off. • Heat is dissipated inside the irradiated medium (mass heating). • Heat transfers from medium to outside. • Due to the mass heating effect, a much faster temperature increase can be obtained (depending upon microwave power and loss factor of material being irradiated).

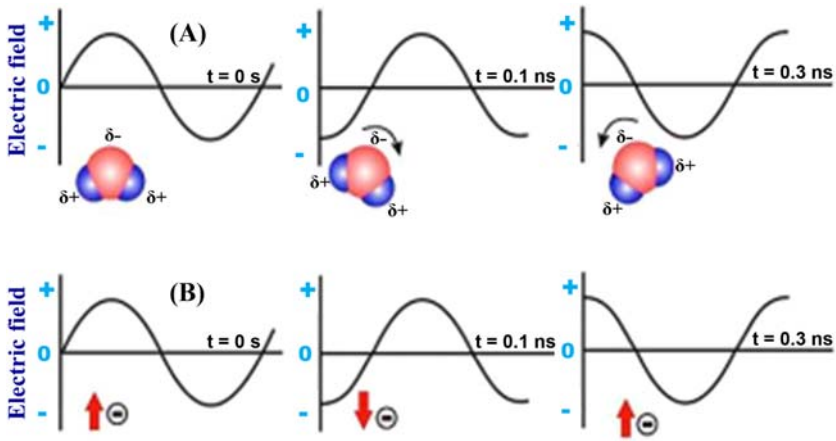

FIGURE 5.7 Two main heating mechanisms under microwave irradiation, (A) dipolar polarization and (B) ionic conduction mechanism.

solvent molecules or reagents) are involved, whereas, in ionic conduction, charged particles (free ions or ionic species) in a substance contribute to heating. When irradiated by MW frequencies, the dipoles in the sample try to align themselves in the direction of the applied electric field. As the electric field oscillates, the molecular dipoles try to follow the alternating electric field streamlines. In such a process, energy is lost in the form of heat through

molecular friction and dielectric loss (dielectric heating). Interactions between materials and microwaves are based on two specific mechanisms:

1. dipole interactions/rotation, and
2. ionic conduction.

Both mechanisms require effective coupling between components of the target material and the rapidly oscillating electric field of the microwaves.

1. *Dipole interactions/rotation*
   - **a.** Dipole rotation is an interaction in which polar molecules try to align themselves with the rapidly changing electric field of the microwave.
   - **b.** Dipole interactions take place with polar molecules. The polar ends of a molecule tend to reorientate themselves and oscillate in step with the oscillating electric field of the microwaves.
   - **c.** Generally, the more polar a molecule, the more effectively it will couple with the microwave field.
   - **d.** The rotational motion of the molecule tries to orient itself with the field, resulting in a transfer of energy.
   - **e.** The coupling ability of this mechanism is related to the polarity of the molecules and their ability to align with the electric field.
   - **f.** Several factors will ultimately determine the dipole rotation coupling efficiency. However, any polar species (solvent/or substrate) that are present will encounter this mechanism of energy transfer.
2. *Ionic conduction*
   - **a.** It results if there are free ions or ionic species present in the substance being heated.
   - **b.** The electric field generates ionic motion as the molecules try to orient themselves to the rapidly changing field.
   - **c.** This causes instantaneous superheating.
   - **d.** The temperature of the substance also affects ionic conduction. As the temperature increases, the transfer of energy becomes more efficient.

In the case of dipolar polarization, the amount of heat generated by this process is directly related to the ability of these dipoles to align themselves with the frequency of the applied MW field. If a dipole does not have enough time to realign (high-frequency irradiation), or reorients too quickly (low-frequency irradiation) with the applied field, no MW heating will take place. The allocated frequency of 2.45 GHz available in all commercial systems lies between these two extremes and gives the molecular dipoles just enough time to align with the field but does not permit them to follow the alternating field precisely.

On the other hand, in the case of ionic conduction, the dissolved charged particles in a sample (usually ions) oscillate back and forth under the influence of the MW field. In this process, these ions collide with their

neighboring molecules and generate heat. The ion conductivity mode provides a much stronger heat-generating capacity than the dipolar rotation mechanism because these effects are particularly evident when considering the heating behavior of ionic liquids in an MW field. The ability of a substance to convert electromagnetic energy into heat at a given frequency and temperature is determined by the so-called loss tangent (tan δ) which is defined as the ratio of dielectric loss (ε'') and dielectric constant (ε'). Thus, the loss tangent gives a measure of heat generated for a certain degree of polarization. In general, a reaction medium with a high tan δ at the standard operating frequency of an MW reactor (2.45 GHz) is required for good absorption and efficient heating. Overall, solvents used in MW chemistry can be classified as high- (tan $\delta > 0.5$), medium- (tan $\delta \approx 0.1-0.5$), and low absorbing (tan $\delta < 0.1$). On the other hand, polar additives, such as ionic liquids or passive heating elements made out of strongly MW absorbing materials to increase the absorbance level of low-absorbing reaction media [2–4].

Kappe et al. conducted a systematic study aimed to elucidate the influence of the electromagnetic field on a chemical transformation, outside of the simple macroscopic change in bulk reaction temperature. To suppress the influence of the electromagnetic field, a silicon carbide (SiC) vessel (which presents a high MW absorptivity) was used to conduct chemical reactions. For comparison, a nonabsorbing MW radiation vessel was used to conduct the same reactions under identical reaction conditions. The obtained results showed that the electromagnetic field has no direct influence on the reaction pathways. It is the overheating phenomenon that drives the enhancements in MW chemistry.

Blanco-Vega et al. synthesized Ni-doped TiO_2 using titanium (IV) isopropoxide and nickel (II) nitrate hexahydrate as the precursors. The precursors were mixed in isopropanol and water. The mixture was stirred at room temperature for 2 h and loaded into the microwave reactor [17]. Another study reported on the preparation of BiOBr-Graphene nanocomposites using the same synthesis method [18]. In short, $Bi(NO_3)_3 \cdot 5H_2O$ was dissolved in ethylene glycol. The mixture was treated in an ultrasonic bath, and subsequently, KBr was added to the solution. Graphene oxide (GO) powder was dissolved in ethylene glycol and the GO solution was added to the former solution. Finally, the mixture was heated at 90°C in a microwave reactor.

Advantages of microwave synthesis methods. The microwave synthesis method is considered superior because of the following reasons:

1. The reaction temperature is quickly achieved and keeps uniform within the time of reaction.
2. The kinetics of crystallization is increased by one-to-two orders of magnitude in comparison to conventional heat treatment. Therefore, different crystalline phases can be fabricated.

3. The physicochemical properties of the materials can be easily improved with slight modifications of the reaction conditions.
4. Low-temperature method for preparation of nanophase materials of different sizes and shapes. Therefore, low power consumption (energy saving).
5. Nanophase materials can be produced either by a batch process or a continuous process.
6. Environment friendly as reactions take place in a closed isolated system.
7. Greener approach to synthesizing materials in a shorter time.

Disadvantages of the microwave synthesis method:

1. The reaction may not complete (therefore, optimization is crucial)
2. An expensive instrument is required
3. It is difficult to scale up the production of materials.

5.7 Chemical vapor deposition

CVD is a generic name for a group of processes that involve the deposition of solid material from a gaseous phase. Microfabrication processes widely use CVD to deposit materials in various forms including thin films, monocrystalline, polycrystalline, amorphous, and epitaxial. CVD is a vacuum deposition method used to produce high-quality and high-performance solid materials. The process is often used in the semiconductor industry to produce thin films. In typical CVD, the wafer (substrate) is exposed to one or more volatile precursors, which react and/or decompose on the substrate surface to produce the desired deposit. Simultaneously, volatile by-products are also produced, which are removed by gas flow through the reaction chamber. Microfabrication processes widely use CVD to deposit materials in various forms, including monocrystalline, polycrystalline, amorphous, and epitaxial. These materials include silicon dioxide, SiC, silicon nitride, silicon oxynitride, carbon fiber, carbon nanofibers, carbon nanotubes, diamond, graphene, fluorocarbons, filaments, tungsten, titanium nitride, and various high-k dielectrics.

CVD is a technique that has been exploited for the preparation of supported semiconductor nanomaterials. Thin films (supported in glass, metallic substrates, or semiconducting substrates), composite materials (SiO_2/TiO_2, activated carbon/TiO_2, amine polymer/TiO_2), mesoporous materials, and TiO_2 nanorods, among others, have been prepared by CVD. Chemical methods are the most popular techniques for manufacturing TiO_2 due to the relative simplicity of control over synthesis, narrow NP size distribution, low cost, and reliable stabilization of NPs in the system. On the other hand, physical methods have been less explored, especially for large-scale production of materials since highly specialized equipment and operators are needed for material development. The CVD method allows the production of high-purity materials. This method does not need the postheat-treatment to

improve the crystallinity of the formed material. However, ultrahigh vacuum and precursors with high vapor pressure are required to attain the material's deposition. Currently, several methods have been developed based on gas deposition principles that present simple differences, such as the type of precursor employed, the type of substrate, the desired degree of thin film uniformity, and reaction conditions. Some examples of these methods include atmospheric pressure chemical vapor deposition (APCVD), plasma-enhanced chemical vapor deposition (PECVD), metalorganic CVD (MOCVD) which is based on metalorganic precursors, and hybrid physical-chemical vapor deposition (HPCVD).

CVD is considered one of the most precise methods when conformal deposition of the material is required. In this way, CVD offers numerous advantages in the deposition of the ordered nanostructured thin film of varied compositions. CVD requires volatile molecular precursors as the source for film growth. The precursor molecules are transported in a stream of carrier gas which may be either chemically inert or reactive. They are converted by chemical reactions in the gas phase near the surface itself into a thin solid film of the desired material. In the CVD process, heated carrier gases drive the deposition reaction. The main chemical events involved in thin film formation using the CVD technique are shown in Fig. 5.8. A typical CVD instrument consists of the following parts:

- sources of and feed lines for gases;
- mass flow controllers for metering the gases into the system;
- a reaction chamber or reactor;
- a system for heating the wafer on which the film is to be deposited; and
- temperature sensors.

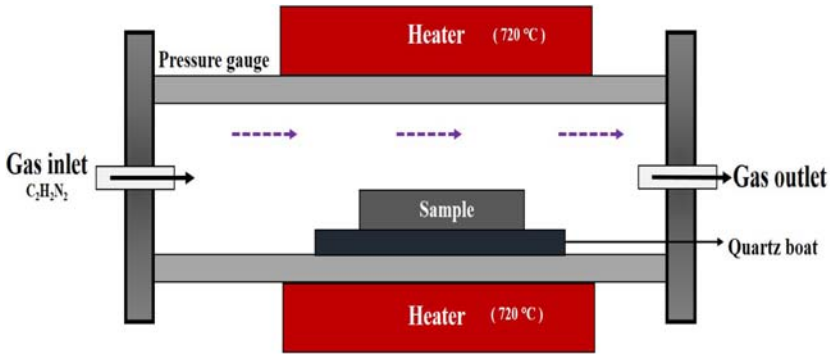

FIGURE 5.8 Fabrication of thin film nanostructured materials using the CVD method.

Generally, the CVD synthesis process consists of the following steps:

- A predefined mix of reactant gases and diluent inert gases are introduced at a specified flow rate into the reaction chamber;
- the gas species move to the substrate;
- the reactants get adsorbed on the surface of the substrate;
- the reactants undergo chemical reactions with the substrate to form the film;
- the gaseous by-products of the reactions are desorbed and evacuated from the reaction chamber.
- During the CVD process, the reactant gases not only react with the substrate material at the wafer surface (or very close to it), but also in the gas phase in the reactor's atmosphere.
- Reactions that take place at the substrate surface are known as *heterogeneous reactions* and are selectively occurring on the heated surface of the wafer where they create good-quality films.
- Reactions that take place in the gas phase are known as *homogeneous reactions.*
- Homogeneous reactions form gas-phase aggregates of the depositing material, which adhere to the surface poorly, and at the same time, form low-density films with lots of defects.
- In short, heterogeneous reactions are much more desirable than homogeneous reactions during the CVD process.

For example, Sarantopoulos et al. fabricated TiO_2 thin films in an isothermal, isobaric, and horizontal low-pressure-CVD reactor using borosilicate glass and Si wafers as substrates and titanium isopropoxide as the molecular precursor [19]. Besides the different substrates employed, the deposition time, the temperature, and the number of precursors varied during the deposition of the films. Different morphologies of the films were obtained due to differences in the experimental conditions. On the other hand, nonflat substrates (glass microfiber) originated columnar growth independent of film thickness. The films were evaluated for the degradation of pollutants in an aqueous solution (malic acid, imazapyr, and orange G) and gas phase (toluene). Higher photocatalytic efficiencies were achieved for films deposited on fibrous substrates because they exhibit a high porosity, a columnar morphology, and a high specific surface area [2–4].

For example, silicon dioxide may be deposited by several different processes. Common source gases include silane and oxygen, dichlorosilane ($SiCl_2H_2$) and nitrous oxide (N_2O), or tetraethylorthosilicate (TEOS; $Si(OC_2H_5)_4$). The reactions are as follows:

$$SiH_4 + O_2 \rightarrow SiO_2 + 2H_2$$

$$SiCl_2H_2 + 2N_2O \rightarrow SiO_2 + 2N_2 + 2HCl$$

$$Si(OC_2H_5)_4 \rightarrow SiO_2 + \text{byproducts}$$

The choice of the source gas depends on the thermal stability of the substrate. For example, aluminum is sensitive to high temperatures. Silane deposits between 300°C and 500°C, dichlorosilane at around 900°C, and TEOS between 650°C and 750°C, result in a layer of low-temperature oxide (LTO). However, silane produces a lower-quality oxide than the other methods (lower dielectric strength, for instance), and it deposits nonconformally. Any of these reactions may be used in low pressure chemical vapor deposition (LPCVD), but the silane reaction is also done in APCVD. CVD oxide invariably has a lower quality than thermal oxide, but thermal oxidation can only be used in the earliest stages of IC manufacturing.

Several forms of CVD are in wide use depending on the conditions. These processes differ in the means by which chemical reactions are initiated (e.g., activation process) and process conditions (e.g., temperature and pressure). For instance, a reactor is said to be a "hot-wall" if it uses a heating system that heats not only the wafer but the walls of the reactor itself. An example of this is radiant heating from resistance-heated coils. "Cold-wall" reactors use heating systems that minimize the heating up of the reactor walls while the wafer is being heated up. An example of this is heating via IR lamps inside the reactor. In hot-wall reactors, films are deposited on the walls in much the same way as they are deposited on the wafers. Therefore, this type of reactor requires frequent wall cleaning. CVD is of different types based on the range of its operating pressure:

1. Plasma methods (see also plasma processing):
   - **a.** Microwave plasma-assisted CVD (MPCVD): It is used to activate hydrocarbon and dissociate molecular hydrogen. A typical 2.45 GHz is used as an excitation source. In general, microwave plasma oscillates electrons producing ions by colliding with gas atoms and molecules [20].
   - **b.** Plasma-enhanced CVD (PECVD): CVD that utilizes plasma to enhance the chemical reaction rates of the precursors. PECVD processing allows deposition at lower temperatures, which is often critical in the manufacture of semiconductors. The lower temperatures also allow for the deposition of organic coatings, such as plasma polymers, that have been used for NPs surface functionalization.
   - **c.** Remote plasma-enhanced CVD (RPECVD): Similar to PECVD except that the wafer substrate is not directly in the plasma discharge region. Removing the wafer from the plasma region allows processing temperatures down to room temperature.
   - **d.** Low-energy plasma-enhanced CVD (LEPECVD): CVD employs a high-density, low-energy plasma to obtain the epitaxial deposition of semiconductor materials at a high rate and low temperature.

2. Atomic-layer CVD (ALCVD): Deposits successive layers of different substances to produce layered, crystalline films. See atomic-layer epitaxy.
3. Combustion CVD (CCVD): CCVD or flame pyrolysis is an open-atmosphere, flame-based technique for depositing high-quality thin films and nanomaterials.
4. Hot filament CVD (HFCVD): Also known as catalytic CVD (Cat-CVD), or more commonly, initiated CVD (iCVD). This process uses a hot filament to chemically decompose the source gases. The filament temperature and substrate temperature, thus, are independently controlled, allowing colder temperatures for better absorption rate at the substrate and higher temperatures necessary for the decomposition of the precursors to free radicals at the filament.
5. HPCVD: This process involves both the chemical decomposition of precursor gas and the vaporization of a solid source.
6. Metalorganic CVD (MOCVD): This CVD process is based on metalorganic precursors.
7. Rapid thermal CVD (RTCVD): This CVD process uses heating lamps or other methods to rapidly heat the wafer substrate. Heating only the substrate rather than the gas or chamber walls helps to minimize unwanted gas-phase reactions that can lead to particle formation.
8. Vapor-phase epitaxy (VPE): This process operates near ambient pressure at high temperatures between 700°C and 800°C. The chemical sources to grow the epitaxial layers are gaseous. This technique has been used to grow several III-V compound semiconductors.
9. Photo-initiated CVD (PICVD): This process uses UV light to stimulate chemical reactions. It is similar to plasma processing, given that plasmas are strong emitters of UV radiation. Under certain conditions, PICVD can be operated at or near atmospheric pressure.
10. Laser CVD (LCVD): This CVD process uses a laser to heat spots or lines on a substrate in semiconductor applications. In microelectromechanical systems (MEMS) and fiber production, the lasers are used to rapidly break down the precursor gas. The process temperature can exceed 2000°C to build up a solid structure in much the same way as laser sintering-based 3-D printers build up solids from powders.

Following are the advantages of the CVD method:

1. It can be used for a wide range of metals and ceramics synthesis
2. It can be used for coatings or freestanding structures
3. Fabricates net or near-net complex shapes
4. Extremely high-purity deposits ($>99.995\%$ purity) can be obtained
5. Conforms homogeneously to curves/linings of the substrate surface
6. The thickness and morphology of the films and coatings can be easily controlled

7. Forms alloys
8. Infiltrates fiber preforms and foam structures
9. It can coat internal passages with high length-to-diameter ratios
10. It can simultaneously coat multiple components
11. It can coat powders.

5.8 Physical vapor deposition

PVD, sometimes (especially in a single-crystal growth context) is also called physical vapor transport (PVT). PVD is a term used to describe a family of coating processes. It is a process carried out in a high vacuum at temperatures between 150°C and 500°C. This designates a variety of vacuum deposition methods which can be used to produce thin films and coatings. PVD is a process in which the material goes from a condensed phase to a vapor phase and then back to a thin film condensed phase. PVD uses a physical process (such as heating or sputtering) to produce a vapor of material, which is then deposited on the object which requires coating. The most common PVD processes are evaporation and sputtering (Fig. 5.9). Evaporation is typically using cathodic arc or electron-beam sources while sputtering is using magnetic enhanced sources or "magnetrons," cylindrical or hollow cathode sources. PVD is fundamentally a vaporization coating technique which involves the transfer of material to an atomic level. It is an alternative process to electroplating. The process is similar to CVD except that the precursors, that is, the material that is going to be deposited starts in solid form, whereas in CVD, the precursors are introduced to the reaction chamber in the gaseous state.

PVD is used in the manufacture of items which require thin films for mechanical, optical, chemical, or electronic applications. Examples include semiconductor devices such as thin films for solar panels, aluminized PET

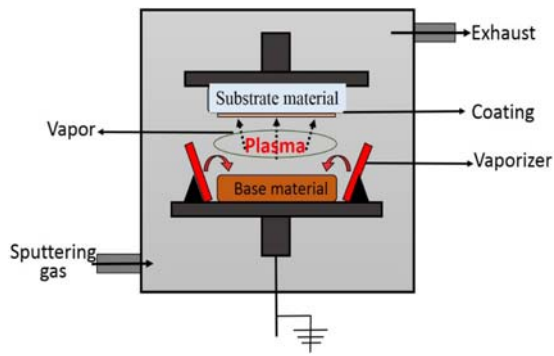

FIGURE 5.9 Schematic presentation of the PVD process.

film for food packaging and balloons, and titanium nitride-coated cutting tools for metalworking. Besides PVD tools for fabrication, special smaller tools (mainly for scientific purposes) have been developed.

In other words, PVD is another deposition method that can be used for the fabrication of bare and doped semiconductors. In contrast to the CVD method, in PVD, thin films are formed from the gas phase, without a chemical transition from the precursor to the product. The basic PVD processes come under two general categories: (1) evaporation and (2) sputtering. Very high deposition rates have been achieved with the advent of electron-beam heated sources. Several PVD techniques are available for the deposition of thin films. Among them are cathodic arc vapor (plasma or arc ion plating) deposition, magnetron sputtering (or sputter ion plating), and combined magnetron and arc processes. These PVD techniques differ concerning the type of evaporation of the precursors and the plasma conditions used during the deposition process. In the case of arc evaporation, a limited cathodic area is evaporated with a very high-energy arc that quickly moves over a spot on the metal surface to be evaporated. The plasma generated consists of highly ionized metal vapor. In the case of sputtering, atoms are ejected mechanically from a target by the impact of ions or energetic neutral atoms (Fig. 5.9). Advances in sputtering techniques have allowed the deposition of different thin films at low temperatures. Owing to this, the use of polymeric substrates has been widely explored for industrial applications. PVD processes are carried out under vacuum conditions. The process mainly involves four steps:

- Evaporation
- Transportation
- Reaction
- Deposition

The high purity, solid coating material (metals such as titanium, chromium, and aluminum) is either evaporated by heat or by bombardment with ions (sputtering). At the same time, a reactive gas (e.g., nitrogen or a gas containing carbon) is introduced; it forms a compound with the metal vapor and is deposited on the tools or components as a thin, highly adherent coating. To obtain a uniform coating thickness, the parts are rotated at a uniform speed about several axes. The properties of the coating (such as hardness, structure, chemical and temperature resistance, and adhesion) can be accurately controlled.

For example, Yang et al. prepared N-doped TiO_2 films by ion-assisted electron-beam evaporation, using rutile and nitrogen ion bombardment at various nitrogen partial pressure. The photocatalytic activity of the films was evaluated for the degradation of methylene blue. Despite the hydrophilicity, uniform composition, and nanometric nature of the films, the photocatalytic degradation process was lengthy (60 h) [2–4,21].

PVD is of different types based on the heating/sputtering source:

1. *Cathodic arc deposition*: A high-power electric arc discharged at the target (source) material blasts away into highly ionized vapor to be deposited onto the workpiece.
2. *Electron-beam PVD*: The material to be deposited is heated to a high vapor pressure by electron bombardment in a "high" vacuum and is transported by diffusion to be deposited by condensation on the (cooler) workpiece.
3. *Evaporative deposition*: The material to be deposited is heated to a high vapor pressure by electrical resistance heating in a "high" vacuum.
4. *Close-space sublimation*: The material and substrate are placed close to one another and radiatively heated.
5. *Pulsed laser deposition*: A high-power laser ablates material from the target into a vapor.
6. *Sputter deposition*: A glow plasma discharge (usually localized around the "target" by a magnet) bombards the material sputtering away as a vapor for subsequent deposition.
7. *Pulsed electron deposition*: A highly energetic-pulsed electron beam ablates material from the target generating a plasma stream under non-equilibrium conditions.
8. *Sublimation sandwich method*: This method is used for creating man-made crystals.

The evaporation methods have certain merits and demerits which have been summarized as follows in Table 5.2.

PVD coatings have their importance. PVD coatings are deposited for numerous reasons. Some of the main reasons are

- Improved hardness and wear resistance.
- Reduced friction.
- Improved oxidation resistance.
- The use of such coatings is aimed at improving efficiency through improved performance and longer component life.
- They may also allow coated components to operate in environments that the uncoated component would not otherwise have been able to perform.

Based on the above discussion, the PVD methods/coatings have their advantages and disadvantages. Following are the advantages and disadvantages of PVD coatings:

5.8.1 Advantages of PVD coatings

- Materials can be deposited with improved properties compared to the substrate material.
- Almost any type of inorganic material can be used as well as some kinds of organic materials.

TABLE 5.2 Merits and demerits of PVD methods based on the evaporation methods.

Method	Merits	Demerits
E-Beam evaporation	1. High temp materials 2. Good for liftoff 3. High purity	1. Some of the processes are sensitive to radiation 2. Difficult to produce alloys 3. Poor step coverage
Filament evaporation	1. Simple to implement 2. Good for liftoff	1. Limited source material (no high temp) 2. Difficult to produce alloys 3. Poor step coverage
Sputter deposition	1. Better step coverage 2. Alloys easy 3. High temp materials 4. Less radiation damage	1. Possible grainy films 2. Porous films 3. Plasma damage/contamination

- The process is more environmentally friendly than processes such as electroplating.
- PVD coatings are generally used to improve hardness, wear resistance, and oxidation resistance.
- PVD coatings are sometimes harder and more corrosion resistant than the coatings applied by the electroplating process

5.8.2 Disadvantages of PVD coatings

- It is a line-of-sight technique meaning that it is extremely difficult to coat undercuts and similar surface features.
- High capital cost.
- Some processes operate at high vacuums and temperatures requiring skilled operators.
- Processes requiring large amounts of heat require appropriate cooling systems.
- The production speed of PVD coatings is slow compared to other coating deposition processes.
- The PVD technique is limited to substrates with complex geometries.

5.9 Electrochemical deposition method

Electrochemical deposition is a process by which a thin and tightly adherent desired coating of metals, metal oxides, or salts can be deposited onto the

surface of a conductor substrate by simple electrolysis of a solution containing the desired metal ion or its chemical complex. In short, it is a process where the metallic ion can become solid metal and deposit on the cathode surface if a sufficient amount of electric current passes through the electrolyte solution.

Electrochemical synthesis is used for the deposition of particles on metallic or conducting substrates. It can be used to prepare advanced thin films such as epitaxial, superlattice, quantum dots, and nanoporous ones. It is the process that exploits the formation of solid materials directly from electrochemical reactions in liquid compositions on substrate materials. It is a process where metal ions are transferred from a solution and are deposited as a thin layer onto the surface of a cathode. The synthesis of solid materials takes place on a substrate using electrochemical reactions in electrolytes in electrochemical synthesis. The instrument used is known as a *potentiostat*. A three-electrode electrochemical cell (a reference electrode, a specially designed cathode, and an anode or counter electrode) is shown in Fig. 5.10. This instrument controls the voltage difference between a working electrode and a reference electrode.

In general, a powder material is dispersed in a solvent where two electrodes are immersed, the conducting substrate and the counter electrode, both arranged in parallel. Then, an electric potential is applied to the system and particles move toward the conducting substrate to make the film. For example, Werta et al., reported on the electrochemical deposition of $Cd_{1-x}Zn_xS$ thin film (Fig. 5.10) using a high-purity graphite rod as a counter electrode. $Cd_{1-x}Zn_xS$ thin films were cathodically deposited on fluorine-doped thin oxide (working electrode) coated glass substrate through two electrode deposition setup. The Cd, Zn, and sulfur sources were from cadmium chloride, zinc chloride, and sodium thiosulphate, respectively.

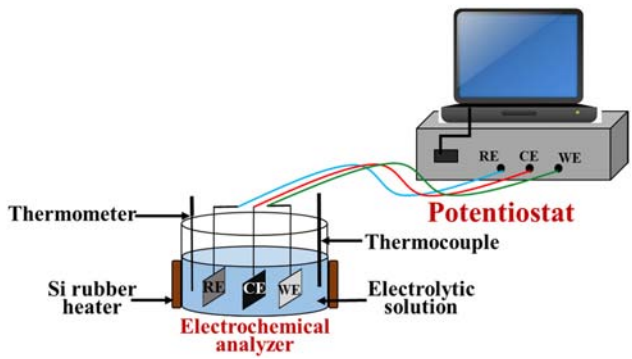

FIGURE 5.10 Thin film deposition by electrochemical deposition methods using a potentiostat [22].

There are several factors affecting the electrodeposition including

- Current density
- The nature of the anions or cations in the solutions
- Bath composition and temperature
- Solution concentration
- Power supply current waveform
- The presence of impurities
- Physical and chemical nature of the substrate surface.

Also, varying electrolysis parameters as mentioned above can easily control the characteristic states of the films. Moreover, the thickness of the electroplated layer on the substrate is determined by the time duration of the plating. Another example is the electrodeposition of TiO_2 films by various Ti compounds such as $TiCl_3$, TiF_4, and $(NH_4)_2TiO(C_2O_4)_2$. The use of titanium inorganic salts in aqueous solutions is always accompanied by difficulties, due to the high tendency of the salts to hydrolyze. Therefore, electrolysis requires both an acidic medium and an oxygen-free environment.

Electrochemical deposition methods have been particularly useful for the fabrication of one-dimensional TiO_2 nanotube and nanowire arrays. In the last decade, these materials have attracted the attention of several research groups since comparative studies show that ordered TiO_2 nanotube arrays present improved characteristics than colloidal TiO_2 for numerous applications (such as sensing, electrochemical water splitting, environmental remediation, dye-sensitized solar cells, drug delivery, and other biomedical applications). Even though TiO_2 nanotubes have been fabricated by different synthetic approaches, anodization of titanium in a fluoride-based electrolyte renders precise control over the morphology and dimensions of the produced materials. By modification and optimization of electrochemical deposition variables, the production of TiO_2 nanotube arrays presenting different morphologies and properties has been accomplished [2–4].

Electrochemical deposition is generally used for the growth of metals and conducting metal oxides because of the following advantages:

1. the thickness and morphology of the nanostructure can be precisely controlled by adjusting the electrochemical parameters,
2. relatively uniform and compact deposits can be synthesized in template-based structures,
3. higher deposition rates are obtained, and
4. the equipment is inexpensive due to the nonrequirements of either a high vacuum or a high reaction temperature.

The main disadvantage is that more chemicals are required for thicker coatings.

5.10 Green synthesis

Green synthesis is an emerging area in the field of bionanotechnology and provides economic and environmental benefits as an alternative to chemical and physical methods. In this method, nontoxic safe reagents which are eco-friendly and biosafe are used. Various natural resources available in nature such as plant extracts, cyclodextrin, chitosan, and many more have been studied for the synthesis of metal oxide nanoparticles. In the green synthesis method, there is no requirement for high pressure, energy, temperature, or toxic chemicals. Hence, nowadays, many researchers are diverting themselves from using synthetic methods. Plants produce more stable NPs compared to other means and are very straightforward to scale up. The risk of contamination is also lower.

It is the development of a clean approach which minimizes the adverse effects on the environment and human health. It is the design of processes that reduces or eliminates the use and/or generation of hazardous substances. It encourages the replacement of existing protocols with new procedures that are more environmentally friendly and pose a low risk to human health. It helps in pollution prevention at the molecular level. It is a synthesis that utilizes a green liquid/solvent, that is, water and it usually takes place at room temperature and atmospheric pressure. The focus is on minimizing the hazard and maximizing the efficiency of synthetic chemical processes and producing nanomaterials and by-products without harming the environment or human health. There are 12 principles of green synthesis Fig. 5.11.

1. It is better to prevent waste formation than to clean up after it is formed.
2. Synthetic methods should be designed to maximize the incorporation of all materials used in the process into the final product.
3. Wherever practicable, synthetic methodologies should be designed to use and generate substances that possess little or no toxicity to human health and the environment.
4. Chemical products should be designed to preserve the efficacy of the function while reducing toxicity.
5. The use of auxiliary substances (e.g., solvents, separation agents) should be made unnecessary wherever possible and innocuous when used.
6. Energy requirements should be recognized for their environmental and economic impacts and should be minimized. Synthetic methods should be conducted at ambient temperature and pressure.
7. A raw material or feedstock should be renewable rather than depleting wherever technically and economically practicable.
8. Reduce derivatives—unnecessary derivatization (blocking group, protection/deprotection, temporary modification) should be avoided whenever possible.

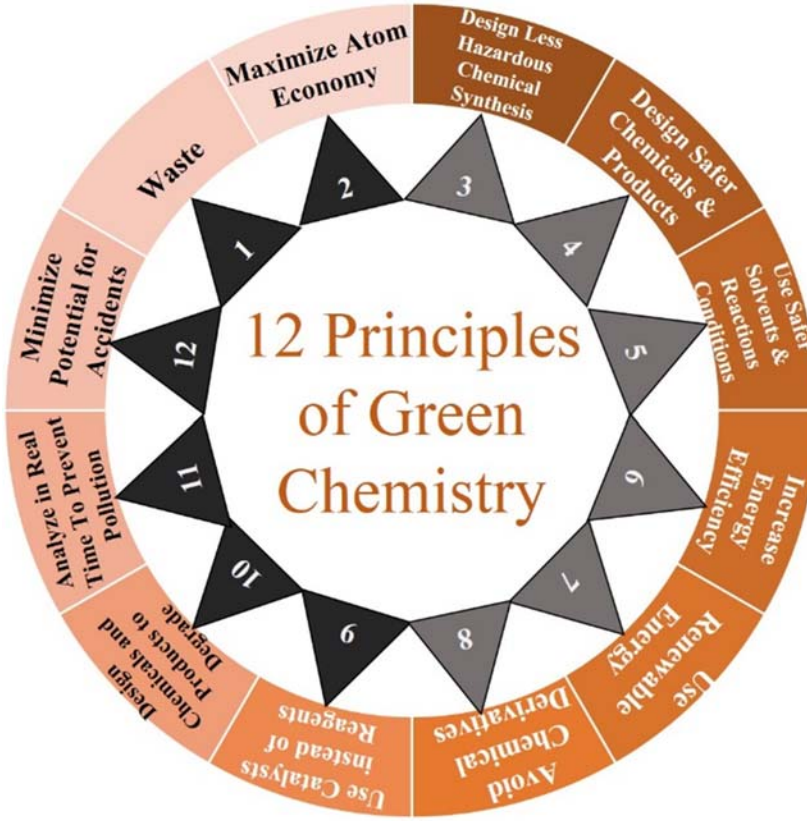

FIGURE 5.11 Twelve principles of green chemistry.

9. Catalytic reagents (as selective as possible) are superior to stoichiometric reagents.
10. Chemical products should be designed so that at the end of their function, they do not persist in the environment and break down into innocuous degradation products.
11. Analytical methodologies need to be further developed to allow for real-time, in-process monitoring and control before the formation of hazardous substances.
12. Substances and the form of a substance used in a chemical process should be chosen to minimize the potential for chemical accidents, including releases, explosions, and fires.

Environmental nanotechnology is considered to play a key role in redefining the current environmental engineering and science field. Due to their unique activity toward recalcitrant contaminants, many nanomaterials are

under active research and development for use in the treatment of water and contaminated sites. Nowadays, continuous increased concern worldwide has been observed for the development of environmental engineering applications. The utilization of metal oxide NPs has received much attention due to their unique properties, such as extremely small size, high surface-area-to-volume ratio, surface modifiability, excellent magnetic properties, and great biocompatibility. Hence, the production of NPs should be economically viable, environmentally sustainable, and well accepted by society.

In the recent past, vast research has been carried out on biological systems, including bacteria, fungi, yeast, and plants and this has led to the transformation of inorganic metal ions to metal nanoparticles. Recent studies have shown that the synthesis, characterization, and application of nanomaterials have been gaining importance in the past couple of decades. The "greener" environmentally friendly processes in chemistry and chemical technology are becoming increasingly popular and are much needed as a result of worldwide problems associated with environmental contamination. Eco-friendly solutions are gaining popularity in this contemporary world.

Having the end product environmentally friendly and using a sustainable process are the keys. To overcome the drawbacks, the green approach to nanoparticles came into existence recently to restrain the ecosystem with a naturally available biodegradable matter for its production. The degradation of any organic compound by the green approach (plant extracts) is mainly due to the presence of polyphenols in the biodegradable material used for treatment purposes. A great deal of research is carried out on a wide range of plant extracts and their chemical constituents.

Metal oxide NPs have been proven to act as a next-generation, economical disinfecting agent, which finds tremendous potential in clinical concerns, contaminant remediation, and other industrial applications due to the achievement of unique properties like antibacterial, antifungal, UV filtering properties, high catalytic, and photochemical activity. Metal oxides such as ZnO, SnO_2, and CeO_2 have been synthesized using plant extracts and have proven to possess such properties [23–36]. These phytochemicals play an essential and useful role in the synthesis of NPs as they can act as oxidizing, reducing, and stabilizing/capping agents.

Green synthesis FeNPs is the process in which plant extracts, microorganisms (bacteria, fungi, algae, and yeast), and enzymes play a significant role in the FeNPs synthesis from naturally biodegradable matter. Among these, synthesis by plant extracts is advantageous because it reduces the risk of further contamination by decreasing the reaction time and maintaining the cell structure [37].

5.10.1 Types of green synthesis

The use of ideal solvent type, that is, water and natural resources is essential to achieve this goal. Green synthesis of metallic nanoparticles has been

adopted to accommodate various biological materials (e.g., bacteria, fungi, algae, and plant extracts).

1. Plant-based extracts-mediated synthesis as shown in Fig. 5.12 (e.g., leaves, seeds, roots, and stems)

   For example, SnO_2 NPs were synthesized using $SnCl_4$ as the precursor and *Tradescantia spathacea* aqueous leaf extract as the solvent as reported by Matussin et al. The leaf extract was carried out at room temperature before mixing with the $SnCl_4$ precursor. The mixture was stirred at 80°C until a paste was produced. The paste was calcined at 800°C to produce SnO_2 NPs [26]. Similarly, the synthesis of ZnO and CeO_2 was reported [29,35].

2. Microorganisms-mediated synthesis (e.g., fungi, bacteria, and algae)

   Srivastava et al. carried out a study on the synthesis of SnO_2 NPs using *Bacterium erwina herbicola*. The bacteria were grown in a Luria broth medium and the biomass was centrifuged. Fresh and clean bacterial cells were added into an aqueous solution of 1 mM $SnCl_2$. The sample was incubated at 30°C. The sample was centrifuged at 12,000 rpm for 10 min for isolation of the nanoparticles from the sample solution. The nanoparticles were then dried in a vacuum oven at 30°C followed by annealing at 150°C [38]. In another study, Sumanth et al. successfully synthesized ZnO using an extract of endophytic fungus isolated from the leaves of *Millingtonia hortensis* [39]. The fungal synthesized ZnO NPs were pure, mainly hexagonal, and size range of 34−55 nm.

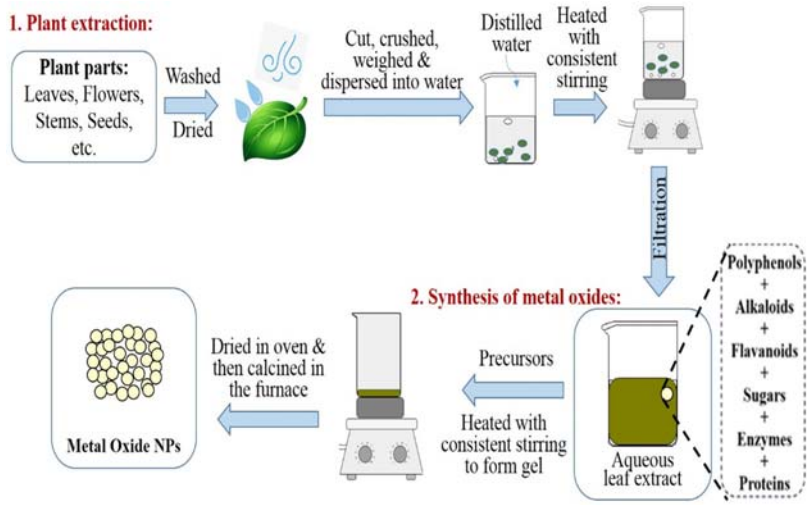

FIGURE 5.12 Green and phytogenic synthesis of metal oxides.

3. Biomolecules-assisted synthesis (e.g., DNA)

   Guo et al. reported on the synthesis of DNA-assisted synthesis AuNPs. In the synthesis, they used a 50 nM aliquot of 10 nM oligonucleotide (complementary to portions of monomeric units of stretched rolling circle products (RCPs)) functionalized (5′-AuNP-TTTTTTGCGTCTAGTGGAGCC-3′). Hybridization of these AuNPs to stretched RCPs was performed at 37°C for 2 h with shaking in a buffer containing 0.5 M NaCl, 20 mM Tris−HCl, 20 mM EDTA, and 0.01% Tween resulting in the RCPs becoming decorated with AuNPs [40].
4. Green reducing agents-mediated synthesis (e.g., glucose and sucrose)

   Lou et al. reported a simple glucose-mediated hydrothermal method for gram-scale synthesis of the SnO_2 nanoparticles. Potassium stannate trihydrate ($K_2SnO_3 \cdot 3H_2O$) was dissolved in 20 mL of 0.8 M aqueous glucose solution. Afterward, the solution was transferred to a Teflon-lined solution [41].

5.11 Summary

In this chapter, various synthesis methods of semiconducting photocatalytic materials such as hydrothermal, solvothermal, sonochemical, and microwave green synthesis have been discussed. Although many synthesis methods have been used to prepare semiconducting photocatalysts, there are selected methods that are proven to design more precise and controlled properties of semiconductors. On the other hand, due to the rising environmental concern, the minimal usage of harsh and toxic chemicals is highly recommended. Therefore, the green synthesis of photocatalysts has attracted much attention because this method uses nontoxic materials which is advantageous to human health and the environment.

References

[1] P.F.M. de Oliveira, J. Quiroz, D.C. de Oliveira, P.H.C. Camargo, A mechano-colloidal approach for the controlled synthesis of metal nanoparticles, Chemical Communications 55 (2019) 14267−14270. Available from: https://doi.org/10.1039/c9cc06199a.

[2] A. Hernández-Ramírez, I. Medina-Ramírez, Photocatalytic semiconductors: synthesis, characterization, and environmental applications, 2015. https://doi.org/10.1007/978-3-319-10999-2.

[3] M.M. Khan, D. Pradhan, Y. Sohn, Nanocomposites for Visible Light-Induced Photocatalysis, Springer International Publishing, Cham, 2017. Available from: https://doi.org/10.1007/978-3-319-62446-4.

[4] H.P. Shivaraju, N. Muzakkira, B. Shahmoradi, Photocatalytic treatment of oil and grease spills in wastewater using coated N-doped TiO_2 polyscales under sunlight as an alternative driving energy, International Journal of Environmental Science and Technology 13 (2016) 2293−2302. Available from: https://doi.org/10.1007/s13762-016-1038-8.

[5] A.S. Ahmed, M. Shafeeq M., M.L. Singla, S. Tabassum, A.H. Naqvi, A. Azam, Band gap narrowing and fluorescence properties of nickel doped SnO_2 nanoparticles, Journal of Luminescence 131 (2011) 1–6. Available from: https://doi.org/10.1016/j.jlumin.2010.07.017.

[6] M. Wang, Y. Che, C. Niu, M. Dang, D. Dong, Effective visible light-active boron and europium co-doped $BiVO_4$ synthesized by sol–gel method for photodegradion of methyl orange, Journal of Hazardous Materials 262 (2013) 447–455. Available from: https://doi.org/10.1016/j.jhazmat.2013.08.063.

[7] T. Moritz, J. Reiss, K. Diesner, D. Su, A. Chemseddine, ChemInform abstract: nanostructured crystalline TiO_2 through growth control and stabilization of intermediate structural building units, ChemInform 28 (2010). Available from: https://doi.org/10.1002/chin.199751032. no-no.

[8] N. Liu, X. Chen, J. Zhang, J.W. Schwank, A review on TiO_2-based nanotubes synthesized via hydrothermal method: formation mechanism, structure modification, and photocatalytic applications, Catalysis Today 225 (2014) 34–51. Available from: https://doi.org/10.1016/j.cattod.2013.10.090.

[9] M. Hu, Z. Zhang, C. Luo, X. Qiao, One-pot green synthesis of Ag-decorated SnO_2 microsphere: an efficient and reusable catalyst for reduction of 4-nitrophenol, Nanoscale Research Letters 12 (2017). Available from: https://doi.org/10.1186/s11671-017-2204-8.

[10] A. Phuruangrat, P. Dumrongrojthanath, N. Ekthammathat, S. Thongtem, T. Thongtem, Hydrothermal synthesis, characterization, and visible light-driven photocatalytic properties of Bi_2 WO_6 nanoplates, Journal of Nanomaterials 2014 (2014) 1–7. Available from: https://doi.org/10.1155/2014/138561.

[11] L. Chen, C.-W. Chen, C.-D. Dong, Hydrothermal synthesis of Se-doped MoS_2 quantum dots heterojunction for highly efficient photocatalytic degradation, Materials Letters 291 (2021) 129537. Available from: https://doi.org/10.1016/j.matlet.2021.129537.

[12] G. Jeevitha, D. Mangalaraj, Ammonia sensing at ambient temperature using tungsten oxide, Materials Today: Proceedings 18 (2019) 1602–1609. Available from: https://doi.org/10.1016/j.matpr.2019.05.254.

[13] B. Qian, D. Wang, H. Wang, H. Zou, Y. Song, X. Zhou, et al., Solvothermal synthesis of columnar $Gd_2O_2S:Eu^{3+}$ and a comparative study with columnar $Gd_2O_3:Eu^{3+}$, Journal of the American Ceramic Society 103 (2020) 356–366. Available from: https://doi.org/10.1111/jace.16747.

[14] P.P. Goswami, H.A. Choudhury, S. Chakma, V.S. Moholkar, Sonochemical synthesis of cobalt ferrite nanoparticles, International Journal of Chemical Engineering 2013 (2013). Available from: https://doi.org/10.1155/2013/934234.

[15] X. Hangxun, B.W. Zeiger, K.S. Suslick, Sonochemical synthesis of nanomaterials, Chemical Society Reviews 42 (2013) 2555–2567. Available from: https://doi.org/10.1039/c2cs35282f.

[16] B. Kumar, K. Smita, L. Cumbal, A. Debut, R.N. Pathak, Sonochemical synthesis of silver nanoparticles using starch: a comparison, Bioinorganic Chemistry and Applications 2014 (2014). Available from: https://doi.org/10.1155/2014/784268.

[17] M.P. Blanco-Vega, J.L. Guzmán-Mar, M. Villanueva-Rodríguez, L. Maya-Treviño, L.L. Garza-Tovar, A. Hernández-Ramírez, et al., Photocatalytic elimination of bisphenol A under visible light using Ni-doped TiO_2 synthesized by microwave assisted sol-gel method, Materials Science in Semiconductor Processing 71 (2017) 275–282. Available from: https://doi.org/10.1016/j.mssp.2017.08.013.

[18] K.-Y. Shih, Y.-L. Kuan, E.-R. Wang, One-step microwave-assisted synthesis and visible-light photocatalytic activity enhancement of BiOBr/RGO nanocomposites for degradation of methylene blue, Materials 14 (2021) 4577. Available from: https://doi.org/10.3390/ma14164577.

[19] C. Sarantopoulos, A.N. Gleizes, F. Maury, Chemical vapor deposition and characterization of nitrogen doped TiO_2 thin films on glass substrates, Thin Solid Films 518 (2009) 1299−1303. Available from: https://doi.org/10.1016/j.tsf.2009.04.070.

[20] M. Roy, Protective hard coatings for tribological applications, Materials Under Extreme Conditions, Elsevier, 2017, pp. 259−292. Available from: https://doi.org/10.1016/B978-0-12-801300-7.00008-5.

[21] M.C. Yang, T.S. Yang, M.S. Wong, Nitrogen-doped titanium oxide films as visible light photocatalyst by vapor deposition, Thin Solid Films 469−470 (2004) 1−5. Available from: https://doi.org/10.1016/j.tsf.2004.06.189.

[22] S.Z. Werta, O.K. Echendu, K.O. Egbo, F.B. Dejene, Electrochemical deposition and characterization of thin-film $Cd_{1-x}Zn_xS$ for solar cell application: the effect of cathodic deposition voltage, Thin Solid Films 689 (2019) 137511. Available from: https://doi.org/10.1016/j.tsf.2019.137511.

[23] S. Matussin, M.H. Harunsani, A.L. Tan, M.M. Khan, Plant-extract-mediated SnO_2 nanoparticles: synthesis and applications, ACS Sustainable Chemistry & Engineering 8 (2020) 3040−3054. Available from: https://doi.org/10.1021/acssuschemeng.9b06398.

[24] S.N. Matussin, A.L. Tan, M.H. Harunsani, M.H. Cho, M.M. Khan, Green and phytogenic fabrication of Co-doped SnO_2 using aqueous leaf extract of *Tradescantia spathacea* for photoantioxidant and photocatalytic studies, Bionanoscience 11 (2021) 120−135. Available from: https://doi.org/10.1007/s12668-020-00820-3.

[25] S.N. Matussin, M.H. Harunsani, A.L. Tan, M.H. Cho, M.M. Khan, Effect of Co^{2+} and Ni^{2+} co-doping on SnO_2 synthesized via phytogenic method for photoantioxidant studies and photoconversion of 4-nitrophenol, Materials Today Communications 25 (2020) 101677. Available from: https://doi.org/10.1016/j.mtcomm.2020.101677.

[26] S.N. Matussin, M.H. Harunsani, A.L. Tan, A. Mohammad, M.H. Cho, M.M. Khan, Photoantioxidant studies of the SnO_2 nanoparticles fabricated using aqueous leaf extract of *Tradescantia spathacea*, Solid State Sciences (2020) 106279. Available from: https://doi.org/10.1016/j.solidstatesciences.2020.106279.

[27] S.N. Matussin, A.L. Tan, M.H. Harunsani, A. Mohammad, M.H. Cho, M.M. Khan, Effect of Ni-doping on the properties of the SnO_2 synthesized using *Tradescantia spathacea* for photoantioxidant studies, Materials Chemistry and Physics (2020) 123293. Available from: https://doi.org/10.1016/j.matchemphys.2020.123293.

[28] A. Rahman, M.H. Harunsani, A.L. Tan, M.M. Khan, Zinc oxide and zinc oxide-based nanostructures: biogenic and phytogenic synthesis, properties and applications, Bioprocess and Biosystems Engineering 44 (2021) 333−1372. Available from: https://doi.org/10.1007/s00449-021-02530-w.

[29] A. Rahman, M.H. Harunsani, A.L. Tan, N. Ahmad, M.M. Khan, Antioxidant and antibacterial studies of phytogenic fabricated ZnO using aqueous leaf extract of *Ziziphus mauritiana* Lam, Chemical Papers 75 (2021) 3295−3308. Available from: https://doi.org/10.1007/s11696-021-01553-7.

[30] A. Rahman, A.L. Tan, M.H. Harunsani, N. Ahmad, M. Hojamberdiev, M.M. Khan, Visible light induced antibacterial and antioxidant studies of ZnO and Cu-doped ZnO fabricated using aqueous leaf extract of *Ziziphus mauritiana* Lam, Journal of Environmental

Chemical Engineering (2021) 105481. Available from: https://doi.org/10.1016/j.jece.2021.105481.

[31] A. Rahman, M.H. Harunsani, A.L. Tan, N. Ahmad, M. Hojamberdiev, M.M. Khan, Effect of Mg doping on ZnO fabricated using aqueous leaf extract of *Ziziphus mauritiana* Lam. for antioxidant and antibacterial studies, Bioprocess and Biosystems Engineering 44 (2021) 875−889. Available from: https://doi.org/10.1007/s00449-020-02496-1.

[32] A. Rahman, M.H. Harunsani, A.L. Tan, N. Ahmad, B.K. Min, M.M. Khan, Influence of Mg and Cu dual-doping on phytogenic synthesized ZnO for light induced antibacterial and radical scavenging activities, Materials Science in Semiconductor Processing 128 (2021) 105761. Available from: https://doi.org/10.1016/j.mssp.2021.105761.

[33] S.N. Naidi, M.H. Harunsani, A.L. Tan, M.M. Khan, Structural, morphological and optical studies of CeO_2 nanoparticles synthesized using aqueous leaf extract of *Pometia pinnata*, BioNanoScience 12 (2022) 393−404. Available from: https://doi.org/10.1007/s12668-022-00956-4.

[34] S.N. Naidi, M.H. Harunsani, A.L. Tan, M.M. Khan, Green-synthesized CeO_2 nanoparticles for photocatalytic, antimicrobial, antioxidant and cytotoxicity activities, Journal of Materials Chemistry B 9 (2021) 5599−5620. Available from: https://doi.org/10.1039/D1TB00248A.

[35] S.N. Naidi, F. Khan, A.L. Tan, M.H. Harunsani, Y.-M. Kim, M.M. Khan, Photoantioxidant and antibiofilm studies of green synthesized Sn-doped CeO_2 nanoparticles using aqueous leaf extracts of *Pometia pinnata*, New Journal of Chemistry 45 (2021) 7816−7829. Available from: https://doi.org/10.1039/D1NJ00416F.

[36] S.N. Naidi, F. Khan, A.L. Tan, M.H. Harunsani, Y.-M. Kim, M.M. Khan, Green synthesis of CeO_2 and Zr/Sn-dual doped CeO_2 nanoparticles with photoantioxidant and antibiofilm activities, Biomaterials Science 9 (2021) 4854−4869. Available from: https://doi.org/10.1039/D1BM00298H.

[37] C.P. Devatha, A.K. Thalla, Green Synthesis of Nanomaterials, Elsevier Ltd, 2018. Available from: https://doi.org/10.1016/b978-0-08-101975-7.00007-5.

[38] N. Srivastava, M. Mukhopadhyay, Biosynthesis of SnO_2 nanoparticles using *Bacterium erwina herbicola* and their photocatalytic activity for degradation of dyes, Industrial and Engineering Chemistry Research 53 (2014) 13971−13979. Available from: https://doi.org/10.1021/ie5020052.

[39] B. Sumanth, T.R. Lakshmeesha, M.A. Ansari, M.A. Alzohairy, A.C. Udayashankar, B. Shobha, et al., Mycogenic synthesis of extracellular zinc oxide nanoparticles from *Xylaria acuta* and its nanoantibiotic potential, International Journal of Nanomedicine 15 (2020) 8519−8536. Available from: https://doi.org/10.2147/IJN.S271743.

[40] M. Guo, I. Hernández-Neuta, N. Madaboosi, M. Nilsson, W. van der Wijngaart, Efficient DNA-assisted synthesis of trans-membrane gold nanowires, Microsystems & Nanoengineering 4 (2018) 1−8. Available from: https://doi.org/10.1038/micronano.2017.84.

[41] X.W. Lou, J.S. Chen, P. Chen, L.A. Archer, One-pot synthesis of carbon-coated SnO_2 nanocolloids with improved reversible lithium storage properties, Chemistry of Materials 21 (2009) 2868−2874. Available from: https://doi.org/10.1021/cm900613d.

Chapter 6

Common characterization techniques for photocatalytic materials

Mohammad Mansoob Khan

6.1 Introduction

In synthetic chemistry, materials science, materials engineering, etc. sample analysis or characterization refers to the general process by which a material's structure and properties are probed and measured. Some definitions limit the use of the term to techniques that study the microscopic structure and properties of materials, while others use the term to refer to any materials analysis process including macroscopic techniques such as density calculation, mechanical testing, and thermal analysis. The scale of the structures observed in materials characterization ranges from angstrom, nanometer, and micrometer such as in the imaging of individual atoms and chemical bonds, up to centimeters, such as in the imaging of coarse grain structures of metals.

Though many characterization techniques have been practiced for centuries, such as basic optical microscopy, new techniques and methodologies are constantly emerging. In particular, the introduction of the electron microscope and secondary ion mass spectrometry in the 20th century has revolutionized the field, allowing the imaging and analysis of structures and compositions on much smaller scales than was previously not possible, leading to a huge increase in the level of understanding as to why different materials show different properties, characteristics, and behaviors. Very recently, atomic force microscopy has further increased the maximum possible resolution for the analysis of certain samples [1].

Material characterization is a crucial step to take before using the materials for any purpose. Depending on the purpose, one can subject the material to mechanical, thermal, chemical, optical, electrical, and other characterizations, depending on the purpose to ensure that the material can perform without failure. The development of particularly new materials requires characterization of their structure across a range of length scales ranging from macro to atomic. Significant advances have been made to enhance the photocatalytic performance

Theoretical Concepts of Photocatalysis. DOI: https://doi.org/10.1016/B978-0-323-95191-3.00002-X

of photocatalytic materials via methods such as structure optimization, doping, surface modification, and fabrication of composites with other photoactive materials. Moreover, there are many fundamental issues regarding the light−matter interaction, structure−property relationship, and photocatalyst−pollutant interaction that are essential for the performance optimization of photocatalysts [2]. Therefore, accurate characterization of the crystal and electronic structures of these materials and their corresponding performance during the photocatalytic process is crucial not only for an in-depth understanding of the photocatalytic mechanism but also for providing experimental guidelines as well as a theoretical framework for the synthesis of high-performance photocatalysts.

For nanomaterials, size becomes an important feature that affects the chemical and physical properties, such as the reactivity and optical band gap energy. Moreover, particle size is of primary importance in heterogeneous photocatalysis, because it is directly related to the efficiency of a catalyst through the enhancement of its specific surface area. Therefore, different characterization techniques are required to deeply study and understand the properties of novel nanomaterials. Currently, various characterization and sample analysis methods are available and are being used effectively [1,3,4]. These characterization methods are broadly categorized into three groups [5,6]:

1. Spectroscopic characterization techniques: Study of the interaction between matter and electromagnetic radiation.
2. Physicochemical characterization techniques: Study of the physical and chemical properties, composition, identification, quality, purity, and stability of a material.
3. Electrochemical characterization techniques: Study of electrical stimulation to analyze the chemical reactivity of a sample surface or a solution.

6.2 Spectroscopic characterization techniques

Historically, spectroscopy originated through the study of visible light dispersed according to its wavelength by a prism. Later the concept was expanded greatly to include any interaction with radiative energy as a function of its wavelength or frequency, predominantly in the electromagnetic spectrum. Although, matter waves and acoustic waves can also be considered forms of radiative energy. Recently, with tremendous difficulty, even gravitational waves have been associated with a spectral signature in the context of the laser interferometer gravitational-wave observatory (LIGO) and laser interferometry.

Spectroscopy is the study of the interaction between matter and electromagnetic radiation, such as electron spectroscopy and atomic spectroscopy. The data obtained from spectroscopy are called a spectrum. A spectrum is a plot of the intensity of energy detected versus the wavelength (or mass or momentum or frequency, etc.) of the energy. Spectroscopic data are often represented by an absorption or emission spectrum, a plot of the response of interest, as a function of wavelength or frequency. Therefore, spectroscopic techniques are

methods that use radiated energy to analyze the properties or characteristics of materials. A spectroscopy spectrum can be used to obtain information about atomic and molecular energy levels, molecular geometries, chemical bonds, interactions of molecules, and related processes. Often, these spectra are used to identify the components of a sample (qualitative analysis). They may also be used to measure the amount of material in a sample (quantitative analysis). They are the basis on which the main class of instrumental analysis and methods were developed and widely used in many areas of modern sciences. The study of molecular structure and dynamics through the absorption, emission, and scattering of light is known as spectroscopy. In short, it is the study of the interaction of electromagnetic radiation in all its forms with matter. The interaction might give rise to electronic excitations (e.g., UV-Vis spectroscopy), molecular vibrations (e.g., Fourier transform infrared (FTIR) and Raman spectroscopy), or nuclear spin orientations (e.g., NMR spectroscopy) [1,3].

6.2.1 Absorption spectroscopy

Absorption spectroscopy is a spectroscopic technique that measures the absorption of radiation as a function of frequency or wavelength due to its interaction with a sample. It is an analytical technique that measures the amount of light absorbed by a sample at a given wavelength. The sample absorbs light in the form of energy, i.e., photons, from the radiating field. The intensity of the absorption varies as a function of frequency and this variation is the absorption spectrum. It can be performed across the electromagnetic spectrum (as shown in Fig. 6.1) depending on the light source. It is

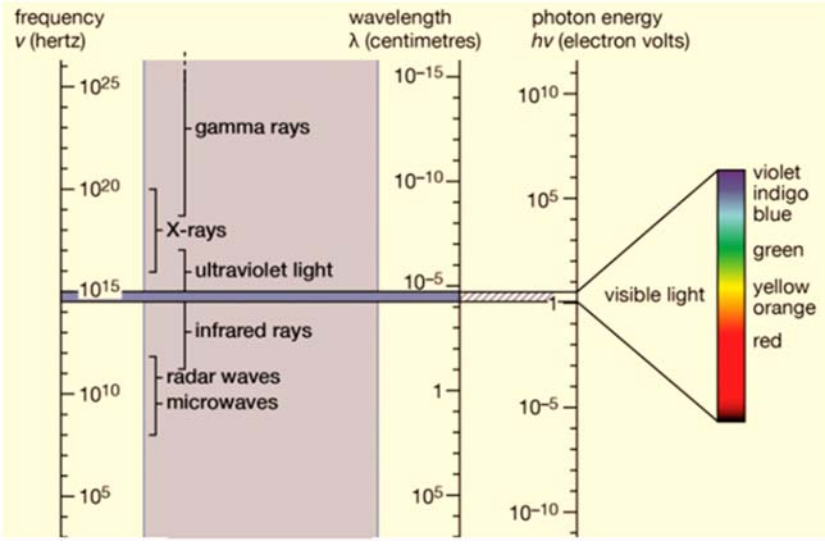

FIGURE 6.1 The electromagnetic spectrum.

used as an analytical tool to determine the presence of a particular substance in a sample, and in many cases, to quantify the amount of the substance present. Ultraviolet-visible and infrared spectroscopy are two examples of absorption spectroscopy. These are the first-hand tools and very common characterization instruments available for sample analysis [1].

6.2.2 Absorption spectroscopy for optical properties

Absorption spectroscopy uses electromagnetic radiation (190−800 nm) which is divided into the ultraviolet range (∼190−400 nm) and the visible range (∼400−800 nm) [7]. In UV-Vis spectroscopy, the light intensity that passes through the sample is measured. Light can either be reflected, scattered, transmitted, or absorbed from matter, and can cause photochemical reactions to occur. The optical properties of a nanomaterial are based on the size, shape, agglomeration, and variation of concentrations. Metal nanoparticles, on the other hand, have unique optical properties which are due to the collective oscillations of conduction electrons when excited by electromagnetic radiation. This phenomenon is called surface plasmon resonances [8].

In general, electrons in the conduction band in nanoparticles collectively oscillate in response to electromagnetic waves. This shows the information on the size, aggregation, structures, etc. of the nanoparticles [9]. Based on the type of samples, i.e., liquid, film, powder, etc. and the optical properties to be measured, UV-Vis spectrophotometry is of two types.

6.2.2.1 UV-visible spectroscopy

UV-visible spectroscopy or spectrophotometry is a quantitative technique used to measure how much a chemical substance absorbs light. This is done by measuring the intensity of light that passes through a sample with respect to the intensity of light through a reference sample or blank. The principle of UV-visible spectroscopy is based on the absorption of ultraviolet light or visible light by chemical compounds, which results in the production of distinct spectra. Spectroscopy is based on the interaction between light and matter.

This method consists of a deuterium or tungsten lamp as a light source for the ultraviolet and visible region wavelengths, respectively, sample and reference beams, a photodetector, and a monochromator (Fig. 6.2). Irradiating the liquid sample by UV light gives the UV spectrum whereas irradiating the liquid sample by UV-Vis light will give the UV-Vis spectrum. Cuvettes are used for sample holding and are kept inside the instrument for introducing samples to the light path. There are different types of cuvettes, namely glass, plastic, silica, or quartz. Plastics and glass cuvettes absorb wavelengths below 310 nm. Therefore, cuvettes made of plastics and glass cannot be used for absorbance studies beyond that wavelength. Hence, quartz cuvettes are used for absorption measurements in the ultraviolet range as they are transparent to

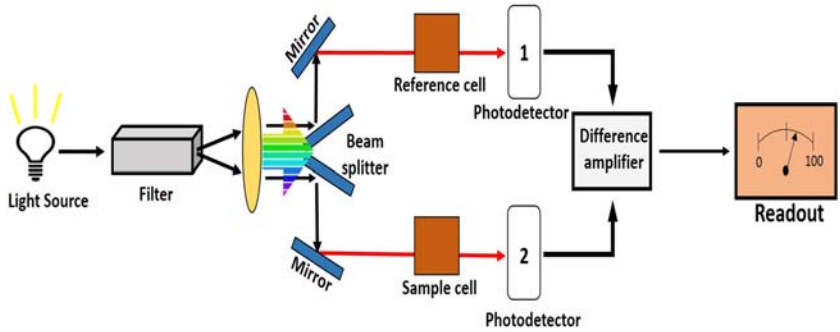

FIGURE 6.2 Schematic of UV-visible spectrophotometer.

wavelengths above 180 nm. There are two types of spectrophotometers which are [10].

- Single-beam spectrophotometers: The light from the monochromator passes through the sample and then to the detector in a single-beam system. Because of the simplicity of the design, fewer optical components are utilized, resulting in a smaller instrument and lower cost. However, a baseline or blank sample must be measured before a sample may be measured. For liquid measurements, the baseline reading is taken to allow for any absorbance of the cuvette and solvent used. The baseline must be measured separately from the sample in a single-beam system. The measurement may be less accurate if there is any variation in the light intensity or system optical performance between the baseline and sample being read separately.
- Double beam spectrophotometers: The light emitted by the monochromator is separated into two beams in the double beam system: a reference beam and a sample beam (Fig. 6.2). The light is usually split with an optical component such as a rotating wheel which has a mirrored segment or a half-silvered mirror called a beam splitter. Each beam follows its optical route into the sample chamber. The reference/blank and sample can be measured at the same time since two beams of the same wavelength are available. This means that the sample measurement can be corrected in real-time for any instrument fluctuations. This real-time adjustment ensures highly accurate measurement.

A beam traveling from the light source to the detector without the sample interaction is used as the reference beam. The light beam interacts with the sample so that it is exposed to ultraviolet light of continuously changing the wavelength. Energy is absorbed when the wavelength emitted corresponds to the energy level that promotes an electron to a higher molecular orbital. The ratio between the sample and reference beam intensities is recorded by the photodetector. The wavelength is determined by the sample's maximum

absorption level. When a difference is found in the intensities that means the reference beam's intensity is higher than the sample, and the particular wavelength is plotted as having a high ultraviolet absorbance. UV-vis spectrum refers to the absorbance or reflectance spectra in the UV-visible region. When the light beam is passed through the solution, a part of the light may be absorbed, and the rest is transmitted through the solution. The ratio of light entering the sample to the light that exits the sample at a fixed wavelength is called transmittance. The negative logarithm of transmittance is called absorbance [1].

When light passes through or is reflected from a sample, the amount of light absorbed is the difference between the incident radiation (I_o) and the transmitted radiation (I). The amount of light absorbed is expressed as absorbance. Transmittance, or light that passes through a sample, is usually given in terms of a fraction of 1 or as a percentage and is defined as

$$T = \frac{I}{I_o} \text{ or } \%T = \frac{I}{I_o} \times 100$$

Whereas absorbance is defined as $A = -\log T$

For most applications, absorbance values are used since the relationship between absorbance and both concentration and path length is normally linear (as per the Beer−Lambert law).

Beer−Lambert law: At a particular wavelength, the absorbance of a sample is directly proportional to the concentration of the absorbing substance and the path length, i.e., $A = \varepsilon cl$, where A is the absorbance, ε is the molar absorptivity (L/mol/cm), c is the concentration (mol/L), and l is the path length (1 cm). The incident radiation should be monochromatic. The absorbing medium should be homogeneous and not scatter the radiation. For example:

1. Colloidal solutions of metal nanoparticles (NPs) within 100 nm diameter scatter the optical light with much efficiency due to their surface plasmon resonance. This is a collective resonance of the conduction electrons in the metal. The bandwidth of the spectrum, magnitude, and wavelength peak of the plasmon resonance is linked to the NPs which depends on the composition of the material, environment, shape, and size of the material.
2. Silver NPs show a plasmon resonance peak featuring an absorption around 410−450 nm. The particle size and dielectric of the medium influence the shape and position of the plasmon absorption in the case of silver NPs. Metal NPs have absorption spectra that can shift toward longer wavelengths as the particle size increases [11].

Energy from incident light causes electrons to transition to different energy levels. Electronic transitions also occur between the vibrational and rotational energy levels of molecules. When a molecule absorbs a UV-visible

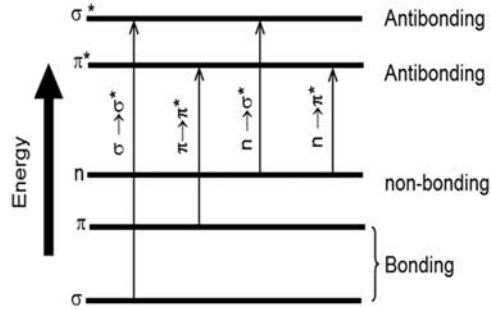

FIGURE 6.3 Electronic transition during UV-visible spectroscopy.

photon (c. 200−700 nm), it promotes a bonding or non-bonding electron into an antibonding orbital as shown in Fig. 6.3. This is called electronic transition [1].

- Bonding ēs appear in *s* and *p* molecular orbitals; non-bonding ēs appear in *n* energy level
- Antibonding orbitals correspond to the bonding ones
- ēs transition can take place between various states. In general, the energy of ēs transition increases in the following order: $(n \rightarrow \pi^*) < (n \rightarrow \sigma^*) < (\pi \rightarrow \pi^*) < (\sigma \rightarrow \sigma^*)$

Even though UV-vis spectroscopy is mainly used to study the synthesis, characterization, and application of colloidal nanoparticles, organic materials, including polymers, metallic nanoparticles, and ceramics with magnetic characteristics can also be used:

- To monitor catalytic/photocatalytic reaction
- To determine the concentration of a particular molecule in solution
- To study biological processes
- For colorimetric detection.

6.2.2.2 *Diffuse reflectance spectroscopy*

In the case of nonhomogeneous, opaque, films, or powdered materials, determination of the band gap is not possible using either the optical transmission−reflection or the spectroscopic ellipsometric methods. Measurement of the diffuse reflectance instead is a more adequate technique. Diffuse reflectance spectroscopy (DRS) is a suitable technique to measure the optical properties of rough surfaces or powders. This technique also provides information about the oxidation state and coordination environment of transition metal ions in catalytic solids. If the surface of the material or sample is microscopically rough, the light rays will reflect and diffuse in many different directions. In this case, each ray follows the law of reflection. However,

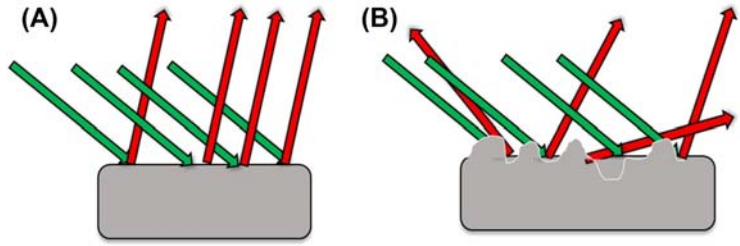

FIGURE 6.4 Comparison between (A) specular reflectance (smooth surface) and (B) diffuse reflectance (rough surfaces).

the roughness of the material makes each ray meets a surface with a different orientation. Subsequently, when the individual rays reflect off the rough surface, they scatter in different directions (see Fig. 6.4).

When electromagnetic radiation is incident upon a sample that can scatter as well as absorb photons, Beer–Lambert law is no longer useful due to two main reasons. (1) The path length l is no longer well defined. (2) The optical response is no longer determined by k but by $\hat{n} = n - ik$.

The diffuse reflectance phenomenon is complex, but in the simplest case of a non-absorbing material ($k = 0$), it only involves the scattering of photons. The scattering of light can be divided into three different types: (1) single scattering, (2) multiple scattering, and (3) dependent scattering. The first type arises when scattering centers are sufficiently apart that each is illuminated only by photons not previously scattered, and on average, there is no phase relationship between the photons scattered from the neighboring particles. In the case of multiple scattering, the scattering centers are still far apart that they may be treated as independent, but each center is now illuminated by photons scattered from adjacent particles. Dependent scattering arises when, in addition to multiple scattering, phase coherence exists between scattered photons from adjacent centers. Dependent scattering is present if the average distance (d) between scattering centers is less than three times the particle diameter.

The division of light scattering systems into the above three categories determines the theoretical approach necessary to describe the scattered light intensity. For single and multiple scattering, the absence of phase coherence ensures that the total scattered light intensity is merely the sum of the intensities of the individual scatters. Both types of scattering can be mathematically treated easily. In contrast, when the particles become so tightly packed that phase coherence becomes important, amplitudes rather than intensities must be summed. This is the case for heterogeneous catalysts because they are always investigated in the form of densely packed powders. Then the radiation transfer theory has to be considered, leading to the well-known Kubelka–Munk theory. The Kubelka–Munk model uses an effective scattering coefficient S and an effective absorption coefficient K to describe the

optical properties of a compact powder sample. A sufficiently thick sample so that all the incident light is absorbed or scattered, no light is considered. Hence, the Kubelka–Munk (K–M) function, $F(R_\infty)$, is related to the apparent absorption (K) and the apparent scattering coefficient (S) as shown by Eq. (6.1):

$$F(R_\infty) = \frac{(1-R_\infty)^2}{2R_\infty} = \frac{K}{S} \tag{6.1}$$

where $R_\infty = \frac{R_{\text{sample}}}{R_{\text{standard}}}$ and it is the equivalent to the Beer–Lambert law for dilute species measured by diffuse reflectance experiments using Eq. (6.2):

$$F(R_\infty) = \frac{\varepsilon C}{S} \tag{6.2}$$

where ε is the molar absorptivity and C is the concentration. For such powder infinitely thick samples, the optical band gap can be easily calculated by substituting α by $F(R_\infty)$. However, as discussed by Murphy, when a thin powder sample (<1 mm) or a rough thin coating on a substrate is measured using DRS, the reflection and transmission of the light through the different interfaces need to be taken into account to avoid the thickness dependence of the optical gap [12]. For this, Murphy in another work proposed a modified K–M two-flux model to calculate the reflectance of the coating as a function of the refractive index, absorption coefficient, scattering coefficient, and thickness [13,14]. Then a fitting procedure is used to correlate the calculated reflectance spectra to the measurements using a spectral-projected gradient algorithm, and in this way, appropriate optical properties can be obtained.

DRS measurements can be performed using a UV-vis spectrophotometer using a special accessory called an integrating sphere. This accessory provides the ability to collect a quantitative reflectance spectrum from highly scattering or irregularly shaped samples, but acquiring only diffuse light, not the specular signal, and so, the Kubelka–Munk theory can be applied.

6.2.3 Vibrational spectroscopy (Fourier transform infrared spectroscopy and Raman spectroscopy)

Vibrational spectroscopy is another type of absorption spectroscopy. Vibrational spectroscopy is a useful method for determining the structure of molecules. The transitions between vibrational states of a molecule are observed experimentally via infrared and Raman spectroscopy. Vibrational spectroscopy reveals the nature of chemical bonds, intramolecular interactions between atoms within a molecule, and intermolecular forces in the condensed phase. To gain such useful information, it is necessary to assign vibrational motion corresponding to each peak in the spectrum. This assignment can be quite difficult due to the large number of closely spaced peaks even in fairly simple molecules.

Vibrational spectroscopy covers a range of techniques, mostly based on absorption spectroscopy. It is a collective term used to describe two analytical techniques, i.e., infrared spectroscopy and Raman spectroscopy. The main difference between these two is the type of vibrations and transitions that are measured. Typically, these two forms of spectroscopies are used in connection with each other to get complete information about the compounds. IR spectroscopy and Raman spectroscopy are both nondestructive and noninvasive tools that provide information about the molecular composition, structure, and interactions within a sample [1,15].

6.2.3.1 Fourier transform infrared spectroscopy

FTIR spectroscopy is vibrational spectroscopy which works in the IR region of the electromagnetic spectrum and uses light with a longer wavelength and lower frequency than visible light. This technique measures vibrational energy levels which are associated with the chemical bonds in the sample as each chemical bond has a unique vibrational energy. Even a carbon−carbon bond will be different from one compound to another depending on what other elements or functional group each carbon is bound to. Due to this unique vibrational energy, each compound will have a unique fingerprint or the output identifying the peak strengths at specific vibrations. This fingerprint can be used to determine the structure of the compounds, identify and characterize the compounds, and identify impurities. This is done by comparing the obtained fingerprint with the fingerprints of known compounds.

It is an analysis tool used for the identification of organic, inorganic, and polymeric materials utilizing infrared light by scanning the samples. Changes in the characteristic pattern of absorption bands clearly indicate a change in the material composition. FTIR is useful in identifying and characterizing unknown materials, detecting contaminants in a material, finding additives, and identifying decomposition, oxidation, and reduction. A schematic diagram of the FTIR spectrophotometer is shown in Fig. 6.5. A typical FTIR spectrometer includes an infrared light source, sample cell, detector, amplifier, A/D converter, and a computer. Radiation from the light source reaches the detector after it passes through the interferometer. The signal is amplified and converted to a digital signal by the A/D converter and amplifier, after which the signal is transferred to the computer where the Fourier transform is carried out.

The infrared radiation of about $100-10{,}000\ \mathrm{cm}^{-1}$ is passed through the sample with part of the radiation absorbed and some passing through. The radiation that is absorbed is converted by the sample to vibrational or rotational energy. The resultant signal obtained at the detector is a spectrum generally from 400 to $4000\ \mathrm{cm}^{-1}$, which represents the sample's molecular fingerprint. Every molecule has a unique fingerprint, which makes FTIR spectroscopy an invaluable tool for chemical identification.

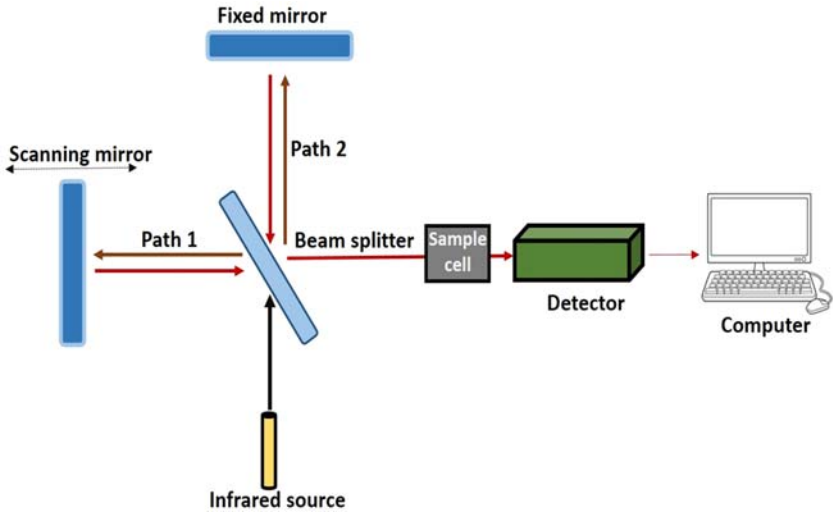

FIGURE 6.5 Schematic diagram of FTIR spectrophotometer.

FTIR spectroscopy has broad use and applicability in the analysis of compounds and molecules in the field of chemical, pharmaceutical, and polymer industries. FTIR spectroscopy instrument is used in industry and academic laboratories to better understand the reaction kinetics, mechanism, and pathways as well as catalytic reactions. In quality assurance and quality control laboratories, FTIR spectroscopy is used to check quality control of final products, purity, minimize impurities, scale-up chemical reactions, and optimize reaction yield. In the chemical laboratory, it is used to ensure that raw materials, intermediates, and final products are according to the plan and purity specifications. In chemical industries, it helps to ensure processes are stable, under control, product formation, and meet end-product specifications and impurity profiles.

6.2.3.2 Raman spectroscopy

Raman spectroscopy is a type of absorption spectroscopy that is used to detect vibrations at the molecular level using Raman scattering. It offers information complementary to that obtained by IR spectroscopy. It provides information about chemical structures and physical forms, which are useful for the identification of substances. This phenomenon was first observed by Raman and Krishnan in 1928. Various samples such as solids, liquids, or vapors in the form of particles or surface layers can be studied using Raman spectroscopy. It is based on inelastic scattering or Raman scattering of monochromatic light generally from the laser in visible, near-IR, or near ultraviolet range.

Typically, a laser beam is used to illuminate the sample (Fig. 6.6). The electromagnetic radiation from the laser hits the spot which is later collected

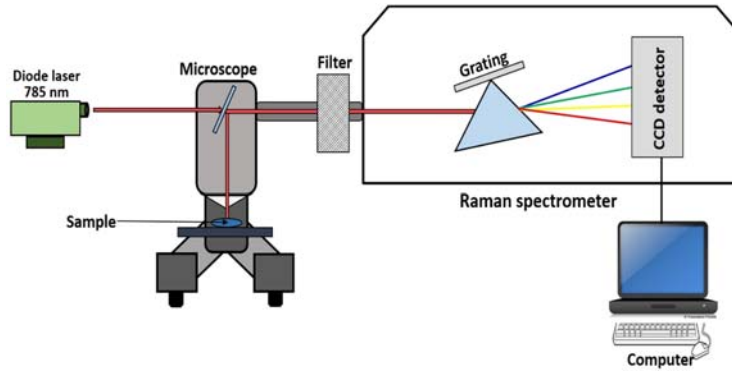

FIGURE 6.6 Schematic of a conventional Raman spectrometer.

with a lens and passed through a collimator. The molecule becomes excited to an excited state from a ground state and is relaxed into a vibrationally excited state. This creates the Stokes-Raman scattering. For example, if the molecules are already in the vibrational state, then it is called anti-Stokes-Raman scattering. A change in polarizability is required for the molecule to exhibit Raman scattering. The intensity of the Raman scattering depends on the change in polarizability whereas the Raman shift is based on the vibrational levels involved.

Raman spectroscopy is a form of vibrational spectroscopy, much like IR spectroscopy, and is used to collect a unique chemical fingerprint of molecules. IR bands arise from a change in the dipole moment of a molecule due to the interaction of light with the molecule, whereas Raman bands arise because of a change in the polarizability of the molecule due to the same interaction.

This means that these observed bands (corresponding to specific energy transitions) arise from specific molecular vibrations. When the energies of these transitions are plotted as a spectrum, they can be used to identify the molecule as they provide a "molecular fingerprint" of the molecule being observed. Each molecule has a different set of vibrational energy levels, and the photons emitted have unique wavelength shifts. It involves collecting and examining these wavelength shifts and using them to identify what is in a sample. Different peaks in the spectrum correspond to different Raman excitations. This is shown in Fig. 6.7.

It is a spectroscopic technique used to observe vibrational, rotational, and other low-frequency modes in a system. It depends on the inelastic scattering (Raman scattering) of monochromatic light, usually from a laser in the visible, near-infrared, or near ultraviolet range. The laser light interacts with molecular vibrations, phonons, or other excitations in the system, resulting in the energy of the laser photons being shifted up or down. The shift in energy gives information about the vibrational modes in the system (Fig. 6.7).

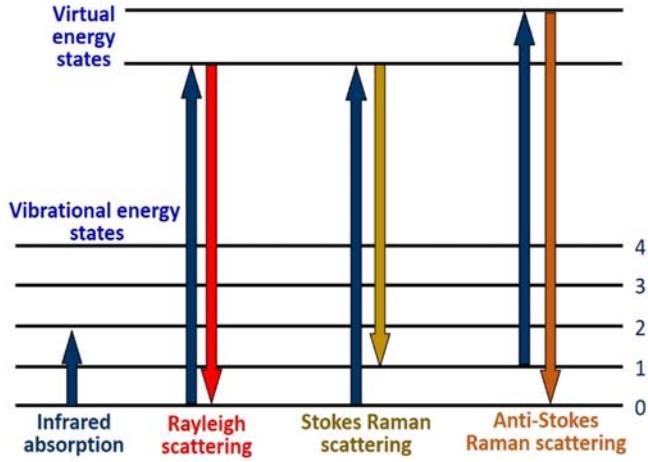

FIGURE 6.7 Types of Raman scattering.

Following are the possible scattering that takes place during Raman scattering measurements:

- Rayleigh (ordinary) scattering is when the photon is absorbed to a higher virtual level and is instantly scattered (emitted) elastically back to the initial level.
- The photons emitted by Stokes-Raman scattering usually have lower energy and frequency than that of the photons absorbed and these photons are inelastically scattered, transferring some of their energy to the molecule.
- The reverse is also possible because emitted photons have higher energy and frequency than the photons absorbed. This is called Anti-Stokes-Raman, but it is not likely at room temperature as electrons prefer to be in the ground state.

When a beam of light is irradiated upon a molecule, photons are absorbed by the material and scattered. The vast majority of these scattered photons have the same wavelength as the incident photons and known as Rayleigh scattering. In Rayleigh scattering, the electron decays back to the same level from which it started. Thus, Rayleigh scattering is often referred to as a form of elastic scattering. In the scattering process, the incident photon excites an electron into a higher "virtual" energy level (or virtual state) and then the electron decays back to a lower level, emitting a scattered photon. In the Raman effect, the electron excited in the scattering process decays to a different level than that where it started and is termed inelastic scattering. Certain vibrations that are allowed in Raman are forbidden in IR spectroscopy, whereas other vibrations may be observed by both techniques although at significantly different intensities.

Apart from materials science and materials engineering, Raman spectroscopy has a wide variety of applications in biology and medicine. It has helped confirm the existence of low-frequency phonons in proteins and

DNA, promoting studies of low-frequency collective motion in proteins and DNA and their biological functions. Raman reporter molecules (RRM) with olefin or alkyne moieties are being developed for tissue imaging with SERS-labeled antibodies. Raman spectroscopy has also been used as a noninvasive technique for real-time, in situ biochemical characterization of wounds. Multivariate analysis of Raman spectra has enabled the development of a quantitative measure for wound healing progress. Spatially offset Raman spectroscopy (SORS), which is less sensitive to surface layers than conventional Raman, can be used to discover counterfeit drugs without opening their packaging and to non-invasively study biological tissue.

The main reason why Raman spectroscopy is so useful in biological applications is that its results often do not face interference from water molecules because they have permanent dipole moments, and as a result, the Raman scattering cannot be picked up on. This is a huge advantage, specifically in biological applications. Raman spectroscopy also has a wide usage for studying biominerals. The advanced version of Raman spectroscopy includes stimulated Raman spectroscopy; surface-enhanced Raman spectroscopy and resonance Raman spectroscopy. Lastly, Raman gas analyzers have many practical applications, including real-time monitoring of anesthetic and respiratory gas mixtures during surgery.

Raman scattering has disadvantages such as sample degradation and fluorescence as a result of which it is the next best option after IR spectroscopy. However, this problem is substantially reduced with modern Raman spectroscopy. At present, tip-enhanced Raman spectroscopy and surface-enhanced Raman scattering are also being used for the chemical imaging of surfaces at the nanometer scale [1,15]. Table 6.1 shows the difference between IR and Raman spectroscopy.

TABLE 6.1 The differences between IR and Raman spectroscopy.

IR spectroscopy	Raman spectroscopy
1. A technique where IR radiation is used to analyze a sample	1. A technique that lies upon the inelastic scattering of photons in the sample
2. Chemical bonds must have the characteristic of an electric dipole	2. Molecules may not have a dipole moment
3. Requires specific sample preparation	3. Does not need specific sample preparation
4. IR active if it causes a change in dipole moment	4. Raman active if it causes a change in polarizability
5. Cannot use water as a solvent due to intense absorption	5. Can use water as a solvent
6. Based on light absorption	6. Based on light scattering
7. Comparatively inexpensive	7. Expensive

6.3 Emission spectroscopy for optical properties

Photoluminescence (PL) spectroscopy is a type of emission spectroscopy. Its main concern is to monitor the light emitted from atoms or molecules after they have absorbed photons. It is suitable for materials that exhibit photoluminescence. It is suitable for the characterization of both organic and inorganic materials of any size and morphology, and the samples can be in solid, liquid, or gaseous forms. It is also useful in the determination of structural features such as defects, size, and composition.

PL spectroscopy uses electromagnetic radiation in the UV and visible range. The PL emission properties of a sample are characterized by four parameters: intensity, emission wavelength, the bandwidth of the emission peak, and emission stability. The PL properties of a material can vary in different ambient environments or in the presence of other molecules. Many nanotechnology-enabled sensors are based on monitoring such changes. Furthermore, as size or dimensions are reduced to the nanoscale, PL emission properties can change. Therefore, a size-dependent shift in the emission wavelength can be observed. Additionally, owing to the released photon which corresponds to the energy difference between the states, PL spectroscopy can also be utilized to study the properties of materials such as band gap energy, recombination mechanisms, and impurity levels.

In a typical PL spectroscopy setup for liquid samples (Fig. 6.8), a solution containing the sample is placed in a quartz cuvette with a known path length. Double beam optics are generally employed. The first beam passes through an excitation filter or monochromator, then through the sample and onto a detector. This impinging light causes photoluminescence, which

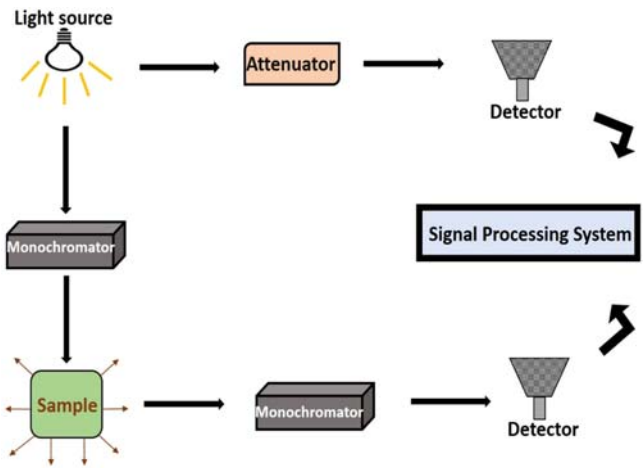

FIGURE 6.8 A typical fluorescence spectrophotometer instrument set up.

is emitted in all directions. A small portion of the emitted light reaches the detector after passing through an optional emission filter or monochromator. A second reference beam is attenuated and compared with the beam from the sample. Solid samples can also be analyzed, with the incident beam impinging on the material (thin film, powder, etc.). Generally, an emission spectrum is recorded, where the sample is irradiated with a single wavelength, and the intensity of the luminescence emission is recorded as a function of wavelength. The fluorescence of a sample can also be monitored as a function of time, after excitation by a flash of light. This technique is called time-resolved fluorescence spectroscopy.

Nanomaterials with PL effects, in particular nanocrystals, can disclose several interesting and improved optical properties. This includes brighter emission, a narrower emission band, and broad UV absorption. For example, semiconductor nanocrystals produce narrower emission peaks than luminescent organic molecules, with a bandwidth of around 30–40 nm. Having a smaller bandwidth, it is much easier to distinguish individual wavelengths originating from multiple sources, such as in an array of nanocrystals. The PL emission intensities and wavelengths are dependent on particle size and materials type. Hence, PL spectroscopy directly enables particle size effects, in particular those in the nanoscale, to be observed and quantified. PL spectroscopy is a contactless, nondestructive method to probe the electronic structure of the materials. The intensity and spectral content of the emitted photoluminescence is a direct measure of important properties of materials such as:

- Band gap determination

  The spectral distribution of PL spectroscopy from a semiconductor can be analyzed to nondestructively determine the electronic band gap energy. This provides a means to quantify the elemental composition of compound semiconductors and is an extremely important material parameter influencing the efficiency of solar cell devices.
- Impurity levels and defect detection

  The PL spectroscopy spectrum at low sample temperatures often reveals spectral peaks associated with impurities contained within the host material. The high sensitivity of this technique provides the potential to identify extremely low concentrations of known and unknown impurities that can strongly affect the material quality and device performance.
- Recombination mechanisms

  The quantity of PL spectroscopy emitted from a material is directly related to the relative amount of radiative and nonradiative recombination rates. Nonradiative rates are typically associated with impurities. Thus, this technique can qualitatively monitor changes in material quality as a function of growth and processing conditions.

6.4 Physiochemical characterization techniques

Physicochemical characterization seeks to define the physical and chemical properties, composition, identification, quality, purity, size, shape, crystal structure, surface area, surface roughness, and stability of the photocatalytic materials. These techniques include particle size analysis, zeta potential, and determination of crystallinity/polymorphism as summarized in Table 6.2.

6.4.1 Structure and phase determination

Phase identification and structure characterization are important in synthetic and materials science. It is a prerequisite to understanding the physical and chemical properties of materials. The structure of a material is inextricably

TABLE 6.2 Summary of the physiochemical techniques that are used for photocatalytic material characterization [16].

No.	Physicochemical characterization technique	Main information derived
1	X-ray diffraction	Crystal structure, composition, crystalline grain size, lattice parameters
2	X-ray fluorescence	Elemental composition of materials
3	Brunauer, Emmett, and Teller	Surface area
4	Mercury porosimetry	The porosity of a material
5	Dynamic light scattering	Hydrodynamic size, detection of agglomerates, surface charge
6	Atomic force microscopy	Particle size and shape in 3D mode, evaluate the degree of covering of a surface with particle morphology,
7	Scanning electron microscopy	Combined with EDX for morphology study, crystal structure, and elemental composition.
8	Transmission electron microscopy	Particle size, monodispersity, shape, aggregation state, detect and localize/ quantify particles in matrixes, study growth kinetics, distinguish monocrystalline, polycrystalline, and amorphous materials, to study defect
9	X-ray photoelectron spectroscopy	Electronic structure, elemental composition, oxidation states, ligand binding (surface-sensitive)

linked to its properties, so determining the structure of your novel or pre-existing molecules is vitally important to many scientific and manufacturing processes, especially for photocatalytic activities. Moreover, the phase/crystal structure of materials also plays a critical role in determining many physical properties, such as cleavage, electronic band structure, and optical transparency.

6.4.1.1 X-ray diffraction

X-ray diffraction (XRD) is a technique used to analyze the atomic or molecular structure of materials. It is known as a nondestructive method and effectively works with amorphous or crystalline materials. In the XRD technique, generally, a monochromatic beam (X-rays of a single wavelength) is used. To obtain this, the unwanted X-ray lines are usually filtered using a foil of a suitable metal whose absorption edge for X-ray lies between the kα and kβ components of the spectrum. Cu kα is the most common radiation used because it is less strongly absorbed by the sample [17].

For diffraction to occur, the interaction between X-rays and substance meets the conditions of Bragg's law (Fig. 6.9). Bragg's law provides the condition for a plane wave to be diffracted by a family of lattice planes, $2d\sin\theta = n\lambda$, where d is the lattice spacing, θ the angle between the wave vector of the incident plane wave, k_o, and the lattice planes, λ its wavelength, and n is an integer, the order of the reflection.

- The angle of incidence is equal to the angle of scattering
- The path length difference is equal to an integer number of wavelengths.

The following are the functions of XRD:

- Measure the average spacings between layers of rows of atoms in a substance
- Determine the orientation of an individual grain or crystal
- Measure the size, shape, and internal stress of small crystalline areas
- Identify the crystal structure of an unknown substance
- To distinguish between crystalline and amorphous materials
- Measurement of sample purity.

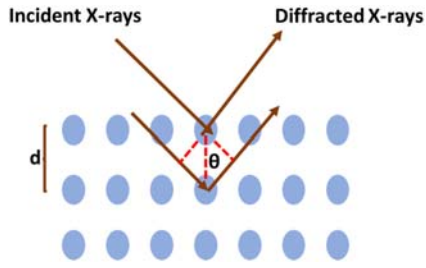

FIGURE 6.9 Schematic representation of Bragg's equation.

To estimate the average crystallite size of a solid/ thin film sample from XRD, following Debye−Scherer Eq. (6.3) is used [18−29]:

$$D = \frac{0.9\lambda}{\beta Cos\theta} \tag{6.3}$$

where D is the crystallite size, β is the full-width half maximum (FWHM) in radians, and θ is the Bragg angle. The crystallite size is a measure of the size of a coherently diffracting domain. The other estimation that can be calculated from the XRD data is the lattice strain (ε) using Eq. (6.4):

$$\varepsilon = \frac{\beta Cos\theta}{4} \tag{6.4}$$

where θ is the diffraction angle and β is the FWHM in radians. The preferential orientation or random growth of preferred plans (hkl) can also be obtained particularly from a thin film sample. This is by calculating the texture coefficient (T_c) using the following Eq. (6.5):

$$T_c = \left| \frac{\frac{I_{(hkl)}}{I_{0(hkl)}}}{\frac{1}{N}\sum \frac{I_{(hkl)}}{I_{0(hkl)}}} \right| \tag{6.5}$$

where $I_{(hkl)}$ is the measured relative intensity of the preferred plane (hkl) and N is the number of reflections observed in the XRD pattern. $I_{0(hkl)}$ is the standard diffraction pattern intensity. If the T_c value <1, it indicates the lack of orientation grain, if $T_c \sim 1$ it indicates random orientation, and if $T_c > 1$, it indicates the higher abundance of crystallites oriented along the (hkl) direction [30].

6.4.1.2 X-ray fluorescence

X-ray fluorescence (XRF) is a nondestructive analytical technique used to determine the elemental composition of materials. The chemistry of a sample is determined by measuring the X-ray emission of fluorescent (secondary) from a sample when it is excited by a primary X-ray source. Each element in a sample produces a unique set of characteristic fluorescent X-rays (which is called a fingerprint). Therefore, XRF is an excellent technology for qualitative and quantitative analysis of material composition.

Following is the process of XRF (Fig. 6.10):

- A sample (solid or liquid) is irradiated with a high-energy X-ray.
- When an atom in the sample is struck with an X-ray of sufficient energy, an electron from one of the atom's inner orbital shells is ejected.
- The atom regains stability, filling the vacancy with an electron from one of the atom's higher energy orbital shells.
- The electron drops to the lower energy state by releasing a fluorescent X-ray.

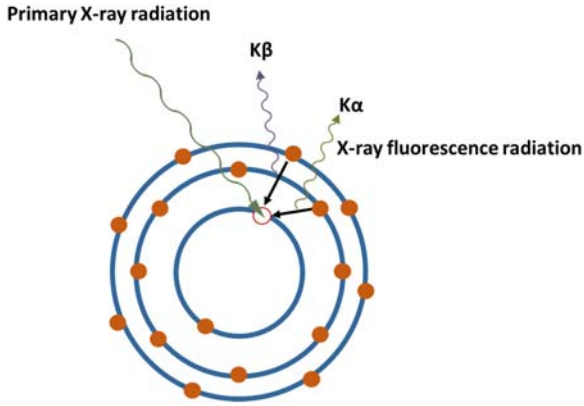

FIGURE 6.10 Schematic representation of the XRF radiation.

There are limitations to XRF as an analytical method which could, in certain circumstances, be disadvantages:

- XRF measurements rely on quantity, so it limits the measurement of low-yield materials.
- It can also face limitations in measuring lighter elements.

6.4.2 Surface area and porosity measurements

Surface area and porosity are important parameters for photocatalytic applications. The surface area depends upon various factors such as particle size, the presence of cracks, surface roughness, and accessible pores. The characteristics of the pores, such as size, volume, and shape, can also greatly affect the photocatalytic performance of the material. The standard methods to determine these properties include direct observation by gas adsorption, mercury porosimetry, optical or electronic microscopy as well as small angle scattering of X-rays (SAXS) or neutrons (SANS). Since the particle size for powders or nanopowder samples is directly related to the surface area, light scattering methods can also be used to determine indirectly the surface area.

6.4.2.1 Surface area and porosity measurements using gas adsorption

Gas adsorption methods are the most prominent and commonly used methods based on the adsorption of inert gas, mainly nitrogen gas, on the surface of a solid material. Gas adsorption takes place on the outer surface and, in the case of porous materials, the surface of pores allows the determination of the specific surface area (SSA). Several methods are used for SSA determination, for example, Brunauer, Emmett, and Teller (BET) and de Boert-Plot methods. However, the BET method is the most commonly used, and it

provides precise SSA evaluation by nitrogen multilayer adsorption, measured as a function of relative pressure using a fully automated analyzer. Monolayer formation of gas molecules on the surface is used to determine the SSA, while the principle of capillary condensation can be applied to assess the presence of pores, pore volume, and pore size distribution. The technique includes external area and pore area evaluations to determine the total SSA in m^2/g. Pore width, pore shape, and effective adsorption potential are the factors that determine pore filling.

According to International Union of Pure and Applied Chemistry (IUPAC), an adsorption isotherm is a function that relates the amount of adsorbed adsorbate to the pressure (or concentration) of the adsorbate in the fluid phase under equilibrium conditions. IUPAC also classified adsorption isotherms into six types as shown in Fig. 6.11. Type I is the characteristic of adsorbents that are microporous, nonporous, or microporous (types II, III, and VI) while types IV and V exhibit a hysteresis loop, i.e., the adsorption and desorption isotherms that do not coincide over a certain region of external pressures [31]. The type IV isotherm is typical for mesoporous adsorbents. Type V hysteresis loop is a typical sign of a weak fluid−wall interaction. It is less common but observed with certain porous adsorbents. Measuring sorption scanning curves helps to identify the underlying mechanism of hysteresis, which is crucial for obtaining an accurate and comprehensive pore size analysis of mesoporous and micro-mesoporous materials.

Pore width, pore shape, and effective adsorption potential are the factors that determine pore filling. In the case of micropores (pore width <2 nm, according to IUPAC classification), pore filling takes place continuously, whereas in the case of mesopores (pore widths in the range $2-50$ nm), pore

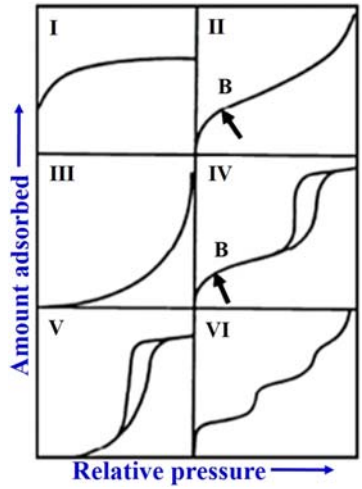

FIGURE 6.11 Classification of adsorption isotherms of BET.

filling happens by pore condensation, which reflects a first-order gas–liquid phase transition. The so-called classical macroscopic, thermodynamic concepts are based on the assumption of a certain pore-filling mechanism. Methods based on the Kelvin equation (e.g., Barrett–Joyner–Halenda, the BJH method) are linked to the pore condensation phenomena, i.e., they are applicable for mesopore size analysis. However, they fail to describe the pore filling of micropores and even narrow mesopores in a correct way [1,15,32].

In contrast to these macroscopic approaches, methods like the density functional theory (DFT) or methods of molecular simulation (Monte Carlo simulation methods, MC), molecular dynamics methods (MD) provide not only a microscopic model of adsorption but also a more realistic description of the thermodynamic properties of the pore fluid. The pore shape can further be obtained from the hysteresis loop from the corresponding isotherm Fig. 6.10.

6.4.2.2 *Surface area and porosity measurements using mercury porosimetry*

Mercury porosimetry uses the non-wetting properties of mercury to gain information on the porosity, pore volume, pore size distribution, and density. The technique consists of applying a high pressure (about 400 MPa for the smallest pores) to force the intrusion of mercury in the sample's smallest pores, whereas mercury intrusion in larger pores already takes place at low pressure. In this way, a wide dynamic range of pore sizes can be measured, and the pore size distribution can be obtained starting from 4 nm up to $\sim 800\,\mu m$. Thus, mercury porosimetry is extremely suitable for materials showing broad distributions of pore sizes or mainly macropores.

Mercury porosimetry is used to measure the porosity of a material by applying controlled pressure to a sample immersed in mercury. External pressure is required for mercury to penetrate the pores of a material due to the high contact angle of mercury. The amount of pressure required to intrude into the pores is inversely proportional to the size of the pores. The larger the pore, the smaller the pressure needed to penetrate the pore. The mercury porosimeter generates volume and pore size distributions from the pressure vs. intrusion data generated by the instrument using the Washburn equation.

The difference between BET and mercury porosimetry is that BET determines equivalent pore diameters, whereas Hg-injection determines pore throat diameters, which is not 1:1 comparable.

6.4.3 Dynamic light scattering

Dynamic light scattering (DLS) is used to determine the size of various particles including proteins, polymers, micelles, vesicles, carbohydrates, nanoparticles, biological cells, and gels (Fig. 6.12). DLS has been used to measure

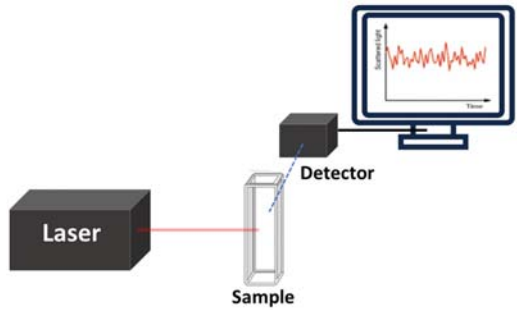

FIGURE 6.12 A schematic diagram of dynamic light scattering setup.

the particle size of dispersing colloidal samples, study the stability of formulations, and detect the presence of aggregation or agglomeration as well as the surface charge. If the system is not dispersed in size, the mean effective diameter of the particles can be determined. This measurement depends on the size of the particle core, the size of surface structures, particle concentration, and the type of ions in the medium.

These days, light scattering techniques have become very popular to measure the size and size distribution of nanoparticles in a solution or colloidal solution. Fundamentally, the techniques consist of shining a monochromatic light beam, such as a laser, onto the solution that contains the spherical particles. The Brownian motion of the particles (movement of particles due to the random collision with the molecules of the liquid that surrounds the particle) causes scattering of the light, and such scattering depends on the particle velocity. For Brownian motion, small particles move quickly and large particles move more slowly. Therefore, the assumption of pure Brownian movement and spherical particles allows the determination of the size and size distribution of particles and molecules.

The measurements of the intensity of the light by a photomultiplier placed at 90 degrees as a function of the frequency lead to a frequency spectrum of the intensity of the scattered light. The spectra acquire the form of a Lorentzian-shaped line whose width depends on the diffusion coefficient (D) and the scattering angle. The assumption of pure Brownian movement and spherical particles allows the determination of the size and size distribution of particles and molecules. This is possible since the probability density function for Brownian movement is well defined and depends mainly on the diffusion coefficient, which according to the Stokes-Einstein equation is a function of the temperature, the viscosity of the solvent, and the size of the particle.

Since DLS essentially measures fluctuations in scattered light intensity due to the diffusion of particles, the diffusion coefficient of the particles can be determined. The DLS software of commercial instruments typically displays the particle population of different diameters. If the system is

monodispersed, there should only be one population, whereas a polydisperse system would show multiple particle populations. If there is more than one size population present in a sample then either the CONTIN analysis should be applied for photon correlation spectroscopy instruments, or the power spectrum method should be applied for Doppler shift instruments [1,15,32].

Stability studies can be done conveniently using DLS. Periodical DLS measurements of a sample can show whether the particles aggregate over time by seeing whether the hydrodynamic radius of the particle remains the same or increases. If particles aggregate, there will be a larger population of particles with a larger radius. In some DLS instruments, stability depends on temperature which can be analyzed by controlling the temperature in situ.

6.4.4 Surface topography using atomic force microscopy

Atomic force microscopy (AFM) is a powerful and versatile microscopy technique used to study samples at the nanoscale. Surface topography or morphology can be observed by contacting or non-contacting techniques. The most commonly used contacting techniques are AFM and profilometry. It takes an image in a three-dimensional topography and provides various kinds of surface measurements, fulfilling the needs of researchers, academicians, and scientists. AFM can generate images at an atomic resolution with angstrom scale resolution height information with less sample preparation. In polymer nanocomposites, it can be used to measure the surface roughness and visualize the surface texture on several types of material. Moreover, it is a nondestructive technique and has a high three-dimensional spatial resolution. An AFM setup is shown in Fig. 6.13. AFM is a contact technique, although, in some operation modes, no real contact takes place. In AFM, the probe consists of a sharp tip with a radius of curvature of a few nanometers, normally made of Si or SiN, which is attached to a very sensitive cantilever.

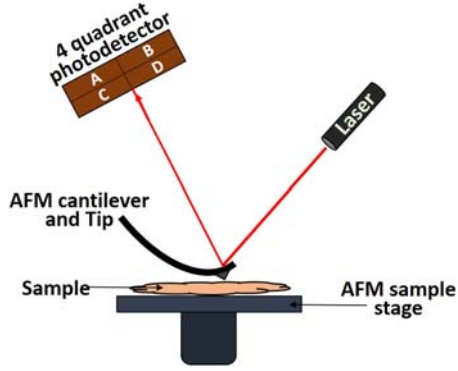

FIGURE 6.13 An AFM probe raster scan over a sample surface.

The AFM has a microscale cantilever, usually made from silicon or silicon nitride. At one end of the cantilever is a sharp tip that has a radius of curvature in the order of nanometers. By bringing the tip into proximity to the sample surface, forces acting between the tip and the sample surface cause the cantilever to bend and deflect in a similar manner to a tiny diving board. The forces are not measured directly. These forces are calculated by measuring the cantilever's deflection. If the stiffness of the cantilever is known, then the force is measured using Hooke's law shown by Eq. (6.6):

$$F = -kz \tag{6.6}$$

where F is the force, k is the stiffness of the cantilever, and z is the distance the lever is bent. The sample is mounted on a piezoelectric stage whose position can be precisely controlled by applying a voltage. The sample is laterally scanned relative to the tip and the cantilever's deflection is measured as a function of position. The cantilever deflection can be detected in several different ways, with the most common measuring laser light that is reflected from the top of the cantilever onto a position-sensitive detector made from an array of photodiodes.

The AFM can be operated in several different modes. The most common is contact mode, where the tip is in intimate contact with the surface. As it is raster-scanned across the surface, it is deflected as it encounters surface corrugations. Another way is the constant force mode, where the distance between the tip and surface is continually adjusted to maintain a constant deflection, and therefore, constant height above the surface [1,15,32].

The tapping mode or dynamic force mode (DFM) is another approach in which a stiff cantilever is brought within proximity of the surface. Then it oscillates and changes in the resonant frequency or amplitude of the cantilever are measured during a scan. During the oscillation, part of the tip intermittently touches or taps the surface. The tapping mode requires very stiff cantilevers to avoid them becoming stuck in the sample surface. The choice of operation modes depends on the sample and its environment. The tapping mode offers improved lateral resolution on soft samples, as lateral forces such as drag, which is common in contact mode, are virtually eliminated. It is also advantageous for materials that are poorly adsorbed on a substrate. In general, for delicate samples, constant force or tapping modes are utilized. The sensitivity of the force measurements is directly related to the size and stiffness of the cantilever, which can range from 1 pN to 1 nN per nm, and the deflection sensor measures motions ranging from several microns to even 0.01 nm. The minimum force that can be measured with the AFM is typically 5 pN.

6.4.5 Scanning electron microscopy

In scanning electron microscopy (SEM), an electron beam is directed toward the specimen instead of a light beam, as in the case of an optical microscope.

A highly concentrated electron beam is shot from an electron gun located at the top of the device. The two main electron gun types are field emission guns, which generate a strong electric field that rips electrons from the atom, and thermionic guns, in which the filament is heated until the electrons stream moves away. The SEM scans the surface of the sample with high-energy electron beams. Thus, SEM differs from conventional light microscopes as they use light waves to create a magnified image. In SEM, when the electron beam strikes the specimen surface, it interacts with the surface. When the incident beam of electrons hits the specimen, X-rays and three types of electrons are emitted: backscattered (or primary) electrons, secondary electrons, and Auger electrons. SEM makes use of the primary, or backscattered, and the secondary electrons. High-resolution images are produced by SEM revealing details of $\sim 1-5$ nm using the secondary electrons. The backscattered electrons are also used to form the image in this technique. For identifying elemental compositions, characteristic X-rays are used by a technique known as Energy-Dispersive X-ray Analyzer (EDX or EDA).

A schematic diagram of the working of SEM is shown in Fig. 6.14. The electron column has the scanning coils and the electron beam is passed through them to the final lens. This deflects the beam in vertical and horizontal directions so that it can perform raster scanning over the surface's rectangular area. Signals are detected and amplified with the help of electronic devices, displaying them as images on a cathode ray tube. Raster scanning is synchronized with the microscope. The displayed image is a distribution map of the signal intensity emitted from the scanned area of the specimen.

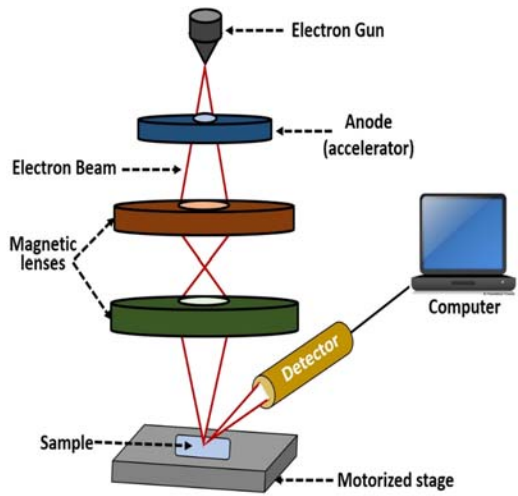

FIGURE 6.14 Schematic of scanning electron microscope.

In short, SEM involves a type of electron microscope that produces images of a sample by scanning the surface with a focused beam of electrons. The electrons interact with atoms in the sample, producing various signals that contain information about the surface topography and composition of the sample. It is a non-contacting technique where a beam of electrons, typically in the energy region of 0.2−40 keV, is focused on the sample's surface to form a spot of about 0.4−5 nm, which is scanned forming a 2D image of the sample. The image is formed by the secondary electrons (SEI), emitted from the valence and conduction bands of the material and whose intensity is proportional to the surface topography. The contrast difference produced from the emitted electrons at different heights (penetration field) produces a three-dimensional appearance of the image. The signals that derive from electron−sample interactions reveal information about the sample including external morphology, size, texture, chemical composition, crystalline structure, and orientation of materials making up the sample. In most applications, data are collected over a selected area of the surface of the sample, and a two-dimensional image is generated that displays spatial variations in these properties [1,15,16,32].

6.4.6 Transmission electron microscopy

Transmission electron microscopy (TEM) has been in use for characterizing nanomaterials, especially because of its high lateral spatial resolution, it can even resolve objects that are separated by less than 0.2 nm. TEM is also versatile as it is capable of producing fine images and also gives diffraction data from the same sample. In addition to the capability of TEM in producing enhanced morphological and structural information of the nanomaterials, it is also capable of giving analytical information, present as separate attachments. For example, electron energy loss spectroscopy can provide information regarding the electronic structure while energy-dispersive X-ray spectroscopy (EDX) can give the chemical composition of the nanomaterials.

Although the components of a TEM are essentially similar to those of a standard SEM, with the arrangement of the electron gun and electromagnetic lenses, condenser, etc., the major difference lies in the sample specimen and its position and how the data are collected from the sample (Fig. 6.15). In the conventional TEM mode, an incident high-energy electron beam is transmitted through a very thin specimen. As the electron beam enters the thin specimen, the electron−electron interaction between the beam and the sample transforms the incident electron into unscattered, elastically scattered, or inelastically scattered electrons. These diffracted electrons (scattered or unscattered) are then focused (using a series of electromagnetic lenses) to produce an electron diffraction pattern. Also, depending upon the density of the unscattered electrons, various images, viz. amplitude-contrast image, a phase contrast image, or shadow image of varying darkness can be produced.

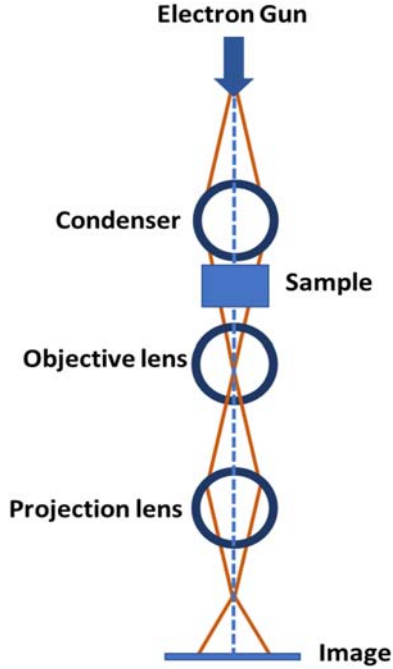

FIGURE 6.15 Schematic of transmission electron microscope.

Both TEM and SEM are capable of revealing information regarding the size and shape of the nanomaterials. These techniques can also provide information on whether the nanomaterials form aggregation and how well they are dispersed. However, TEM has the advantage of providing superior spatial resolution to SEM. While using TEM, a significant trade-off is made using a high vacuum with the additional requirement of a very thin sample specification so that an electron beam can penetrate the sample during TEM measurements. It is a long and complex process to make the sample thin enough for data acquisition, and often, the sample might be damaged or its structure could get altered while thinning it down to 50−100 nm. Another concern is that TEM uses a very high-energy electron beam as a result of which the specimens can be damaged or even destroyed by these intense, high-voltage electron beams. However, a good sample preparation with uniform thickness can give maximum information about the material with minimum complex interpretations [1,15,16,32].

Selected area (electron) diffraction (SAD or SAED) is a crystallographic experimental technique performed using a TEM. It can be used to determine crystal orientation, and measure lattice constants and their defects. The scattered electrons from a specific region are collected by SAED targeted with nanoscale precision using a specialized aperture in the electron beam's path.

TABLE 6.3 Differences between SEM and TEM.

SEM	TEM
1. Electron beam scans over the surface sample	1. Electron beam passes through the thin sample
2. Scan any thickness of the sample	2. Specially prepared thin samples
3. Specimen stage at the bottom of the column in the chamber	3. Specimen stage in the middle of the column
4. Image is of the surface of the sample	4. Image is a two-dimensional projection of the sample

In addition, SAED offers s spatial resolution up to several hundred times greater than XRD techniques.

In summary, there are a few differences between SEM and TEM. These differences have been summarized in Table 6.3.

6.4.7 X-ray photoelectron spectroscopy for elemental composition

X-ray photoelectron spectroscopy (XPS) is a surface-sensitive quantitative spectroscopic technique based on the photoelectric effect that can identify the elements that exist within a material (elemental composition) or are covering its surface, as well as their chemical state and the overall electronic structure and density of the electronic states in the material. XPS is a powerful measurement technique because it not only shows what elements are present but also what other elements they are bonded to. The technique can be used in line profiling of the elemental composition across the surface or in-depth profiling when paired with ion-beam etching. It is often applied to study chemical processes in the materials in their as-received state or after cleavage, scraping, exposure to heat, reactive gasses or solutions, ultraviolet light, or during ion implantation.

The phenomenon used for photoelectron spectroscopy is based on the photoelectric effect outlined by Einstein where the concept of the photon was used to describe the ejection of electrons from a surface when photons impinge upon it. For XPS, also known as electron spectroscopy for chemical analysis (ESCA), the photon energies of choice are the fundamental emissions from Al-κα (1486.6 eV) or Mg-κα (1253.6 eV) cathodes. The XPS technique is highly surface specific due to the short inelastic mean free path (IMFP) of the photoelectrons that are excited from the solid. The energy of the photoelectrons leaving the sample is the characteristic of each element present.

Each peak area is proportional to the number of atoms present in the material. The shape of the peak and the BE can be slightly altered by the

chemical site of the emitting atom. Hence, XPS can provide chemical bonding information as well. The fundamental equation that relates the BE of the emitted photoelectron with the measured electron kinetic energy (KE) is given by Eq. (6.7):

$$BE = h\nu - KE - \phi \tag{6.7}$$

where ($h\nu$) is the incident photon energy and (ϕ) is the work function, which has to be well defined for each piece of equipment to determine precisely the BE that is usually measured in reference to the material's Fermi level. The analysis of the XPS spectrum (counts per BE) allows to obtain the surface elemental composition by comparing it to standard materials (quantitative) or using XPS databases (semiquantitative). The depth of analysis in XPS is about 1−10 nm depending on the incidence energy of the photons, the KE of the outgoing electrons, and the angle of collection (angle-resolved XPS, ARPES). The XPS technique requires ultra-high vacuum conditions (UHV, pressure in a range from 108 to 1010 mbar), and so the samples have to be evaluated always in dry conditions. The XPS is essentially a nondestructive technique but is very sensitive to surface contamination. Therefore, in some cases, an in situ cleaning process is applied using an ion gun.

XPS detects only electrons that have escaped from the sample into the vacuum of the instrument. To escape from the sample, a photoelectron must travel through the sample. Photo-emitted electrons can undergo inelastic collisions, recombination, excitation of the sample, recapture, or trapping in various excited states within the material, all of which can reduce the number of escaping photoelectrons. These effects appear as an exponential attenuation function as the depth increases, making the signals detected from analytes at the surface much stronger than the signals detected from analytes deeper below the sample surface. Thus, the signal measured by XPS is exponentially surface-weighted signal, and this fact can be used to estimate analyte depths in layered materials. In short, XPS is a surface-sensitive quantitative spectroscopic technique that measures:

- the elemental composition at the parts per thousand range
- empirical formula
- chemical state
- electronic state of the elements that exist within a material
- binding energy (BE)
- layer thickness in the upper portion of surfaces.

In short, XPS spectra are obtained by irradiating a material with a beam of X-rays while simultaneously measuring the KE and the number of electrons that escape from the top 0−10 nm of the material being analyzed [1,15,16,32].

6.5 Electrochemical characterization technique

The electrochemical characterization technique is an effective tool to study oxidation-reduction reactions in a variety of media. It can be applied in electrolytic salt solution and it uses an electrochemical cell made up of inert materials. This technique uses an instrument known as a "potentiostat" (Fig. 6.16). This instrument is used to measure the thermodynamic, kinetic, and photocatalytic properties of the nanomaterials or photocatalysts.

Generally, it is based on applied potential and electron transfer between the interfaces and the electrodes. It is the study of the relations between chemical reactions and electricity, interconversion of chemical energy and electrical energy, as well as redox reactions. It involves the transfer of electrons from one substance to another substance. Its analytical calculations are based on the measurement of electrical quantities (i.e., current, potential, charge, or resistance) and their relationship to chemical parameters. These characteristics are measured in electrolytes having a buffer and an inert atmosphere using a potentiostat. It deals with the relationship between electricity and chemistry, i.e., electrochemistry. One of its important uses is to characterize chemical samples to know the thermodynamic, kinetic, and photocatalytic properties.

In electrochemical characterization, the measurement of potential, charge, or current is used to determine an analyte's concentration or to characterize an analyte's chemical reactivity [33]. The potential, charge, and current are the basic electrochemical signals that act as analytical signals. Hence, these signals form the core experimental designs for all the electrochemical characterization techniques.

6.5.1 Thermodynamic properties using electrochemical techniques

6.5.1.1 The band gap energy

Band gap energy (E_g), i.e., the forbidden energy, is a very important parameter related to the electronic structure of semiconducting materials. This parameter has to match at least the energy difference of ~ 1.23 eV between the redox levels H_2O/H_2 and O_2/H_2O required for water splitting. The absorption

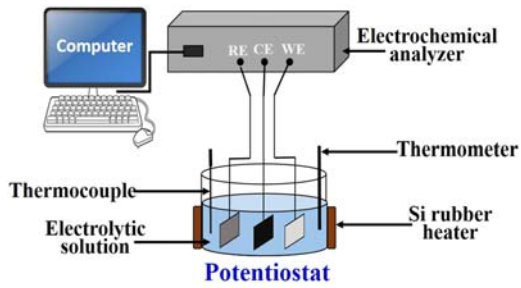

FIGURE 6.16 Schematic of a potentiostat.

coefficient (α) of a crystalline material depends on the photon energy according to Eq. (6.8):

$$\propto = A\left(h\nu - E_g\right)^n / h\nu \tag{6.8}$$

where A is a proportionality constant and E_g is the band gap energy. For crystalline semiconductors, n depends on the electron transition type, 1/2 for direct transition and 2 for indirect transition. However, 2 has been mostly preferred to analyze the passive film. The band gap energy for a passive film can be determined from an $(i_{ph}h\nu)^{1/2}$ versus $h\nu$ plot and is estimated at the photon energy value where the i_{ph} equals 0, provided that the photocurrent (i_{ph}) for the film is proportional to the absorption coefficient, i.e.,

$$i_{ph} = A\left(h\nu - E_g\right)^n / h\nu \tag{6.9}$$

This method was applied to obtain the E_g of the passive film zircaloy-4 using a conventional three-electrode cell of 1−l multineck flask with a quartz window as a photon inlet, using the zircaloy-4 as a working electrode and saturated calomel electrode (SCE) and Pt, respectively, as reference and counter electrodes. A 300 W Xenon (Xe) arc lamp combined with a scanning digital monochromator was used to impose a monochromatic illumination (200−800 nm) to the working electrode. The band gap energy for the inner anhydrous ZrO_2 was calculated (4.30 ± 0.15 eV) by extrapolation from the $(i_{ph}h\nu)^{1/2}$ versus $h\nu$ plot.

6.5.1.2 Fermi level

Another very important parameter in the discussion of solid-state materials is the Fermi level. The Fermi energy (E_F) of a semiconductor is defined as the energy of the topmost filled orbital at a temperature of absolute zero. For an n-type semiconductor, the Fermi level lies just below the conduction band (CB), whereas for a p-type semiconductor, it lies just above the valence band (VB). In addition, as with metal electrodes, the Fermi level of a semiconductor electrode varies with the applied potential. For example, moving to more negative potentials will raise the Fermi level.

The semiconductor solid-state physics community has adopted electron energy in a vacuum as a reference, whereas electrochemists have traditionally used the standard hydrogen electrode (SHE) scale. While estimates vary, SHE appears to lie at -4.5 eV with respect to the vacuum level. We are now in a position to relate the redox potential E_{redox} (as defined with reference to SHE) with the Fermi level E_F, redox expressed versus the vacuum reference as shown by Eq. (6.10):

$$E_{F,\text{redox}} = -4.5\ eV - eE^{\circ}_{\text{redox}} \tag{6.10}$$

6.5.1.3 The double layer at the semiconductor

The electrical double layer (EDL) is the result of the variation of electric potential near a surface. It has a significant influence on the behavior of

colloids and other surfaces in contact with solutions or solid-state fast ion conductors.

The primary difference between a double layer on an electrode and one on an interface is the mechanisms of surface charge formation. With an electrode, it is possible to regulate the surface charge by applying an external electric potential. This application, however, is impossible in colloidal and porous double layers, because for colloidal particles, one does not have access to the interior of the particle to apply a potential difference.

Electrodes prepared with a photocatalytic semiconductor can be used in a photoelectrochemical cell to measure properties such as band gap energy, flat-band potential, and kinetics of hole and electron transfer. The semiconductor must be supported on an electronic conductor substrate and put into an electrochemical cell in contact with the electrolytic solution. Since in a photoelectrode, the electron transfer occurs necessarily at the interface between the semiconducting photoanode and the electrolyte, first, an explanation of the semiconductor−electrolyte interface is important. The band bending is a result of interface phenomena and the characteristic charge transfer reactions across the solid electrolyte that represents the basis of an electrode.

The band bending is also affected by the external voltage (V_B). For a given semiconductor and electrolyte, there exists a unique potential for which the potential drop between the surface and the bulk is zero and there is no space-charge layer. This is the flat-band potential (V_{Fb}) or, in other words, the applied potential (V) at which the semiconductor energy bands are "flat" leading up to the solution junction. For an n-doped semiconductor, the flat-band potential is close to the CB edge, and experimentally, the two concepts are sometimes treated as interchangeable.

6.5.1.4 The flat-band potential

The electrochemical methods to determine the flat-band potential are well established and known. The two most common methods are described as follows:

1. The first one stems from the impedance spectroscopy in the dark
2. Current−voltage characteristics under a light pulse.

The flat-band potential of the *p*-type electrode is more anodic (positive) than that of the *n*-type electrode. This difference in the flat-band potential between the two types of the same semiconductor electrode is nearly equivalent to the band gap of the semiconductor.

6.5.1.5 Light pulse techniques

The light pulse technique (LPT) and the scanning light pulse technique (SLPT) are photoelectric methods used to determine the electrical parameters of metal oxide semiconductor structures. The LPT method may be used to determine the V_{Fb} value of the entire semiconductor device, while the SLPT

method allows the determination of the distribution of local V_{Fb} values over the gate area. In most cases, the area is scanned by a small light beam. Photocurrent versus potential curves is typically obtained by applying a scan potential to the semiconductor−electrolyte interface in combination with an appropriated chopped light illumination to inhibit the effect of the electron recombination on the charge transfer kinetics. It requires a typical three-electrode photoelectrochemical cell (PEC) consisting of a semiconductor photoanode; a cathode, generally made up of Pt; and an SCE as a reference electrode. The light incidence must be as a spot of the controlled area.

Photocurrent intensity has been regarded as one of the most efficient methods to evaluate the photocatalytic activity of a photocatalyst. It has been recognized that a high photocurrent intensity suggests a high efficiency for $\bar{e}$ and $h+$ generation and separation, and thus, high photocatalytic activity. The expected accuracy of the LPT method is typically ± 10 mV (for the most common potentiostat), while the accuracy of the V_{Fb} determination methods based on measurement of the capacitance characteristic is rarely better than ± 50 mV.

6.5.1.6 *Electrochemical determination of the* V_{FB} *of particles in suspension*

The above-mentioned methods are appropriate for solid semiconductor electrodes or semiconductors deposited on a substrate (electronic conductor). However, these techniques are not appropriate when the photocatalysts are suspended. An electrochemical method to calculate the V_{fb} for semiconductors in suspension has been established. This method is based on the measurement of the photovoltage developed under light irradiation of a suspension containing an electron acceptor such as methyl viologen (MV^{2+}; 1,1′-dimethyl-4,4′-bipyridinium dichloride). This is a very simple method for determining the E_{fb} of semiconductor particles in suspension.

6.5.2 Kinetic properties using electrochemical techniques

6.5.2.1 *Electrochemical impedance spectroscopy for charge separation, transport, storage, and reaction elements in nanostructured oxide semiconductor electrodes*

Electrochemical impedance spectroscopy (EIS) is an electrochemical technique that is very advantageous for characterizing and understanding the characteristics of nanomaterials as well as in applications in corrosion, biosensors, battery development, fuel cell development, paint characterization, sensor development, and physical electrochemistry. It is a powerful technique for examining the

- separation efficiency of the photogenerated electrons−holes
- photoinduced charge carriers' separation

- transport properties
- charge transfer resistance across the surface of photoelectrodes.

At the same time, electronic conductivity and interfacial electron transfer in nanostructured oxide electrodes permeated with electrolytes can be measured and used to calculate and obtain various other information. Moreover, nanoparticulate films prepared on optically transparent electrodes (OTE) have been extensively studied due to their wide applications in photoelectrocatalysis.

EIS spectra are typically measured in a three-electrode cell using a standard potentiostat equipped with an impedance spectra analyzer. The amplitude of the *ac* signal ($|\Delta E|_{ac}$) used is about 10 mV, while the frequency is typically scanned between 100 kHz and 20 mHz. All the interfacial potentials must be referred to against an appropriated reference electrode that controls the *dc* potential (E_{dc}) of the electrode/electrolyte interface. The counter electrodes can be Pt, Au, or W wires. The obtained spectra for films having a thickness l can be fitted to the equivalent circuit as shown in Fig. 6.17.

The electronic conductivity of the films is modeled by series resistances (r_1) representing the electron transport resistance through the electrode thickness ($R_1 = r_1 l$) and the electrolyte resistance (R_2) that separates working and reference electrodes. The electronic conductivities of the nanoporous oxide films (σ_n) are calculated using Eq. (6.11), where A and ρ represent the geometric area and porosity of the film, respectively:

$$\sigma_n = \frac{1}{R_1 A(1-\rho)} \tag{6.11}$$

On the other hand, electron transfer at the oxide/electrolyte interface is modeled by constant-phase elements (CPEs, q_3) representing the charge storage into the film ($Q_3 = q_3 l$) and parallel resistances (r_3) standing for the charge transfer resistance ($R_3 = r_3/l$) which is strongly dependent on the *dc* potential.

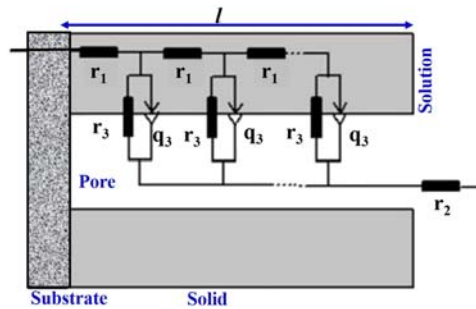

FIGURE 6.17 The equivalent circuit is used to fit EIS spectra at different dc interfacial potentials.

6.5.2.2 Interparticle electron transport through semiconductor nanostructured films

Since the particle diameter is of the same order or smaller than the space-charge layer thickness in semiconductor thin films having high surface areas, the transportation of photoexcited electrons ($\bar{e}$) and holes (h^+) through the films is controlled by diffusion. This phenomenon is reasonable when the formation of necks between the particles takes place during the thermal sintering of the films. The contact zone between n-type oxide nanoparticles is small, thus generating an energy barrier at this contact because the space-charge layer is as thick as or thicker than the contact diameter particle. In this way, photoexcited electrons cannot be easily transported through the oxide films, and the electrons photogenerated in the particles not bonded to the surface do not give photocurrent (j_{ph}) at the external circuit [1,15,16,32].

6.5.3 Photocatalytic efficiency using electrochemical techniques

6.5.3.1 Photochemical thermodynamic efficiency factor

The photochemical thermodynamic efficiency factor (PTEF) is an energy ratio equating the energy used to achieve the photocatalytic conversion of organic molecules over the energy absorbed by the photocatalyst and evaluates the performance of photocatalytic reactors on a thermodynamic basis with the equation of the reactor's efficiency (Eq. 6.12):

$$PTEF = \eta = \frac{Q_{\text{used}}}{Q_a} \tag{6.12}$$

where Q_a represents the irradiation energy absorbed and Q_{used} represents the irradiation energy used for the formation of $^{\bullet}$OH free radicals which then interact with the adsorbed species. The PTEF is a very applicable parameter because it is not restricted to a homogeneous or heterogeneous photoconversion chemical process.

The PTEF is a dimensionless quantity, as required by thermodynamic consistency. The PTEF definition can be broadly applied, covering various kinetic models and being appropriate for various photochemical reactors, either homogeneous (in solution) or heterogeneous (in the interface). The PTEF for photocatalytic air treatment units is a parameter relating to the energy utilized for the $^{\bullet}$OH free radical formation over the irradiated energy on the photocatalyst.

One can expand the PTEF definition of photocatalytic reactors for air treatment by introducing a judiciously selected photocatalytic reaction network and kinetics as well as relevant thermodynamic and irradiation parameters. The PTEF parameter equates the enthalpy of formation of consumed $^{\bullet}$OH and H$^{\bullet}$ free radicals with their absorbed photon energy. Therefore, the PTEFs provide information on the efficiency of photon energy utilization.

6.5.3.2 Relative photonic efficiency (ξ_r)

Photon efficiency (ξ) is used to facilitate the comparison of the efficacy of reactor designs (which differed in size, and hence, the residence time), as shown by Eq. (6.13):

$$\xi = \frac{C_o V}{I_o} \tag{6.13}$$

where C_o is the initial concentration, V is the volume flow rate, and I_o is the light intensity. In the case of relative photonic efficiency, a specific wavelength (ξ_r) is in order.

6.5.3.3 Quantum yield (ϕ)

The quantum yield (ϕ) is a measure of the efficiency of photon emission as defined by the ratio of the number of photons emitted to the number of photons absorbed. In other words, it is the number of times a specific event takes place per photon absorbed by the system. The quantum yield for the decomposition of a reactant molecule in a decomposition reaction is defined as shown by Eq. (6.14):

$$\Phi = \frac{\text{no. of molecules decomposed}}{\text{no. of photons absorbed}} \tag{6.14}$$

Quantum yield can also be defined for other events such as fluorescence as follows using Eq. (6.15):

$$\Phi = \frac{\text{no. of photons emitted}}{\text{no. of photons absorbed}} \tag{6.15}$$

Here, quantum yield is the emission efficiency of a given fluorophore.

For example, quantum yield is used in modeling photosynthesis as shown by Eq. (6.16):

$$\Phi = \frac{\mu\text{mol } CO_2 \text{ fixed}}{\mu\text{mol photons absorbed}} \tag{6.16}$$

In a chemical photodegradation process, when a molecule dissociates after absorbing a light quantum, the quantum yield is the number of decomposed molecules divided by the number of photons absorbed by the system. Since not all photons are absorbed effectively, the typical quantum yield will be less than 1.

Quantum yields greater than 1 are possible for photoinduced or radiation-induced chain reactions, in which a single photon may trigger a long chain of transformations. For example, the reaction of H_2 with Cl_2, in which as many as 10^6 molecules of HCl can be formed per quantum of the blue light absorbed.

In optical spectroscopy, the quantum yield is the probability that a given quantum state is formed from the system initially prepared in some other

quantum state. For example, a singlet to triplet transition quantum yield is the fraction of molecules that, after being photoexcited into a singlet state, cross over to the triplet state.

The fluorescence quantum yield is defined as the ratio of the number of photons emitted to the number of photons absorbed. Experimentally, relative fluorescence quantum yields can be determined by measuring the fluorescence of a fluorophore of known quantum yield with the same experimental parameters (excitation wavelength, slit widths, photomultiplier voltage, etc.) as the substance in question. The quantum yield is then calculated using Eq. (6.17):

$$\Phi = \Phi_R \times \frac{Int}{Int_R} \frac{1 - 10^{-A_R}}{1 - 10^{-A}} \frac{n^2}{n_R^2} \tag{6.17}$$

where ϕ is the quantum yield, *Int* is the area under the emission peak (on a wavelength scale), A is absorbance (also called "optical density") at the excitation wavelength, and n is the refractive index of the solvent. The subscript R denotes the respective values of the reference substance [1,15,16,32].

6.6 Conclusion

In this chapter, the role of several different techniques for the characterization of photocatalytic materials including spectroscopic, vibrational, emission, physicochemical, and electrochemical characterization techniques have been discussed. The fundamentals of each characterization technique help to understand the physical and chemical properties of the novel synthesized materials for various photocatalytic applications. Furthermore, this chapter covers the similarities and differences of each characterization method to better understand the process of each characterization method.

References

[1] A. Hernández-Ramírez, I. Medina-Ramírez, Photocatalytic Semiconductors: Synthesis, Characterization, and Environmental Applications, Springer International Publishing, Cham, 2015. Available from: https://doi.org/10.1007/978-3-319-10999-2.

[2] C. Luo, X. Ren, Z. Dai, Y. Zhang, X. Qi, C. Pan, Present perspectives of advanced characterization techniques in TiO_2-based photocatalysts, ACS Applied Materials & Interfaces 9 (2017) 23265−23286. Available from: https://doi.org/10.1021/acsami.7b00496.

[3] M.M. Khan, D. Pradhan, Y. Sohn, Nanocomposites for Visible Light-Induced Photocatalysis, Springer International Publishing, Cham, 2017. Available from: https://doi.org/10.1007/978-3-319-62446-4.

[4] M.M. Khan (Ed.), Chalcogenide-Based Nanomaterials as Photocatalysts, first ed., Elsevier, 2021. Available from: https://doi.org/10.1016/C2019-0-01819-5.

[5] P.S. Nnamchi, C.S. Obayi, Electrochemical characterization of nanomaterials, Characterization of Nanomaterials, Elsevier, 2018, pp. 103−127. Available from: https://doi.org/10.1016/B978-0-08-101973-3.00004-3.

[6] J.D. Clogston, A.K. Patri, Importance of Physicochemical Characterization Prior to Immunological Studies, World Scientific, 2013, pp. 25–52. Available from: https://doi.org/10.1142/9789814390262_0002.

[7] G. George, R. Wilson, J. Joy, Ultraviolet spectroscopy: a facile approach for the characterization of nanomaterials, Spectroscopic Methods for Nanomaterials Characterization, Elsevier, 2017, pp. 55–72. Available from: https://doi.org/10.1016/B978-0-323-46140-5.00003-0.

[8] D.D. Evanoff, G. Chumanov, Synthesis and optical properties of silver nanoparticles and arrays, ChemPhysChem 6 (2005) 1221–1231. Available from: https://doi.org/10.1002/cphc.200500113.

[9] A. López-Serrano, R.M. Olivas, J.S. Landaluze, C. Cámara, Nanoparticles: a global vision. Characterization, separation, and quantification methods. Potential environmental and health impact, Analytical Methods 6 (2014) 38–56. Available from: https://doi.org/10.1039/c3ay40517f.

[10] S.M. Nilapwar, M. Nardelli, H.v Westerhoff, M. Verma, Absorption spectroscopy, Methods in Enzymology, Academic Press Inc., 2011, pp. 59–75. Available from: https://doi.org/10.1016/B978-0-12-385118-5.00004-9.

[11] M.M. Khan, S. Kalathil, J. Lee, M.H. Cho, Synthesis of cysteine capped silver nanoparticles by electrochemically active biofilm and their antibacterial activities, Bulletin of the Korean Chemical Society 33 (2012) 2592–2596. Available from: https://doi.org/10.5012/bkcs.2012.33.8.2592.

[12] A.B. Murphy, Band-gap determination from diffuse reflectance measurements of semiconductor films, and application to photoelectrochemical water-splitting, Solar Energy Materials and Solar Cells 91 (2007) 1326–1337. Available from: https://doi.org/10.1016/j.solmat.2007.05.005.

[13] A.B. Murphy, Modified Kubelka-Munk model for calculation of the reflectance of coatings with optically-rough surfaces, Journal of Physics D: Applied Physics 39 (2006) 3571–3581. Available from: https://doi.org/10.1088/0022-3727/39/16/008.

[14] A.B. Murphy, Optical properties of an optically rough coating from inversion of diffuse reflectance measurements, Applied Optics 46 (2007) 3133–3143. Available from: https://doi.org/10.1364/AO.46.003133.

[15] D. Titus, E. James Jebaseelan Samuel, S.M. Roopan, Nanoparticle Characterization Techniques, Elsevier Inc, 2019. Available from: https://doi.org/10.1016/b978-0-08-102579-6.00012-5.

[16] S. Mourdikoudis, R.M. Pallares, N.T.K. Thanh, Characterization techniques for nanoparticles: comparison and complementarity upon studying nanoparticle properties, Nanoscale 10 (2018) 12871–12934. Available from: https://doi.org/10.1039/C8NR02278J.

[17] C. Suryanarayana, M.G. Norton, X-rays and diffraction, X-Ray Diffraction, Springer US, Boston, MA, 1998, pp. 3–19. Available from: https://doi.org/10.1007/978-1-4899-0148-4_1.

[18] S.N. Matussin, A.L. Tan, M.H. Harunsani, M.H. Cho, M.M. Khan, Green and phytogenic fabrication of Co-doped SnO_2 using aqueous leaf extract of tradescantia spathacea for photoantioxidant and photocatalytic studies, Bionanoscience 11 (2021) 120–135. Available from: https://doi.org/10.1007/s12668-020-00820-3.

[19] S.N. Matussin, M.H. Harunsani, A.L. Tan, M.H. Cho, M.M. Khan, Effect of Co^{2+} and Ni^{2+} co-doping on SnO_2 synthesized via phytogenic method for photoantioxidant studies and photoconversion of 4-nitrophenol, Materials Today Communications 25 (2020) 101677. Available from: https://doi.org/10.1016/j.mtcomm.2020.101677.

[20] S.N. Matussin, M.H. Harunsani, A.L. Tan, A. Mohammad, M.H. Cho, M.M. Khan, Photoantioxidant studies of the SnO_2 nanoparticles fabricated using aqueous leaf extract of Tradescantia spathacea, Solid State Sciences (2020) 106279. Available from: https://doi.org/10.1016/j.solidstatesciences.2020.106279.

[21] S.N. Matussin, A.L. Tan, M.H. Harunsani, A. Mohammad, M.H. Cho, M.M. Khan, Effect of Ni-doping on the properties of the SnO_2 synthesized using Tradescantia spathacea for photoantioxidant studies, Materials Chemistry and Physics (2020) 123293. Available from: https://doi.org/10.1016/j.matchemphys.2020.123293.

[22] A. Rahman, M.H. Harunsani, A.L. Tan, N. Ahmad, M.M. Khan, Antioxidant and antibacterial studies of phytogenic fabricated ZnO using aqueous leaf extract of Ziziphus mauritiana Lam, Chemical Papers 75 (2021) 3295−3308. Available from: https://doi.org/10.1007/s11696-021-01553-7.

[23] A. Rahman, A.L. Tan, M.H. Harunsani, N. Ahmad, M. Hojamberdiev, M.M. Khan, Visible light induced antibacterial and antioxidant studies of ZnO and Cu-doped ZnO fabricated using aqueous leaf extract of Ziziphus mauritiana Lam, Journal of Environmental Chemical Engineering (2021) 105481. Available from: https://doi.org/10.1016/j.jece.2021.105481.

[24] A. Rahman, M.H. Harunsani, A.L. Tan, N. Ahmad, M. Hojamberdiev, M.M. Khan, Effect of Mg doping on ZnO fabricated using aqueous leaf extract of Ziziphus mauritiana Lam. for antioxidant and antibacterial studies, Bioprocess and Biosystems Engineering 44 (2021) 875−889. Available from: https://doi.org/10.1007/s00449-020-02496-1.

[25] A. Rahman, M.H. Harunsani, A.L. Tan, N. Ahmad, B.K. Min, M.M. Khan, Influence of Mg and Cu dual-doping on phytogenic synthesized ZnO for light induced antibacterial and radical scavenging activities, Materials Science in Semiconductor Processing 128 (2021) 105761. Available from: https://doi.org/10.1016/j.mssp.2021.105761.

[26] S.N. Naidi, M.H. Harunsani, A.L. Tan, M.M. Khan, Structural, morphological and optical studies of CeO_2 nanoparticles synthesized using aqueous leaf extract of Pometia pinnata, Bionanoscience 12 (2022) 393−404. Available from: https://doi.org/10.1007/s12668-022-00956-4.

[27] S.N. Naidi, M.H. Harunsani, A.L. Tan, M.M. Khan, Green-synthesized CeO_2 nanoparticles for photocatalytic, antimicrobial, antioxidant and cytotoxicity activities, Journal of Materials Chemistry B 9 (2021) 5599−5620. Available from: https://doi.org/10.1039/D1TB00248A.

[28] S.N. Naidi, F. Khan, A.L. Tan, M.H. Harunsani, Y.-M. Kim, M.M. Khan, Photoantioxidant and antibiofilm studies of green synthesized Sn-doped CeO_2 nanoparticles using aqueous leaf extracts of Pometia pinnata, New Journal of Chemistry 45 (2021) 7816−7829. Available from: https://doi.org/10.1039/D1NJ00416F.

[29] S.N. Naidi, F. Khan, A.L. Tan, M.H. Harunsani, Y.-M. Kim, M.M. Khan, Green synthesis of CeO_2 and Zr/Sn-dual doped CeO_2 nanoparticles with photoantioxidant and antibiofilm activities, Biomaterials Science 9 (2021) 4854−4869. Available from: https://doi.org/10.1039/D1BM00298H.

[30] R. Romero, D. Leinen, E.A. Dalchiele, J.R. Ramos-Barrado, F. Martín, The effects of zinc acetate and zinc chloride precursors on the preferred crystalline orientation of ZnO and Al-doped ZnO thin films obtained by spray pyrolysis, Thin Solid Films 515 (2006) 1942−1949. Available from: https://doi.org/10.1016/j.tsf.2006.07.152.

[31] Z.A. ALOthman, A review: fundamental aspects of silicate mesoporous materials, Materials 5 (2012) 2874−2902. Available from: https://doi.org/10.3390/ma5122874.

[32] P.H. Salame, V.B. Pawade, B.A. Bhanvase, Characterization Tools and Techniques for Nanomaterials, Elsevier Inc, 2018. Available from: https://doi.org/10.1016/B978-0-12-813731-4.00003-5.

[33] Y.S. Choudhary, L. Jothi, G. Nageswaran, Electrochemical characterization, Spectroscopic Methods for Nanomaterials Characterization, Elsevier, 2017, pp. 19−54. Available from: https://doi.org/10.1016/B978-0-323-46140-5.00002-9.

Chapter 7

Applications of photocatalytic materials

Mohammad Mansoob Khan

7.1 Introduction

The exponential growth of research activities has taken place in materials sciences, materials chemistry, nanoscience, and nanotechnology in the past decades. When the size of the material becomes smaller and smaller down to the nanometer (nm) scale, it acquires novel chemical, physical, and electronic properties. These properties also differ in terms of changes in the shape and size of the nanomaterials. Among the unique properties of nanomaterials, the movement of electrons (ēs) and holes (h^+s) in semiconductor nanomaterials is primarily controlled by the quantum confinement effect and the transport properties that are related to the phonons. Photons are largely influenced by the type, morphology, and geometry of the materials by a considerable amount with the decrease in the size of the material. The small surface area of particle size is helpful to many devices which are based on metal oxides, such as TiO_2, making an easy interaction between the devices and the interactive media, which mainly happens on the surface or at the interfaces and considerably depends on the surface of the material. Therefore, TiO_2 is one of the most popular commercially available nanosize semiconducting materials that has found application in a variety of fields owing to its wide availability, low cost, biocompatibility, nontoxicity, and high chemical stability [1–3].

Photocatalysts have attracted a great amount of multidiscipline research due to their distinctive potential for solar-to-chemical-energy conversion applications, ranging from water and air purification to hydrogen and chemical fuel production. Moreover, photocatalysis has been considered a key technology to face the global concerns of environmental pollution and the ever-increasing energy demands by utilizing environmentally benign earth-abundant materials and renewable energy sources, such as solar energy. The performance of photocatalysts depends on several parameters such as concentration, mass, light intensity, wavelength of light, pH, temperature, nature of photocatalysts,

Theoretical Concepts of Photocatalysis. DOI: https://doi.org/10.1016/B978-0-323-95191-3.00003-1

particle size, surface area, adsorption nature, and concentration of the substrate. Apart from that many efforts have been accordingly focused on the design and fabrication of advanced photocatalytic materials relying on modification approaches [4]. Moreover, materials' modifications also boost light harvesting and photon capture, charge separation, and mass transfer that play a pivotal role in photocatalytic environmental remediation and solar-to-chemical-energy conversion applications. These modifications are not limited to coupling with plasmonic nanoparticles, surface engineering, and formation of heterostructure with other semiconducting and/or graphene-based nanomaterials, as well as tailoring the materials' structure and morphology (e.g., nanotubes, nanowires, and photonic crystals). There are several applications of metal oxides such as TiO_2 because of their perfect properties, such as water purification, air purification, antibacterial, decontamination, UV protection, toothpaste, sensing, photocatalysis, and paint. Some approaches have been adopted which include improving the TiO_2 surface by hydrophilic polymer dispersants such as polyethylene glycol with paint. Photocatalytic materials with outstanding properties make them a better choice [5–8]. Fig. 7.1 shows some of the applications of photocatalytic materials. The excellent properties include

- better surface appearance
- perfect chemical resistance

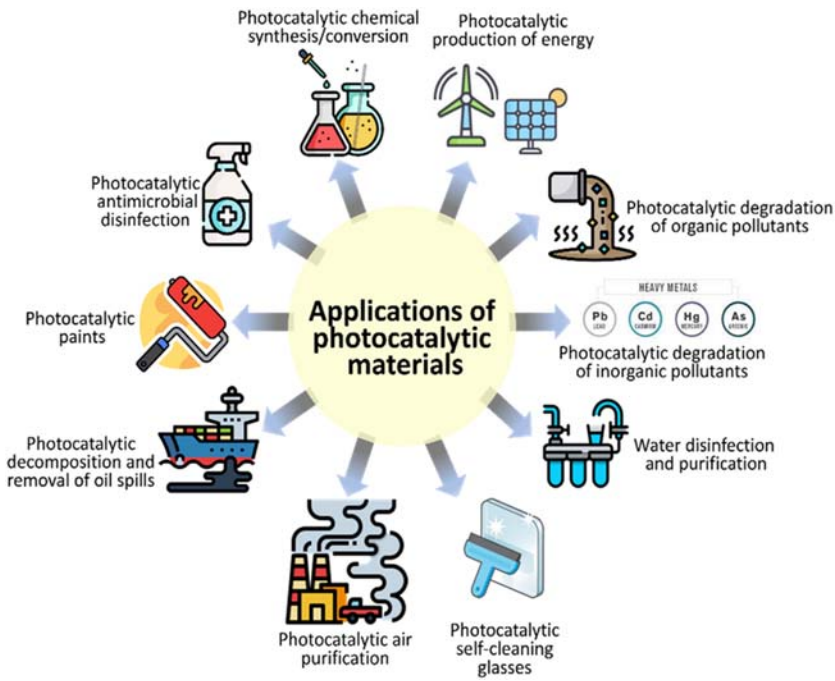

FIGURE 7.1 Examples of various photocatalytic applications.

- reduction in permeability to a corrosive environment
- better anticorrosion properties
- optical clarity
- increase in modulus
- thermally stable
- simple to clean surface
- antiskid
- antifogging
- antifouling characteristics
- perfect thermal and electrical conductivity
- perfect retention of gloss
- other mechanical characteristics such as scratch resistance, antireflective in nature, chromate and lead-free, and good adherence to various types of materials.

The following sections discuss some of the selected photocatalytic applications of semiconductors as photocatalysts. These methods are considered a green photocatalytic approach because most of the applications take place at normal temperature and pressure, do not involve high energy inputs, and the end byproducts are water and carbon dioxide which are not harmful and toxic.

7.2 Energy production using photocatalysis

Overuse of fossil fuels has depleted traditional energy sources and contributed to contamination of the water, soil, and air environments. Renewable and green energy are widely expected to be used to address the energy issue and environmental pollution. Solar energy is an extremely attractive natural energy source. Solar energy conversion to chemical energy via chemical reactions is a promising method of generating renewable energy. Photocatalysis is artificial photosynthesis as it is inspired by the natural photosynthesis of green plants and some other microorganisms, which convert solar energy to chemical energy in the form of carbohydrates or hydrogen [9]. Photocatalytic H_2 production via solar H_2O splitting is one of the promising solutions for sustainable energy and environmental remedy issues with no reliance on fossil fuels and no CO_2 emission. Existing photocatalytic systems for H_2O splitting can be divided into two primary types.

1. Splitting H_2O into H_2 and O_2 gases using a single visible-light-responsive photocatalyst with sufficient potential to achieve overall H_2O splitting. In this type, the photocatalyst should have a suitable thermodynamic potential for H_2O splitting, that is, a sufficiently narrow band gap energy to harvest visible light photons and stability against photocorrosion. Because of these stringent requirements, the number of reliable and reproducible photocatalysts suitable for one-step H_2O splitting is limited.

2. A two-step excitation mechanism using two different photocatalysts. This type of photocatalyst was inspired by natural photosynthesis that takes place in green plants. This is known as the *Z*-scheme. The advantages of H_2O splitting using the *Z*-scheme system are
   - **a.** A wide range of visible light is available. So a change in Gibbs free energy required to drive each photocatalyst can be reduced as compared to the one-step water splitting system
   - **b.** Separation of obtained H_2 and O_2 gases is possible. It is possible to use a semiconductor that has either an H_2O reduction or oxidation potential for one side of the system. For example, some metal oxides (e.g., WO_3 and $BiVO_4$) act as a good O_2 evolution photocatalyst in a two-step H_2O splitting system using a proper redox mediator, although they are unable to reduce H_2O [10,11].

Water splitting is the chemical reaction in which H_2O is broken down into H_2 and O_2 gases as shown by the following equation:

$$H_2O_{(l)} \rightarrow 2H_{2(g)} + O_{2(g)}$$

Efficient and economical photochemical H_2O splitting would be a technological breakthrough that could support a hydrogen economy. At the industrial level, H_2O splitting with pure H_2O has not yet been reported. However, the two products, that is, H_2 and O_2 production are well-known. The reverse of water splitting is the basis of the hydrogen fuel cell.

Electricity produced by photovoltaic systems potentially offers the cleanest way to produce H_2 gas than nuclear, wind, geothermal, and hydroelectric. Here too, H_2O is broken down into H_2 and O_2 gases by electrolysis, however, the electrical energy is obtained by a photoelectrochemical cell (PEC) process. This system is named artificial photosynthesis.

Photocatalytic H_2O splitting is an artificial photosynthesis process with photocatalysis in a photoelectrochemical cell used for the dissociation of H_2O into its constituent components, H_2, and O_2 gases, using either artificial or natural light. Theoretically, only light energy (photons), water, and a catalyst are needed. This topic is the focus of considerable research, however, so far no technology has been commercialized.

Hydrogen fuel production has gained much attention as public understanding of global warming has increased. Methods such as photocatalytic H_2O splitting are being investigated to produce H_2 gas, which is a clean-burning fuel for the future. Water splitting holds particular promise since it utilizes H_2O which is an inexpensive renewable resource. Photocatalytic H_2O splitting has the simplicity of using a photocatalyst and sunlight to produce H_2 gas from H_2O.

Population growth and industrial development have greatly increased the formation of waste products and consumption of energy worldwide. This situation creates the need for a clean and sustainable alternative source of energy.

In the 1960s, Fujishima et al. unfolded the fascinating characteristics of TiO_2 as a semiconductor photocatalyst. H_2 gas is considered an ideal energy carrier for the future having a high energy capacity. It is an environment-friendly fuel since it does not produce any air pollutants or greenhouse gases. This minimizes the concern of global warming issues. It is considered the cleanest source of energy for transportation and other industrial use.

Semiconductor photocatalyst-assisted H_2O splitting under sunlight is an effective way to the production of environment-friendly H_2 gas. Research in the area of solar H_2 gas production started in 1972 with the well-known Honda-Fujishima effect. H_2 gas was produced by photoelectrochemical (PEC) H_2O splitting using TiO_2 as a photoanode and Pt as a cathode. When light is irradiated with energy larger than the band gap energy of TiO_2, electron-hole ($\bar{e}$-h^+) pairs are formed in the conduction band (CB) and valence band (VB), respectively. The electrons ($\bar{e}$s) then migrate toward the Pt cathode on the application of an anodic potential to an external circuit. Therefore, $\bar{e}$s participates in the reduction reaction and produces H_2 gas, whereas, h^+ carries out the oxidation reaction and produces O_2 gas. The overall reaction mechanism is shown in Fig. 7.2A [10–12]. Similarly, Pt-loaded TiO_2 can be a good photocatalyst for H_2 production (Fig. 7.2B) under ambient conditions.

Numerous photoelectrochemical cells have been designed and reported by researchers across the globe for the effective utilization of solar energy. However, the development of a suitable photoelectrode with high stability and thermodynamic properties, such as suitable band gap energy and band edge position, is a great challenge (Fig. 7.2). The solar H_2 formation approach can be broadly classified as

1. photoelectrochemical (PEC)-assisted H_2O splitting and
2. photocatalytic or photochemical H_2O splitting.

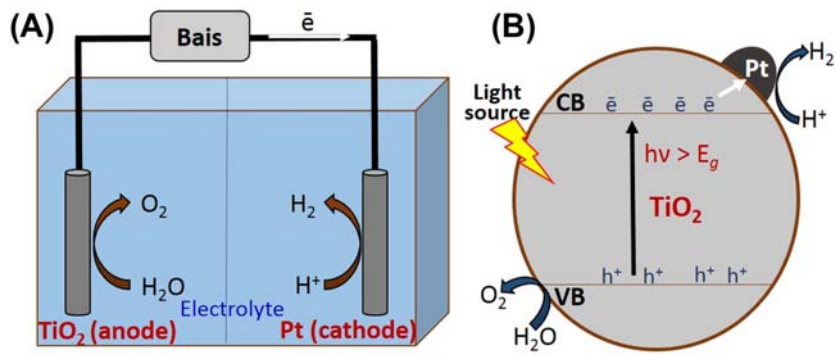

FIGURE 7.2 (A) PEC water splitting using a TiO_2 photoanode and Pt cathode and (B) Photocatalytic water splitting using Pt-loaded TiO_2.

Remarkable research has been done to achieve photocatalytic H_2O splitting to generate H_2 gas considering sunlight as the most powerful source of energy that continuously provides the power of $\sim 1.2 \times 10^{17}$ W.

Photocatalysts must confirm several key principles to be considered effective for H_2O splitting. A key principle is that H_2 and O_2 production should take place in a stoichiometric ratio of 2:1. Significant deviation could be due to a flaw in the experimental setup and/or a side reaction, neither of which indicate a reliable photocatalyst for H_2O splitting. The prime measure of photocatalyst effectiveness is quantum yield (QY), which is shown in Eq. (7.1):

$$\mathrm{QY}(\%) = \frac{\text{Photochemical reaction rate}}{\text{Photon absorption rate}} \times 100 \tag{7.1}$$

This quantity is a reliable determination of how effective a photocatalyst is. However, it can be misleading due to varying experimental conditions. To assist in comparison, the rate of gas formation can also be used. This method is challenging on its own because it is not normalized. However, it can be useful for rough comparisons and is consistently reported in the literature. Overall, the best photocatalyst should have a high QY and provide a high rate of H_2 gas production.

The other deciding and important factor for a photocatalyst is the range of light being absorbed. Though UV light-based photocatalysts perform better per photon than visible light-based photocatalysts owing to the higher photon energy, however, more visible light reaches the Earth's surface than UV light. Thus, a less efficient photocatalyst that absorbs visible light (longer wavelength) may ultimately be more useful than a more efficient photocatalyst absorbing only light with smaller wavelengths, that is, UV light. The utility of material for photocatalytic H_2O splitting is typically investigated for one of the two redox reactions at a time. To achieve this, a three-component system is employed:

1. a catalyst,
2. a photosensitizer, and
3. a sacrificial electron acceptor such as persulfate when investigating water oxidation and a sacrificial electron donor (e.g., triethylamine) when studying proton reduction. The use of sacrificial reagents simplifies the process and prevents unfavorable charge recombination [10–12].

Recent advancements in the development of novel nanomaterial for energy production and storage with improved energy efficiencies, lower costs, and energy savings, contribute significantly to global energy sustainability as demand is continuously increasing. Nanostructured solar cells such as TiO_2 and ZnO nanotube-based dye-sensitized solar cells have the potential to be cheaper and easier to install with recent advancements in their print-like manufacturing process and can be made into flexible rolls rather than discrete

panels [11,12]. It is also inevitable that the abundant water resource and sunlight as energy to have hydrogen derived from water as the future source of clean energy. The advancement in research on improving the efficiency of H_2 production and light harvesting using different metal oxide nanostructures such as TiO_2, ZnO, Ce/TiO_2, and CeO_2-graphene is expanding very fast [11,12]. This would serve as a major source of clean energy to the world and help in energy sustainability for future generations.

7.3 Photocatalytic degradation of organic pollutants

Textile-colored dyes, other industrial dyes, and colorless organic pollutants constitute one of the largest groups of organic compounds that are a major threat to environmental danger. The dyes which are frequently used on the industrial scale are azo, anthraquinone, sulfur, indigoid, triphenylmethyl (trityl), and phthalocyanine derivatives. About 1%−20% of the total world production of dyes is used for dying processes and unused dyes are released into various water bodies as textile wastewater effluents. The release of colored wastewater in the environment is a considerable source of nonaesthetic pollution which leads to eutrophication and other environment-related issues. It can produce toxic and dangerous byproducts through reduction, oxidation, hydrolysis, or other chemical reactions taking place in the wastewater [1,2].

Another class of chemicals that causes water pollution and contamination is pesticides. During the last two decades, worldwide pesticide usage has dramatically increased, coinciding with changes in farming policies and increasing intensive agricultural practices. Pesticides appearing on water surfaces and groundwater can be classified according to their specific biological activities on a target species (e.g., insecticides, weedicides, herbicides, fungicides, and acaricides) or by their chemical composition (e.g., phenylurea and phenoxy-acid pesticides, organochlorine compounds, chlorophenolic substances, triazines, carbamates, thiocarbamates, and organophosphorus insecticides) [12]. For instance, Hanh et al. have successfully synthesized Cu-doped ZnO using the hydrothermal method with different Cu percentages (i.e., 1, 2, 3, and 4 wt.%) for photocatalytic degradation of monocrotophos pesticide [13]. The synthesized photocatalysts showed enhanced activity for photocatalytic degradation of monocrotophos into CO_2, H_2O, and harmless inorganic ions even under irradiation of visible light. They have also reported that 3 wt.% Cu-doped ZnO photocatalyst showed the highest monocrotophos degradation efficiency among the other synthesized Cu-doped ZnO.

Several reports have shown that Degussa P25 (TiO_2) and modified-TiO_2 have been able to photocatalytically degrade various types of organic pollutants in the presence of artificial light (UV and visible range) or solar radiation. The photocatalytic degradation of dyes such as methyl orange (MO), reactive red 195, acid orange 7, reactive yellow 81, and reactive violet 1 using Degussa P25 as photocatalysts has been extensively investigated [14,15].

The advantages and disadvantages of the use of TiO_2-assisted heterogeneous photocatalysis for the photocatalytic degradation of dyes have been described in widespread literature. However, evaluation of the mineralization by total organic carbon (TOC) analysis and information concerning the evolution of toxicity and biodegradability of the treated samples have been scarce. The toxicity and biodegradability of the byproducts during the photocatalytic degradation of the azo dyes and acid orange 7 were evaluated using artificial UV light as the source of radiation and TiO_2 Degussa P25 as photocatalyst. The Microtox assay indicated that the toxicity of the pollutants was significantly minimized after the treatment. Additionally, the photocatalytic process showed an enhancement in the degradability of the polluted water sample after 6 h of treatment. Therefore, this advanced oxidation process (AOP) could be used as a pretreatment method to degrade biorecalcitrant organic dyes [6,14,15].

7.4 Removal of inorganic pollutants from wastewater

Rapid industrialization and population increase may cause major inorganic pollutants affecting the environment. Inorganic pollutants have a greater risk to the environment as well as human health which vary on interaction at both extracellular and intracellular levels [16]. There is a variation of inorganic pollutants, for example, metals with their biological importance may have harmful effects depending on their degree of consumption. Moreover, alkali and alkaline metals salts could also degrade both the physical and chemical environment of soil which could lead to difficulty in water and nutrient uptake. However, toxic heavy metals interact more strongly with soil constituents compared to alkali metals. Therefore, major inorganic pollutants include alkali metals and heavy metal ions [16–18].

In wastewater treatment systems, the common inorganic pollutants are nitrates, nitrites, selenium, cyanides, heavy metals like arsenic, lead, copper, cadmium, mercury, iron, phosphates, fluorides, calcium, aluminum, and other compounds of cyanides. Great amounts of phosphates and nitrates collectively can cause eutrophication [19]. On the other hand, fluoride contamination in water may cause dental ailments and fluorosis disease which affects millions of people globally [20]. Inorganic pollutants mainly comprise heavy metals which are toxic even at low concentrations. Heavy metals such as arsenic, mercury, lead, and chromium can enter the body system through water, food, and air which may cause some health issues [16–18].

7.4.1 Removal of toxic and heavy metals and metalloids using photocatalysis

Metals are quite problematic because they are not biodegradable and can accumulate in living tissues. In developing countries, with the rapid development

of industries such as metal plating industries, mining industries, fertilizer industries, tanneries, batteries, paper industries, pesticides, and wastewaters containing heavy metals are directly or indirectly discharged into various water bodies. Any metal (or metalloid) species may be considered a "contaminant'" if it occurs where it is unwanted, or in a form or concentration that causes a detrimental effect on humans or the environment. Table 7.1 shows different heavy metals and their effects on human health and their acceptable limits.

Thus, the photocatalytic removal of heavy metals and metalloids is rapidly gaining importance for wastewater treatment. The photocatalytic treatment process can convert ionic species into their metallic solid forms and deposit them over the semiconductor surface or transform them into less toxic and soluble species. The redox level of the metallic couples related to the levels of the CB and VB can be considered the most important parameter for predicting the feasibility of the transformation of the species. For the reduction of photocatalytic chemical species, the CB of the semiconductor photocatalyst must be more negative than the reduction potential of the chemical species. In contrast, photooxidation can take place only when the potential of the VB is more positive than the oxidation potential of the chemical species [3,5,6].

For example, chromium (Cr) exists in the aquatic environment mainly in two oxidation states, trivalent Cr(III) and hexavalent Cr(VI). Cr(VI) species are known to be carcinogenic and toxic whereas Cr(III) is less toxic and can be readily precipitated out of solution in the form of $Cr(OH)_3$. Cr(VI) is a frequent contaminant in wastewater produced by several industries, such as electroplating, leather tanning, and paints. The frequently found Cr(VI) species in aqueous solutions are $Cr_2O_7^{2-}$, CrO_4^{2-}, H_2CrO_4, and $HCrO_4$. Although the relative distribution depends on the pH of the solution, the concentration of Cr(VI), and the redox potential. However, none of these Cr(VI) species form insoluble precipitates, making their separation through direct precipitation not feasible. In this oxidation state, the Cr is extremely mobile in water and soil. Thus, to form a Cr in the solid phase, which can be easily separated from the aqueous media, it is necessary to change the oxidation state. The use of heterogeneous photocatalysis for the reduction of Cr(VI) has been described as an alternative option for the removal of Cr(VI) found in wastewater bodies and industrial effluents [22].

The removal of Cr(VI) using TiO_2 as a photocatalyst has been favored at lower solution pH values due to an increased potential difference between the CB of TiO_2 and Cr(VI)/Cr(III) and the anionic-type adsorption of Cr(VI) onto the surface of TiO_2. The reaction can be accelerated by the addition of the scavengers such as citric acid, humic acid, oxalate, nitrilotriacetic acid, ethylenediaminetetraacetic acid, phenol, and isopropyl alcohol. In particular, size, shape, and surface area are very important factors in determining the photocatalytic activity of TiO_2. In this context, a sea-urchin-like rutile TiO_2

TABLE 7.1 Types of toxic and heavy metals and their effects on human health [21].

Heavy metals	Major sources	Effect on human health	Permissible amount (mg/L)
Arsenic	Pesticides, fungicides, metal smelters, unintended release during the mining of gold and lead, from the combustion of coal	Bronchitis, dermatitis, poisoning	0.02
Cadmium	Welding, electroplating, pesticides, fertilizers	Renal dysfunction, lung disease, lung cancer, bone defects, kidney damage, bone marrow	0.06
Lead	Paint, pesticides, automobile emission, mining, burning of coal, ore and metals processing, piston-engine aircraft operating on leaded aviation fuel	Mental retardation in children, development delay. Fatal infant encephalopathy, chronic damage to the nervous system, liver and kidney damage	0.1
Manganese	Welding, fuel addition, ferromanganese production	Inhalation or contact damage to the central nervous system	0.26
Mercury	Pesticides, batteries, paper industry	Tremors, gingivitis, protoplasm poisoning, damage to the central nervous system, spontaneous abortion	0.01
Zinc	Refineries, brass manufacture, metal plating	Damage to the nervous system, dermatitis	15
Chromium	Mine, mineral sources	Damage to the nervous system, irritability	0.05
Copper	Mining, pesticide production, chemical industry	Anemia, liver and kidney damage, stomach irritation	0.1

superstructure with ultrathin nanorods and exposed {110} facets exhibited excellent photocatalytic activity for the removal of Cr(VI) ions from plating wastewater effluents. This special morphology exhibited a structure-enhanced photocatalytic activity because it facilitates the transport of photoelectrons to

the rutile nanorod {110} facets and prevents them from recombining with holes. The percent removal was nearly 100% at initial Cr concentrations below 53.7 mg/L after 3 h of solar radiation [22].

7.4.2 Removal of cyanides using photocatalysis

Cyanide (CN^-) is one of the common water contaminants mainly released into the water bodies by different types of industries. It is a highly toxic priority pollutant to human beings and aquatic organisms even at very low concentrations. The presence of free and complex cyanides in industrial effluent, therefore, causes many environmental problems. It is predominantly used in electroplating, metal plating, and the extraction of gold and silver in mining industries, where it is produced in large quantities. It is also used in textiles, plastics, and paper industries. CN^- may be present in waste streams and environmental matrixes in a variety of forms, such as free cyanide (CN^-), simple and complex cyanides, cyanates (OCN^-), and nitriles ($-C\equiv N$). The most toxic form of cyanide is free cyanide, which includes the cyanide anion itself and hydrogen cyanide (HCN) either in a gaseous or aqueous state.

A promising method of cyanide detoxification is the photocatalytic approach. During the removal process, the toxic CN^- species are converted into cyanate species (OCN^-) at the semiconductor surface and can also be transformed into N_2 and CO_2 as byproducts which are less toxic to the environment and human beings. The use of TiO_2 in the slurry form for the photocatalytic degradation of both free and complex cyanide compounds under artificial UV light irradiation has been extensively investigated, studied, and reported [12].

The mechanism in Fig. 7.3A shows that the released cyanide is proposed to be the photooxidative radical scavenger, being oxidized to cyanate (OCN^-), and resulting in Fe photoreduction in the absence of oxygen. Fig. 7.3B shows the possible direct and indirect mechanisms for the [Fe $(CN)_6^{3-}$] selective degradation where h^+ and $^{\bullet}OH$ radicals are trapped by the t-ButOH. Fig. 7.3C shows that the indirect reduction by the indirect

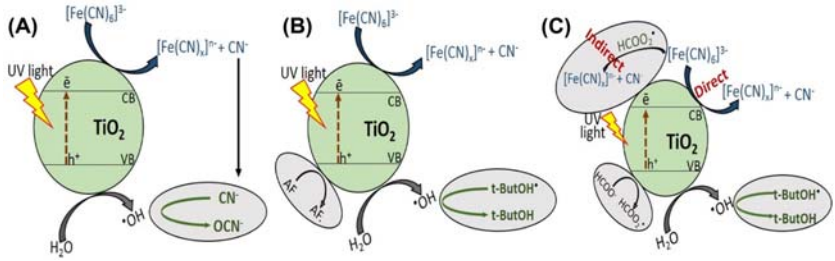

FIGURE 7.3 Possible mechanisms for the photocatalytic degradation of $[Fe(CN)_6]^{3-}$, (A) without scavengers, (B) with scavengers, and (C) complete proposed direct and indirect mechanisms.

transfer of one electron to iron from the intermediate species to the iron cyano complex is possible in the bulk of the reactor and not on the surface.

As the electron in the CB has a reductive potential superior to the Fe $(CN)_6^{3-}$, the direct reduction is possible. Also, the scavenger acceptors generate species such as the formate radical ion $HCOO^{\bullet -}$, which is a highly reductive radical with a redox potential between -1.98 and -1.1 V, even more reductive than the TiO_2 CB E(vs (NHE)) = -0.5 V at pH 7.0.

In contrast, the direct reaction of Fe^{3+} with t-butanol as a radical does not take place. Thus, the indirect reduction for this radical is discarded. Therefore, adding a mixture of scavengers has a synergistic effect on the photoreductive degradation of the $[Fe(CN)_6^{3-}]$, which is evidenced by the presence and increase of CN^- and the total removal of Fe in the solution. Hence, the selective reduction of the metal and the degradation of the cyano complex can be reached without the oxidation of cyanide, which may be an option for cyanide recovery for the reuse of water in the process [23].

7.5 Water disinfection and purification

The main aim of water disinfection and purification is the prevention of waterborne diseases among human beings, pet animals, and crops. In general, during a sizable fraction of the disease outbreak, the etiologic agent was not identified. However, in many of these cases, enteric bacteria or enteric viruses are believed to be the causative agents. The mechanisms for microbial inactivation and removal might include the following process:

- Laceration of the cell wall
- Modification of cell permeability
- Modification of the nature of the protoplasm
- Alteration of nucleic acids
- Disruption of protein synthesis
- Induction of abnormal redox process
- Inhibition of enzyme activity

The declaration of many new regulations for the control of microbiological and chemical pollutants in drinking water has prompted the search for a suitable and cost-effective alternative method for primary disinfection. Of particular concern are the disinfection byproducts (DBPs) of chlorination and that groundwater high in natural organic matter (NOM) may be incompatible with the more traditional chemical disinfectants. Even the alternatives currently considered such as chloramines may be inappropriate because they are weak virucides and may not meet primary disinfection requirements [12].

A variety of chemical agents can be used to inactivate microorganisms. These include halogens and their derivatives (Cl_2, Br_2, I_2, HOCl, OCl, ClO_2, HOBr, HOI, and polyiodide anion exchange resins), oxygenated and highly oxidizing compounds (ozone, hydrogen peroxide, phenols, alcohols, persulfate

and percarbonate, peracetic acid, and potassium permanganate), metal ions (Ag^{+}, Cu^{2+}, etc.), dyes, quaternary ammonium compounds, strong acids and bases, and enzymes. There are also physical processes that are included in the disinfection such as electromagnetic radiation (ultrasonic waves, heat, visible light, UV light, gamma radiation, and X-rays), particle radiation (electron beam), and electrical current.

A variety of factors influence the disinfection efficacy which include

- contact time
- chemical nature
- concentration of the disinfecting agent
- the initial mixing mode and point of injection
- nature and intensity of the physical agents
- temperature of the microorganisms
- type of microorganisms
- concentration of the microorganisms
- age of the microorganisms
- the nature of the liquid carrier

Following are the common features of the important chemical disinfectants (Cl_2, OCl, ClO_2, and O_3):

- Highly potent microorganism inactivation and relatively highly toxic to human beings and animals
- Active interaction (normally oxidation or addition) with organic matter and with inorganic reducing agents
- Sufficient solubility in aqueous media (except the dihalogens due to their nonpolar nature)
- Penetration capability through surfaces and cell membranes
- Moderate to good deodorizing ability

The relative stabilities of these chemicals follow the order $Cl_2 > OCl > ClO_2$, O_3, and their relative costs are $O_3 > ClO_2$, $OCl > Cl_2$. Undesirable characteristics include DBP production, membrane attack, corrosivity to metallic materials, and discoloration of tints and dyes. It has been stated that it would be ideal to separate the oxidation and disinfection functions in the water treatment system.

The fundamental mechanism of the photocatalytic oxidation process has been well established in the case of TiO_2 photocatalyst irradiated by UV light. For the inactivation of microorganisms, the photocatalytic inactivation process is quite similar to the process of degradation of organic pollutants. It is because the microorganisms, such as bacterial cells, are 70%−90% water, and the major cellular constituents, such as polysaccharides, lipids, proteins, and nucleic acids, are organic compounds in nature and can be attacked by reactive oxygen species (ROSs) and subsequently lead to cell death. Fig. 7.4 shows the typical photocatalytic disinfection process. The photoreaction is

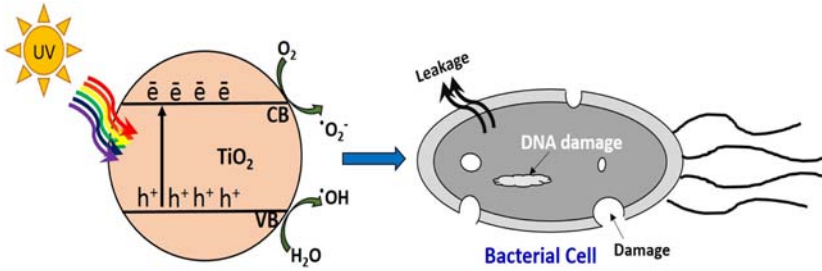

FIGURE 7.4 Schematic diagram showing the mechanism of photocatalytic disinfection using TiO_2 under UV light irradiation.

initiated by absorbing photons with energy higher than the band gap energy (E_g) of the semiconductor. Then, the photon-generated electron-hole ($\bar{e}$-h^+) pairs are separated and migrate to the surface or interface of the photocatalyst, where a variety of redox reactions take place with the generation of various ROSs. The photon-generated $^{\bullet}OH$, $O_2^{\bullet -}$, and H_2O_2 are usually perceived to be the reactive species responsible for bacterial inactivation. The direct bactericidal effects of $\bar{e}$s and h^+s have also been revealed recently [24–26].

In previous studies, several factors affecting the efficiency of photocatalytic materials in water disinfection and purification have been investigated, and even so, further research is needed to address practical applications [27]. These factors include

- Catalyst dose: The amount of catalyst is determined by the type and dimensions of the reactor and it changes depending on the type of pollutant. In theory, higher concentrations of catalysts provide a greater number of active sites, and therefore, higher rates of reactive radicals' generation. However, an excess of catalyst will cause particle aggregation and an increase in solution opacity, reducing the effective path length of radiation.
- Light intensity and wavelength: The photochemical process and the production of electron-hole pairs are highly influenced by light intensity. The rate of photon generation and electron-hole pair formation increases as the intensity of radiation increases.
- Dissolved oxygen: The photocatalytic reaction is also affected by dissolved oxygen. Oxygen improves or hinders photodegradation depending on the mechanism/pathway of the reaction but does not affect the adsorption of pollutants on surface photocatalytic materials.
- Effect of oxidants incorporation: The addition of external oxidant/electron acceptors has been also studied to inhibit the electron-hole recombination in photocatalytic materials and improve their photocatalytic performance toward water pollutants. Because the formation of radicals has a decisive role in water disinfection and purification, several authors have studied the effect of the incorporation of electron scavengers, such as H_2O_2, O_3, and $(NH_4)_2S_2O_8$.

7.5.1 Photocatalytic disinfection process

The present meaning of the photocatalytic process and various other steps involved in this approach have been discussed previously. Heterogeneous photocatalysis (HPC) is among the most successful applications of the AOPs as suggested by the wide variety of research groups, scientific reports, facilities, and patents about the use of this technology for the removal of toxic substances found in polluted water, air, and soil. However, the use of HPC for water disinfection is a developing field of investigation which has given rise to the design and synthesis of novel nanostructured photocatalysts having interesting and demanding properties for more efficient environmental applications.

The photocatalytic processes for organic pollutants removal and mass transfer are an important part of the inactivation using HPC processes. Initial practical approaches for a quantitative description of HPC kinetics have been commonly carried out using the Langmuir−Hinshelwood (L−H) kinetics model. This mathematical model assumes that the reaction takes place on the surface of the photocatalyst. According to the L−H model, the rate of reaction (r) is proportional to the fraction of particle surface covered by the pollutant (θ_x). Mathematically, it can be shown in Eq. (7.2):

$$r = -\frac{dC}{dt} = k_r\theta_x = \frac{k_r KC}{1 + KC + K_s K_s} \tag{7.2}$$

where k_r is the rate of reaction constant, K is the pollutant adsorption constant, C is the pollutant concentration at any time, K_s is the solvent adsorption constant, and C_s is its concentration. Several authors have reported the data using the L−H kinetic approach. However, despite that the L−H kinetic approach fits properly with the experimental data. It does not consider the role of the radiation field on the mechanism.

Other kinetic studies on HPC suggest that the rate of reaction increases with photocatalyst concentration to get a maximum value concentration depending on the pollutants and the reactor used. Over these concentrations, the rate of reaction remains unchanged or decreases with further increments of photocatalyst concentration [12].

7.6 Photocatalytic self-cleaning glasses

Self-cleaning glass is a specific type of glass with a surface that keeps itself free of dust and grime. The field of self-cleaning coatings on glass is divided into two categories:

1. hydrophobic self-cleaning coatings
2. hydrophilic self-cleaning coatings

These two types of coating both clean themselves through the action of water, the former by rolling droplets and the latter by sheeting water that

carries away dust. Hydrophilic coatings based on TiO_2, however, have an additional property: they can chemically break down absorbed dust in sunlight.

TiO_2 NPs are well-known to decompose organic matter when irradiated with ultraviolet light. This fact has long been known as an obstructing phenomenon that takes place with paint containing a TiO_2 pigment. During a self-cleaning process with a photocatalyst, contaminants on substrates get photodecomposed, wherein radicals and active oxygen species generated by UV light irradiation on a photocatalyst decompose the organic contaminants into CO_2, thereby, allowing the surface of the substrate to remain clean. It has been reported that a positive hydrophilic effect appears when a TiO_2 photocatalyst is irradiated by UV light. This characteristic is widely applied to glasses, mirrors, and building materials. If a TiO_2 photocatalytic coating material is used in an outdoor location exposed to rainwater, organic contaminants on the surface of the coating are decomposed by light irradiation and the residual inorganic particles are readily washed away by the rainwater. Hence, the coated surface exhibits the expected self-cleaning effect. Free radicals and ROSs generated by the activity of TiO_2 photocatalyst are effective in decomposing and preventing the propagation of bacteria and fungi. Because of their small selectivity against bacterial species and their ability to decompose the toxins produced by bacteria, TiO_2 photocatalysts have been increasingly used for interior finishing materials in hospitals and medical equipment.

On the other hand, the intensity of UV light available indoors is one digit lower compared with that available outdoors. Hence, it is difficult to offer sufficient photocatalytic activities with UV light in a room. In addition, there are many places where the intensity of UV light is lower than expected such as in cars that are equipped with UV-cut glasses. To operate effectively in these locations, novel photocatalysts responsive to visible light and capable of performing within the visible light spectrum of 500−600 nm wavelength as well as the UV region have been developed and commercialized. It should be understood from the spectra of sunlight that the energy harvesting efficiency of photocatalysts under sunlight has improved with the expansion of the effective wavelength to 500−600 nm.

Visible light-responsive photocatalysts have been fabricated through a change in the band structure. This can be achieved by the addition of new energy levels by doping TiO_2 photocatalyst with another element such as nitrogen or sulfur. The photocatalyst thus obtained is yellower compared with conventional anatase-type photocatalysts and is capable of absorbing a portion of the visible light. Generally, the particle size of the visible-light-responsive photocatalysts is designed to be bigger than that of conventional anatase-type photocatalysts. This is to avoid a shift in the optical absorption edge to a shorter wavelength owing to the quantum confinement effect which takes place when the particle size is <10 nm.

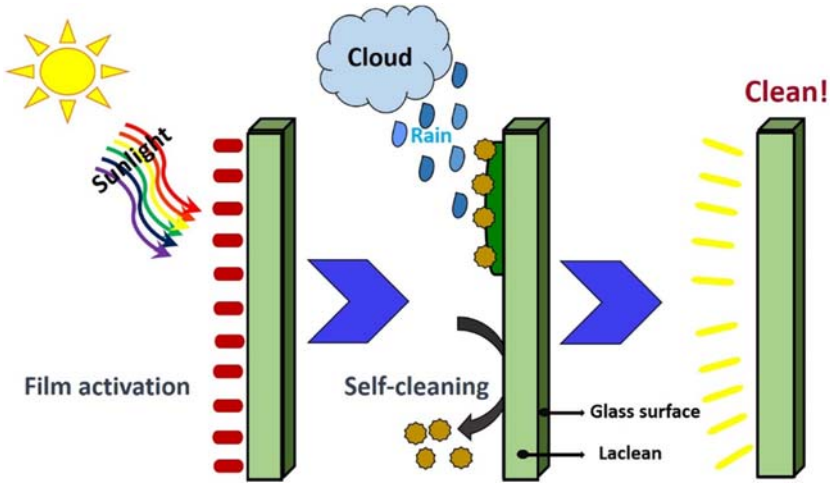

FIGURE 7.5 Schematic diagram of the photocatalytic self-cleaning surface.

The commercialized applications of antibacterial visible light-responsive photocatalyst include window blinds and wallpapers. A photocatalyst layer on the surface of these resin-coated products, a transparent primer coating agent, composed principally of inorganic components, is applied to form an intermediate layer to improve durability, and then a coating, containing photocatalyst particles, is applied to form the top layer. Fig. 7.5 shows the schematic of self-cleaning glass and surfaces [5,6,28].

7.7 Photocatalytic air purification

Photocatalytic air purification is a promising technology that mimics nature's photochemical process, but its practical applications are still limited despite considerable research efforts in recent decades. Using light to clean up polluted air is an ideal technology that mimics nature's process and has great potential to be developed as a key technology for air purification, which still needs breakthroughs in several areas.

In the advanced photocatalytic oxidation (APCO) reaction, pure or doped metal oxide semiconductors (e.g., TiO_2, ZnO, CdS, and Fe (III)-doped TiO_2) are commonly used as photocatalysts. An important step of photoreaction is the formation of $\bar{e}$-h^+ pairs which need the energy to overcome the band gap energy (E_g) between VB and CB. When the energy provided (photon) is larger than the E_g, the $\bar{e}$-h^+ pairs are created in the semiconductor, and the charge transfers between the $\bar{e}$-h^+ pairs and adsorbed species (reactants) on the semiconductor surface, and then photooxidation occurs. The common light sources used are UV light and visible light. In the presence of air or

oxygen, UV-irradiated TiO_2 is capable of completely decomposing many organic pollutants. The activation of TiO_2 by UV light is shown as

$$TiO_2 + hv \rightarrow TiO_2(\bar{e} + h^+)$$

In this reaction, h^+ and $\bar{e}$ are powerful oxidizing and reductive agents, respectively. The oxidative and reductive reactions are expressed as

Oxidative reaction:

$$OH^- + h^+ \rightarrow {}^{\bullet}OH$$

Reductive reaction:

$$O_{2ads} + \bar{e} \rightarrow O^-_{2ads}$$

In the photocatalytic degradation of organic pollutants, the hydroxyl radicals ($^{\bullet}OH$), which are formed from the oxidation of adsorbed H_2O or adsorbed OH^-, are the primary oxidants and the presence of oxygen can prevent the recombination of the $\bar{e}$-h^+ pairs. For a complete APCO reaction, the final products of the reactions are CO_2 and H_2O.

$$\text{Pollutants} + {}^{\bullet}OH + O_2 \rightarrow \text{Mineralized products } (CO_2,\ H_2O,\ \text{etc.})$$

Studies on the photocatalytic oxidation of NO_x and VOCs have been carried out intensively as shown in Fig. 7.6. Hoffmann et al. reviewed the environmental applications of semiconductor photocatalysis. Reaction mechanism and kinetics, especially using the Langmuir–Hinshelwood model, were studied. The workability of the semiconductors, especially TiO_2 and doped-TiO_2 with Fe on photochemical oxidation was investigated, and photoreactors for H_2O and air purification were studied with different pollutants [12,29].

The main advantages of the photocatalytic air purification process are

1. no need for external energy input or chemicals except light, which is not expensive when utilizing sunlight or ambient light.
2. safe operation under ambient conditions and relatively humidity-insensitive activity

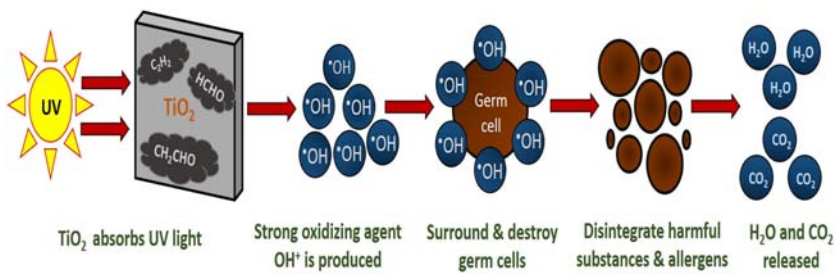

FIGURE 7.6 Schematic showing the photocatalytic air purification process.

3. able to fully mineralize the volatile organic compounds (VOCs) to CO_2 and H_2O byproducts which are not toxic and harmful.
4. able to kill or remove the microorganisms such as bacteria and viruses.

On the other hand, this process suffers from low photon utilization efficiency and slow removal rate, the difficulty of scaling up, and the fouling/deactivation of photocatalysts during long use.

7.8 Photocatalytic decomposition and removal of oil spills

An oil spill is the release of liquid petroleum hydrocarbons into the environment, especially in the marine ecosystem, due to different human activities, which cause various forms of pollution. Oil spills take place when there is the failure of the oil drilling machinery due to human error, carelessness, deliberate acts, or mistakes, or because of natural disasters or marine accidents, especially for refineries or tankers shipping any form of petroleum products.

The primary oil pollutants in the ocean and sea may be caused by leaking of oil from a shipwreck, prospecting and excavating of oil on the sea, dropping of oil and gas in the atmosphere, shipping maintenance industry, offshore industry, and harbor contamination. In addition to the release of toxic substances from oil spills, oil slicks may cover the sea surface to reduce the photosynthesis of algae and dissolve oxygen therein. Oil slicks on the ocean surface resulting from spills from ships, oil, and gas platforms as well as natural seeps from the ocean bottom, are a kind of marine pollution. Oil slicks are primarily composed of hydrocarbons which often have long residence times in the environment.

The negative impacts of oil spills on the ecosystems of the ocean or the environment of the sea surface may be very serious and unexpected. The conventional methods for the treatment of oil spills are skimming, oil booms, oil inhalations, and oil recovery. However, the emergency and large-scale treatments of oil spills generally have a high unit price and great workforce is required. The small amounts or low concentration of oil spills in the harbor may need an economically attractive method. Chemical methods invariably result in significant secondary pollution. Furthermore, chemical approaches will be ineffective unless the chemical substances are well dispersed. Apart from these conventional methods, researchers also explored bioremediation treatment and it was able to overcome some of the drawbacks of the other two methods, but it cannot be recycled due to the lower survival capacity of microbes against oil contaminants. In recent years, photocatalytic oxidation technology has emerged as a new technology for environmental pollution treatment because of its advantages of low energy consumption, no secondary pollution, and sustainability [30]. However, the existing methods that degrade oil by photocatalytic techniques are still limited.

TiO_2 has been widely used in the photocatalytic degradation of toxic organic pollutants. Using photocatalysts such as TiO_2 and UV-A (330−430 nm) light from the Sun results in the complete oxidation of oil spills and hydrocarbons into H_2O and CO_2 on the surface of the water. Photocatalytic degradation of toluene (70%) and 1-decene (25%) could be photocatalyzed on P25 (TiO_2) and T805 (Degussa TiO_2). T805 has a greater efficiency for photocatalytic degradation of toluene and dodecane in seawater than P25 by about two-fold. Ziolli and Jardim have reported that 90% of the oil in the seawater was photocatalytically degraded. Photocatalytic degradation of polycyclic aromatic hydrocarbons in the oil affected by TiO_2 thin films was also studied by gas chromatography-mass spectrometry. Generally, TiO_2 can be effectively excited under UV light [31].

One study conducted by Tetteh et al. reported that TiO_2 (80% anatase and 20% rutile) was able to degrade phenol and soap oil and grease (SOG) found in a local South African oil refinery wastewater in 90 min of UV light irradiation [32]. The percentage removal of phenol and SOG was found to be 76% and 88%, respectively. Moreover, the predicted models developed results showing reasonable agreement with the experimental data which confirm the adaptability of the models.

7.9 Photocatalytic paints

Photocatalytic paints use light energy to neutralize and control environmental pollution. Although mineral paints already contain environmentally friendly and sustainable materials, TiO_2, as a catalyst that allows the photocatalytic reaction, is a good choice. The catalyst is not used up during the reaction and continues to remediate the environment till the life of the paint. The photocatalytic reaction converts NO_x, SO_x, and other harmful pollutants including formaldehyde and acetaldehyde into harmless nitrates and respective end products. The photocatalytic reaction helps to break down organic pollutants and contaminants into harmless and mineralized byproducts, keeping the surface clean. TiO_2 used in conventional paints can break down the organic paint itself, reducing the lifespan of the paints.

Super-hydrophilic surfaces achieve a self-cleaning effect by retaining a thin film of water on the surface which prevents dust from adhering to the surface. This strategy can be combined with photocatalysis owing to the super-hydrophilic nature of photocatalytic TiO_2. The formation of highly reactive free radicals such as $^{\bullet}OH$ and $O_2^{\bullet -}$ is catalyzed by the photocatalyst as it absorbs UV light. The free radicals have an extremely high oxidation potential and can decompose organic pollutants which have immobilized on the surface.

Introducing such materials into an organic paint system is very difficult because the strongly oxidizing $^{\bullet}OH$ and $O_2^{\bullet -}$ free radicals, generated as a result of UV exposure, can decompose the organic resin in the paints.

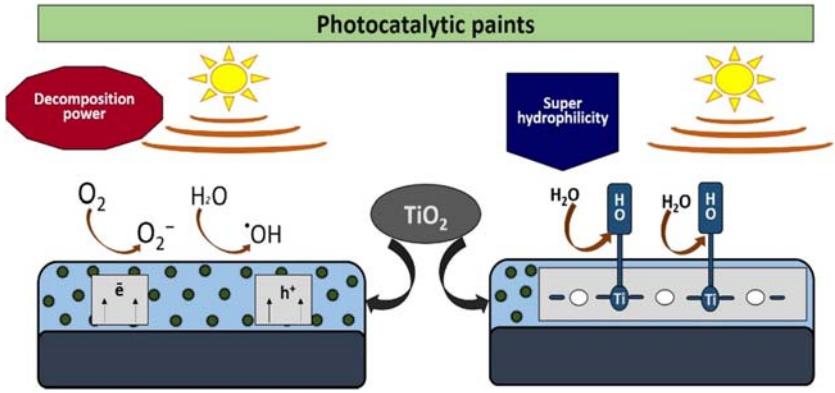

FIGURE 7.7 Reaction mechanism showing photocatalytic self-cleaning by paint.

The destructive effect of TiO_2 pigments on organic binders has for a long time been known to the paint industry that is why most TiO_2 pigments today are stabilized to reduce their photoactivity.

Photocatalytic paints have mostly been formulated with anatase TiO_2 NPs (Fig. 7.7) due to the high photoactivity of such particles. However, these attempts have not been sufficiently successful owing to the rapid degradation of the binder. Photocatalytic paints are a very interesting option for paints intended for wood protection. In addition to making a surface self-cleaning, the $^{\bullet}OH$ and $O_2^{\bullet-}$ free radicals can potentially keep the surface free of microorganisms. Guidelines about the use of toxic antimicrobial chemicals are continuously becoming stricter which limits the application of currently used solutions and makes it more expensive and difficult to introduce new chemicals. Photocatalysis is, therefore, an attractive strategy for keeping a surface free of dust and microorganisms because TiO_2 is nontoxic and has no environmental limitations. Furthermore, the effect is long-lasting as TiO_2 only functions as a photocatalyst and is not used up in the reaction. It is necessary to develop a more robust photocatalytic organic paint where the effect of the photocatalyst on the binder is decreased [33,34].

7.9.1 Mechanism behind photocatalytic paints

Photocatalytic paints have been marketed and declared to be superior to any other regular paint due to their various characteristics and advantages. Their ability to decompose pollutants and dust when in contact with the coated surface can be explained by photocatalysis and proposed mechanisms (Fig. 7.7). Basically, when light irradiates and get absorbs onto the photocatalyst particles, the electrons get excited and move from VB to CB, leaving behind holes. The hole and electron act as charge carriers. Free radicals, $^{\bullet}OH$ and $O_2^{\bullet-}$ are generated by the reactions of water and oxygen molecules on the

photocatalyst surface. These radicals are responsible for the oxidative decomposition of the pollutants. The reaction mechanism of nano TiO_2 in photocatalytic paints is shown in the following chemical reactions [34]:

$$TiO_2 + hv(UV) \rightarrow TiO_2(e^-_{CB} + h^+_{VB})$$

$$TiO_2\left(h^+_{VB}\right) + H_2O \rightarrow TiO_2 + H^+ + OH^-$$

$$TiO_2(h^+_{VB}) + OH^- \rightarrow TiO_2 + OH^\bullet$$

$$TiO_2(e^-_{CB}) + O_2 \rightarrow TiO_2 + O_2^{\bullet -}$$

$$O_2^{\bullet -} + H^+ \rightarrow HO_2^\bullet$$

$$\text{Pollutants} + OH^\bullet \rightarrow \text{Degradation products}$$

$$\text{Pollutants} + h^+_{VB} \rightarrow \text{Oxidation products}$$

$$\text{Pollutant} + e^-_{CB} \rightarrow \text{Reduction products}$$

Acetaldehyde is a recurrent VOC present in indoor environments that can also be formed during combustion processes and emitted by different sources in homes like building materials, hardwood, plywood, laminate floorings, adhesives, paints, and varnishes. It can cause eye, skin, and respiratory tract irritation, and it is classified as a probable carcinogen. Because of their negative effects, these outdoor and indoor air pollutants must be removed before their concentrations reach harmful levels. Acetaldehyde undergoes photocatalytic oxidation by forming a sequence of stable intermediates as follows:

$$\text{Acetaldehyde} \rightarrow \text{Formaldehyde} \rightarrow \text{Formic acid} \rightarrow \text{Carbon dioxide}$$

The nitrogen oxides (NO_x) include nitric oxide (NO) and nitrogen dioxide (NO_2) among other highly reactive gases. They are mainly formed in urban areas through combustion processes in vehicles, power plants, and other industrial sources and can cause photochemical smog and acid rain, which contribute to global warming. In the case of NO_x decomposition on a photocatalytic paint embedded with TiO_2 NPs, the reasonable reaction sequence and intermediates formed are as follows:

$$NO \rightarrow NO_2 \rightarrow HNO_3$$

To support the above reaction sequence, Han et al. listed the photocatalytic reaction equation of the oxidation of NO on the TiO_2 surface as shown in the following equation. Equation ($2HNO_3$ + NO) is the reaction where HNO_3 accumulates onto the surface of TiO_2. The issue of accumulation has been tackled commercially by the addition of an acid scavenger ($CaCO_3$ or NaOH) into the paint formula.

$$4NO + O_2 + 2H_2O \xrightarrow{hv,TiO_2} 4HNO_2$$

$$4HNO_2 + O_2 \xrightarrow{hv,TiO_2} 4NO_2 + 2H_2O$$

$$2H_2O + 4NO_2 + O_2 \xrightarrow{hv,TiO_2} 4HNO_3$$

$$2HNO_3 + NO \xrightarrow{hv,TiO_2} 3NO_2 + H_2O$$

$$2NO + O_2 \xrightarrow{hv,TiO_2} 2NO_2$$

Other species produced in this photocatalytic reaction are hydrogen peroxide (H_2O_2) and nitrous acid (HONO), which can have certain health implications. H_2O_2 is a strong oxidizing agent that aids in converting sulfur dioxide (SO_2) to particulate sulfate. According to Gandolfo et al., the formation of HONO and NO and the species yield are dependent on pigment volume concentration (PVC) and the porosity of the paint. They have found that the low porosity of paint led to the formation of HONO, whereas high porosity led to the formation of NO. Thus, the proposed mechanism for the formation of HONO and NO has been shown in the following equations:

$$NO_2 + O_2^- \left(+ H^+\right) \longrightarrow NO_2^- (HONO) + O_2$$

$$NO_2(ads) \xrightarrow{hv,TiO_2} NO(ads) + O$$

$$NO(ads) + OH(ads) \xrightarrow{TiO_2} HONO$$

Thus, an in-depth understanding of the mechanisms is required in identifying the possible byproducts formed from the photocatalytic reactions and minimizing the implications of these species on human health and the environment. This field of study is still new to conclude the exact mechanism behind these reactions as it requires proper and deeper investigation and understanding [35–37].

7.9.2 Factors affecting the efficiency of photocatalytic paints

From the literature review of photocatalytic paints and coatings, it can be seen that very wide results on the contaminant degradation and selectivity were obtained. This large variability in results comes principally from the employment of different photoreactor configurations and sizes, operating conditions, tested pollutants, photocatalytic materials, and paint compositions. Thus, the direct comparison between all these systems is not appropriate, at least by evaluating only the pollutant conversion.

Several factors are responsible for the photocatalytic degradation of pollutants by photocatalytic paints (as illustrated in Fig. 7.8), which include the photocatalytic materials added, porosity, quantity, size, morphology, PVC, and paint formulation.

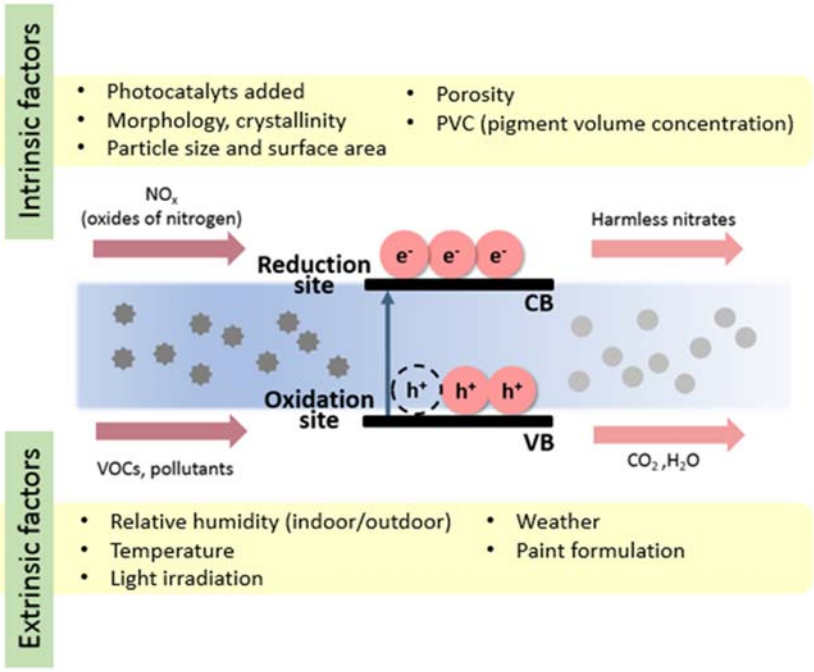

FIGURE 7.8 Intrinsic and extrinsic factors affect the photocatalytic performance of the paint.

Other parameters or factors that need to be examined are the operating conditions, such as light intensity, amount and type of pollutants present, surface temperature, humidity, and artificial weathering.

For example, two sets of experiments were set up to investigate the effect of UV light and visible light irradiation on MO dye against a plain concrete block and a concrete block coated with CdS/TiO_2 [38]. It was found that the coated concrete block was able to degrade MO dye under UV light irradiation. The reason is that under visible light irradiation, the temperature was increased up to 60°C due to the heat coming off from the visible light. This caused undissolved MO solid to dissociate making the absorbance of MO higher with time.

7.10 Photocatalytic antibacterial disinfection

Photocatalysis has recently emerged as an effective green solution for antimicrobial disinfection applications. Photocatalytic disinfection has been observed to be efficient in the deactivation of numerous varieties of organisms mainly microorganisms. Several gram-positive and gram-negative bacterial strains, such as *Escherichia coli*, *Staphylococcus aureus*, and *Streptococcus pneumonia*, have been studied. Similarly, fungal strains, such as *Aspergillus niger*,

Fusarium graminearum, algae (*Tetraselmis suecica*, *Amphidinium carterae*, etc.), and viral strains have also been examined in this decade. In recent years, it has been explored that photocatalytic antibacterial agents have no drug resistance and side effects due to their rapid and efficient bactericidal efficacy. They are becoming one of the most optimistic replacements for antibiotics for dealing with bacterial diseases and water pollution caused by certain pathogens. Photocatalysis has unique advantages in the antibacterial field and its controllability plays a unique role [25,26].

Photocatalyst not only kills the bacterial cells but also decomposes and mineralizes the bacterial cells. TiO_2 as a photocatalyst is more effective than any other antibacterial agent because the photocatalytic reaction works even when the cells are covering the surface while the bacteria are actively propagating. The endotoxins produced at the death of cells are also expected to be decomposed and mineralized by photocatalytic action. TiO_2 does not deteriorate and it shows a long-term antibacterial effect. Mostly, disinfections by TiO_2 are 1.5 times higher than ozone and 3 times greater than chlorine. TiO_2 as a nano photocatalyst has strong oxidation effects on single-celled organisms that include all bacteria and fungus. The very strong oxidizing power of TiO_2 can destroy the cell membrane of bacteria, (Fig. 7.4) causing leakage of the cytoplasm, which inhibits the activities of bacteria and ultimately results in the death, decomposition, and mineralization of the bacteria.

The antibacterial activities of nanoparticles (pigments) are found inversely proportional to particle size and relate to their intrinsic ability to generate active carriers giving rise to active surface species. Pigments calcined at higher temperatures, consequently with fewer structural defects, are more active because sometimes defects act as recombination centers for the $\bar{e}$s and h^+s. Hence, the antibacterial efficiency of TiO_2 is not determined by surface area but by the ability to generate active carrier species resulting in the formation of effective chemical species such as peroxides (hydrogen peroxide). This is not surprising because of the size of bacteria relative to the pigments—the majority of the surface area offered by a pigment is sterically unavailable to the bacterial cells.

In terms of future building developments, especially in the medical world, this would offer significant advantages for eliminating the potential of methicillin-resistant *S. aureus* (MRSA). Current building work pilot trials show high efficiency in reducing fungal growth on walls, windows, and roofing structures [39,40].

In brief, the mechanisms of antibacterial activity can be summarized as follows and are illustrated in Fig. 7.9:

- Generation of ROS
- Disruption of the bacterial cell membrane
- Penetration of the bacterial cell membrane
- Induction of intracellular antibacterial effects, including interactions with DNA and proteins

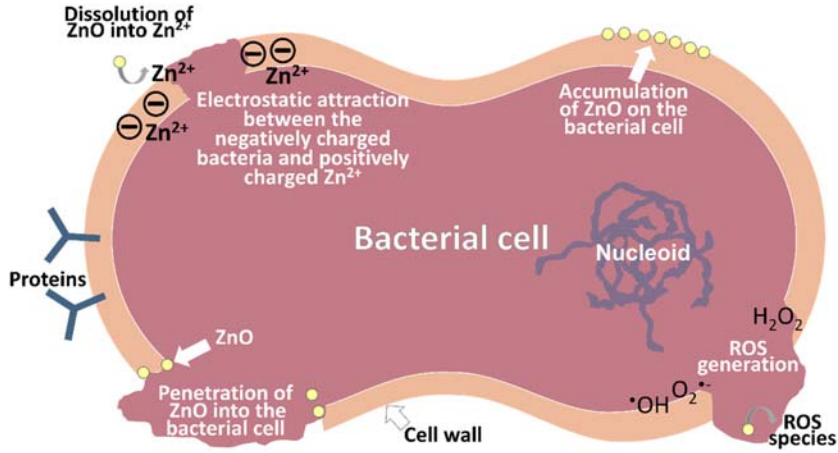

FIGURE 7.9 Schematic diagram of photocatalytic antibacterial mechanisms of ZnO under irradiation of light.

For example, Happy et al. reported that ZnO at a concentration of 50 μg/mL demonstrated potential inhibition of bacterial growth after 10 h of incubation. This may be due to the positively charged ZnO interacting with the negatively charged bacterial membrane leading to a loss in membrane integrity and intracellular protein leakage [41]. Steffy et al. reported that *Aristolochia indica* synthesized ZnO exhibited strong bactericidal properties against clinically isolated multidrug-resistant strains isolated from diabetic foot ulcers [42]. The authors also conducted a protein leakage analysis and found out that the bactericidal effects of green synthesized ZnO are due to cell membrane damage. This led to the outflow of protoplasmic inclusions and the amount of protein leaked from the bacterial cells depended on the concentration and time of contact of ZnO. Previous studies have shown that the effect of ZnO varies for the microorganism tested/species, size, and concentration. The size of synthesized ZnO also plays a vital role in the antibacterial activity because the cellular membranes in the bacterial cells contain nanosized pores as reported by Babu et al. [43]. Apart from that the antibacterial efficiency of ZnO is directly related to its shape, surface-to-volume ratio, surface charge, and the number of oxygen vacancy sites.

7.11 Photocatalytic chemical synthesis and/or conversions

Artificial photosynthetic systems are based on photosensitization or photocatalysts that facilitate light-induced charge separation. Separated charges ($\bar{e}$-h^+) are involved in the reduction and oxidation process. Photocatalytic systems can be based on molecular materials, such as natural photosynthesis,

or crystalline solids, such as semiconductor-based heterogeneous photocatalysis. The later type frequently offers higher stability and photostability as well as an easy separation of products. In heterogeneous, semiconductor-based photocatalytic systems, several syntheses of organic compounds have been reported [44,45].

Synthesis and/or conversions of organic compounds in the semiconductor-based heterogeneous photocatalysis results from redox reactions initiated by electrons in the CB and h^+ in the VB. However, mechanisms of the reactions may involve a direct ē transfer between an organic substrate and the photocatalyst, or an indirect ē transfer, encompassing activation (oxidation or reduction) of small molecules as initial steps of the overall reaction shown in Fig. 7.10.

H_2O and OH^- anions are the main small molecules being oxidized in these processes. The formed hydroxyl radicals ($^{\bullet}OH$) are responsible for the consecutive oxidation of organic substrates. $^{\bullet}OH$ is a very reactive and strong oxidant which usually shows a low selectivity in oxidation reactions. Furthermore, $^{\bullet}OH$-free radicals may lead to complete oxidation of organics to CO_2, H_2O, and simple inorganic anions. Formation of $^{\bullet}OH$-free radicals takes place mainly at metal oxides (TiO_2, ZnO, etc.). The difference between

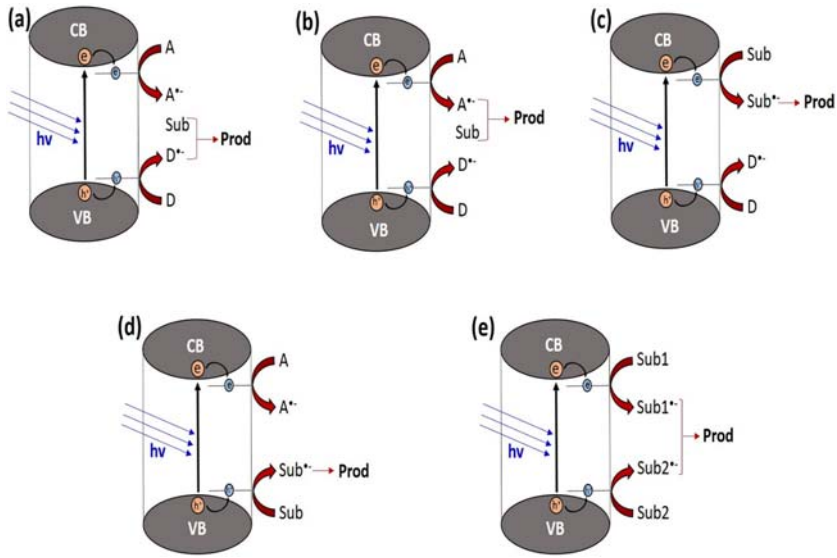

FIGURE 7.10 Primary redox reactions leading to photocatalytic synthesis of organic compounds (Prod) from substrates (Sub, Sub1, Sub2) and small molecules acting as electron donors (D) or acceptors (A): (a, b) reaction involving reduction and oxidation of two small molecules (A, D); (c) reaction involving reduction of an organic substrate (Sub) and oxidation of a small molecule (D); (d) reaction involving reduction of a small molecule (A) and oxidation of an organic substrate (Sub); and (e) reaction involving reduction and oxidation of organic substrates (Sub1, Sub2).

the direct oxidation of an organic molecule by photogenerated holes and its indirect oxidation involving photogenerated hydroxyl radicals may be quite difficult.

Dioxygen, CO_2, H_2O, and H_2O_2 are major small molecules undergoing reduction reactions with electrons from the CB. Superoxide ($O_2^{\bullet -}$), $CO_2^{\bullet -}$, and H_2O are the primary products of these processes, respectively. Also, inorganic ions may act as electron acceptors.

Two decades ago, Kisch proposed a classification of photocatalytic reactions based on the role of primary oxidation and reduction reactions in the formation of products. According to this classification, semiconductor photocatalysts of type A encompass the formation of two different products as a result of reactions involving photogenerated ēs and h^+s as shown in Fig. 7.10A–D. As a result of semiconductor photocatalysts of type B, only one product is formed, as shown in Fig. 7.10E. In this case, products of primary redox reactions (free radicals) couple together, yielding a new stable molecule, as depicted in Fig. 7.10E. This is because photocatalysts of type B require the coupling of two radicals and their lifetimes strongly affect the overall efficiency of the reaction [44].

Photocatalytic organic synthesis using metal oxides is well-known and in the progress. Choi et al. recently reported the photocatalytic synthesis of 2-hydroxyterephthalic acid (HTPA) using terephthalic acid (TPA). In this synthesis, HTPA was treated with novel photocatalysts ZnO and ZnS under visible light irradiation for 6 h, which in situ generated $^{\bullet}OH$ radicals and reacted with HTPA which led to the formation of TPA [45].

Another study was done by Almquist et al. on the photocatalytic oxidation of cyclohexane on TiO_2 in various solvents to determine the effect of the solvent media [46,47]. Selectivity to cyclohexanol and cyclohexanone was found to be affected by the polarity of the solvents. In polar solvents, cyclohexanol was less strongly adsorbed on TiO_2 due to the competition with the solvent. Hence, higher selectivity was observed. In nonpolar solvents, the selectivity was low due to the adsorbed cyclohexanol on the TiO_2 being mineralized to CO_2.

The photocatalytic synthesis of phenol was conducted by Park et al. using TiO_2 NPs. The surface of TiO_2 was modified using Fe^{3+}, H_2O_2, $Fe^{3+} + H_2O_2$, or polyoxometalate [48]. The surface modifications were found to enhance the phenol production yield and selectivity in TiO_2 suspensions. The photocatalytic oxidation of alcohols by TiO_2 has been extensively studied. For example, Wang et al. have reported the photocatalytic oxidation pathway of methanol from its aqueous solution [49]. From the study, water is the dominant surface species and the oxidation pathway is through the generated $\cdot OH$ radicals. If the amount of water is lower than the critical ratio (in which the critical molar ratio between water and methanol was found to be 300), the direct oxidation of methanol by the photogenerated holes will be the predominant process at the TiO_2 surface.

Following is the photocatalytic pathway for oxidation of alcohol:

$$TiO_2 \rightarrow TiO_2\left(h^+ + \bar{e}\right)$$

$$TiO_2\left(h^+\right) + OH^- \rightarrow TiO_2 + {}^{\bullet}OH$$

$$TiO_2\left(h^+\right) + H_2O \rightarrow TiO_2 + {}^{\bullet}OH + {H_{aq}}^+$$

$${}^{\bullet}OH + RCH_2OH \rightarrow R \cdot CHOH + H_2O$$

$$TiO_2\left(h^+\right) + RCH_2OH \rightarrow TiO_2 + R \cdot CHOH + H^+$$

$$R \cdot CHOH + O_2 \rightarrow RCHO + HO_2^{\bullet}$$

7.12 Summary

In this chapter, various semiconducting photocatalytic applications, such as energy production, pollutants degradation, removal of heavy metals, water purification, self-cleaning glasses, air purification, removal of oil spills, photocatalytic paints, and photocatalytic chemical synthesis and/or conversions have been discussed. Energy and environment-related photocatalytic applications have attracted much attention because these applications are green and advantageous to human health and the environment. The photocatalytic semiconductors have been growing very fast and attracting the attention of researchers worldwide. Semiconductors have found application in a variety of fields due to their wide availability, biocompatibility, low cost and nontoxicity, and high chemical stability. There are many fields of applications including air purification, water purification, decontamination, antibacterial, toothpaste, UV protection, photocatalysis, sensing, and paint application. Some of the selected photocatalytic applications have been discussed.

References

[1] M.M. Khan, D. Pradhan, Y. Sohn, Nanocomposites for Visible Light-induced Photocatalysis, Springer International Publishing, Cham, 2017. Available from: https://doi.org/10.1007/978-3-319-62446-4.

[2] M.M. Khan (Ed.), Chalcogenide-Based Nanomaterials as Photocatalysts, Elsevier, 2021. Available from: https://doi.org/10.1016/C2019-0-01819-5.

[3] M.M. Khan, S.F. Adil, A. Al-Mayouf, Metal oxides as photocatalysts, Journal of Saudi Chemical Society 19 (2015) 462–464. Available from: https://doi.org/10.1016/j.jscs.2015.04.003.

[4] F. Fresno, R. Portela, S. Suárez, J.M. Coronado, Photocatalytic materials: recent achievements and near future trends, Journal of Materials Chemistry A 2 (2014) 2863–2884. Available from: https://doi.org/10.1039/c3ta13793g.

[5] M.M. Khan, Metal oxide powder photocatalysts, Multifunctional Photocatalytic Materials for Energy (2018) 5–18. Available from: https://doi.org/10.1016/B978-0-08-101977-1.00002-8.

[6] M.M. Khan, Principles and mechanisms of photocatalysis, Photocatalytic Systems by Design, Elsevier, 2021, pp. 1–22. Available from: https://doi.org/10.1016/B978-0-12-820532-7.00008-4.

[7] A. Rahman, M.M. Khan, Chalcogenides as photocatalysts, New Journal of Chemistry. 45 (2021) 19622–19635. Available from: https://doi.org/10.1039/D1NJ04346C.

[8] A. Kumar, G. Pandey, A review on the factors affecting the photocatalytic degradation of hazardous materials, Material Science & Engineering International Journal 1 (2017). Available from: https://doi.org/10.15406/MSEIJ.2017.01.00018.

[9] X. Chen, J. Zhao, G. Li, D. Zhang, H. Li, Recent advances in photocatalytic renewable energy production, Energy Materials. (2022). Available from: https://doi.org/10.20517/energymater.2021.24.

[10] K. Maeda, K. Domen, Photocatalytic water splitting: recent progress and future challenges, The Journal of Physical Chemistry Letters 1 (2010) 2655–2661. Available from: https://doi.org/10.1021/jz1007966.

[11] A.A. Ismail, D.W. Bahnemann, Photochemical splitting of water for hydrogen production by photocatalysis: a review, Solar Energy Materials and Solar Cells 128 (2014) 85–101. Available from: https://doi.org/10.1016/j.solmat.2014.04.037.

[12] A. Hernández-Ramírez, Photocatalytic Semiconductors, Springer International Publishing, Cham, 2015. Available from: https://doi.org/10.1007/978-3-319-10999-2.

[13] N.T. Hanh, N. le Minh Tri, D. van Thuan, M.H. Thanh Tung, T.-D. Pham, T.D. Minh, et al., Monocrotophos pesticide effectively removed by novel visible light driven Cu doped ZnO photocatalyst, Journal of Photochemistry and Photobiology A: Chemistry 382 (2019) 111923. Available from: https://doi.org/10.1016/j.jphotochem.2019.111923.

[14] M.M. Khan, S.A. Ansari, D. Pradhan, M.O. Ansari, D.H. Han, J. Lee, et al., Band gap engineered TiO_2 nanoparticles for visible light induced photoelectrochemical and photocatalytic studies, Journal of Materials Chemistry A 2 (2014) 637–644. Available from: https://doi.org/10.1039/C3TA14052K.

[15] M.M. Khan, S.A. Ansari, M.I. Amal, J. Lee, M.H. Cho, Highly visible light active Ag@TiO_2 nanocomposites synthesized using an electrochemically active biofilm: a novel biogenic approach, Nanoscale 5 (2013) 4427. Available from: https://doi.org/10.1039/c3nr00613a.

[16] N. Sidana, H. Kaur, P. Devi, Organic linkers for colorimetric detection of inorganic water pollutants, Inorganic Pollutants in Water, Elsevier, 2020, pp. 135–152. Available from: https://doi.org/10.1016/b978-0-12-818965-8.00008-1.

[17] A. Kumar, I.J. Schreiter, A. Wefer-Roehl, L. Tsechansky, C. Schüth, E.R. Graber, Production and utilization of biochar from organic wastes for pollutant control on contaminated sites, Environmental Materials and Waste: Resource Recovery and Pollution Prevention, Elsevier Inc., 2016, pp. 91–116. Available from: https://doi.org/10.1016/B978-0-12-803837-6.00005-6.

[18] S. Singh, K.L. Wasewar, S.K. Kansal, Low-cost adsorbents for removal of inorganic impurities from wastewater, Inorganic Pollutants in Water, Elsevier, 2020, pp. 173–203. Available from: https://doi.org/10.1016/b978-0-12-818965-8.00010-x.

[19] N. Bombuwala Dewage, A.S. Liyanage, C.U. Pittman, D. Mohan, T. Mlsna, Fast nitrate and fluoride adsorption and magnetic separation from water on α-Fe_2O_3 and Fe_3O_4 dispersed on Douglas fir biochar, Bioresource Technology 263 (2018) 258–265. Available from: https://doi.org/10.1016/j.biortech.2018.05.001.

[20] A. Banerjee, Groundwater fluoride contamination: a reappraisal, Geoscience Frontiers 6 (2015) 277–284. Available from: https://doi.org/10.1016/j.gsf.2014.03.003.

[21] R. Singh, N. Gautam, A. Mishra, R. Gupta, Heavy metals and living systems: an overview, Indian Journal of Pharmacology 43 (2011) 246. Available from: https://doi.org/10.4103/0253-7613.81505.

[22] F.E. Bortot Coelho, V.M. Candelario, E.M.R. Araújo, T.L.S. Miranda, G. Magnacca, Photocatalytic reduction of Cr(VI) in the presence of humic acid using immobilized Ce−ZrO_2 under visible light, Nanomaterials 10 (2020) 779. Available from: https://doi.org/10.3390/nano10040779.

[23] L.A. Betancourt-Buitrago, O.E. Ossa-Echeverry, J.C. Rodriguez-Vallejo, J.M. Barraza, N. Marriaga, F. Machuca-Martínez, Anoxic photocatalytic treatment of synthetic mining wastewater using TiO_2 and scavengers for complexed cyanide recovery, Photochemical & Photobiological Sciences 18 (2019) 853−862. Available from: https://doi.org/10.1039/C8PP00281A.

[24] M. Pawar, S. Topcu Sendoğdular, P. Gouma, A. Brief, Overview of TiO_2 photocatalyst for organic dye remediation: case study of reaction mechanisms involved in Ce-TiO_2 photocatalysts system, Journal of Nanomaterials 2018 (2018) 1−13. Available from: https://doi.org/10.1155/2018/5953609.

[25] S.N. Naidi, M.H. Harunsani, A.L. Tan, M.M. Khan, Green-synthesized CeO_2 nanoparticles for photocatalytic, antimicrobial, antioxidant and cytotoxicity activities, Journal of Materials Chemistry B 9 (2021) 5599−5620. Available from: https://doi.org/10.1039/D1TB00248A.

[26] A. Rahman, M.H. Harunsani, A.L. Tan, M.M. Khan, Zinc oxide and zinc oxide-based nanostructures: biogenic and phytogenic synthesis, properties and applications, Bioprocess and Biosystems Engineering 44 (2021) 1333−1372. Available from: https://doi.org/10.1007/s00449-021-02530-w.

[27] C. Belver, J. Bedia, A. Gómez-Avilés, M. Peñas-Garzón, J.J. Rodriguez, Semiconductor photocatalysis for water purification, Nanoscale Materials in Water Purification, Elsevier, 2019, pp. 581−651. Available from: https://doi.org/10.1016/B978-0-12-813926-4.00028-8.

[28] A.J. Haider, Z.N. Jameel, I.H.M. Al-Hussaini, Review on: titanium dioxide applications, Energy Procedia 157 (2019) 17−29. Available from: https://doi.org/10.1016/j.egypro.2018.11.159.

[29] M.R. Hoffmann, S.T. Martin, W. Choi, D.W. Bahnemann, Environmental applications of semiconductor photocatalysis, Chemical Reviews 95 (1995) 69−96. Available from: https://doi.org/10.1021/cr00033a004.

[30] Y. Zhou, M. Elchalakani, P. Du, C. Sun, Cleaning up oil pollution in the ocean with photocatalytic concrete marine structures, Journal of Cleaner Production 329 (2021) 129636. Available from: https://doi.org/10.1016/j.jclepro.2021.129636.

[31] R.J. Berry, M.R. Mueller, Photocatalytic decomposition of crude oil slicks using TiO_2 on a floating substrate, Microchemical Journal 50 (1994) 28−32. Available from: https://doi.org/10.1006/mchj.1994.1054.

[32] E.K. Tetteh, S. Rathilal, D.B. Naidoo, Photocatalytic degradation of oily waste and phenol from a local South Africa oil refinery wastewater using response methodology, Scientific Reports 10 (2020) 8850. Available from: https://doi.org/10.1038/s41598-020-65480-5.

[33] A. Galenda, F. Visentin, R. Gerbasi, M. Favaro, A. Bernardi, N. el Habra, Evaluation of self-cleaning photocatalytic paints: are they effective under actual indoor lighting systems? Applied Catalysis B: Environmental 232 (2018) 194−204. Available from: https://doi.org/10.1016/j.apcatb.2018.03.052.

[34] F. Salvadores, M. Reli, O.M. Alfano, K. Kočí, M. de los M. Ballari, Efficiencies evaluation of photocatalytic paints under indoor and outdoor air conditions, Frontiers in Chemistry 8 (2020). Available from: https://doi.org/10.3389/fchem.2020.551710.

[35] A. Hashemi Monfared, M. Jamshidi, Synthesis of polyaniline/titanium dioxide nanocomposite (PAni/TiO_2) and its application as photocatalyst in acrylic pseudo paint for benzene removal under UV/VIS lights, Progress in Organic Coatings 136 (2019) 105257. Available from: https://doi.org/10.1016/j.porgcoat.2019.105257.

[36] R. Han, R. Andrews, C. O'Rourke, S. Hodgen, A. Mills, Photocatalytic air purification: effect of HNO_3 accumulation on NO_x and VOC removal, Catalysis Today 380 (2021) 105−113. Available from: https://doi.org/10.1016/j.cattod.2021.04.017.

[37] A. Gandolfo, V. Bartolomei, D. Truffier-Boutry, B. Temime-Roussel, G. Brochard, V. Bergé, et al., The impact of photocatalytic paint porosity on indoor NO_x and HONO levels, Physical Chemistry Chemical Physics 22 (2020) 589−598. Available from: https://doi.org/10.1039/C9CP05477D.

[38] K. He, Y. Chen, M. Mei, Study on influencing factors of photocatalytic performance of CdS/TiO_2 nanocomposite concrete, Nanotechnology Reviews 9 (2020) 1160−1169. Available from: https://doi.org/10.1515/ntrev-2020-0074.

[39] J.M. Coronado, F. Fresno, M.D. Hernández-Alonso, R. Portela, Design of Advanced Photocatalytic Materials for Energy and Environmental Applications, Springer London, London, 2013. Available from: https://doi.org/10.1007/978-1-4471-5061-9.

[40] Z. Zhou, B. Li, X. Liu, Z. Li, S. Zhu, Y. Liang, et al., Recent progress in photocatalytic antibacterial, ACS Applied Bio Materials 4 (2021) 3909−3936. Available from: https://doi.org/10.1021/acsabm.0c01335.

[41] A. Happy, M. Soumya, S. Venkat Kumar, S. Rajeshkumar, R.D. Sheba, T. Lakshmi, et al., Phyto-assisted synthesis of zinc oxide nanoparticles using *Cassia alata* and its antibacterial activity against *Escherichia coli*, Biochemistry and Biophysics Reports 17 (2019) 208−211. Available from: https://doi.org/10.1016/j.bbrep.2019.01.002.

[42] K. Steffy, G. Shanthi, A.S. Maroky, S. Selvakumar, Enhanced antibacterial effects of green synthesized ZnO NPs using *Aristolochia indica* against multi-drug resistant bacterial pathogens from Diabetic Foot Ulcer, Journal of Infection and Public Health 11 (2018) 463−471. Available from: https://doi.org/10.1016/j.jiph.2017.10.006.

[43] A.T. Babu, R. Antony, Green synthesis of silver doped nano metal oxides of zinc & copper for antibacterial properties, adsorption, catalytic hydrogenation & photodegradation of aromatics, Journal of Environmental Chemical Engineering 7 (2019) 102840. Available from: https://doi.org/10.1016/j.jece.2018.102840.

[44] M. Kobielusz, P. Mikrut, W. Macyk, Photocatalytic synthesis of chemicals, Advances in Inorganic Chemistry, Academic Press Inc., 2018, pp. 93−144. Available from: https://doi.org/10.1016/bs.adioch.2018.05.002.

[45] Y.I. Choi, S. Lee, S.K. Kim, Y.-I. Kim, D.W. Cho, M.M. Khan, et al., Fabrication of ZnO, ZnS, Ag-ZnS, and Au-ZnS microspheres for photocatalytic activities, CO oxidation and 2-hydroxyterephthalic acid synthesis, Journal of Alloys and Compounds 675 (2016) 46−56. Available from: https://doi.org/10.1016/j.jallcom.2016.03.070.

[46] D. Friedmann, A. Hakki, H. Kim, W. Choi, D. Bahnemann, Heterogeneous photocatalytic organic synthesis: state-of-the-art and future perspectives, Green Chemistry 18 (2016) 5391−5411. Available from: https://doi.org/10.1039/c6gc01582d.

[47] C.B. Almquist, P. Biswas, The photo-oxidation of cyclohexane on titanium dioxide: an investigation of competitive adsorption and its effects on product formation and selectivity, 2001.

[48] H. Park, W. Choi, Photocatalytic conversion of benzene to phenol using modified TiO_2 and polyoxometalates, Catalysis Today (2005) 291−297. Available from: https://doi.org/10.1016/j.cattod.2005.03.014.

[49] C. Wang, H. Groenzin, M.J. Shultz, Direct observation of competitive adsorption between methanol and water on TiO_2: an in situ sum-frequency generation study, Journal of the American Chemical Society 126 (2004) 8094−8095. Available from: https://doi.org/10.1021/ja048165l.

Chapter 8

Photocatalysis: laboratory to market

Mohammad Mansoob Khan

8.1 Introduction

Photocatalysis is one of the effective and promising methods for solving numerous current environmental and energy-related issues [1]. Photocatalysis is a chemical reaction that takes place in the presence of a photocatalyst and suitable light. In other words, it is a reaction that uses light to generate a pair of excited electrons and positive holes to induce redox reactions as the first step with both positive and negative Gibbs-energy change. Photocatalysis promises a solution to challenges associated with the intermittent nature of sunlight that is considered a renewable and ultimate energy source for power and energy-related activities on the Earth. Other examples are water splitting, hydrogen production, water treatment and disinfection, removal of pollutants from contaminated water and air, photocatalytic tiles, photocatalytic paints, self-cleaning window panels based on photoactive materials, and many more issues [1]. Hence, there is a need to understand the fundamental concepts of photocatalysis in a simple and applied way.

A photocatalyst is a material that harvests light to bring it to a higher energy level and provides such energy to a reacting substance to make a chemical reaction take place. An appropriate photocatalyst should be non-toxic, not expensive, and highly effective to utilize light [2]. The overall catalytic performance of a photocatalyst usually depends on three factors: light harvesting, photogenerated charge carriers' separation, transfer, and surface reaction. On the one hand, light absorption is closely related to the energy band structure of photocatalysts, however, most of the existing stable photocatalysts have a wide bandgap, indicating a narrow light absorption range, which restricts the photocatalytic efficiency. On the other hand, only the photogenerated electrons and holes that migrate to the photocatalyst surface can participate in the photocatalytic reaction, whereas most of them are readily recombined in the bulk phase of the photocatalysts. In addition, some photogenerated electrons or holes may corrode the photocatalyst rather than participate in the target photocatalytic reaction.

Theoretical Concepts of Photocatalysis. DOI: https://doi.org/10.1016/B978-0-323-95191-3.00013-4

Pollutants from the persistent organic chemicals are present in wastewater from the rapid growth of industries and factories as well as from normal households and in landfill leachates. Most organic dyes are non-biodegradable, chemically stable, and carcinogenic which can harm human health as well as marine life. Therefore, it is very important to remove these dyes and photocatalysis is a promising method to do so. Hence, the application of photocatalysts can be a promising method for solving industrial wastewater issues and environmental pollution. To utilize solar energy effectively, semiconductor photocatalysts, especially visible light active photocatalysts, have been developed for the degradation of organic dye pollutants [3–6], inactivation of bacteria [7,8], photoelectrochemical conversion [9,10], and hydrogen production [11,12]. The advantages of visible light active photocatalysts are that they can utilize energy from the freely available abundant sunlight effectively, are inexpensive, and do not produce any harmful byproducts.

For example, in recent times, air pollution has become one of the world's major problems. Besides, air pollution also includes the pollutants found in indoor air. It has been found that indoor air has a high concentration of volatile organic compounds (VOCs). These pollutants can have harmful effects on human beings such as sick building syndrome, headaches, and many more [13]. A semiconductor as a photocatalyst shows a promising result in removing these harmful and toxic substances to improve indoor air quality [14]. A few advantages of these photocatalysts are as follows: light is used as energy, they can be made versatile by incorporating a dopant to the semiconductor to improve its characteristics based on the desired properties, and they also do not release any harmful toxins or toxic byproducts. This technology has the potential to mimic nature's ways to clean the environment by removing various types of pollutants found in the atmosphere [15].

Another example is photocatalytic dye degradation and removal which is a process that breaks down large dye molecules into smaller molecules and harmless byproducts (such as H_2O and CO_2) in the presence of light. In photocatalysis, the appropriate type and amount of light should be harvested or absorbed by the photocatalysts. Also, photocatalysis depends on the capability of the photocatalyst to harvest UV or visible light. Generally, there are four different steps involved in a photocatalytic reaction. First, the absorption of light (UV or visible), then the next step is the separation of electrons (e^-) and holes (h^+), followed by a redox reaction, and finally the desorption of byproducts from the surface of the photocatalysts. By illuminating photocatalysts with light energy equal to or greater than the band gap energy (E_g) level, the electrons in the valence band (VB) are excited to the conduction band (CB) thus creating charge carriers (e^- and h^+), consisting of electrons and holes, which can lead to oxidation and reduction reactions (as a primary reaction) [16–18]. The photogenerated electrons have a reduction capability whereas photogenerated holes have an oxidation capability. The photogenerated

electron-hole pairs react with some of the species in the dye solution (dissolved gases, water, etc.) and produce highly reactive free radicals such as hydroxyl ($^{\bullet}OH$), $OH_2^{\bullet}$, and superoxide ($O_2^{\bullet-}$). These radicals can then break down organic pollutants (via secondary reaction) and produce non-harmful byproducts such as H_2O and CO_2. The energy levels of the photocatalyst can affect the reaction performance. Therefore, the band gap energy (E_g), which is the energy difference between the top of the VB and the bottom of the CB in the photocatalyst, is important.

Other than band gap energy and charge carrier mobility, the band edge positions are also very important and crucial for photocatalytic activities because it is one of the keys to catalytic reactions which take place at the surface of the photocatalysts. The photocatalyst has an intrinsic band structure that sets its electronic transport properties. To achieve excellent photocatalytic degradation performance during photocatalysis, a photocatalyst must have appropriate bend edge positions and the photogenerated electrons and holes have to be separated efficiently and effectively for more charge carriers to be available during photocatalytic reactions [19–21]. During photocatalysis, the electrons and holes can recombine after being formed. Therefore, to improve photocatalytic performance, the recombination rate must be reduced and minimized.

Despite a lot of work been done on basic photocatalytic research, there is still a vast gap between laboratory, industry, and applied applications. Laboratory findings can take no account of the cost, catalyst recycling, energy consumption, environmental protection, and other issues, but only prove the feasibility and mechanism of the photocatalytic system. However, there are numerous uncontrollable factors in the actual production process in the case of amplifying industrial applications. Moreover, the synthesis conditions of the photocatalysts will not be as controllable and stable as in the laboratory. Hence, there is a need to understand the fundamentals of photocatalysis, photocatalysts, and the demand of the market and the users.

8.2 Photocatalysis from laboratory to real life

Photocatalytic technology has been mainly applied for the treatment of industrial wastewater treatment which comprises dyeing, papermaking, printing, electroplating industry, etc. As for other photocatalysis research fields, such as solar water splitting, photocatalytic CO_2 reduction, nitrogen fixation, photocatalytic CH_4 activation, and photocatalytic fine chemicals synthesis, they are often stuck at the proof-of-concept level.

Although a lot of work has been done on basic photocatalytic research, there is still a lot of gap between laboratory and industrial applications. Laboratory studies can take no account of the cost, catalyst recycling, energy consumption, environmental protection, and other issues, but only prove the feasibility and mechanism of the photocatalytic system. However, in the case

of intensifying industrial application, there are several uncontrollable factors in the real manufacturing process, and the preparation conditions of the photocatalysts will not be as controllable and stable as in the laboratory. Therefore, the development of feasible, stable, cost-effective, and large-scale manufacturing methods is the key to realizing the industrial and real applications of photocatalytic systems.

Large-scale production of photocatalysts and related technology based on photocatalysis for real-life applications have been developing in various ways to solve the environmental problems taking place in the rapidly growing industrialized world (Fig. 8.1). There are a few large-scale productions using photocatalysis that have been developed for real-life applications. These technologies help to improve indoor air quality, road making, paint to improve air pollution, water pollution, and cosmetics sunscreen. In the following discussions, a few real-life applications using different types of photocatalysts have been compiled.

First of all, the elimination of air pollutants present in the air is very important because it harms human health and their surroundings. To improve indoor air quality, air purification systems have been developed using photocatalytic materials such as photocatalytic paints. To apply in real-life conditions, photocatalytic paints have to be applied to the walls of the buildings. Therefore, a photocatalyst chosen was modified TiO_2, which is active under visible light that is the dominant spectrum in an indoor environment. This material was advantageous to such applications where visible light is the main light that is being used for lighting houses, lighting buildings, lighting schools, and all our surroundings. To be precise, the production of a

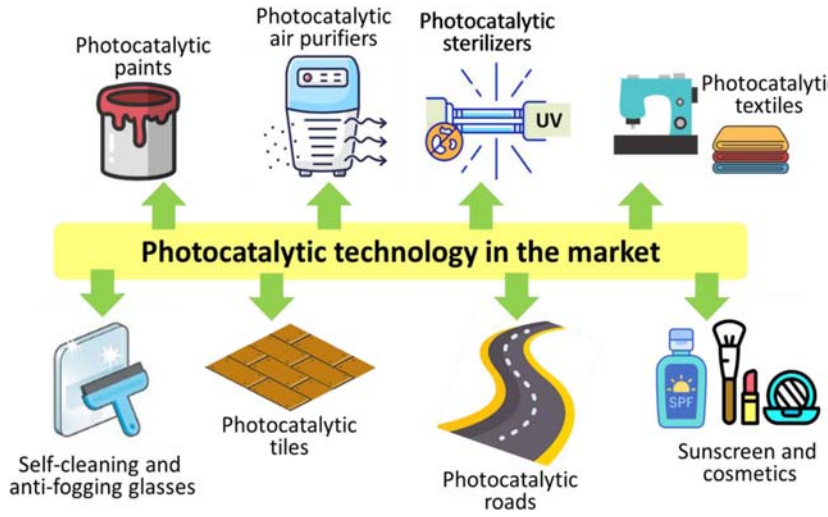

FIGURE 8.1 Selected photocatalytic technologies that are available in the market.

photocatalytic Mn-doped TiO_2 was used in the process. Moreover, a powder named TCM-1 has been successfully synthesized and has a magnificent outcome for the oxidation of air pollutants in an indoor-like environment. The powder TCM-1 can degrade volatile compounds (VOCs) such as BTX (benzene, toluene, and xylene) and nitrogen oxides (NOx) [22].

A study reported by Maggos et al. carried out the photocatalytic paint investigation on the absence and the presence of photocatalysts using NO and toluene as the pollutants in the reactor. It was observed that as the visible light irradiation is turned on, a drastic decrease in NO concentration was seen. However, only a slight decrease in toluene concentration was observed. Hence, it was confirmed that the degradation efficiency of the photocatalytic paint for the elimination of NO was higher as compared to toluene [23].

In short, Maggos et al. experimented to evaluate the air quality using Mn-doped TiO_2 photocatalyst paint on a laboratory scale and a real scale [23]. It was observed that photocatalytic paint can convert NO into radicals. Since NO has acidic properties so NO is well absorbed by alkaline constituents of the paints. Therefore, the reaction potential of NO has increased with HO_x radicals. On the other hand, toluene showed lower photocatalytic removal in the same photocatalytic process in the laboratory and real-scale experiments. This is because the paint surface consists of a tremendously hydroxylated surface which restricts its interaction with the active radicals. Thus, this makes toluene to be readily absorbed in a less hydrophilic TiO_2 surface than on a more hydroxylated surface. When Maggos et al. compared the results of laboratory experiments and real-scale experiments, it was found that both pollutants (NO and toluene) showed a higher value of degradation in the laboratory experimental results than in real-scale experimental results. This is because the transition from laboratory to real-scale experiment is challenging due to the involvement of many other factors such as traffic and environmental parameters. The environmental parameters that are present were temperature, relative humidity, wind speed, and light intensity. Therefore, these factors greatly affect the more complex real-life application results and have a significant difference that characterizes the photocatalytic efficiency of the paint. Furthermore, the potential for pollutant removal is highly dependent on the intrinsic properties of gas and the chemical nature of the paint in which Mn-doped TiO_2 was incorporated during the synthesis.

The urban air quality was majorly influenced by the pollutants, namely nitrogen oxides (NO_x), sulfur oxides (SO_x), hydrocarbons, and carbon monoxide (CO) that are caused by the vehicles discharged as the number of automobiles is increasing every year and the formation of secondary long-range pollutants, which are the ozone and photochemical smog from the action of sunlight on NO_2 and VOCs. Therefore, photocatalyst materials can be added to the surface of the pavement and building materials. Thus, when these photocatalytic materials are exposed to sunlight, the oxidation and/or reduction process takes place and the pollutants get oxidized and/or reduced and

precipitated on the surface of the pavement or building materials. When in contact with rain or washing water, this precipitate can be easily removed and washed off from the surface.

For instance, for concrete pavement blocks, the wearing layers of the pavers were added with anatase TiO_2 (about 8 mm thick) [24]. It was found that modified TiO_2 was present on the surface even if some abrasion takes place by automobiles. The involvement of TiO_2 in the cement causes the NO_x to transform into NO_3^- due to the alkalinity of concrete and the NO_3^- can be easily adsorbed on the surface. Moreover, in the presence of a cement matrix, a synergetic effect plays an important role. The NO and NO_2 gas can be trapped with nitrate salt and the deposited nitrate can be washed away. In the laboratory, the physical parameters play an important role in the photocatalytic reaction of air purification. The parameters that need to be investigated are light intensity, temperature, relative humidity, and contact time (controlled by flow velocity, surface area, and height of airflow). It is clear that with increasing relative humidity, the reduction of NO_x concentration in the air decreases. This is mainly because water in the air contributes to the adhesion of the pollutants at the pavement surface or surface of the buildings. Moreover, as the relative humidity increases, the H_2O molecules and NO_x in the air can cause a competition effect. It can be seen that with a longer contact time (lower air velocity, higher surface area, and smaller height of air flow), the reduction of NO_x increases. For example, from 2004 to 2005, the first pilot project of 10,000 m^2 of photocatalytic pavement blocks was built in Antwerp, Belgium.

Several successful applications have been performed and observed in the laboratory and real life. Accordingly, photocatalytic products have been brought to the industries and then to the market (Fig. 8.2).

8.3 Photocatalysis from laboratory to market

The global demand for the use of photocatalysts has grown over the years until their market size was reported at 2072.6 million USD in 2020 as shown in Table 8.1. While the compound annual growth rate (CAGR) for their market size is expected to rise by 7.1% from 2021 to 2027 [25].

The Grand View Research, Inc., has set an expectation of the global photocatalyst market size to be achieved at 4.58 billion USD by 2025. This resulted in the increased demand for photocatalysts because of their self-cleaning properties and low maintenance cost which drives the growth of the marketing industry [25].

The materials typically used among the photocatalysts could be TiO_2, ZnO, SnO_2, CeO_2, etc. Interestingly, a report has stated that the consumption of TiO_2 has dominated globally over the rest of the materials by 85% due to

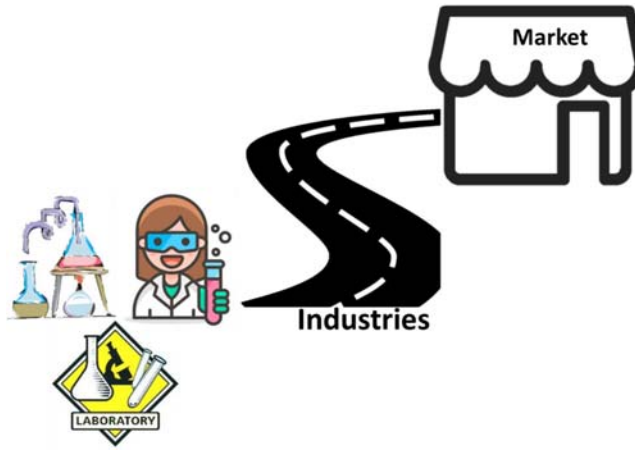

FIGURE 8.2 Schematic diagram showing photocatalytic techniques from laboratory to industry to the market.

TABLE 8.1 Data of present global photocatalyst market trends.

Present global photocatalysts market			
Study year	2020	**Study year in the forecast**	2027
Market size	USD 2072.6 million	**Forecast market size in 2025**	USD 4.58 billion
Forecast CAGR from 2021 to 2027	7.10%		
Dominant by material	Titanium dioxide		
Dominant by application	Paints and coatings		
Dominant by region	Asia Pacific		

its high chemical and physical stability as well as low cost as shown in Fig. 8.3. Thus, the global market share of TiO_2 has been seen to be the largest in 2020 [25]. Also, it is a superior material used as photocatalysts in all constructions and industries.

However, Qamar et al. believe that the rate of reaction and mineralization exhibited by ZnO is much more rapid and generates free radicals such as $^{\bullet}OH$ more comparatively against TiO_2 [26] while the data on the market share of TiO_2 showed that it is expected to grow rapidly more than ZnO throughout the rest of the year until 2026 [27].

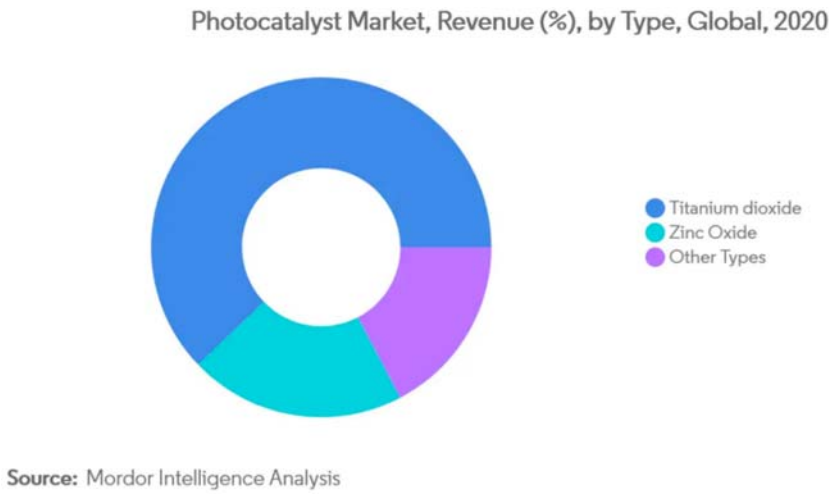

FIGURE 8.3 Annual global market total revenue in % segmented by material type in 2020 [25].

8.4 Photocatalytic self-cleaning and anti-fogging glass

The well-known TiO_2 as a hydrophilic and super-oxidative compound has been commercially used for developing self-cleaning and anti-fogging materials [28]. In addition to that, the application of TiO_2 has also been studied in paints for the degradation of air pollutants and decontamination purposes [29]. Moreover, the unique properties of TiO_2 have also been proven with its whiteness, scattering of light, and high refractive index while these properties have attracted a high number of consumers for their usage in paints and coatings formulations. A lot of companies have exploited the photoinduced TiO_2 as a photocatalytic material for several applications such as photocatalytic glasses and tiles as shown in Tables 8.2 and 8.3.

Several developed countries have successfully manufactured self-cleaning products in previous years. Considering the rising number of industrial activities, the emission of pollutants has propelled the usage of those products that can reduce environmental pollution. Some examples of manufactured products are shown in Table 8.3.

A recent photoinduced superhydrophilicity-based technology called Hydrotech has been successfully developed by the Japanese company TOTO Ltd. The technology is mainly recognized as waterproofing which has been successfully utilized in several coatings, paints, roofing, and building materials. Moreover, it requires sunlight to break down contaminants that are then rinsed away by rain or water. The illustration shown in Fig. 8.4 summarized the series of mechanisms of photocatalytic self-cleaning materials. The self-cleaning procedure acquires the build-up of contaminants on the glass, activation of photocatalyst on the coating by

TABLE 8.2 The use of TiO_2 as self-cleaning materials.

Substratum	Applications	Properties	References
Tiles	Roof, walls, kitchen, and bathroom	Self-cleaning	[30]
Glasses	Vehicle mirrors, indoor glass, windows, mirrors	Self-cleaning, anti-fogging	[31]
Plastics	Automobiles, buildings	Self-cleaning	[32,33]
Textiles/ fibers/cotton	Protective clothing, interior furniture	Self-cleaning	[34]

TABLE 8.3 Examples of manufactured self-cleaning products.

Type of product	TiO_2 properties	Features	References
Hydrotech	Self-cleaning	• High thermal stability	[28]
Activ	Self-cleaning	• High mechanical durability • Reproducible photocatalyst • Low visible reflectance • High transmittance	[35]

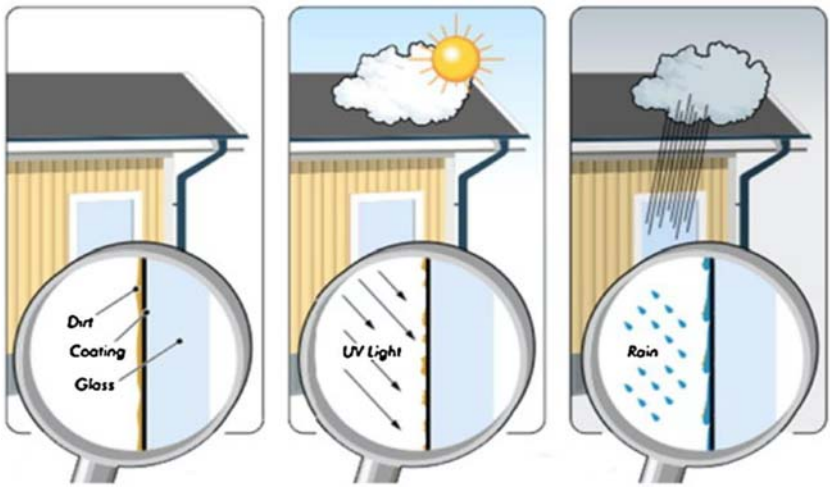

FIGURE 8.4 Illustration showing the mechanism. (From left to right) for self-cleaning of glass [28].

sunlight, breakdown of contaminants by the photocatalytic coating, and the rinse down of decomposed materials by rain or water [28].

Generally, photocatalytic coatings are made up of a liquid suspension of TiO_2 which is sprayed onto the surface. According to Yan et al., the modification of self-cleaning products requires high processing temperatures to obtain the optimal thermal stability of the photocatalytic active TiO_2 in anatase form [36]. This is because the developed self-cleaning materials are favored because of the high thermal stability of the active anatase TiO_2 phase [37]. The material is sintered in the range 600°C−800°C to firmly adhere the TiO_2 layer to the surfaces [28]. Moreover, Yan et al. studied that non-doped TiO_2 in anatase form also promotes high thermal stability [28]. However, the recombination of electrons and holes is increased and eventually reduces its photocatalytic activity in this particular condition.

Another developed product based on the photocatalytic TiO_2 is called Activ by Pilkington glass which has been mostly applied in private buildings worldwide as transparent glass windows. The self-cleaning glass was manufactured with a thick film of nanocrystalline TiO_2 by 15 nm and uploaded on a glass window. Its unique dual-action coating uses the forces of nature to help keep the glass free from dirt, giving not only the practical benefit of less cleaning but also clearer and better-looking windows. The unique dual-action self-cleaning coating is located on the external glass pane which possesses photocatalytic and hydrophilic properties and works in two stages [35]:

- **Stage 1:** The coating absorbs natural daylight or sunlight to break down and loosen organic dust and pollutants.
- **Stage 2:** When it rains, instead of forming droplets, the water spreads evenly over the surface of the glass, forming a thin film and helping to wash away any dirt and reduce streaks. During long dry periods, the glass can be cleaned by simply hosing it with clean water.

Interestingly, Mills et al. have studied the Pilkington Activ glass based on its significant biodegradable activity toward stearic acid [38]. Moreover, the great mechanical durability and reproducible photocatalytic activity of Activ make it ideal for its use as photocatalytic reference material. In addition to this, the product displayed 7% low visible reflectance and transmittance properties which are important for light absorption and enhance its photocatalytic activity. Meanwhile, similar products like Radiance Ti, Sunclean, and Bioclean have been introduced in the market of photocatalyst self-cleaning materials as well [39−41].

8.5 Photocatalytic paints

The development of photocatalytic paints has gained interest in recent years due to their benefits. Photocatalytic paints involve incorporating photocatalysts such as TiO_2 which acts as the main ingredient in photocatalytic paints.

The presence of light is required in photocatalytic paints and is used as a main source of energy. Once the photocatalyst gets excited, it causes various reactions to take place on the surface of the paint. Thus, when light is irradiated on the photocatalytic paints used on the walls of the interior or exterior buildings, the stimulation of light on the photocatalyst causes the coated surface to acquire properties such as air purification and self-cleaning [42].

The photocatalytic coatings are designed in such a way to be transparent making them suitable to be applied to a wide variety of surfaces. It is also reported that with exposure to light, the active ingredients used in photocatalyst coatings such as TiO_2 help to decompose stain, smog, and pollution and convert these substances into harmless non-toxic byproducts [43]. The light-energized TiO_2 adsorb H_2O and O_2 from the air undergoing primary reaction on the surface of the photocatalyst to form strong oxidizing species, i.e., $^{\bullet}OH$ and $O_2^{\bullet -}$, which will then react with the pollutants and microbial growth present in the environment to perform self-cleaning ability. Whereas, the superhydrophilicity where water is strongly attracted to the surface of TiO_2 results in a major reduction in the contact angle of water that covers the surface to prevent the formation of droplets. Moreover, there are several benefits of using photocatalytic paints such as self-cleaning, minimizing maintenance, air purification, lasting for a prolonged time, and reduced cleaning.

Paint manufacturers have started working on using photocatalysts in paints. However, the major challenge is to produce a photocatalyst that attacks organic substances and does not attract or destroy the organic binding agents. In other words, the photocatalytic process virtually destroys itself as it breaks down the binding agents on the surface. This will result in chalking and premature weathering with a corresponding shorter life expectancy for photocatalytic paints.

KEIM Soldalit-ME has succeeded in engineering a long-lasting photocatalytic paint with enhanced self-cleaning properties. These properties are by combining a photocatalytically acting pigment with mineral binder systems. The company has manufactured paints with several advantages. In terms of having clean facades, silicate facade paint becomes hydrophilic under the irradiation of light. This gives a self-cleaning effect, fast drying speed, and anti-static and non-thermoplastic properties. In terms of getting clean air, the photocatalytically active mineral coatings help to break down air pollutants. Moreover, this contributes to the decomposition of atmospheric air pollutants such as VOCs, SO_x, NO_x, greenhouse gases, and superficial contaminations (Fig. 8.5) [44].

Moreover, EXOCOAT nano-titanium oxide-based coatings exhibited excellent self-cleaning performance. It is a smart coating because these coatings actively destroy dirt particles with the aid of light. The coating can generate free radicals in moist air. These radicals can oxidize dirt to H_2O and CO_2. The second feature of these coatings is their superhydrophilicity. After

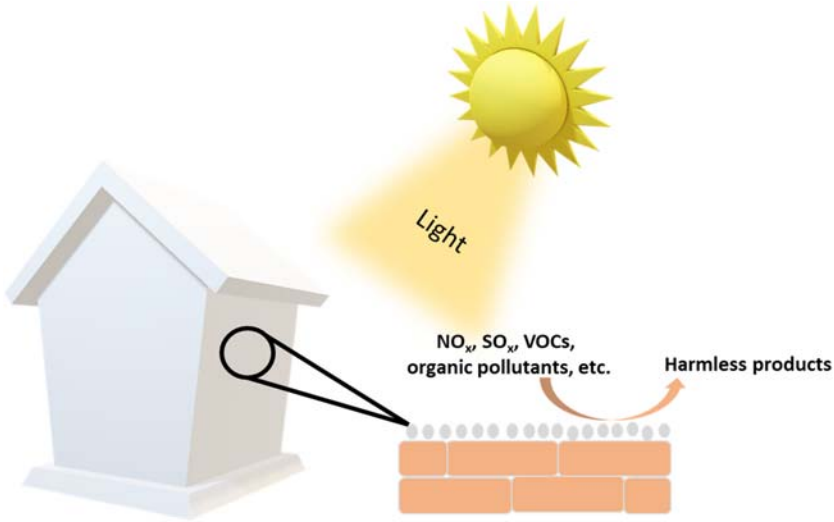

FIGURE 8.5 Photocatalytic paint is coated to reduce harmful gases and air pollutants.

the photocatalytic reaction, water may flush down the dirt particles. However, the photocatalytic reaction and the rinsing with water do not necessarily have to take place simultaneously, although it is advantageous [45].

8.6 Photocatalytic tiles

One of the most valuable applications over the periods has been the self-cleaning tiles or also known as the photocatalytic tiles. As the development of photocatalysts advances, photocatalytic tiles would prove their usefulness in raising the living standards in residential housing and the healthcare performances in industrial, hospitality, and medical treatment buildings [46]. Furthermore, it reduces the amount of time, effort, and chemical detergents for surface cleaning of buildings [47]. Photocatalytic tiles are tiles coated with thin layers of TiO_2 on their surface, which show properties of antimicrobial, antibacterial pollutants decomposition upon exposure to sunlight, oxygen, and moisture as well as superhydrophilicity, resulting in healthier environments with lower costs than surface cleaning [46,48–50].

With new technologies, ceramic tiles with TiO_2 surface coating have been largely and particularly researched as photocatalytic tiles due to their efficiency and positive functionality [49]. The use of TiO_2 as a coating material for ceramic tiles has been very effective due to its properties. However, depending on the intended use, high sintering temperatures, the reaction and adhesion factors between TiO_2 and the substrate, and changes in the appearance of the tile surface need to be considered carefully [49,51]. The purpose

of using TiO_2 in ceramic tiles was to create self-sterile ceramic tiles that can kill fungi and bacteria on the surface of ceramic tiles [49,52].

One of the commercialized photocatalytic tiles is known as ACTIVE SURFACES ceramics. ACTIVE SURFACES ceramics offers photocatalytic, anti-pollution, antibacterial, and antiviral tiles which are produced as the result of 100% Italian research that began about 10 years ago (cooperation between the Iris Ceramica Group and the Department of Chemistry of the University of Milan). ACTIVE SURFACES are distinguished by four important properties as shown in Fig. 8.6 [53]:

1. Anti-pollution effectiveness: ACTIVE SURFACES ceramics can permanently and continuously eliminate polluting molecules present in the air.
2. Antibacterial and antiviral: (99% effective against coronavirus SARS-CoV-2) – ACTIVE SURFACES ceramics can destroy the bacteria that come into contact with the surface. The presence of silver makes the antibacterial properties work even in the dark.
3. Anti-odor effectiveness: ACTIVE SURFACES ceramics can degrade the molecules responsible for bad odors effectively even under LED lights.
4. Self-cleaning effectiveness: ACTIVE SURFACES ceramics facilitate the removal of dirt. In indoor environments, this property reduces the use of detergents that are aggressive and toxic to human beings.

A Japanese company, TOTO Ltd, the world's largest toilet manufacturer founded HYDTROTECT, an environmental cleaning technology utilizing photocatalysts that harness the power of light and water to purify the air and clean surface automatically [54]. The HYDROTECT tiles include the following features [55]:

- Air cleaning effect: The toxic substances in the air that negatively affect people are dissolved and cleaned by the reactive oxygen species (ROS) generated from photocatalysis using the clean energy of sunlight.

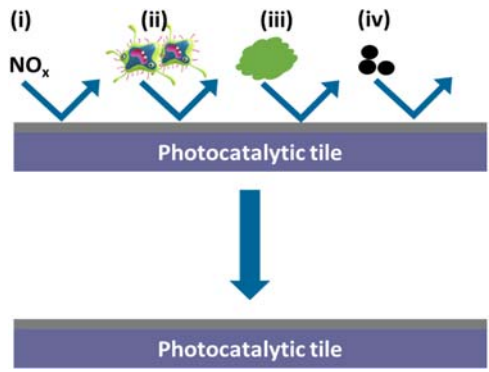

FIGURE 8.6 The schematic properties of photocatalytic tiles.

Moreover, they claimed that HYDROTECT tile also eliminates nitrogen oxides (NO_x) at the outer walls of buildings similar to plants.

- Self-cleaning effect: The surface of the tiles is stain-resistant and easy to clean. Apart from the power of light and rain that keep buildings constantly clean, this economical photocatalytic tile retains its beauty for a long time and requires little maintenance. Furthermore, detergent and water for maintenance can be reduced, which contributes to environmental conservation.

8.7 Photocatalytic air purifiers

Airborne hazards such as chemicals, particulate matter, biological pollutants, and microorganisms may endanger not only human health but other living organisms. Major chemicals (also known as air pollutants) such as sulfur oxides (SO_x), nitrogen oxides (NO_x), and VOCs result from human activity [56]. The development of respiratory diseases or even premature deaths has been associated with exposure to these hazardous substances. In fact, sulfur dioxide (together with sulfur trioxide) contributes to acid rain; oxides of nitrogen react with hydrocarbons which give rise to urban smog while the chemical nature of either man-made or naturally occurring VOCs has significant vapor pressures which may impact both the environment and human health. Therefore, to control the production of these pollutants as well as to improve air quality, the reinforcement of highly efficient and viable purification technologies is necessary. Fig. 8.7 shows the simple mechanism of photocatalytic air purifiers.

Moreover, in recent times, many people are more conscious of pathogens found in the air due to the coronavirus pandemic. Therefore, research in the

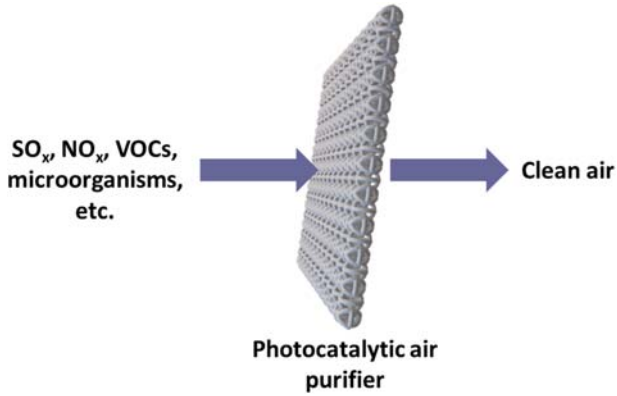

FIGURE 8.7 Schematic of photocatalytic air purifiers.

disinfection of microorganisms by photocatalysts is highly sought to bring about a better quality of life. Microorganisms generally have a cell membrane that is made up of a phospholipid bilayer which protects and regulates the cell function. Any damage to the cell membrane will cause the inactivation of microorganisms. Similarly, with organic pollutants, the $^{\bullet}OH$ radicals formed by reacting with the phospholipid bilayer get oxidized, and therefore, destroy the structure of the cell membrane which leads to the death of the microbial cells [57].

In recent years, air purification systems have incorporated photocatalytic oxidation (PCO) technology for the degradation of pollutants. This involves the utilization of a light-activated catalyst in the presence of solar (or artificial) light under ambient conditions. PCO is not only cost-effective as it does not require chemicals or any other external energy except light, but it also safely operates under ambient conditions and is a relatively humidity-insensitive activity. Finally, it is capable of fully degrading VOCs into carbon dioxide (CO_2) and water (H_2O) [15]. TiO_2 is a photosensitive semiconductor that has widely been employed in PCO technology for its effectiveness in absorbing ultraviolet (UV) light in the presence of oxygen and water vapor to form reactive hydroxyl radicals ($^{\bullet}OH$) and superoxide radicals ($O_2^{\bullet-}$) [56,58]. These free radicals may react with pollutants in a series of reactions, such as substitution, bond cleavage, and electron transfer and oxidize as well as decompose the pollutants into harmless end byproducts [58].

Research institutes and technology companies in South Korea have been working on photocatalytic air purification for several years. Airodoctor air purifier has a quadruple filter that uses a highly effective photocatalysis technology for sustainable and hazard-free air purification which is now patented. The first three filter steps are similar to those of conventional air purifiers, namely particles (large or small) are filtered out through prefilters, activated carbon, and high-efficiency particulate air (HEPA) filters. Photocatalysis takes place at the fourth filter. TiO_2 is irradiated by UV-A light from highly powerful LED modules. Photocatalysis results in the decomposition and neutralization of viruses, bacteria, allergens, and harmful gases. Similarly, Airtech is an air purifier with a deodorizing function that incorporates a TiO_2 photocatalyst and a HEPA filter [59]. This air purifier consisted of multi-layer filtration to produce clean air and works as follows:

- Washable Pre-filter: It filters visible dust and hair. It can be cleaned with water. No need to replace it. Completely extend HEPA filter service life by filtering dust and hair.
- High-efficiency HEPA filter: Able to filter particles $>0.3-0.5\,\mu m$ at 99.998%.

- UV-LED PhotoCatalyst: A photocatalyst filter coated with TiO_2 can intercept the floating matter in the air. After the filter is exposed to UV light, the substances are decomposed for an odor-free environment.

8.8 Photocatalytic roads

One of the major global concerns includes environmental pollution which causes an urgent need to develop new technologies and cleaner processes. Atmospheric pollution is defined as the presence of certain pollutants at levels that impact human health, the environment, and cultural heritage negatively. Emission from the vehicles such as nitrogen oxides (NO_x), hydrocarbons (HCs), and carbon monoxide (CO) has an impact on the overall air quality [24,60]. These are highly harmful pollutants causing the formation of acid rain, tropospheric ozone, global warming, and human diseases, particularly diseases related to the respiratory and immune systems. To treat the air pollution caused by automobiles, vehicles, etc. one of the solutions can be the treatment of the pollutants as close to the source as possible. Therefore, photocatalysts can be added to the surface of road materials. In combination with sunlight/light and photocatalysts, the pollutants can be oxidized and/or reduced and precipitated on the surface of the material or roads (Fig. 8.8). Afterward, the precipitated pollutants or byproducts can be removed from the surface by rain or by cleaning/washing with water [24,60].

PlusTI Ti-intro CME all-purpose penetrant is a TiO_2-enhanced cationic molecular emulsion and is a carrier liquid that deeply penetrates asphalt and concrete pavement. The Pavement Technology, Inc (PTI) research and development team worked closely with a leading US-based university to ensure deep penetration of a TiO_2-based formulation. To develop a sustainable photocatalytic self-cleaning surface that removes NO_x, SO_x, VOCs, and other

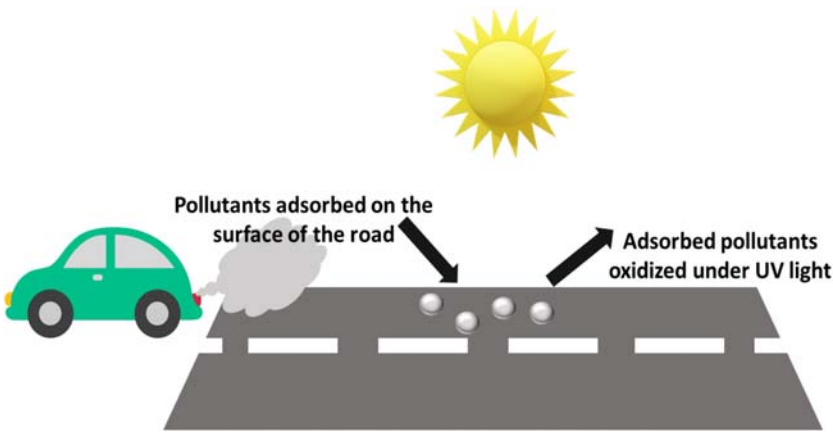

FIGURE 8.8 Schematic of photocatalytic road.

TABLE 8.4 NO_x reduction efficiency of a photocatalyst [61].

Compound	NO_x reduction efficiency (%)					
Application rate (gsy)	**Controlled sample**	**0.05**	**0.06**	**0.08**	**0.10**	**0.12**
Ti-Intro CME	NEGL	48%	52%	55%	58%	53%

pollutants, factors such as humidity, temperature, flow rates, and method of applications were tested and evaluated. Table 8.4 shows the NO_x reduction efficiency of photocatalysts.

8.9 Photocatalytic sterilization

Antibacterial agents are commonly divided into two types: organic antibacterial agents and inorganic antibacterial agents [62]. Inorganic antibacterial agents are mainly based on silver ions (Ag^+) to kill bacteria; however, they fail to break down endotoxins. The shortcoming of silver ions can be overcome using TiO_2 photocatalytic sterilization. This might be due to the high reaction energy of active free hydroxyl radicals ($^{\bullet}OH$, 120 kcal/mol) that are generated by the TiO_2 through photocatalytic reaction, which is higher than that of various chemical bonds in organic compounds. Therefore, $^{\bullet}OH$ radicals can effectively decompose organic compounds, particularly the main component of the bacterium [63]. Furthermore, the synergy activity of free $^{\bullet}OH$ radicals and other reactive radicals generated from photocatalysis makes the attacks on bacteria more frequent which causes extensive damage to biological cell structures [64].

Advanced oxidation processes (AOPs) involving TiO_2-mediated photocatalysis technology have attracted considerable interest. The process includes generating ROS, although hydroxyl radicals are considered responsible for the disinfection property against bacteria as shown in Fig. 8.9. Furthermore, other ROS species such as singlet oxygen and hydrogen peroxide also play a role in sterilization as these free radicals/ions can actively participate in the oxidation of cellular components, membrane leakage of the microbial cell wall, and other processes [65].

Kaltech's photocatalytic technology has developed its photocatalytic sterilization and deodorization devices (KL-W01 and KL-B01) which is the industry's first photocatalyst-only sterilization/deodorization device without an absorbent filter. This photocatalytic sanitizer and deodorizer device can efficiently decompose organic substances with a photocatalyst [66].

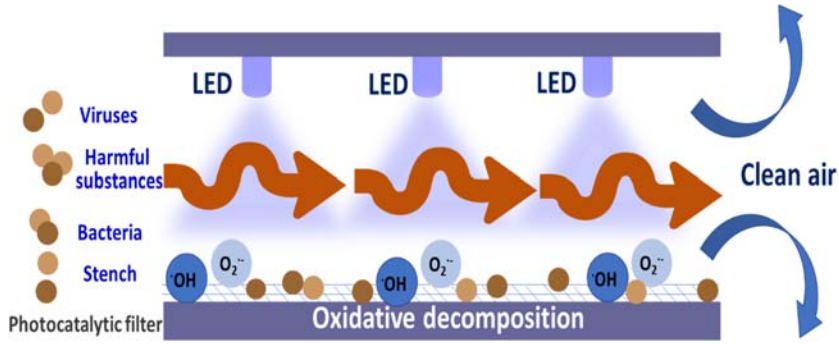

FIGURE 8.9 A schematic diagram of photocatalytic sterilization.

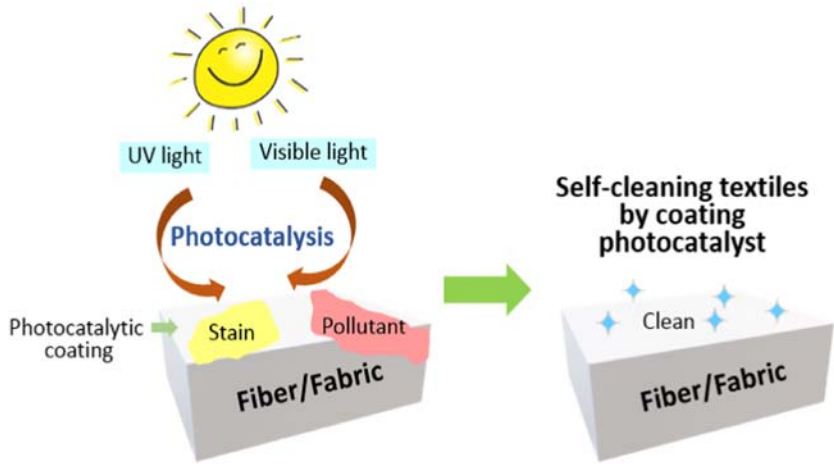

FIGURE 8.10 Mechanism showing removal of stains and contaminants using photocatalysis by photocatalytic textiles.

8.10 Photocatalytic textiles

Textiles are often regarded as our second skin. They decorate and protect our bodies while bringing comfort into our lives. The development of nanotechnological processes for the chemical and morphological modification of textile substrates has enabled a breakthrough in the production of multifunctional smart high-performance textiles with added value. Fig. 8.10 shows the mechanism of photocatalytic textiles for the removal of stains, pollutants, etc.

The application of photocatalyst-based additives and nano-/microstructures of different types of materials to textile surfaces has opened an infinite potential for the development of new advanced nanocomposite textile

products for personal protection, medical applications, pollutant degradation, filtration, wearable electronics, solar cells, and sensor devices. Takashi Nohmura, chief research and development officer of Taiyo Kogyo Corp., Tokyo, Japan, and chairman of the Japanese Association of Photocatalytic Products collaborated with Nippon Soda Co. Ltd to paint photocatalysts manually onto a PVC fabric sample. They conducted an outdoor exposure test for several months and found that it showed an overwhelming antifouling property. Moreover, Kuraray Co. Ltd. has developed photocatalytic awning fabric Excellence based on the Taiyo and Nippon Soda photocatalytic license. The fabric has excellent resistance to dirt, and it offers the aesthetic advantage to awnings and cuts the cost of cleaning and maintenance significantly. As long as TiO_2 stays chemically intact, the antifouling properties will last on the fabrics and textiles [67] (Table 8.5).

8.11 Sunscreens and cosmetics

Sunscreens provide temporary protection against UV radiation. The active ingredients found in sunscreens are classified into organic and inorganic UV filters based on chemical composition and mechanism of action. Organic filters are aromatic compounds that work by absorbing UV light whereas inorganic filters are minerals that can absorb, reflect, and scatter UV light as shown in Fig. 8.11. There are advantages and disadvantages associated with both kinds of filters, and both filters are frequently found in commercially available formulations [74]. The most frequently used inorganic UV filters are TiO_2 and ZnO. TiO_2 possesses a higher refractive index than diamond, does not absorb visible rays, and is highly chemically stable. Therefore, it is widely used in paints and cosmetics as a white pigment and as a UV-absorbing agent. There are three types of crystal structures of TiO_2 which are anatase, rutile, and brookite. The industrially used ones are anatase and rutile. The anatase phase can be converted to the rutile phase at a temperature of $\sim 700^{\circ}C$. TiO_2 exhibits UV shielding effects, hence, rutile TiO_2 is widely used in the cosmetics sector, especially in sunscreens. Anatase TiO_2 displays photocatalytic functions and offers self-cleaning capabilities under sunlight, air cleaning, water quality improvement, and antimicrobial and anti-mold functions. Similar to TiO_2, the mode of action of ZnO is to either scatter or reflect UV light. This particular property allows for an increase in the optical pathway of the photons, which enhances the sun protection factor (SPF) and thus increases the efficacy of the product. ZnO typically protects the UVA region, whereas TiO_2 covers UVB and part of the UVA region [74].

The DSM company has developed PARSOL TX which is fully compliant with the scientific committee for consumer safety. PARSOL TX is an aluminum-free, inorganic UV filter, made of 100% pure TiO_2 in rutile form. It has excellent photostability and outstanding compatibility with other UV filters. Moreover, PARSOL TX's hydrophobic coating strongly contributes

TABLE 8.5 Summary of photocatalytic textiles integrated with various nanomaterials.

Nanomaterials used	Integration method	Textile substrate	Functionality	References
ZnO/Gallic acid	Sonochemical deposition	Cotton	Biocompatible and antimicrobial fabrics	[68]
TiO_2	Impregnation method	Cotton	Self-cleaning textile	[69]
Au/TiO_2 film	Photo-deposition	Cotton	Self-cleaning textile	[70]
Copolymer/SiO_2 nanocomposite	Silks screen printing	Polyester fabric	Self-cleaning for textiles coating	[71]
Janus SiO_2	Chemical deposition	Poly-(ethylene terephthalate) (PET)	Water-repellent textiles	[72]
[a]PANI/TiO_2	Not mentioned	Cotton	UV Protective clothes	[73]

[a]*Polyaniline.*

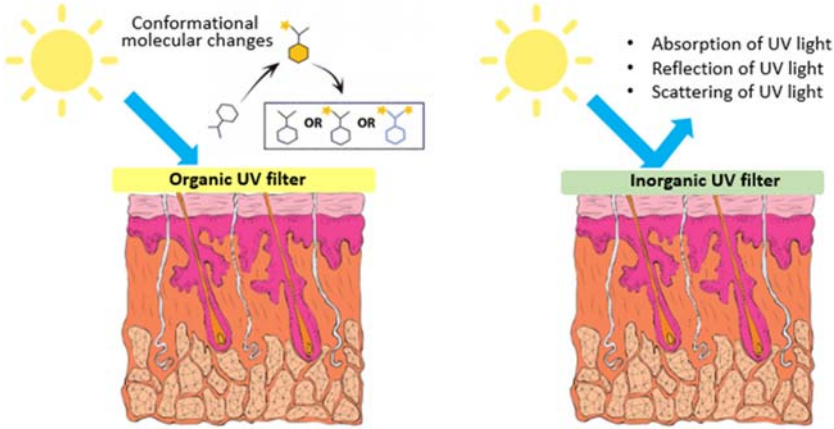

FIGURE 8.11 Mechanism of action of organic and inorganic UV filters.

to its aesthetic appeal in formulation and its pleasing and sensory feel. Due to its simple and easy formulation properties, it offers unrivaled flexibility across a wide range of sun- and skin-care product formulations including make-up products and the latest additions in the personal care market's BB and CC cream formulations [75].

8.12 Summary

Due to the rapid industrialization of the world, environmental problems have arisen leading to the large-scale production of photocatalysts. Although laboratory-based production has been successfully developed, the use of photocatalysis for real-life experiments is in demand. Moreover, photocatalysts in the markets should reach the human beings to counter environmental problems. A report stated that TiO_2 has dominated globally over the rest of other materials owing to its high chemical and physical stability as well as its low cost. This resulted in an increased demand for photocatalysts. Owing to their self-cleaning properties and low maintenance cost, they further drive the growth of the marketing industry.

References

[1] D. Ravelli, D. Dondi, A. Albini, A multi-faceted concept for green chemistry, Photocatalysis (2011) 1999–2011. Available from: https://doi.org/10.1039/b714786b.

[2] C. Tian, Q. Zhang, A. Wu, M. Jiang, Z. Liang, B. Jiang, Cost-effective large-scale synthesis of ZnO photocatalyst with excellent performance for dye photodegradation, ChemComm (2012) 2858–2860. Available from: https://doi.org/10.1039/c2cc16434e.

[3] X. Wang, J. Ma, Y. Kong, C. Fan, M. Peng, S. Komarneni, Synthesis of p-n heterojunction Ag_3PO_4/$NaTaO_3$ composite photocatalyst for enhanced visible-light-driven photocatalytic

performance, Materials Letters 251 (2019) 192–195. Available from: https://doi.org/10.1016/j.matlet.2019.05.078.

[4] C. Li, B. Wang, F. Zhang, N. Song, G. Liu, C. Wang, et al., Performance of Ag/BiOBr/GO composite photocatalyst for visible-light-driven dye pollutants degradation, Journal of Materials Research and Technology 9 (2020) 610–621. Available from: https://doi.org/10.1016/j.jmrt.2019.11.001.

[5] Y. Yao, J. Liang, Y. Wei, X. Zheng, X. Xu, G. He, et al., One-pot synthesis of visible-light-driven photocatalyst for degradation of Rhodamine B: graphene based bismuth/bismuth(III) oxybromide, Materials Letters 240 (2019) 246–249. Available from: https://doi.org/10.1016/j.matlet.2019.01.021.

[6] E.E. El-Katori, M.A. Ahmed, A.A. El-Bindary, A.M. Oraby, Impact of CdS/SnO_2 heterostructured nanoparticle as visible light active photocatalyst for the removal methylene blue dye, Journal of Photochemistry and Photobiology A: Chemistry 392 (2020) 112403. Available from: https://doi.org/10.1016/j.jphotochem.2020.112403.

[7] R. Gupta, B. Boruah, J.M. Modak, G. Madras, Kinetic study of Z-scheme C_3N_4/$CuWO_4$ photocatalyst towards solar light inactivation of mixed populated bacteria, Journal of Photochemistry and Photobiology A: Chemistry 372 (2019) 108–121. Available from: https://doi.org/10.1016/j.jphotochem.2018.08.035.

[8] Y. Li, H. Wang, L. Huang, C. Wang, Q. Wang, F. Zhang, et al., Promoting LED light driven photocatalytic inactivation of bacteria by novel β-Bi_2O_3@BiOBr core/shell photocatalyst, Journal of Alloys and Compounds 816 (2020) 152665. Available from: https://doi.org/10.1016/j.jallcom.2019.152665.

[9] Z. Zhu Yang, C. Zhang, G. Ming Zeng, X. Fei Tan, D. Lian Huang, J. Wu Zhou, et al., State-of-the-art progress in the rational design of layered double hydroxide based photocatalysts for photocatalytic and photoelectrochemical H_2/O_2 production, Coordination Chemistry Reviews 446 (2021) 214103. Available from: https://doi.org/10.1016/j.ccr.2021.214103.

[10] S. Kikkawa, Y. Nakatani, K. Teramura, H. Asakura, S. Hosokawa, T. Tanaka, Photoelectrochemical investigation of the role of surface-modified Yb species in the photocatalytic conversion of CO_2 by H_2O over Ga_2O_3 photocatalysts, Catalysis Today 352 (2020) 18–26. Available from: https://doi.org/10.1016/j.cattod.2020.02.016.

[11] Y.C. Chang, S.Y. Syu, Z.Y. Wu, Fabrication of ZnO-In_2S_3 composite nanofiber as highly efficient hydrogen evolution photocatalyst, Materials Letters 302 (2021) 130435. Available from: https://doi.org/10.1016/j.matlet.2021.130435.

[12] I. Ahmad, S. Shukrullah, M.Y. Naz, M. Ahmad, E. Ahmed, M.S. Akhtar, et al., Efficient hydrogen evolution by liquid phase plasma irradiation over Sn doped ZnO/CNTs photocatalyst, International Journal of Hydrogen Energy (2021). Available from: https://doi.org/10.1016/j.ijhydene.2021.06.147.

[13] Indoor Air Quality | US EPA, n.d. https://www.epa.gov/report-environment/indoor-air-quality (accessed November 7, 2021).

[14] E.S. Karafas, M.N. Romanias, V. Stefanopoulos, V. Binas, A. Zachopoulos, G. Kiriakidis, et al., Effect of metal doped and co-doped TiO_2 photocatalysts oriented to degrade indoor/outdoor pollutants for air quality improvement. A kinetic and product study using acetaldehyde as probe molecule, Journal of Photochemistry and Photobiology A: Chemistry 371 (2019) 255–263. Available from: https://doi.org/10.1016/j.jphotochem.2018.11.023.

[15] F. He, W. Jeon, W. Choi, Photocatalytic air purification mimicking the self-cleaning process of the atmosphere, Nature Communications 12 (2021) 10–13. Available from: https://doi.org/10.1038/s41467-021-22839-0.

[16] R. Molinari, C. Lavorato, P. Argurio, Visible-light photocatalysts and their perspectives various liquid phase chemical conversions, Catalysts (2020) 1–38.

[17] C. Lavorato, P. Argurio, R. Molinari, Hydrogen production and organic synthesis in photocatalytic membrane reactors: a review, International Journal of Membrane Science and Technology 7 (2020) 1–14. Available from: https://doi.org/10.15379/2410-1869.2020.07.01.01.

[18] F. Ja'afar, C.H. Leow, V. Garbin, C.A. Sennoga, M.-X. Tang, J.M. Seddon, Surface charge measurement of SonoVue, definity and optison: a comparison of laser doppler electrophoresis and micro-electrophoresis, Ultrasound in Medicine & Biology 41 (2015) 2990–3000. Available from: https://doi.org/10.1016/j.ultrasmedbio.2015.07.001.

[19] A.S. Basaleh, R.M. Mohamed, Synthesis and characterization of Cu-$BaTiO_3$ nanocomposite for atrazine remediation under visible-light radiation from wastewater, Journal of Materials Research and Technology 9 (2020) 9550–9558. Available from: https://doi.org/10.1016/j.jmrt.2020.06.081.

[20] M. Ahmadi, H. Ramezani Motlagh, N. Jaafarzadeh, A. Mostoufi, R. Saeedi, G. Barzegar, et al., Enhanced photocatalytic degradation of tetracycline and real pharmaceutical wastewater using MWCNT/TiO_2 nano-composite, Journal of Environmental Management 186 (2017) 55–63. Available from: https://doi.org/10.1016/j.jenvman.2016.09.088.

[21] S. Wang, H. Gao, Y. Wei, Y. Li, X. Yang, L. Fang, et al., Insight into the optical, color, photoluminescence properties, and photocatalytic activity of the N-O and C-O functional groups decorating spinel type magnesium aluminate, CrystEngComm 21 (2019) 263–277. Available from: https://doi.org/10.1039/c8ce01474d.

[22] C. Cacho, O. Geiss, J. Barrero-moreno, V.D. Binas, G. Kiriakidis, L. Botalico, et al., Studies on photo-induced NO removal by Mn-doped TiO_2 under indoor-like illumination conditions, Journal of Photochemistry & Photobiology, A: Chemistry 222 (2011) 304–306. Available from: https://doi.org/10.1016/j.jphotochem.2011.04.037.

[23] T. Maggos, V. Binas, V. Siaperas, A. Terzopoulos, P. Panagopoulos, G. Kiriakidis, A promising technological approach to improve indoor air quality, Applied Sciences 9 (2019) 4837. Available from: https://doi.org/10.3390/app9224837.

[24] E. Boonen, A. Beeldens, Photocatalytic roads: from lab tests to real scale applications, European Transport Research Review 5 (2013) 79–89. Available from: https://doi.org/10.1007/s12544-012-0085-6.

[25] Grand View Research, Photocatalyst market size worth $4.56 billion by 2025, (2021). https://www.grandviewresearch.com/press-release/global-photocatalyst-market.

[26] M. Qamar, M. Muneer, A comparative photocatalytic activity of titanium dioxide and zinc oxide by investigating the degradation of vanillin, Desalination 249 (2009) 535–540. Available from: https://doi.org/10.1016/j.desal.2009.01.022.

[27] Maximize Market Research, Global photocatalyst market: industry analysis and forecast (2020–2026) by material, application, end use, and region, 2020–2026, 2021. https://www.maximizemarketresearch.com/market-report/global-photocatalyst-market/94833/.

[28] S. Banerjee, D.D. Dionysiou, S.C. Pillai, Self-cleaning applications of TiO_2 by photo-induced hydrophilicity and photocatalysis, Applied Catalysis B: Environmental. 176–177 (2015) 396–428. Available from: https://doi.org/10.1016/j.apcatb.2015.03.058.

[29] F. Salvadores, O.M. Alfano, M.M. Ballari, Kinetic study of air treatment by photocatalytic paints under indoor radiation source: Influence of ambient conditions and photocatalyst content, Applied Catalysis B: Environmental 268 (2020) 118694. Available from: https://doi.org/10.1016/j.apcatb.2020.118694.

[30] T.-H. Xie, J. Lin, Origin of photocatalytic deactivation of TiO_2 film coated on ceramic substrate, The Journal of Physical Chemistry C 111 (2007) 9968−9974. Available from: https://doi.org/10.1021/jp072334h.

[31] H. Yaghoubi, N. Taghavinia, E.K. Alamdari, Self cleaning TiO_2 coating on polycarbonate: surface treatment, photocatalytic and nanomechanical properties, Surface and Coatings Technology 204 (2010) 1562−1568. Available from: https://doi.org/10.1016/j.surfcoat.2009.09.085.

[32] W.S. Tung, W.A. Daoud, Self-cleaning fibers via nanotechnology: a virtual reality, Journal of Materials Chemistry 21 (2011) 7858. Available from: https://doi.org/10.1039/c0jm03856c.

[33] C. Kapridaki, L. Pinho, M.J. Mosquera, P. Maravelaki-Kalaitzaki, Producing photoactive, transparent and hydrophobic SiO_2-crystalline TiO_2 nanocomposites at ambient conditions with application as self-cleaning coatings, Applied Catalysis B: Environmental 156−157 (2014) 416−427. Available from: https://doi.org/10.1016/j.apcatb.2014.03.042.

[34] K. Liu, M. Cao, A. Fujishima, L. Jiang, Bio-inspired titanium dioxide materials with special wettability and their applications, Chemical Reviews 114 (2014) 10044−10094. Available from: https://doi.org/10.1021/cr4006796.

[35] Self-Cleaning, n.d. https://www.pilkington.com/en/us/products/product-categories/self-cleaning# (accessed June 6, 2022).

[36] M. Yan, F. Chen, J. Zhang, M. Anpo, Preparation of controllable crystalline titania and study on the photocatalytic properties, The Journal of Physical Chemistry B 109 (2005) 8673−8678. Available from: https://doi.org/10.1021/jp046087i.

[37] P. Periyat, S.C. Pillai, D.E. McCormack, J. Colreavy, S.J. Hinder, Improved high-temperature stability and sun-light-driven photocatalytic activity of sulfur-doped anatase TiO_2, The Journal of Physical Chemistry C 112 (2008) 7644−7652. Available from: https://doi.org/10.1021/jp0774847.

[38] A. Mills, A. Lepre, N. Elliott, S. Bhopal, I.P. Parkin, S.A. O'Neill, Characterisation of the photocatalyst Pilkington Activ™: a reference film photocatalyst? Journal of Photochemistry and Photobiology A: Chemistry 160 (2003) 213−224. Available from: https://doi.org/10.1016/S1010-6030(03)00205-3.

[39] Glass on Web, AFG industries announced the introduction of radiance-TiTM, a new self-cleaning glass that helps keep windows clean on the outside, 2001. https://www.glasson-web.com/news/afg-radiance-ti-new-self-cleaning-glass.

[40] Glass online, PPG introduces SunClean self-cleaning glass for commercial applications, 2012. https://www.glassonline.com/ppg-introduces-sunclean-self-cleaning-glass-for-commercial-applications/.

[41] Glass Solutions, Self cleaning glass-bioclean, n.d. https://glassolutions.co.uk/en-gb/products/bioclean-self-cleaning-glass.

[42] A. Fujishima, K. Honda, Electrochemical photolysis of water at a semiconductor electrode, Nature 238 (1972) 37−38. Available from: https://doi.org/10.1038/238037a0.

[43] M.L. Ibrahim, N.N.A. Nik Abdul Khalil, A. Islam, U. Rashid, S.F. Ibrahim, S.I. Sinar Mashuri, et al., Preparation of Na_2O supported CNTs nanocatalyst for efficient biodiesel production from waste-oil, Energy Conversion and Management 205 (2020) 112445. Available from: https://doi.org/10.1016/j.enconman.2019.112445.

[44] KEIM Mineral Paints, KEIM Soldalit®-ME − an exterior sol-silicate photocatalytic mineral paint, n.d. https://www.keimpaints.co.uk/mineral-products/keim-exterior-paints/soldalit-me/.

[45] EXOCOAT Technology | Axcentive, n.d. https://www.axcentive.com/smart-coatings/exo-coat-technology/ (accessed June 6, 2022).
[46] J. Rangineni, Photocatalytic tiles: uses and limits, 2011. https://www.tile-magazine.com/articles/86384-photocatalytic-tiles-uses-and-limits.
[47] R. Ameta, S.C. Ameta, Photocatalysis: Principles and Applications, CRC Press, 2017.
[48] A. Shakeri, D. Yip, M. Badv, S. Imani, M. Sanjari, T. Didar, Self-cleaning ceramic tiles produced via stable coating of TiO_2 nanoparticles, Materials 11 (2018) 1003. Available from: https://doi.org/10.3390/ma11061003.
[49] A.L. da Silva, M. Dondi, M. Raimondo, D. Hotza, Photocatalytic ceramic tiles: challenges and technological solutions, Journal of the European Ceramic Society 38 (2018) 1002−1017. Available from: https://doi.org/10.1016/j.jeurceramsoc.2017.11.039.
[50] R. Ameta, S. Benjamin, A. Ameta, S.C. Ameta, Photocatalytic degradation of organic pollutants: a review, Materials Science Forum 734 (2012) 247−272. Available from: https://doi.org/10.4028/http://www.scientific.net/MSF.734.247.
[51] D. Synnott, N. Nolan, D. Ryan, J. Colreavy, S.C. Pillai, Self-cleaning tiles and glasses for eco-efficient buildings, Nanotechnology in Eco-Efficient Construction: Materials, Processes and Applications, Elsevier Ltd., 2013, pp. 327−342. Available from: https://doi.org/10.1533/9780857098832.3.327.
[52] Q. Jiang, T. Qi, T. Yang, Y. Liu, Ceramic tiles for photocatalytic removal of NO in indoor and outdoor air under visible light, Building and Environment 158 (2019) 94−103. Available from: https://doi.org/10.1016/j.buildenv.2019.05.014.
[53] Iris ceramica, Where design and science meet, beauty and well-being live, n.d. https://www.irisceramica.com/active-surfaces.
[54] HYDROTECT | Tile | Products | TOTO GLOBAL SITE, n.d. https://jp.toto.com/en/products/tile/hydro/ (accessed June 6, 2022).
[55] Hydrotect tile|NITTAI-KOGYO Co., Ltd. − The experts in tiles, n.d. https://www.nittai-kogyo.co.jp/english/information/hydro.html (accessed June 6, 2022).
[56] A. Zaleska, A. Hanel, M. Nischk, Photocatalytic air purification, Recent Patents on Engineering 4 (2011) 200−216. Available from: https://doi.org/10.2174/187221210794578637.
[57] M. Sagir, M.B. Tahir, U. Waheed, M.H. Qasim, Role of photocatalysts in air purification, Encyclopedia of Smart Materials (2022) 597−603. Available from: https://doi.org/10.1016/b978-0-12-815732-9.00003-6.
[58] L. Zhong, F. Haghighat, Photocatalytic air cleaners and materials technologies − abilities and limitations, Building and Environment 91 (2015) 191−203. Available from: https://doi.org/10.1016/j.buildenv.2015.01.033.
[59] Deodorising Photocatalytic Air Purifiers | Airtech System Taiwan, n.d. https://www.airtech.com.tw/pro-deodorising-photocatalytic-air-purifiers.html (accessed June 6, 2022).
[60] J.G. Mahy, C.A. Paez, J. Hollevoet, L. Courard, E. Boonen, S.D. Lambert, Durable photocatalytic thin coatings for road applications, Construction and Building Materials 215 (2019) 422−434. Available from: https://doi.org/10.1016/j.conbuildmat.2019.04.222.
[61] Pavement Technology Inc., PlusTITM Ti-intro CME® all-purpose penetrant, n.d. https://www.pavetechinc.com/pollution-reducing-penetrant/ (accessed June 8, 2022).
[62] W. Raza, S.M. Faisal, M. Owais, D. Bahnemann, M. Muneer, Facile fabrication of highly efficient modified ZnO photocatalyst with enhanced photocatalytic, antibacterial and anticancer activity, RSC Advances 6 (2016) 78335−78350. Available from: https://doi.org/10.1039/C6RA06774C.
[63] S. Sepahvand, S. Farhadi, Fullerene-modified magnetic silver phosphate ($Ag_3PO_4/Fe_3O_4/C_{60}$) nanocomposites: hydrothermal synthesis, characterization and study of

photocatalytic, catalytic and antibacterial activities, RSC Advances 8 (2018) 10124–10140. Available from: https://doi.org/10.1039/C8RA00069G.

[64] M. Gong, S. Xiao, X. Yu, C. Dong, J. Ji, D. Zhang, et al., Research progress of photocatalytic sterilization over semiconductors, RSC Advances 9 (2019) 19278–19284. Available from: https://doi.org/10.1039/C9RA01826C.

[65] P.V. Laxma Reddy, B. Kavitha, P.A. Kumar Reddy, K.-H. Kim, TiO_2 -based photocatalytic disinfection of microbes in aqueous media: a review, Environmental Research 154 (2017) 296–303. Available from: https://doi.org/10.1016/j.envres.2017.01.018.

[66] TurnedK, Photocatalyts sterilization and deodorization device, n.d. https://turnedk.com/en/kl-b01/.

[67] K. Tagawa, Photocatalyst technology adds value to fabric, 2005. https://fabricarchitecture-mag.com/2005/05/01/photocatalyst-technology-adds-value-to-fabric/.

[68] M. Salat, P. Petkova, J. Hoyo, I. Perelshtein, A. Gedanken, T. Tzanov, Durable antimicrobial cotton textiles coated sonochemically with ZnO nanoparticles embedded in an in-situ enzymatically generated bioadhesive, Carbohydrate Polymers 189 (2018) 198–203. Available from: https://doi.org/10.1016/j.carbpol.2018.02.033.

[69] G. Zhang, D. Wang, J. Yan, Y. Xiao, W. Gu, C. Zang, Study on the photocatalytic and antibacterial properties of TiO_2 nanoparticles-coated cotton fabrics, Materials 12 (2019) 2010. Available from: https://doi.org/10.3390/ma12122010.

[70] M.J. Uddin, F. Cesano, D. Scarano, F. Bonino, G. Agostini, G. Spoto, et al., Cotton textile fibres coated by Au/TiO_2 films: synthesis, characterization and self cleaning properties, Journal of Photochemistry and Photobiology A: Chemistry 199 (2008) 64–72. Available from: https://doi.org/10.1016/j.jphotochem.2008.05.004.

[71] H.M. Ahmed, M.M. Abdellatif, S. Ibrahim, F.H.H. Abdellatif, Mini-emulsified Copolymer/Silica nanocomposite as effective binder and self-cleaning for textiles coating, Progress in Organic Coatings 129 (2019) 52–58. Available from: https://doi.org/10.1016/j.porgcoat.2019.01.002.

[72] A. Synytska, R. Khanum, L. Ionov, C. Cherif, C. Bellmann, Water-repellent textile via decorating fibers with amphiphilic janus particles, ACS Applied Materials & Interfaces 3 (2011) 1216–1220. Available from: https://doi.org/10.1021/am200033u.

[73] J. Yu, Z. Pang, C. Zheng, T. Zhou, J. Zhang, H. Zhou, et al., Cotton fabric finished by PANI/TiO_2 with multifunctions of conductivity, anti-ultraviolet and photocatalysis activity, Applied Surface Science 470 (2019) 84–90. Available from: https://doi.org/10.1016/j.apsusc.2018.11.112.

[74] S.E. Mancebo, J.Y. Hu, S.Q. Wang, Sunscreens, Dermatologic Clinics 32 (2014) 427–438. Available from: https://doi.org/10.1016/j.det.2014.03.011.

[75] DSM UV filter PARSOL® TX fully compliant with latest SCCS opinions on nano form of titanium dioxide, n.d. https://www.dsm.com/personal-care/en_US/events-and-news/press-releases/2014/11-02-filter-parsol-tx-compliant.html (accessed June 7, 2022).

Chapter 9

Future challenges for photocatalytic materials

Mohammad Mansoob Khan

9.1 Introduction

Photocatalysis using semiconductors is certainly an appropriate tool in dealing with environmental applications such as wastewater treatment, biological applications, and energy-related applications [1]. It is a promising method to be used to help and solve world environmental issues and it is an important technique to work on. Several recent advances in photocatalysis have been understood by the selective control of the morphology of nanomaterials, element doping, design of photocatalytic reactors, and porous material support [2]. However, there are extensive challenges to the production of high-quality semiconductor nanomaterials. It is crucial to search for new modification methods to improve the transfer efficiency of the charge carrier which leads to the reduction in the recombination of electrons ($\bar{e}$s) and holes (h^+s). A survey shows that efforts in exploring suitable materials and attempts to optimize their band gap energy tuning for the design and fabrication of advanced photocatalysts in the context of nanotechnology have been introduced. Additionally, other features, such as morphological architecture, choice of semiconductor materials, and surface properties affecting photocatalysis, have been considered when designing a stable and efficient photocatalyst material. The present theoretical understanding of key aspects of photocatalytic materials is progressing at its pace [3].

As photocatalysis offers excellent prospects for the treatment of wastewater or pretreatment of drinking water and other environmental issues, it needs further in-depth research and understanding. However, the commercialization of such techniques yet suffers many interferences and there are many areas where the technology could be further improved, such as the design and efficiency of the photocatalysts, operation conditions, and reactor design. As of today, the design and operation conditions of the proposed reactor are fairly reliable for small-scale applications. However, to effectively use the technology on a larger scale, it is important to explore all available options to

Theoretical Concepts of Photocatalysis. DOI: https://doi.org/10.1016/B978-0-323-95191-3.00014-6

enhance the activity of photocatalysts and understand the underlying mechanisms of photocatalytic degradation of pollutants and disinfection. Apart from this, measuring the degree of pollutant's mineralization gives a better value to any study of photocatalytic degradation of pollutants. It is also important to design photocatalytic reactors to be energy efficient and determine the appropriate reaction conditions based on pollutant concentration and type, keeping in mind the possible influence of interfering parameters and compounds present in real water bodies and other related items [4].

The prospects of using semiconductor nanomaterials in photocatalysis offer a range of unique advantages related to spatially extended charge separation and visible-light absorption, which have been confirmed through a convincing performance in reducing half-reactions. However, for such systems to become practical, additional challenges need to be resolved. These challenges include photocorrosion, short-excited state lifetimes of charge carriers, and poor control over energy transfer to catalytic sites of the semiconductors. To resolve these issues, several emerging strategies have been proposed and discussed. Among potential solutions, utilizing nanocrystals as triplet sensitizers of photoredox coordination compounds is expected to enhance the absorption characteristics while decreasing the damage to the semiconductor. Assemblies of inorganic colloids can also be used for directing the photoinduced energy to reactive sites like the action of chlorophylls in PSII. Such materials having this geometry and type could inspire a cascade-like design of photosynthetic assemblies for water oxidation and other photocatalytic applications [3].

In short, a photocatalyst absorbs photons with an energy that is larger than the band gap energy and this generates electron−hole pairs within the conduction band (CB) and valence band (VB) which initiate redox reactions. In ideal conditions, continuous photocatalysis is used for the removal of pollutants or maintaining the release of waste and pollutants into the environment [5]. Other than that, as non-renewable energy tends to deplete over time, the search for alternative and greener sources has developed and increased as it is important for the future. Photocatalysis provides such an alternative to save energy as well. Such an example is by utilizing solar photoreactions. Solar photoreactions were studied and extensively applied in various ways in different industries such as fine chemical production, architecture and construction, water and air treatment, hygiene and sanitation, environmental protection, and the automotive industry [6].

Apart from the above, photocatalysis can help in alternative sources of energy and help in the reduction of waste and pollutants to the environment. It also plays potential roles in the medicinal world. Photocatalysis can also help in biomedical sensors such as anticancer applications and antibacterial applications. As redox processes can yield free scavenging radicals, these free radicals can effectively help in degrading any unwanted substances such

as toxic substances or even reactive cancer cells in the body [7]. Hence, photocatalysis can be used in laboratories for commercial purposes.

The following sections explore some of the selected photocatalytic applications. These applications are still in their initial and progressing stages.

9.2 Energy production using photocatalysis

Hydrogen can be considered an alternative to fossil fuels as it is a renewable, zero-emission fuel, and environmentally friendly [8]. Currently, green and inexpensive techniques for H_2 generation have gained interest for photocatalyst researchers. Among all other factors, to accomplish the overall water splitting reaction, the band position (VB and CB) of the photocatalyst should locate in an inappropriate position. Therefore, the lowest energy level of CB should be more negative than the hydrogen evolution potential and the highest energy level of the VB should be more positive than the oxygen evolution potential [9]. Moreover, pH, charge transfer and separation, charge recombination, and light intensity are among the other factors that affect the efficiency of hydrogen production [10].

In the last decade, in the search for visible-light responsive photocatalysts, significant effort has been made for the development of active sites on photocatalysts and explaining reaction mechanisms, which led to significant progress in the field of heterogeneous photocatalysis for H_2O splitting. Photocatalysts such as $Rh_{2-y}Cr_yO_3$-loaded GaN:ZnO (one-step water splitting system) and a two-step system consisting of $Pt/ZrO_2/TaON$ and Pt/WO_3 with an IO_3^-/I^- shuttle redox mediator have been developed, with respective apparent quantum yields of about 5.1% at 410 nm and 6.3% at 420.5 nm. However, researchers continue to search for more active photocatalytic systems which are capable of harvesting more visible-light photons. Solar energy conversion efficiency increases when one can achieve overall H_2O splitting under visible-light irradiation, i.e., longer wavelength. This is because the number of available photons in the solar spectrum increases with the increase of the wavelength.

In relation to such a system processing, a unique reactor for photoelectrochemical H_2 production was proposed as shown in Fig. 9.1. The development of a photocatalyst with a wider absorption band is highly desirable. While there is an activation barrier for surface chemical reactions that evolve H_2 and O_2 gas, a photocatalyst with a 600 nm absorption edge would be optimal. Recently developed materials, such as $LaTiO_2N$, Ta_3N_5, and $Sm_2Ti_2S_2O_5$, have a band gap of $\sim$2.0 eV (an absorption edge near 600 nm). Although, the photocatalytic activities of these 600 nm class materials are insufficient to achieve overall water splitting at present. Recent progress in materials chemistry toward reducing the density of defects should enable the use of such materials. Fortunately, in a two-step water splitting system, the absorption wavelengths available for H_2 and O_2 formation have been

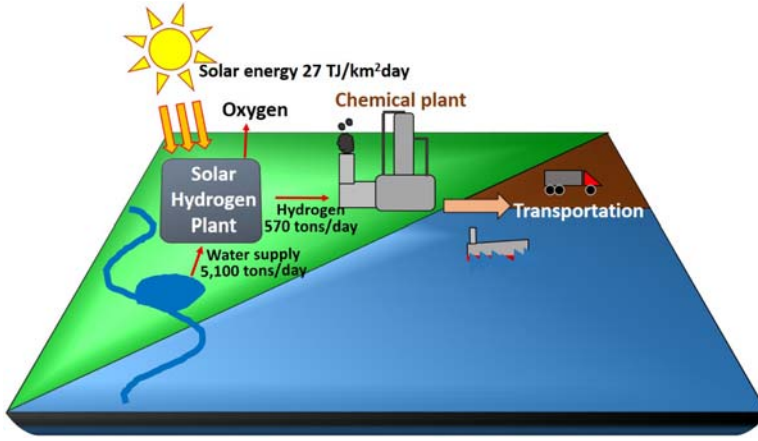

FIGURE 9.1 A possible scheme for large-scale water splitting for H_2 production using sunlight.

increased to 660 nm (using $BaTaO_2N_{12}$) and 600 nm (using Ta_3N_5), respectively. It is also significant to examine the type of defects in photocatalysts, which can facilitate undesirable electron−hole recombination because less than 10% of the incident photons are used by current reaction systems for overall photocatalytic water splitting [11].

Designing a promising visible-light absorber material that has favorable band alignment for H_2O oxidation that possesses a relatively long photo lifetime is an obligatory requisite. This type of new material should not be restricted by poor carrier transport, deviations from ideal stoichiometry, and other defects. In particular, the selection of materials and approaches for future innovations is quite limited for surface protection, surface-state passivation, and selective charge extraction. New deposition approaches would be needed to fabricate promising materials that are semiconductor sensitive. For this purpose, extensive knowledge is required regarding interface energetics, the dynamic behaviors of interfaces during operation, and the electrolyte and temperature dependence of interface properties to design robust interfaces.

Although significant development has been made in this area in the past decade, continuous growth is required for a proper understanding of surface and interface engineering. This is to meet the demand for the progress of photoanodes with higher efficiencies in the practical application of photoelectrochemical water splitting. It is necessary to improve the understanding of the limitations of numerous surface modifications and how different parameters are involved in charge separation. The choice of the right amalgamation may be possible by considering the transport mechanism of different semiconductors, thereby helping to reduce the risk that may arise because of potential materials which help to accelerate the development of material

screening. Finally, the problem related to charge transport could be solved by developing a strong theoretical base in addition to knowledge regarding computational optimization and experimental skill. All of these would enable the design of novel materials for innovative research and applications [12].

Some of the challenges in photocatalytic water splitting are stated below [13,14]:

- The production of renewable hydrogen is an appealing solution to the energy crisis and environmental pollution. It is expected that about 10% solar to hydrogen (STH) conversion of a 2,500,000 km^2 area can provide one-third of the energy needed. However, conventional photovoltaic (PV)-assisted photoelectrochemical cells (PEC) are expensive and complex to design on a large scale even though PV-assisted PEC manifests high STH conversion efficiencies [15].
- Cost-effective and flexible particulate photocatalytic H_2O splitting systems are shown to have superiority over the PEC system. However, achieving STH conversion of 10% is also challenging. The photocatalysts should absorb the visible light of wavelength 600 nm with an apparent quantum efficiency (AQE) value of more than 60%. One way to overcome this is to drive the oxidation and reduction of water efficiently. This requires a minimum band gap of more than 2.0 eV which overall restricts the performance of a photocatalyst [16].
- The charge (electron−hole pair) recombination is also one of the major challenges regarding photocatalytic water splitting. It is also important to investigate the nature of the defects, which can facilitate the undesirable electron−hole recombination in photocatalysts because fewer than 10% of the incident photons are used by current reaction systems for photocatalytic overall water splitting.
- There are multiple strategies to improve STH efficiency which include metal-doping. However, finding suitable dopants has also become a challenge as well as finding the optimum amount of the dopant. Besides, more studies should be focused on finding a cheap dopant in exchange for expensive noble-metal dopants. Moreover, a suitable sacrificial reagent used as a hole scavenger in the hydrogen production reaction should be studied as well [8].
- Various effective UV-light-responsive photocatalysts have been well established, although most of them suffer from photocorrosion and are not active under visible light which accounts for 45% of the energy of the solar spectrum. The photocorrosion phenomena are the major challenges, which lower the overall photocatalytic performance. Therefore, designing visible-light-driven photocatalysts for water splitting represents a major mission for photocatalytic water splitting to maximize solar energy conversion and storage [13].
- A technology to separate simultaneously produced H_2 and O_2 would be required. The system-processing study, including the construction of the

water splitting reactor, H_2 and O_2 gas separator, a solar hydrogen chemical plant, and so on, is expected to be more important for realizing practical application in the future [15].

- Backward reaction: H_2 and O_2 are produced in the same environment, and they can back react to form water. This is an unfortunate event because it implies a loss of products, and thus, a loss of energy/efficiency. To achieve high efficiency of photocatalytic water splitting, this back-reaction must be avoided. Therefore, modifications and optimization to suppress the water formation reaction (water splitting back reaction) are required.
- Sluggish kinetics: The first step of water splitting, the O_2 evolution reaction, is a thermodynamically uphill reaction that involves a four-electron oxidation process of water molecules. It leads to the sluggish water oxidation kinetics of many promising semiconductors. The use of cocatalysts has been an established approach to accelerate the sluggish water oxidation kinetics for water splitting. While many single cocatalyst configurations have been well documented, cocatalytic systems that consist of multiple components with different functions may allow for better performance.
- Another concerning factor is the impractical typical photoreactor which includes the photocatalyst particles being stirred in the water suspension. This needs to be studied more as additional energy input is required during stirring. Therefore, sheet-like systems fixed on solid plates can be promising in exchange for catalytic materials [17].

9.3 Photocatalysis in environmental aspects

The implementation of green approaches has been investigated in the past few decades for the removal of various pollutants in the environment. Pollutants, such as organic molecules, toxic and harmful gases, and heavy metal ions can be degraded, mineralized, or reduced to harmless inorganic substances through photocatalytic reaction [18]. Many technological processes produce unwanted by-products, which give rise to pollution and reduce natural resources, hence, damaging the environment. Applications of new technology influence the values and culture of a society and frequently pose new ethical questions. To improve any present systems in society, it is normal practice that such systems must be compared with a hypothetical and predicted system known as the "ideal system." The word "Ideal system" refers to a system that has ideal characteristics, i.e., perfect in all means. It is what the mind pictures as being perfect. The concept of ideal engine, ideal switch, ideal voltage source, ideal current source, and ideal semiconductor devices like ideal diodes, ideal transistors, and amplifiers have been defined and taken as standards to improve the quality and performance of such practical devices or systems. It is found that, by keeping such hypothetical

devices or systems in mind, researchers have continuously been improving the characteristics and properties of practical devices and systems to upgrade their performances. Hence, an ideal technology model is essential to plan the improvement in the performance of any practical technology. The concept of ideal technology can be predicted as a technology that can solve all basic needs of human beings and provide luxurious comfortable life without affecting the society and environment. Ideal technology should have characteristics to elevate the quality of life to a unique level with perfect equality so that every human being in this universe should lead a happy and comfortable life and understand the so-called concept of heaven on earth. Based on various factors which decide the characteristics of an ideal technology system, a model consisting of input conditions, output conditions, system requirements, and environmental conditions should be proposed. The following are such important properties and conditions.

The important input conditions/properties are

1. Manipulate the fundamental nature of matter to provide solutions to basic and advanced problems of human beings.
2. Inexpensive and self-reliable in terms of resources to make it attractive to be used by people and countries of varied economic situations.
3. Global so that the technology provides solutions and services at any time, anywhere, and at any amount of time to the users.
4. Affordable to everyone so that it uses common materials available in nature and manipulate effectively to the need of human beings at an affordable price.

The important output conditions/properties are

1. Solve basic needs like food, drinking water, renewable energy, clothing, shelter, health, and a clean environment.
2. Provide comfortable life to the users by providing solutions to their needs.
3. Equality—ideal technology provides equal opportunity and similar solutions to every user irrespective of their gender, education, background, economic status, religion, and country of origin.
4. Automation—ideal technology automates all processes in every type of industry to avoid human interference in work/control to provide an expected output based on programming.
5. Immortality is the ultimate goal of ideal technology so that it can create a path for the permanent situation or enhancement of the human life span.

The important system requirements are

1. General purpose technology to support all fields and problems of human and living beings on the earth.
2. Self-directed, self-controlled, and self-regulated so that the technology can control itself to achieve its goal.

3. Easy, simple, quick, and user-friendly to solve all types of problems and to provide a quick ideal solution.
4. Scalable so that it is used for solving small and simple problems to large and complex problems of life.
5. Expert in identifying and solving problems and providing comfort to human beings.
6. Exploring new opportunities to improve and discover comfortability and freedom in the life of people.
7. Infinite potential for further development of life in the universe.

The important environment and external properties are

1. Maintain a clean environment through its processes and avoid the footprint of processes while achieving specific functions.
2. Infinite business opportunities by creating new products and services with ideal characteristics.
3. Adaptive to any situation to achieve the stated goal.
4. No side effects so it should be safe for users and the environment.

Any technology which has the above properties and characteristics is considered an ideal technology and conventional technologies have serious drawbacks or limitations in terms of the above properties [19].

The advancement in photocatalysis to cure environmental pollutants and dye-contaminated industrial effluents is by categorizing the photocatalysts into three generations. First-generation photocatalysts proved to be inadequate for dye removal as they were limited by their large band gap energy and interfacial charge recombination. With the progress in this research field, better knowledge of diverse functional properties (e.g., the optoelectronic, physical, and band gap characteristics) has unlocked a new avenue to develop a second generation of photocatalysts. Among photocatalysts, the second-generation photocatalysts were studied most extensively due to their excellent charge separation, faster reaction kinetics, visible light utilization, and remarkable quantum yields (QYs) for dye degradation and other organic pollutants removal. To expand the photocatalyst applications to an industrial scale, the post-separation problems associated with the first- and second-generation materials were addressed by the third-generation photocatalysts. The low QYs of the third-generation photocatalysts (e.g., due to reduced surface area and reaction sites after deposition) presented a new opportunity to develop and improve immobilization technologies [20].

Besides the design of the photocatalysts, the underlying mechanisms that govern the photocatalytic degradation process are of immense importance. In this regard, the Z-scheme mechanism that duplicates the natural degradation process of chlorophyll is ideal for designing photocatalysts for dye degradation. Moderate reusability and low catalyst dosage ($100-200\ g/m^3$) are also advantageous for wastewater treatment and other organic pollutants removal.

The uncertainties regarding process parameters, material design, and treatment of real wastewater make an impression of doubt toward photocatalysts. However, the limitations and challenges that currently undermine the industrial applications of photocatalysts can be resolved. In short, the third-generation materials hold tremendous potential for the future of wastewater treatment on an industrial scale and other related applications [19].

Therefore, the main challenges of photocatalysis for a green and clean environment are as follows [21]:

- Slow reaction process and low ROSs transformation: By considering the working conditions (type of light, the concentration of pollutants, type and dosage of catalyst, presence of interfering species, pH, etc.), it could be deduced in general that the photocatalytic technology alone is not fast enough to be competitive concerning other existing technologies.
- Photocatalyst deactivation: Industrial applications require continuous processing. Unfortunately, photocatalytic materials suffer from the issue of surface deactivation after a certain time of use which requires stopping the process and a regeneration step is needed.
- Complicated synthesis of photocatalysts and unconvincing testing: The majority of photocatalytic materials are not suitable for real use, not because of efficiency or stability, but due to the use of expensive reagents along with very long and complicated synthesis procedures to prepare a few grams of photocatalytic materials [22]. Moreover, in the tests to evaluate the photocatalysts, most research studies report the photoactivity of the materials toward the removal of single pollutants under well-controlled lab-scale conditions that are far away from the real environment.
- Although photocatalysts for environmental remediation are highly studied nowadays, the usage of harsh chemicals and conditions to produce photocatalysts are mainly used. This might become a major threat to the environment. Therefore, the synthesis methods must be green, facile, energy efficient, high-throughput, and more feasible for large-scale manufacturing.
- The amount of photocatalysts used is another concern as a higher amount of photocatalysts suspended in water will aggregate together and might become a threat to the water system or environment. Therefore, producing effective photocatalysts and using only a small amount of the photocatalysts will become another challenge.
- Many applications of environmental remediation require sacrificial agents or noble-metal cocatalysts to improve the activities. These are normally not eco-friendly apart from them being expensive. Tuning the photocatalysts' properties becomes a challenge to producing efficient photocatalysts.
- Since it is reported that photocatalysis in the environment is mostly dependent on the shape and size of the photocatalysts, therefore, controlled production of photocatalyst particles is highly recommended.

9.4 Water purification and disinfection using photocatalysis

Solar photocatalysis is often cited as a possible solution for ensuring a safe drinking water supply in developing countries. While the main challenge in developed countries is the maintenance of existing infrastructure and the treatment of wastewater, in developing countries, the priority is obtaining safe drinking water by eradicating pathogenic microorganisms. Similar to water treatment for pollutant removal, despite successes in lab-scale experiments, industrial-scale photocatalytic disinfection is impractical [23].

Other challenges to the drinking water supply in developing countries include the natural scarcity of water sources in several areas. Floods can produce more siltation problems in river systems as well as the contamination of rivers and large dams giving rise to source receptor issues. Climate change and water scarcity are also some of the concerns. Stratification problems in lake abstraction points and aeration of abstraction points to break down the thermocline layer are needed which require much energy. Poor access to water and poor water resource management must be addressed. Poor water productivity in the agricultural sector can impact water quality. Water affordability issues and the challenges of investing in water infrastructure need to be addressed. Storage and confidence in storage facility containers to prevent contamination need education and awareness of cross-contamination [20].

Nowadays, significant technologies such as reverse osmosis have been extensively implemented to produce clean water from seawater. However, practical applications are limited by the high expense and energy consumption. Therefore, the research and development of cost-effective, low-energy-intensive, scalable manufacturing, and efficient freshwater products are in-demand [24].

Solar-driven photocatalysis certainly represents one of the most promising and alternative water disinfection technologies. Compared with the traditional bulk materials, these photocatalysts with low-dimensional nanostructures (i.e., 0D, 1D, and 2D nanostructures) possess excellent optical and photocatalytic activities due to high $\bar{e} - h^+$ separation efficiency and large surface area providing more active sites. Remarkable research opportunities lie in the development of nanophotocatalysts with the design of different sizes and morphologies for various microorganism inactivation and treatments (Fig. 9.2).

Following research fields for the photocatalyst design and developments need to be paid particular attention to

1. The development of controllable synthetic methods for 0D, 1D, and 2D low-dimensional nanomaterials with desired size, morphology, and surface functionalization still poses challenges and needs further exploration. The key strategy is to control the crystal nucleation and growth process. For instance, to grow a 1D nanostructure, it has to promote the growth of one dimension while limiting the other two dimensions based on crystal

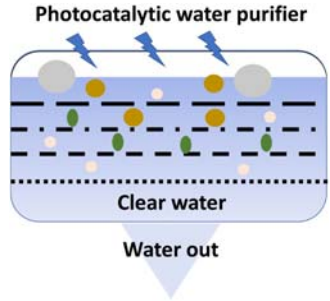

FIGURE 9.2 A schematic diagram of the photocatalytic water purification process.

structure asymmetry by adding organic ligands, surfactants, or hard/soft templates. Several wet chemical methods, such as the hot-injection pyrolysis, liquid−solid−solution (LSS) strategy, and reverse microemulsion route are useful for the synthesis of monodisperse nanoparticles with controlled dimension by precisely adjusting the precursor's type and concentration. Furthermore, the "bottom-up" self-assembly technology to construct hierarchical nanostructures and their underlining structure−property relationship in photocatalytic bacterial inactivation is also important and could be one of the future research directions.

2. From the environmental point of view, metal-free photocatalysts, especially elemental photocatalysts such as red phosphorus and α-sulfur, have shown much more promising indications to achieve cost-effective photocatalytic applications, as these photocatalysts consist of only one element. However, the photocatalytic inactivation efficiency of these photocatalysts is still far from acceptable for practical application. To further improve the photocatalytic bactericidal activity of these photocatalysts, the known strategies such as heterostructuring, doping heteroatoms, nanoscaling, and faceting, which are extensively used in traditional semiconductor photocatalysts, can be applied to modify the elemental photocatalysts to achieve the goals.
3. Chemically synthetic photocatalysts have displayed their significant role as highly efficient photocatalysts but are limited by complicated fabrication procedures, low quantity (in several grams), and high costs. In this regard, naturally occurring minerals may be the most favorable photocatalysts due to their extremely low costs that can be readily obtained in large amounts. One of the disadvantages that hamper the application of natural minerals is the large particle size. To overcome this, further downsizing of the natural mineral particles into nanoscale by ball milling, in addition to simple heat treatment to increase crystallinity or trigger phase transformation to make nano-heterojunctions, could be a promising approach.

4. Current studies about the photocatalyst design have evolved from UV light to visible light region. However, the studies intended to utilize near-infrared (NIR) light, although the NIR light constitutes ~44% of the solar spectrum, are rather limited compared with the overwhelmed studies on visible-light-driven (VLD) photocatalysts. Developing NIR-driven photocatalysts by using up conversion materials is highly desired to combine with UV and VLD photocatalysts. Thus, eventually achieving full spectrum solar-driven photocatalysts for water disinfection.
5. It is well known that photocatalytic bacterial inactivation is based on reactive species (RSs) formation that shows no oxidation selectivity. All types of microorganisms, no matter harmful or not, will be removed without any preference. In this regard, much effort is needed to design molecular imprinting photocatalysts based on the specific cell surface for selective inactivation of particular microorganisms with high efficiency.
6. Besides the development of photocatalysts, important issues about catalyst immobilization, recycling methods, photocatalytic reactor design as well as optimization of disinfection parameters need to be addressed for future practical applications. In addition, the photostability of these emerging nanostructured materials also needs to be taken into consideration for practical use. Although these issues still pose challenges, it is expected that the next few years will bring major advancements in both basic and applied research in solar-driven photocatalytic water disinfection using various natural and synthesized nanostructured materials [25].
7. Photothermal-assisted photocatalytic pollutant degradation, sterilization, and H_2 production have been validated to generate fresh water, although several challenges need to be addressed. For example, the exploration of the fundamental mechanism of photothermal-assisted photocatalysis as well as the optimization of hybrid composites in terms of photothermal materials [24].

9.5 Photocatalysis in biomedical aspects

Among various semiconductor photocatalysts, metal oxide, such as TiO_2, has proven to be the most widely used, owing to its long-term photostability, low toxicity, strong oxidizing power, and ease of availability. To emphasize the vital importance of TiO_2, which is promising to benefit human beings, the primary studies on biomedical applications of TiO_2 during the past decade, such as photodynamic therapy (PDT) for cancer, drug delivery system, cell imaging, biosensor, and genetic engineering are being investigated. Other biomedical applications of TiO_2 are also beneficial to human beings.

For example, with the extended life span, the need for medical implants, which are used to replace or act as a fraction of the whole biological structure, has also increased. Owing to its biocompatibility, TiO_2-based implants have been widely used in clinics, particularly in orthopedics and dental

implant procedures, giving hope to millions of patients. The reactive oxygen species (ROS) induced by photoactivated TiO_2 can kill not only cancer cells (Fig. 9.3), but also many pathogenic organisms, such as bacteria and fungi. Consequently, TiO_2 is also considered an effective antimicrobial drug.

In addition, TiO_2 irradiated by UV light could increase the chemotherapeutic drug accumulation in targeted cancer cells, inhibiting the multiple drug resistance, which is the main hurdle to the successful consequence of chemotherapy. Furthermore, it has been reported that TiO_2 can also be irradiated by ultrasound, resulting in its application as a new material to treat cancer and infection. Despite the promising biomedical applications of TiO_2, certainly, there are still some challenges that need to be undertaken as soon as possible, to make TiO_2 beneficial for human beings to the utmost soon (Fig. 9.4) [26–28].

1. Among all the biomedical applications, TiO_2-based implants have been successfully applied in clinics, especially in orthopedics and dentistry, while most of the investigations are confined in vivo and/or in vitro. Moreover, many scientists have focused on the modifications of this semiconductor material to improve its efficiency and extend its applications. The results showed that some of these modifications are effective. However, relative studies between different methods have been rarely performed. Thus, until now, there has been no consensus on the best. In the twenty-first century, translational medicine is certain to become a new concept and a new direction in the medical field. Therefore, it is authoritative for researchers to develop controlled and standardized research to find out the optimal TiO_2 or TiO_2 nanocomposites, and then, perform research in vivo and in vitro, with the reasonable help of doctors, nurses, and pharmacists. In this way, TiO_2 can ultimately be widely and successfully applied in clinics.

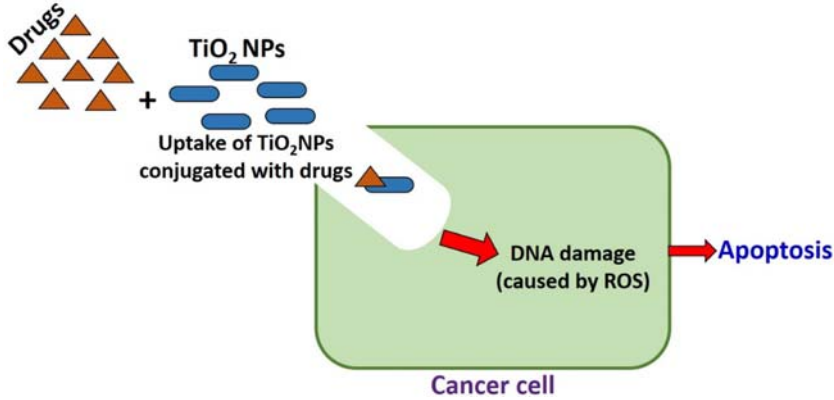

FIGURE 9.3 Schematic showing cancer treatment using TiO_2 nanoparticles.

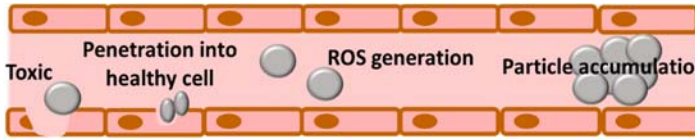

FIGURE 9.4 Schematic diagram of challenges in biomedical applications.

2. Compared with the validity, the safety issue of TiO_2 is even more important when assessing whether it could be used for human beings or not. The ROS (Fig. 9.3) generated by the illumination of TiO_2 is the basis of its biomedical applications, especially in PDT and genetic engineering. However, ROS generation has also been suggested for the cytotoxicity and other adverse effects of TiO_2 NPs. But previous investigations have shown that TiO_2 might have a potentially adverse effect on human health, particularly harming the lungs, brain, and skin. Therefore, the potentially toxic effects of TiO_2 and its nanocomposites on human health and the mechanisms underlining the process should be further studied. Besides, how to reduce the side effects should also be intensely investigated in the future.
3. The application of TiO_2 in PDT might be the widely reported research. However, there are some limitations to its practical use in the future. Mostly, UV light is not the best means of excitation in PDT owing to its shallow penetration depth and low content in the light. Furthermore, considering excessive exposure to UV light is the main risk cause of skin cancer. It is even unsafe to treat patients using UV light. So far, great efforts have been invested to extend the optical absorption of TiO_2 to the visible light region, which provides the basis for TiO_2 in treating skin diseases and natural orifices in the future. Compared with UV light and visible light, infrared rays and laser rays have deep penetration depth into tissues. Both of them have been applied in clinical trials, especially in cancer treatment. If TiO_2 can also be irradiated by infrared rays and/or laser rays, it will be quite interesting and needs to be confirmed. If so, then, TiO_2 as a promising approach can be applied to treat diseases that are located quite deeper.
4. Some new concepts should be proposed to fabricate new classes of nanocomposites featuring diagnostic and therapeutic properties. These multifunctional nanocomposites have potential applications in the early diagnosis and effective treatment of diseases. So far, rapid progress in science and technology has paved the way for the fabrication of such multifunctional TiO_2 nanocomposites. With careful confidence, the introduction of novel TiO_2 nanocomposites is expected, which can find out the targeted cells or tissues accurately in the early stage of diseases and bind with and remove the targeted cells precisely with high proficiency.

5. Gene therapy can not only be viewed as a modality in the treatment of genetic diseases but also be applied as a treatment for other diseases, such as cardiovascular disease and cancer, which are the foremost reasons for the death of human beings. The improvement of gene therapy is largely dependent on the development of genetic engineering tools. TiO_2 can be used as a light-inducible gene knock-out device, which may be an excellent tool for gene therapy. However, additional efforts need to be made in this field and there should be more progress. It is worthwhile to indicate that there is a bright future that lies ahead for TiO_2, which may be a great contribution to humankind. To achieve this, researchers from different disciplines should collaborate and work together to gain more achievements [27].
6. The hazardous effects of photocatalysts, especially in their nanoparticle forms, also drew the attention of many researchers. Several works to analyze the toxicity of the nanoparticles have been carried out. The studies reported the toxic effects of particles that have properties such as the small size of nanoparticles. Although the efficiency of the nanoparticles is increased with smaller particle size, this, however, could lead to the accumulation of particles inside undesired cells or tissues which can lead to toxic effects. Furthermore, size is inversely proportional to its mobility. Therefore, smaller particles have an immense mobility rate which can invade various internal tissues or cells. The accumulation leads to toxic effects and pathway blockage. Nevertheless, nanoparticles tend to aggregate to attain stability which sometimes leads to physiological abnormalities [29].
7. Another limitation is the increase in surface area of particles which leads to an increase in their chemical reactivity. This usually leads to the production of ROS that can cause oxidative stress, inflammation, and damage to DNA, proteins, and membranes. Changes in nanoparticle form and structure may lead to different properties in such a way that 100 nm particles are non-hazardous while 1 nm particles are toxic or vice versa. Furthermore, nanoparticles are highly dependent on environmental particles that may disintegrate or aggregate leading to toxicity [29].

9.6 Air purification using photocatalysis

Air pollution is rapidly increasing, transported, and more difficult to control than water pollution. As a result, its control and prevention pose several challenging issues in developed and developing countries. As air pollution is getting severe in many parts of the world, the need for clean air has increased, hence, demand for environment-friendly and more efficient air purification technologies is increasing. Photocatalysis is being actively investigated as a sustainable air purification technology because of its environmentally benign nature. It decomposes air pollutants into harmless CO_2 and

H_2O end products under ambient conditions, which makes it particularly suitable for indoor air purification.

Unlike other systems, for air purification, no chemicals or external energy input are needed, except for light, which is not expensive when using ambient light or sunlight. At present, the purification of photocatalytic air offers the following advantages:

- It can be used safely under environmental conditions and activity relatively insensitive to moisture.
- Large capacity to fully mineralize volatile organic compounds (VOCs) to CO_2 and H_2O.
- Unlike other options, the purification of photocatalytic air does not retain particles or contaminants as these are eradicated or transformed in their entirety.
- Most photocatalytic air purification systems do not require constant maintenance.

As the large purification capacity of the photocatalytic process is mainly based on the photon flux, photocatalytic air purification is most efficient when it is applied to air in a confined space like an indoor environment. However, there are two critical limitations of photocatalysis that delay its practical application for air purification, i.e., the limited utilization of ambient light (mostly visible light and IR) and fouling or deactivation of photocatalysts [30].

In recent years, visible light utilization has been the hot and most studied subject as well as the most wanted goal in environmental photocatalysis. However, it should be understood that visible light can be utilized at the expense of redox power. Visible light excitation produces less energetic electrons and holes than UV light excitation. Therefore, visible light-assisted photocatalytic degradation (PCD) cannot be efficient in degrading intractable air pollutants that need strong oxidants such as highly reactive free radicals $^{\bullet}OH$ and $O_2^{\bullet -}$. As a result, visible light photocatalysis is not always the best option for air purification applications and it should be the choice only when ambient visible light (e.g., room light, sunlight) is used as a light source. Visible light-assisted photocatalysts may not be essentially needed when UV light lamps can be installed inside an air cleaner blocking the possible exposure of harmful UV irradiation to human beings. However, considering that the most ideal way of utilizing photocatalysts for air cleaning (particularly indoor air) is to use ambient light with photocatalysts coated on the surface of indoor environments (e.g., windows, doors, walls, ceilings, and furniture) (Fig. 9.5). Alternatively, photocatalytic materials that should exceed TiO_2-based materials in visible light activity need to be developed.

Even though the expansion of visible light active nanomaterials is an exclusive part of photocatalytic air purification technology advancement, the present research appears to exaggerate this topic. Furthermore, despite many

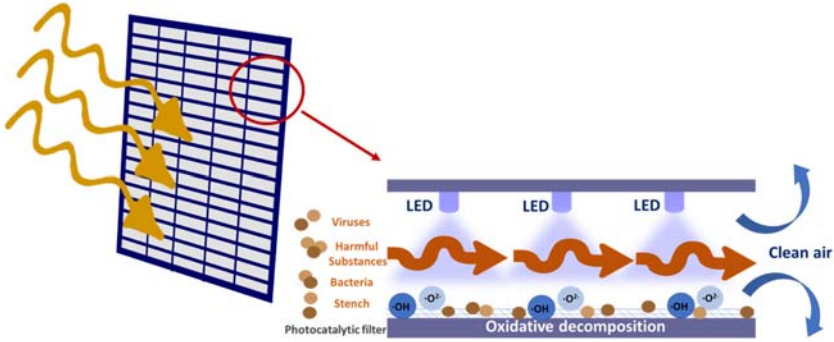

FIGURE 9.5 Schematic diagram of photocatalytic air purification.

photocatalytic materials reported in the literature, it is very difficult to compare their PCD performances on an objective basis and to identify the best photocatalytic material required for a specific case of air purification. Since each photocatalytic report showed different target VOCs and different experimental conditions. At the same time, there is a large gap between the laboratory research results and the requirements for practical applications. It should also be noted that the development of photoreactors and system engineering is mostly ignored, which can provide alternative solutions for enhancing the PCD performance of photocatalytic materials. Optimizing appropriate reactor design parameters may overcome serious hurdles (e.g., low photon absorption efficiency, mass transfer limitation, low surface area, catalyst deactivation, slow reaction kinetics, etc.) that currently delays the commercialization of photocatalytic air purification. Future research efforts on photocatalytic air purification should fill the gaps by providing missing knowledge and practical solutions for the commercialization of this technology. The following issues should be systematically and prudently addressed in future studies of photocatalytic air purification [30]:

1. The stability of the selected photocatalytic materials.
2. The efficiency of the PCD on the operation parameters (humidity, temperature, airflow rate, reactor volume and residence time, irradiation wavelength and intensity, photocatalyst loading, etc.)
3. Photocatalytic reactor and system design to achieve the given treatment goal of a target air system.
4. The formation of stable by-products has become the main issue as it is unavoidable under certain circumstances. Many by-products are known to be more toxic than the parent pollutant itself (e.g., CO production during photocatalytic degradation of methanol). Additional purification steps are required to minimize the production of by-products. Moreover, it can also be minimized by employing high reaction temperatures which are often at the expense of increased operational cost [31].

5. The photocatalytic air purification systems demand suitable sources of light energy. Furthermore, they show low mineralization efficiencies for the most difficult to remove pollutants and multiple by-products which make the systems unfeasible for real-world operation.
6. Specific operational challenges such as blockage of active surface sites of the catalyst due to the deposition of dust, salt, dirt, stones, etc., should be considered.
7. The optimization of reactor design for scale-up purposes should not be ignored. The reactor system should be effective in mass transfer processes and reaction kinetics for real-world applications.
8. The development of this technology is slow, as is the production of the materials needed for its operation. Most photocatalysis processes are still at an early stage, so more in-depth studies are needed to elucidate synergistic mechanisms and solve practical engineering problems.
9. Research in the field of photocatalysis should focus not only on scientific development but also on the resolution and attention to everyday problems related to poor air quality.
10. Photocatalyst fouling/deactivation [32].

9.7 Photocatalysis in the food-processing industry

Although photocatalytic properties of semiconductors have been utilized quite extensively in several application areas, such as optics, electronics, photovoltaics, solar cells, cosmetics, and environmental clean-up, their use in the food sector is relatively new, and most of the research in this area is still in its infancy. In the last decade, considerable efforts have been directed at the applications of semiconductor photocatalysis in the areas of food safety and food quality as shown in Fig. 9.6 [33–35].

Plastic packaging contributes to environmental issues resulting in the high demand for developing safe, smart, and active food packaging films. This is also to ensure fresh and safe food. For the past years, researchers have used biological macromolecules for developing degradable food packaging films for food preservation [36]. However, biomaterials such as biopolymeric films are hydrophilic and are not physically practical. Hence, they are limited applications in active packaging. Furthermore, microbial spoilage during storage has become one of the issues with packaging. Therefore, using active packaging films with antibacterial properties is required to avoid food-borne diseases [37].

TiO_2–assisted photocatalysis as a non-thermal antibacterial method offers an alternative approach for reducing the risks of microbial contamination on different types of food items including fruits, vegetables, drinks, etc. TiO_2–assisted photocatalysis can enhance food safety in solid, liquid, and gas phase food systems to maintain the food quality and shelf life. Improved disinfection efficiency can be obtained in liquid-phase systems in comparison

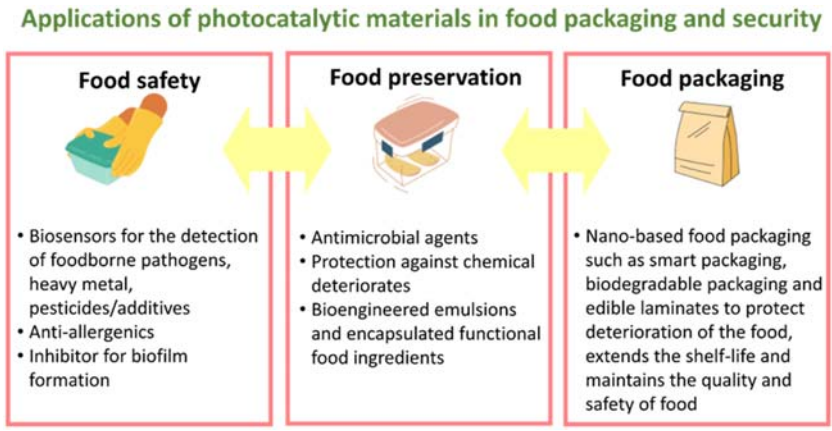

FIGURE 9.6 Example of applications of photocatalytic materials in the food-processing industry.

to solid- and gas-phase systems. The role of TiO_2 in gas phase systems is more likely to decompose ethylene ($H_2C = CH_2$, C_2H_4) from the surrounding ambient of postharvest products. On the other hand, for solid phase systems, the suspended TiO_2 with a higher surface area provides an improvement in the photocatalytic activity with more effective disinfection of microbes than the immobilized TiO_2. However, it is difficult to separate the photocatalyst from the suspension after usage. This is another greatest challenge for the researchers.

The photogenerated ROSs ($^{\bullet}OH$, $O_2^{\bullet -}$, etc.) are responsible for inactivating microorganisms and decomposing organic matter. The critical factors of photocatalytic disinfection and degradation are closely related to the ability of ROS generated during photoreaction processes and the possibility of the target to contact the surface of the catalyst. The formation of ROS is restricted by the excitation light source, and the TiO_2−assisted photocatalysis shows low utilization of visible light, which weakens the photoactivity and the efficiency of removal of targets by widening the range of light responses and minimizing the recombination of electron−hole pairs. The modification of TiO_2 provides a reasonable and effective approach to inhibiting bacterial growth in foods, especially for heat-sensitive products. It is worth stating that high photocatalytic activity can improve the efficiency of inactivation, but may also accelerate the oxidation, adversely affecting the sensual value of the products. Furthermore, the photoinduced ROS usually stays on the surface of the photocatalyst, and seldom migrates into other places or sites. Thus, limiting the application of TiO_2−assisted photocatalysis to a certain extent. The amalgamation of TiO_2−assisted photocatalysis with coating and packaging films offers suitability and practicality for using the technology in the food industry and the amalgamation of TiO_2−assisted

photocatalysis with high hydrostatic pressure (HHP) can also provide synergistic effects. Therefore, amalgamating TiO_2−assisted photocatalysis with other technologies utilizes the advantages of both TiO_2−assisted photocatalysis and the other techniques with outstanding disinfection efficiency. Future advances in modification of the technology and its amalgamation with other techniques should present great opportunities for improving photocatalytic antibacterial efficiency and enhancing food safety, shelf life, and quality for the food industry [34]. The applications of nanotechnology in the food industry have become more advanced; however, food nanotechnology is facing major challenges in terms of environmental issues and human health and safety [35]:

- Toxin accumulation might take place after long-term storage. This might be due to the gradual penetration of degraded photoactivated materials. Therefore, it is necessary to establish the safety of photoactivated materials before application [38].
- Innovative packaging that has multiple functions such as providing mechanical protection, gas and moisture barrier, antimicrobial and antioxidant properties, and detection of food quality and safety (smart materials) should be studied and created.
- Nanotoxicity: Uncertain cytotoxicity of the materials incorporated or migrated in food products.
- Consumer's health concern: Public concern for adverse effects and health hazards of nano-based food due to a lack of sufficient knowledge among the consumers about the risk factors.
- Environmental concern: Dissemination of toxic, persistent photocatalytic materials used in the food industry leading to harmful impacts on the environment.

9.8 Summary

Many applications have been using photocatalysts on a real-life scale to improve energy, environmental, air, and water purification as well as food technologies. Semiconductor photocatalysts have gained major attention in dealing with energy, environment as well as in biological applications due to their excellent properties. However, to produce an excellent photocatalytic system, many researchers have overlooked the important factors that affect the quality of the systems, especially in real-life applications. The effectiveness of the photocatalytic systems must be suitable for long-term usage. Moreover, fundamental things such as fast recombination and less stability should have been studied and investigated more. Therefore, extensive studies on producing excellent photocatalysts are required to produce better a world environment. Hence, researchers are constantly working on the advancement of photocatalysis to be applied to environmental issues in the future.

References

[1] S. Zhu, D. Wang, Photocatalysis: basic principles, diverse forms of implementations and emerging scientific opportunities, Advanced Energy Materials 7 (2017) 1700841. Available from: https://doi.org/10.1002/aenm.201700841.

[2] S.-H. Guan, K.-F. Zhao, Q. Tong, Q.-X. Rao, L. Cheng, W. Song, et al., A review of photocatalytic materials application on nonylphenol degradation, Environmental Challenges 4 (2021) 100172. Available from: https://doi.org/10.1016/j.envc.2021.100172.

[3] Y. Li, F. Chen, R. He, Y. Wang, N. Tang, Semiconductor photocatalysis for water purification, Nanoscale Materials in Water Purification, Elsevier, 2019, pp. 689–705. Available from: https://doi.org/10.1016/B978-0-12-813926-4.00030-6.

[4] S.N. Ahmed, W. Haider, Heterogeneous photocatalysis and its potential applications in water and wastewater treatment: a review, Nanotechnology 29 (2018) 342001. Available from: https://doi.org/10.1088/1361-6528/aac6ea.

[5] C. Zhang, Y. Li, M. Li, D. Shuai, X. Zhou, X. Xiong, et al., Continuous photocatalysis via photo-charging and dark-discharging for sustainable environmental remediation: performance, mechanism, and influencing factors, Journal of Hazardous Materials 420 (2021). Available from: https://doi.org/10.1016/j.jhazmat.2021.126607.

[6] D. Spasiano, R. Marotta, S. Malato, P. Fernandez-Ibañez, I. Di Somma, Solar photocatalysis: materials, reactors, some commercial, and pre-industrialized applications, A Comprehensive Approach, Applied Catalysis B: Environmental 170–171 (2015) 90–123. Available from: https://doi.org/10.1016/j.apcatb.2014.12.050.

[7] D. Hariharan, P. Thangamuniyandi, A. Jegatha Christy, R. Vasantharaja, P. Selvakumar, S. Sagadevan, et al., Enhanced photocatalysis and anticancer activity of green hydrothermal synthesized Ag@TiO_2 nanoparticles, Journal of Photochemistry and Photobiology B: Biology 202 (2020) 111636. Available from: https://doi.org/10.1016/j.jphotobiol.2019.111636.

[8] M. Ismael, A review and recent advances in solar-to-hydrogen energy conversion based on photocatalytic water splitting over doped-TiO_2 nanoparticles, Solar Energy 211 (2020) 522–546. Available from: https://doi.org/10.1016/j.solener.2020.09.073.

[9] B.C. Marepally, C. Ampelli, C. Genovese, E.A. Quadrelli, S. Perathoner, G. Centi, Production of Solar Fuels Using CO_2, 2019, pp. 7–30. https://doi.org/10.1016/B978-0-444-64127-4.00001-X.

[10] R. Acharya, B. Naik, K. Parida, Cr(VI) remediation from aqueous environment through modified-TiO_2-mediated photocatalytic reduction, Beilstein Journal of Nanotechnology 9 (2018) 1448–1470. Available from: https://doi.org/10.3762/bjnano.9.137.

[11] A. Hossain, K. Sakthipandi, A.K.M. Atique Ullah, S. Roy, Recent progress and approaches on carbon-free energy from water splitting, Nano-Micro Letters 11 (2019) 103. Available from: https://doi.org/10.1007/s40820-019-0335-4.

[12] P.S. Aithal, S. Aithal, Opportunities & challenges for green technologies in 21st century, 2016. http://www.rdmodernresearch.com.

[13] X. Chen, Z. Zhang, L. Chi, A.K. Nair, W. Shangguan, Z. Jiang, Recent advances in visible-light-driven photoelectrochemical water splitting: catalyst nanostructures and reaction systems, Nano-Micro Letters 8 (2016) 1–12. Available from: https://doi.org/10.1007/s40820-015-0063-3.

[14] B. Samanta, Á. Morales-García, F. Illas, N. Goga, J.A. Anta, S. Calero, et al., Challenges of modeling nanostructured materials for photocatalytic water splitting, Chemical Society Reviews 51 (2022) 3794–3818. Available from: https://doi.org/10.1039/D1CS00648G.

[15] K. Maeda, K. Domen, Photocatalytic water splitting: recent progress and future challenges, The Journal of Physical Chemistry Letters 1 (2010) 2655−2661. Available from: https://doi.org/10.1021/jz1007966.

[16] S. Chen, T. Takata, K. Domen, Particulate photocatalysts for overall water splitting, Nature Reviews Materials 2 (2017) 17050. Available from: https://doi.org/10.1038/natrevmats.2017.50.

[17] S.K. Lakhera, A. Rajan, R. T.P., N. Bernaurdshaw, A review on particulate photocatalytic hydrogen production system: progress made in achieving high energy conversion efficiency and key challenges ahead, Renewable and Sustainable Energy Reviews 152 (2021). Available from: https://doi.org/10.1016/j.rser.2021.111694.

[18] H. Wang, X. Li, X. Zhao, C. Li, X. Song, P. Zhang, et al., A review on heterogeneous photocatalysis for environmental remediation: from semiconductors to modification strategies, Chinese Journal of Catalysis 43 (2022) 178−214. Available from: https://doi.org/10.1016/S1872-2067(21)63910-4.

[19] H. Anwer, A. Mahmood, J. Lee, K.-H. Kim, J.-W. Park, A.C.K. Yip, Photocatalysts for degradation of dyes in industrial effluents: opportunities and challenges, Nano Research 12 (2019) 955−972. Available from: https://doi.org/10.1007/s12274-019-2287-0.

[20] J. Treacy, Drinking water treatment and challenges in developing countries, The Relevance of Hygiene to Health in Developing Countries, IntechOpen, 2019. Available from: https://doi.org/10.5772/intechopen.80780.

[21] R. Djellabi, R. Giannantonio, E. Falletta, C.L. Bianchi, SWOT analysis of photocatalytic materials towards large scale environmental remediation, Current Opinion in Chemical Engineering 33 (2021) 100696. Available from: https://doi.org/10.1016/j.coche.2021.100696.

[22] H. Tong, S. Ouyang, Y. Bi, N. Umezawa, M. Oshikiri, J. Ye, Nano-photocatalytic materials: possibilities and challenges, Advanced Materials 24 (2012) 229−251. Available from: https://doi.org/10.1002/adma.201102752.

[23] A.B. Djurišić, Y. He, A.M.C. Ng, Visible-light photocatalysts: prospects and challenges, APL Materials 8 (2020) 030903. Available from: https://doi.org/10.1063/1.5140497.

[24] Y. Lu, H. Zhang, D. Fan, Z. Chen, X. Yang, Coupling solar-driven photothermal effect into photocatalysis for sustainable water treatment, Journal of Hazardous Materials 423 (2022). Available from: https://doi.org/10.1016/j.jhazmat.2021.127128.

[25] W. Wang, G. Li, D. Xia, T. An, H. Zhao, P.K. Wong, Photocatalytic nanomaterials for solar-driven bacterial inactivation: recent progress and challenges, Environmental Science: Nano 4 (2017) 782−799. Available from: https://doi.org/10.1039/C7EN00063D.

[26] L.-D. Piveteau, M.I. Girona, L. Schlapbach, P. Barboux, J.-P. Boilot, Thin ®lms of calcium phosphate and titanium dioxide by a sol-gel route: a new method for coating medical implants, n.d.

[27] Z. Fei Yin, L. Wu, H. Gui Yang, Y. Hua Su, Recent progress in biomedical applications of titanium dioxide, Physical Chemistry Chemical Physics 15 (2013) 4844. Available from: https://doi.org/10.1039/c3cp43938k.

[28] C. Zhang, Y. Li, D. Shuai, Y. Shen, D. Wang, Progress and challenges in photocatalytic disinfection of waterborne viruses: a review to fill current knowledge gaps, Chemical Engineering Journal 355 (2019) 399−415. Available from: https://doi.org/10.1016/j.cej.2018.08.158.

[29] T. Sahu, Y.K. Ratre, S. Chauhan, L.V.K.S. Bhaskar, M.P. Nair, H.K. Verma, Nanotechnology based drug delivery system: current strategies and emerging therapeutic

potential for medical science, Journal of Drug Delivery Science and Technology 63 (2021). Available from: https://doi.org/10.1016/j.jddst.2021.102487.

[30] S. Weon, F. He, W. Choi, Status and challenges in photocatalytic nanotechnology for cleaning air polluted with volatile organic compounds: visible light utilization and catalyst deactivation, Environmental Science: Nano 6 (2019) 3185−3214. Available from: https://doi.org/10.1039/C9EN00891H.

[31] K. Vikrant, S. Weon, K.H. Kim, M. Sillanpää, Platinized titanium dioxide (Pt/TiO_2) as a multi-functional catalyst for thermocatalysis, photocatalysis, and photothermal catalysis for removing air pollutants, Applied Materials Today 23 (2021). Available from: https://doi.org/10.1016/j.apmt.2021.100993.

[32] F. He, W. Jeon, W. Choi, Photocatalytic air purification mimicking the self-cleaning process of the atmosphere, Nature Communications 12 (2021) 2528. Available from: https://doi.org/10.1038/s41467-021-22839-0.

[33] V.K. Yemmireddy, Y.-C. Hung, Using photocatalyst metal oxides as antimicrobial surface coatings to ensure food safety-opportunities and challenges, Comprehensive Reviews in Food Science and Food Safety 16 (2017) 617−631. Available from: https://doi.org/10.1111/1541-4337.12267.

[34] Z. Zhu, H. Cai, D.-W. Sun, Titanium dioxide (TiO_2) photocatalysis technology for nonthermal inactivation of microorganisms in foods, Trends in Food Science & Technology 75 (2018) 23−35. Available from: https://doi.org/10.1016/j.tifs.2018.02.018.

[35] S.D. Lamabam, R. Thangjam, Progress and challenges of nanotechnology in food engineering, Impact of Nanoscience in the Food Industry, Elsevier, 2018, pp. 87−112. Available from: https://doi.org/10.1016/B978-0-12-811441-4.00004-2.

[36] M. Alizadeh Sani, M. Maleki, H. Eghbaljoo-Gharehgheshlaghi, A. Khezerlou, E. Mohammadian, Q. Liu, et al., Titanium dioxide nanoparticles as multifunctional surface-active materials for smart/active nanocomposite packaging films, Advances in Colloid and Interface Science 300 (2022). Available from: https://doi.org/10.1016/j.cis.2021.102593.

[37] P. Suppakul, J. Miltz, K. Sonneveld, S.W. Bigger, Active packaging technologies with an emphasis on antimicrobial packaging and its applications, Journal of Food Science 68 (2003) 408−420. Available from: https://doi.org/10.1111/j.1365-2621.2003.tb05687.x.

[38] H. Xu, L. Chen, D. Julian McClements, Y. Hu, H. Cheng, C. Qiu, et al., Progress in the development of photoactivated materials for smart and active food packaging: photoluminescence and photocatalysis approaches, Chemical Engineering Journal 432 (2022). Available from: https://doi.org/10.1016/j.cej.2021.134301.

Index

Note: Page numbers followed by "*f*" and "*t*" refer to figures and tables, respectively.

O

P

T

U

V

W

X

Z

Theoretical Concepts of Photocatalysis

Mohammad Mansoob Khan, Professor, Inorganic Chemistry, Department of Chemical Sciences, Faculty of Science, Universiti Brunei Darussalam, Brunei Darussalam.

Theoretical Concepts of Photocatalysis offers a concisely structured and systematic overview of photocatalysis as well as explores the theory and experimental studies of charge-carrier dynamics in photocatalysis. This book introduces the fundamental concepts of photocatalytic reactions involving different types of photocatalysts for various applications such as treatment of polluted water, wastewater, polluted air, food packaging, and biomedical and medical fields. This book also details the chemistry of visible light-induced photocatalysis, shown by different classes of photocatalysts for novel energy and environment-related applications. Photocatalysis using different types of photocatalysts (such as metal oxides, chalcogenides, their composites, etc.) is a green technology that has been widely applied for environment remediation and energy production. Its significant advantages, such as low cost, high efficiency, stability, and harmlessness, are discussed alongside future perspectives and challenges of photocatalysis. Focusing on nanostructure control, synthesis methods, activity enhancement strategies, environmental applications, and perspectives of semiconductor-based nanostructures. This book offers guidelines for designing novel semiconductor-based photocatalysts with low cost and high efficiency to meet the demands of the efficient utilization of solar energy in the area of energy production and environment remediation.

Key features:

- Covers the fundamentals and theoretical aspects of photocatalysis
- Includes different types of photocatalysts and related photocatalytic reactions
- Offers theoretical and practical concepts of energy and environmental applications
- Summarizes the fundamentals of semiconductor-based nanomaterials for various applications
- Highlights the future perspective and challenges

About the author:

Mohammad Mansoob Khan is a professor of inorganic chemistry at the Department of Chemical Sciences, Faculty of Science, Universiti Brunei Darussalam, Brunei Darussalam. He has worked in India, Ethiopia, Oman, and South Korea and has demonstrated excellence in teaching and novel research. He used to teach various courses at undergraduate and postgraduate levels. His expertise are in the cutting-edge area of nanochemistry, nanosciences, nanotechnology, materials sciences, and materials chemistry, especially in the field of inorganic and nanohybrid materials such as synthesis of noble metal nanoparticles, their nanocomposites, metal oxides (such as TiO_2, ZnO, SnO_2, CeO_2, etc.), and chalcogenides (such as CdS, ZnS, MoS_2, etc.). He is also extensively working on the bandgap engineering of semiconductors (such as metal oxides and chalcogenides). The synthesized nanostructured materials are used for heterogeneous photocatalysis, hydrogen production, photoelectrodes, solar cells, sensors, and biological applications such as antibacterial, antifungal, antibiofilm activities, etc.

ISBN 978-0-323-95191-3

9 780323 951913

ELSEVIER elsevier.com/books-and-journals